UNIVERSIDAD PONTIFICIA COMILLAS DE MADRID
ESCUELA TÉCNICA SUPERIOR DE INGENIERIA (ICAI)
Instituto de Investigación Tecnológica

DESIGN OF UFLS SCHEMES OF SMALL ISOLATED POWER SYSTEMS

DISEÑO DE ESQUEMAS DE DESLASTRE DE CARGAS POR FRECUENCIA DE PEQUEÑOS SISTEMAS AISLADOS

Tesis para la obtención del grado de Doctor

Directores: Prof. Dr. D. Ignacio Egido Cortés
Prof. Dr. D. Luis Rouco Rodríguez

Autor: Ing. él. dipl. EPF D. Lukas Sigrist

Madrid 2010

UNIVERSIDAD PONTIFICIA ICAI ICADE COMILLAS MADRID

ESTUDIOS DE TERCER CICLO - DOCTORADO– MODELO 15 b)

NOTIFICACIÓN AL INTERESADO DE LA CALIFICACIÓN DE LA LECTURA Y DEFENSA DE LA TESIS (OPCIONAL)

Se hace constar que **D. Lukas Sigrist**

ha leído y defendido en el día de la fecha su tesis titulada **"DESIGN OF UNDERFREQUENCY LOAD-SHEDDING SCHEMES OF SMALL ISOLATED POWER SYSTEMS"** ante el Tribunal constituido por los siguientes Profesores:

Presidente:	Dr. D. Antonio Gómez Expósito
Vocales:	Dr. D. Antonio Jesús Conejo Navarro
	Dr. D. Joao Abel Peças Lopes
	Dr. D. Enrique Lobato Miguélez
Secretario:	Dr. D. Fidel Fernández Bernal

habiendo recibido la calificación de SOBRESALIENTE CUM LAUDE UNANIMIDAD

Madrid, 17 de Diciembre de 2010

EL SECRETARIO DEL TRIBUNAL

Destino de este documento una vez cumplimentado
Original: interesado

Für Mami, Vati, Tobi, Annettli

ABSTRACT

This dissertation addresses the problem of designing robust and efficient underfrequency load-shedding (UFLS) schemes of small isolated power systems. UFLS schemes are a well-established remedy against frequency instabilities.

Frequency stability is a major issue for small isolated power systems. In small isolated power systems, frequency instability occurs in the form of continuous frequency decay or of sustained frequency swings leading to tripping of generating units. Main reasons for the continuous frequency decay are insufficient spinning reserve or the loss of a major generating unit. However, the ultimate reason for frequency instability comes from the fact that generating units are equipped with underfrequency protection devices which trip the generating units in case of underfrequency conditions. Thus, if additional counter-measures, such as UFLS, fail, underfrequency protection devices trip the generating units and the power system collapses due to frequency instability. In addition, increasing penetration of decoupled power generation enhances the risk of frequency instability due to its negligible frequency-control capabilities and the absence of inertial response. Decoupled power generation refers to those solar and wind-power generating units which are mechanically decoupled form the power system through a stage of power electronic converters.

UFLS schemes are implemented to avoid system collapses. These schemes trip loads to restore the power equilibrium and to arrest frequency decay. UFLS schemes can be grouped in conventional and advanced schemes. This dissertation is concerned with conventional UFLS schemes which trip predefined amounts of load at specified frequency thresholds. The instant of tripping is determined by underfrequency and rate of change of frequency (ROCOF) relays, monitoring continuously frequency and ROCOF and comparing them to underfrequency and ROCOF thresholds.

The design of such UFLS schemes is usually based on the evaluation of the responses of the power system to a set of contingencies. These evaluations in turn are realized by means of simulations of a model of the power system of interest. A simple but still accurate model has been developed to simulate frequency dynamics of a power system. This so-called non-linear multi-generator system frequency dynamics (SFD) model is a low-order model which reduces the computational cost with respect to a fully detailed model maintaining the essential frequency dynamics of the original model. The

ability of the non-linear multi-generator SFD model to accurately reproduce short-term frequency dynamics has been checked by comparing the SFD model with more detailed power-system models.

Several methods have been reported in literature to design conventional UFLS schemes, but there exists no generally accepted method for the design of UFLS schemes. These methods are mostly based on simulations of a set of operating and contingency scenarios. However, these operating and contingency scenarios are usually determined by the common practice of scenario selection, which does not necessarily guarantee the selection of the most appropriate operating and contingency scenarios. Furthermore, some design methods do not guarantee an optimal UFLS scheme performance in terms of shed load. Thus, a method for the design of robust and efficient UFLS schemes of small isolated power system has been elaborated. Efficiency is tantamount to shedding a minimum amount of load, whereas robustness denotes efficiency for a set of operating and contingency scenarios. This proposed method for the design of robust and efficient UFLS schemes is based upon the SFD model approach.

To guarantee a robust UFLS scheme design, adequate operating and contingency scenarios need to be selected. A method based on Data Mining has been proposed to identify and select representative operating and contingency scenarios. Several Data Mining techniques such as K-Means, Fuzzy C-Means and KSOM have been applied. Efficiency of the UFLS scheme can be achieved by applying an optimization algorithm to adjust the parameters of the UFLS scheme, corresponding with the tunable parameters of the underfrequency and ROCOF relays. The main objective of the optimization stage is to minimize the amount of shed load without jeopardizing the system stability. Adaptive Simulated Annealing algorithm has been suggested as optimization algorithm.

The proposed method for the design of efficient and robust UFLS schemes comprises thus two tasks: the selection of adequate operating and contingency scenarios by means of Data Mining techniques and the optimal tuning of the UFLS parameters by means of adaptive Simulated Annealing optimization algorithm. To confirm the feasibility of the approach, the proposed method has been applied to the design of the UFLS schemes of the La Palma and the Gran Canaria power systems. In addition, the proposed UFLS scheme has been compared to a simply optimized UFLS scheme which uses operating and contingency scenarios determined by the common practice of scenario selection.

Finally, methods for the design of UFLS schemes are in general based upon certain assumptions concerning design conditions and power-system behavior and in particular, variability of UFLS scheme step sizes. Usually, implemented step sizes do not correspond with actual step sizes due to changing operating conditions. Thus, the impact of varying design conditions and varying step sizes has also been extensively studied.

The analysis of varying design conditions is addressed by designing different UFLS schemes resulting from a variation of one of the design conditions. These design conditions can be roughly classified into those affecting the selection of operating and contingency scenarios and those affecting the formulation of the optimization problem, i.e. the objective function, the constraints, the decision variables or the optimization algorithm. Some of these modified design conditions coincide with other design methods proposed in the literature.

In order to address step-size variations and step-size reduction in particular, a method for the design of UFLS backup steps has been proposed which first designs several combinations of different backup steps settings heuristically, based on simplified variations of UFLS scheme step sizes, and in a second step, the proposed designs are validated using a Monte-Carlo simulation approach. Monte-Carlo simulations make use of a probability density function, modeling step-size variation as combination of feeder-load variation and feeder outages and breaker failures. The necessity of backup steps has been reaffirmed by the Monte-Carlo simulation approach.

ACKNOWLEDGEMENTS

Gratus sum, non quia expedit, sed quia iuvat.

At this point, I would like to show my most sincere appreciation towards all people who directly or indirectly contributed to the realization of this dissertation.

First, I would like to express my deepest gratitude to my supervisors, Luis Rouco and Ignacio Egido, for their continuous support, their advice and especially for their confidence and encouragement. One easily gets lost in the oceanic adventure of investigation, and I found my island thanks to their guidance. Daily collaboration was and is a real pleasure!

Second, I wish to thank the IIT for providing the opportunity to do a PhD. Special thanks go to all colleagues and staff for creating a marvelous ambience. To list them all would lead to another two hundred pages and forgetting one of them would be inexcusable. Sometimes, it is necessary to suspend research activities and to redirect the attention to slightly different, maybe more artistic investigations or to have a beer while discussing whether it is froth or foam, etc. Thank you all for those moments.

I also want to mention here the considerate support provided by Red Eléctrica de España for the research reported in this dissertation. This support is gratefully acknowledged; in particular, I wish to thank Santiago Marín, Jesús Rupérez, Alfredo Rodríguez and Cristóbal Castro who have provided valuable comments and discussions throughout the collaboration.

Thanks are also due to Unelco Endesa Generación and especially due to Jordi Magriñá for his support at the very beginning of this investigation.

I am also grateful to Rachid Cherkaoui who introduced me to the IIT and to Luis Rouco in particular.

Finally, I would like to thank my family too, particularly my parents, Dieter and Brigitta, as well as my siblings, Tobias and Annette, and their families for their continuous encouragement. Probably the best family in the world! Even if I am far from home, I never feel alone. And last but not least, I also want to express my gratitude to Ana for her support and her patience, which is a kind of magic seeing that I dedicated several weekends to this dissertation. Every little thing she does is magic!

CONTENTS

LIST OF SYMBOLS

POWER SYSTEM MODELING

Symbol	Description
H	Equivalent inertia
H_i	Inertia of generator i
K_i	Generator model gain in $M_{base,i}$
k_i	Generator model gain in S_{base}
$\hat{K}$	Total gain
k_{eq}	Equivalent gain in S_{base}
$a_{j,i}$	Generator model poles
$b_{j,i}$	Generator model zeros
T_i	Generator model first-order time constant
p_e	Electrical power
$p_{d,i}$	Power demand of generator i equivalent to p_e
$\Delta p_{d,i}$	Variation of power demand of generator i
$\Delta p_{d,tot}$	Total variation of power demand
$p_{m,i}$	(Mechanical) output power of generator i
Δp_m	Generator output power variation
$\Delta p_{m,i}$	Output power variation of generator i
$\Delta p_{m,tot}$	Total power output variation
$\Delta p_{i,max}$	Maximum output power variation of generator i
$\Delta p_{i,min}$	Minimum output power variation of generator i
$p_{loss,j}$	Lost power in scenario j
$p_{loss,max}$	Maximum lost power
$p_{loss,min}$	Minimum lost power
$M_{base,i}$	Machine base of generator i

Symbol	Description
S_{base}	System base
ω	Frequency
$\Delta\omega$	Frequency deviation
ω_j	Frequency of scenario j
$\Delta\omega_j$	Frequency deviation of scenario j
ω_{max}	Maximum frequency
$\Delta\omega_{max,allowable}$	Maximum allowable frequency deviation
$\Delta\omega_{max,j}$	Maximum frequency deviation in scenario j
ω_{min}	Minimum frequency
$\Delta\omega_{min}$	Minimum frequency deviation
$\Delta\omega_{min,allowable}$	Minimum allowable frequency deviation
$\Delta\omega_{min,j}$	Minimum frequency deviation in scenario j
$t_{\omega min,j}$	Instant of minimum frequency in scenario j
$t_{max,j}$	Maximum time $\Delta\omega_{min,j} < \Delta\omega_{min,allowable}$
$\Delta\omega_{ref}$	Governor reference deviation
$\Delta\omega_{ss}$	Post-disturbance steady-state frequency deviation
$\Delta\omega_{ss,j}$	Post-disturbance steady-state deviation in scenario j
e_1	Internal voltage magnitude
δ	Angle of the internal voltage with respect to the infinite bus voltage
t_m	Mechanical torque
V	Lyapunov function
v	Voltage magnitude of the infinite bus
x_t	Total external reactance
$\mathbf{x}_s$	Vector of state variables
$\mathbf{f}$	System of non-linear differential equations
h	Integration step

DESIGN AND ANALYSIS OF UFLS SCHEMES

Symbol	Description
$\omega_{thrshld}$	Frequency threshold
$\omega_{thrshld,uf}$	Frequency threshold of underfrequency relays
$\omega_{thrshld,rocof}$	Frequency threshold of ROCOF relays
t_{int}	Intentional time delay
$t_{int,uf}$	Intentional time delay of underfrequency relays
$t_{int,rocof}$	Intentional time delay of ROCOF relays
$d\omega/dt_{thrshld}$	Rate of change of frequency threshold
t_{opn}	Time delay
p_{step}	Step size
$p_{step,uf}$	Step size of underfrequency stages

Symbol	Description
$p_{step,rocof}$	Step size of ROCOF stages
p_{shd}	Load shed
$p_{shd,j}$	Shed load in scenario j
$t_{shd,j}$	Instant of shedding in scenario j
$\mathbf{\Omega}$	Learning set containing responses of the system frequency
t_{sim}	Simulation time
f_d	Damped oscillation frequency
ω_n	Natural oscillation frequency
ς	Damping
$\mathbf{x}_e$	Input vector for Data Mining
$\mathbf{c}_c$	Centroid
u_{ec}	Degree of membership
f	Objective function
h_l	Equality constraints function
g_l	Inequality constraints function
$\mathbf{x}_d$	Vector of decision variables
$\alpha_{f,j}$	Objective function weighting coefficient related to $p_{shd,j}$
$\beta_{f,j}$	Objective function weighting coefficient related to $\Delta\omega_{min,j}$
$\gamma_{f,j}$	Objective function weighting coefficient related to $\int\Delta\omega_j dt$
$\delta_{f,j}$	Objective function weighting coefficient related to $\Delta\omega_{ss,j}$
σ_ω	Difference between two consecutive frequency thresholds
τ_k	Temperature at iteration k
a_τ	Geometric cooling schedule parameter
b_τ	Rational cooling schedule parameter
Φ	Penalty function
M	Iteration dependent penalty parameter
d_l	Indicator whether constraint l is active or not
$C_{1,l}$	Penalty constant related to the importance of constraint l
$C_{2,l}$	Penalty constant related to the amount of violation of constraint l
g_a	Normal probability density function
b_e	Bernoulli probability density function
p	Failure probability
gb	Probability function describing step-size variations

ACRONYMS

Acronym	Description
UFLS	Underfrequency load shedding
ROCOF	Rate of change of frequency
DPG	Decoupled power generation

Acronym	Description
SFD	System frequency dynamics
SA	Simulated Annealing
GA	Genetic Algorithm
SQP	Sequential Quadratic Programming
ANN	Artificial neural networks
KSOM	Kohonen self-organizing maps
REE	Red Eléctrica de España
UCTE	Union for the Co-ordination of Electricity Transmission
NGET	National Grid Electricity Transmission
HECO	Hawaiian Electric Company

CHAPTER ONE

INTRODUCTION

1-1 PROBLEM STATEMENT

This dissertation addresses the problem of designing underfrequency load-shedding (UFLS) schemes of small isolated power systems. UFLS schemes are a well-established remedy against frequency instabilities. Frequency stability is a major issue for small isolated power systems.

Several power-system blackouts occurred during the past few years around the world, characterized inter alia by frequency instabilities and involving underfrequency load-shedding actions. A summary of large frequency disturbances and blackouts can be found in [CIGRE'99] and in [Bonian'05], including the 1965 blackout in New York or the Malaysian blackout of 1996. Recent blackouts of small isolated power systems have been reported in Oahu (Hawaii, USA) [POWER HECO'09] and in Mallorca-Menorca (Spain) [Endesa'09], both in 2008, and in Tenerife (Spain) in 2009. For example, the short-circuit-based disconnection of more than 50% of total power generation in the Mallorca-Menorca power system instigated a very fast frequency decay, which could not be successfully stopped by load-shedding actions, and the system finally collapsed due to cascading outage of the remaining generating units. More successful load-shedding actions during the partial blackout in 1995 of Israeli power system could, at least, stabilize the northern island after splitting into two subsystems [Hain'97]. The southern island collapsed among other things because a protection-initiated power station tripping prevented load-shedding automatics from stabilizing this island.

These incidents show the importance of underfrequency load shedding in protecting power systems against frequency instability. Unsuccessful load-shedding actions necessarily implicate a review of designs of currently installed UFLS schemes. This dissertation focuses therefore on the design of robust and efficient UFLS schemes of small isolated power systems.

1-1-1 Frequency stability in small isolated power systems

A power system needs to be reliable and secure. Reliability is defined as the probability of the satisfactory operation of a power system, whereas security denotes the degree of

risk in the ability of a power system to survive imminent disturbances. Stability is related to both reliability and security [Elgerd'82; IEEE/CIGRE'04]. In fact, stability refers to the continuance of intact operation following a disturbance. Further, it is a concept used in assessing system robustness[1].

According to [IEEE/CIGRE'04], power-system stability can be defined as "*the ability of an electric power system, for a given initial operating condition, to regain a state of operating equilibrium after being subjected to a physical disturbance, with most system variables bounded so that practically the entire system remains intact.*" This definition applies to a power system as a whole. Often, however, the stability of a particular generator or group of generator can also be of interest. Furthermore, due to the non-linear nature of power systems and due to a constantly changing environment, stability depends on the operating conditions as well as the nature of the disturbance. Congruously, power-system stability can be further classified based on the following considerations:

- The physical nature of the resulting mode of instability as indicated by the main system variable in which instability can be observed.
- The size of the disturbance considered which influence the method of calculation and prediction of stability.
- The devices, processes, and the time span that must be taken into consideration in order to assess stability.

Figure 1-1 (taken form [IEEE/CIGRE'04]) summarizes the classification of the power-system stability problem, identifying its categories. Power-system stability is divided into rotor angle, voltage and frequency stability, according to its underlying physical nature. Furthermore, a distinction is made between small disturbance and large disturbance stability as well as between short-term and long-term stability. A disturbance is large when the non-linear differential equations that describe the power system dynamic behavior cannot be linearized for analysis purposes. Small disturbances continually occur in the form of load changes, whereas large disturbances comprises short-circuits, generator outages, etc. Unlike small disturbances, large disturbances may lead to structural changes in the power system topology. Short-term stability is determined by the dynamics of the generators, their prime movers and the primary controls. Long-term stability is largely affected by the dynamics of the energy sources of the generators (boilers, nuclear reactors, hydro stations with complicate hydraulic circuits, etc) and the secondary controls. Note that in the case of frequency stability, there is no distinction between small disturbance and large disturbance stability. In fact, frequency stability is always a large disturbance stability problem since it depends on specified operating and contingency scenarios.[2]

[1] In fact, security is often also referred as the robustness against one, two, or several contingencies.

[2] Inhere, the terms disturbance and contingency are considered as synonyms. For the sake of completeness, disturbance refers generally to an action of disturbing, whereas contingency refers to a future event which is possible but cannot predicted with certainty.

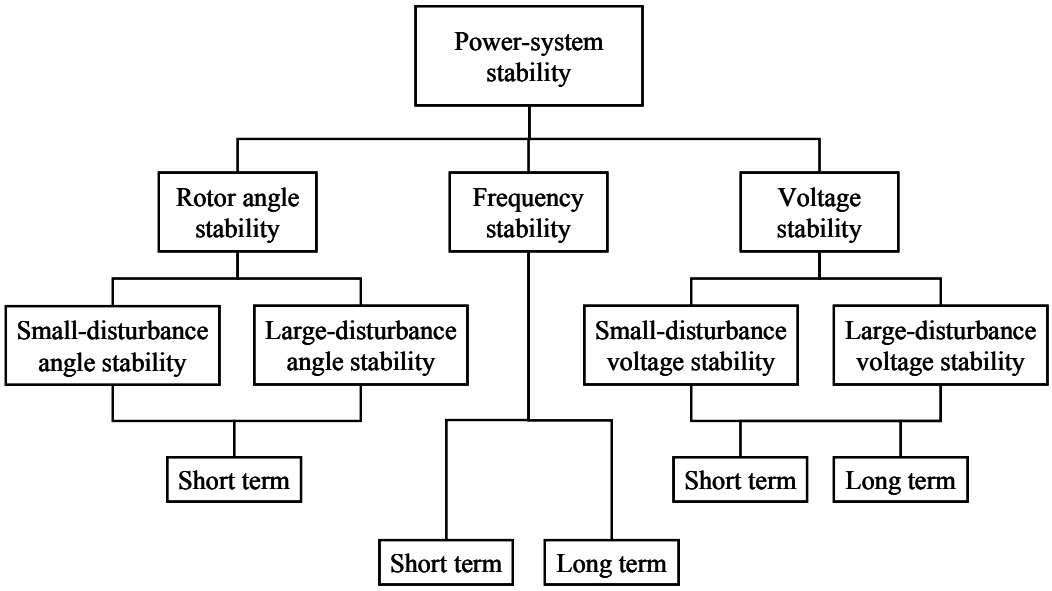

Figure 1-1: Classification of power-system stability [IEEE/CIGRE'04].

Frequency stability refers to the ability of a power system to maintain frequency within an acceptable range following a severe system upset resulting in a significant imbalance between real-power generation and load demand [IEEE/CIGRE'04]. Severe system upsets have their origin in the generation and transmission system. The ability to maintain frequency within an acceptable range is tantamount to maintain or restore equilibrium between real-power generation and load demand. As previously mentioned, frequency stability can be further divided into short-term and long-term frequency stability, according to the involved dynamics[3]. Focus is on short-term frequency stability, which is predominantly determined by the dynamics of the prime movers and their primary controls.

In case of an imbalance between real-power generation and load demand, frequency deviates from its nominal value of 50 Hz. Frequency decreases, if load demand exceeds power generation, whereas frequency increases, if more active power is generated than consumed. In both cases, primary frequency controls try to restore the power equilibrium. However, in general, the situation of lack of generation (i.e. load demand exceeds power generation) is more problematic with regard to possible equipment damages due to limited spinning reserves. Thus, attention is principally paid to situations of lack of generation and consequently, to underfrequency conditions.

In large interconnected power systems, significant frequency deviations normally occur only when the system is split into several islands with substantial power excess or deficit. By contrast, small isolated power systems are very sensitive to power imbalances, usually originating from outages of generating units. From a frequency stability point of view, a small isolated power system can be described as a system which is not interconnected to any other power system and in which any individual

[3] Sometimes, a third distinction with respect to the time span considered is reported. Apart from short-term and long-term stability, also mid-term stability has been analyzed. Mid-term stability studies connect short-term and long-term frequency dynamics. In other words, both generators, especially their turbine-governor systems, and energy supply systems are modeled in detail. Two software tackle the mid-term dynamics: EPRI T/M Stability program and EUROSTAG [EPRI'79; Antoine'92]. They differ in the fact that EPRI uses a manually controlled step-size integration algorithm (the trapezoidal rule), whereas EUROSTAG is based upon a variable step-size integration algorithm.

generating unit in-feed presents a substantial portion of the total demand [Horne'04]. This directly implies that the number of generating units involved in power generation is relatively small compared with a large interconnected power system.

In small isolated power systems, instability occurs in the form of a continuous frequency drop or of sustained frequency swings leading to tripping of generating units [IEEE/CIGRE'04]. A typical example of short-term frequency instability is the unaltered drop of frequency due to insufficient spinning reserve and/or insufficient underfrequency load shedding, which finally causes a system collapse within a few seconds due to underfrequency generator tripping. Another origin of instability might be a huge loss of power generation, albeit enough spinning reserve is available. In a small isolated power system, a huge loss is given by the loss of the largest generating unit[4]. A huge loss instigates a very rapid decay of frequency for which primary control is unable to act in due time – even if sufficient spinning reserve is available. Figure 1-2 illustrates short-term frequency instabilities. The horizontal line describes the minimum allowable frequency before generating units are tripped by underfrequency protection.

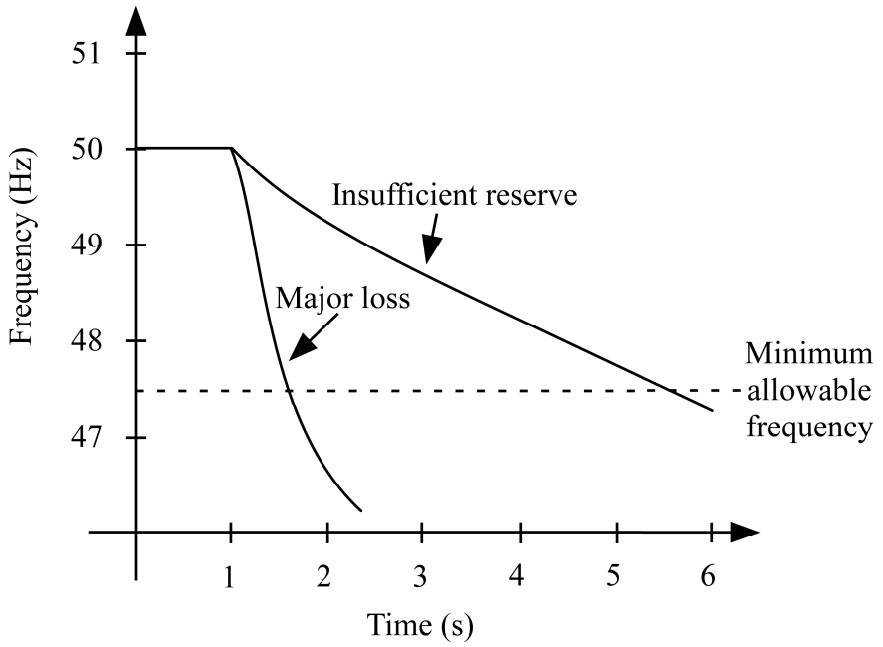

Figure 1-2: Causes of frequency instability.

Hence, frequency stability problems are associated with inadequacies in equipment response or insufficient generation reserves. However, the ultimate reason for frequency instability lies in poor coordination of control and protection equipment. In fact, generating units are equipped with underfrequency protection devices which trip the generating units in case of an underfrequency conditions. The main problem of underfrequency frequency operation is the excitation of resonant conditions of mechanical components such as turbine blades and compressor airfoils of steam turbines and combustion engines. Further problems arise due to reduced output of power-plan auxiliaries such as fans and pumps which reduce the power generation further and may cause thermal overload. Thus, if additional counter-measures such as

[4] This is a common incident in small isolated power systems. A single generating unit may provide up to 50% of the total load demand as in the case of the La Palma (Canary Islands) power system. The loss of 50% of the total generation as in Mallorca-Menorca on November 13, 2008, could jeopardize a power system and lead to a system collapse.

underfrequency load shedding fail, underfrequency protection devices trip the generating units and the power system collapses due to frequency instability. Failures in counter-measures usually originate in poor designs and/or coordination.

1-1-2 Underfrequency load shedding

The magnitude of a frequency excursion mainly depends on the magnitude of the power imbalance and on the way the power system behaves following the disturbance. To avoid damages of generation and load-side equipment, it is crucial to operate the power system within an established, acceptable frequency range or at least, to prevent longer frequency excursions out of this established range. This is achieved by restoring as fast as possible power equilibrium.

In theory, the equilibrium between power generation and load demand can be regained or by readjusting the power generation by means of primary frequency control or by readjusting the load demand. However, for large disturbances, primary frequency control action is usually not fast enough to restore the power equilibrium and to confine frequency excursions to acceptable values. Furthermore, the available spinning reserve could be insufficient to cover the lost power generation. An efficient alternative consists therefore in readjusting the load demand by shedding load.

Underfrequency load-shedding (UFLS) schemes are a last-resort tool to protect the power system in case of a severe contingency, giving rise to a dangerous underfrequency condition. Their primary objective is to arrest frequency decay. UFLS schemes provide an initial underfrequency protection for generating units to prevent a possible cascading power outage. If a small isolated power system collapses in consequence of frequency instability, system restoration takes long, in the order of several hours. In addition, power outages negatively affect utilities by damaging the equipment and causing a substantial loss of revenue, and they may also lead to a loss of costumer confidence [Cote'01]. By contrast, if the system survives as a result of successful load shedding, fewer customers are affected and system restoration is accomplished within a much shorter time (in the order of minutes). Hence, UFLS schemes not only protect generation and load-side equipment, but they also improve power-system reliability and security and they minimize the socio-economical impact on utilities and customers.

In a first stage, UFLS schemes can be divided into manual and automatic UFLS schemes. Manual UFLS actions are generally applied to frequency restoration problems and rarely intervene in the confinement of frequency excursions[5]. By contrast, automatic UFLS schemes are used to arrest frequency decay. In fact, there exist different types of automatic UFLS schemes according to their mode of operation. Figure 1-3 resumes the classification of different UFLS schemes.

[5] In general, UFLS schemes are also used for frequency restoration. Frequency restoration refers to additional load-shedding action to bring back frequency to an acceptable steady-state value. Frequency restoration actions take place after primary UFLS action to stop frequency decay. Thus, frequency restoration is rather a long-term problem and is consequently not considered.

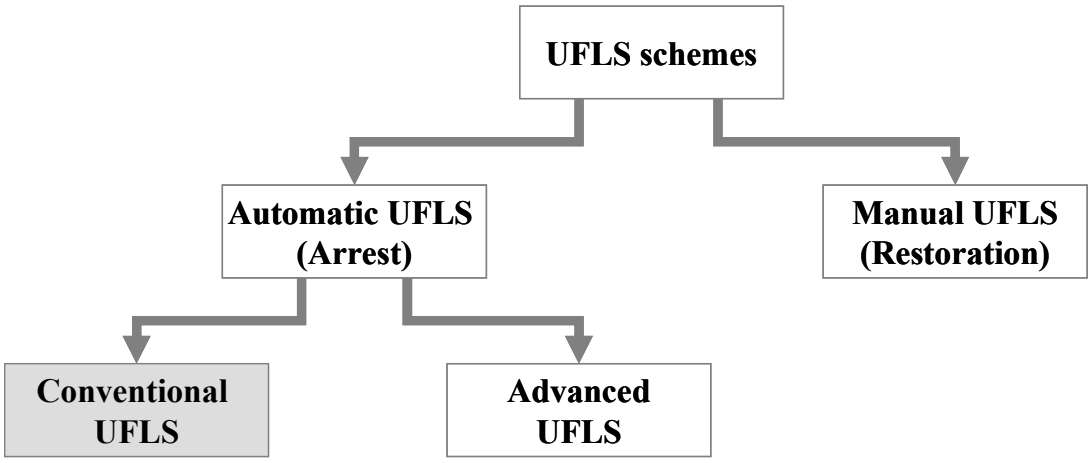

Figure 1-3: Classification of UFLS schemes.

Two UFLS schemes can be distinguished: conventional and advanced UFLS schemes. Conventional UFLS schemes continuously measure frequency and eventually the rate of change of frequency (ROCOF) and shed a predefined amount of load in case of frequency and/or the rate of change of frequency fall below a certain threshold. By contrast, advanced UFLS schemes also use additional information and measurements such as power generation, voltage, etc. to compute the amount of load which needs to be shed. In addition, advanced UFLS schemes are highly adaptive in the sense that they adjust their reaction in function of the actual power-system conditions. However, utilities still use conventional UFLS schemes to protect the power system. Thus, the focus of this dissertation lies on conventional UFLS schemes.

An important task before implementing an UFLS scheme is the adequate design of the UFLS scheme. The design is usually divided into two steps: first, a set of possible operating and contingency scenarios is selected and then, the UFLS scheme parameters are tuned according to some specified criteria. For example, the UFLS scheme should act such that the system integrity is guaranteed for all possible disturbances including worst-case scenarios. In addition, to reduce to impact on customer, overshedding should be avoided and the curtailed amount of load reduced to a minimum. To date, there exists no generally accepted method for the design of UFLS schemes. Some methods have been proposed, but there is no guaranty for an optimal UFLS scheme performance in terms of shed load. As a consequence, there is a need for a systematic method which should lead to robust and efficient UFLS schemes. Finally, the impact of varying UFLS scheme step sizes should also be considered since a reduction of the step sizes might have a jeopardizing impact on system stability.

1-1-3 Review of load-shedding practices

Underfrequency load-shedding practices vary from power system to power system, depending on the characteristics of the system and its operation criteria imposed by the system operator. For the purpose of reviewing load-shedding practices, two larger, a medium-size and two smaller power systems are contemplated. First operating criteria are resumed and subsequently, load-shedding practices are compared.

The larger power systems are the British NGET and the Nordel system, which coordinates power-system operation in the Scandinavian countries as well as in Denmark and Iceland. Both NGET and Nordel power systems are part of the UCTE system and comply with UCTE operation rules. These specify among other things amount and availability of spinning reserve and locate critical underfrequency operating condition at 47.5 Hz [UCTE'04]. Nordel requires generating units to operate within the

frequency band of 50 to 47.5 Hz for 30 minutes, including a possible output reduction of 15% at 47.5 Hz [Nordel'07]. For frequencies lower than 47.5 Hz, large thermal plants start to disconnect. NGET (National Grid of Electricity Transmission) grid code is more demanding in this regard since it requires continuous operation for frequencies even between 47.5 and 47 Hz for 20 s [NGET'09]. Similar conditions are imposed by EirGrid, Irish system operator and owner of the system operator of Northern Ireland [EirGrid'09]. In fact, generating units are required to remain synchronized during 60 minutes for frequencies between 52 and 47.5 Hz and during 20 s for frequencies within 47.5 and 47 Hz. Both NGET and EirGrid grid codes determine the amount of available spinning reserve in accordance with the loss of the largest power generation station. Knowing that Iceland's Landsnet conditions on underfrequency operation of generating units comply with Nordel requirements and resemble those of EirGrid, it seems that Northern European system operators impose quite similar conditions.

By contrast, grid codes of Spanish and Hawaiian isolated power systems are less demanding with respect to extended underfrequency operation of generating units. In fact, Hawaiian system operator (HECO) requires continuous operation for frequencies below 56 Hz for only 6 s [HECO'08; Matsuura'09]. Similar conditions are imposed by the Spanish system operator (REE) where generating units need to continue operating during 3 s for frequencies below 47.5 Hz [MITyC'06]. This is mainly due to the reduced size of these power systems. As in the case of EirGrid, spinning reserves are also determined in function of the loss of the major generating unit. It is noteworthy at that time that the Hawaiian power systems of Maui and Hawaii do not carry spinning reserve capacity but only a regulating reserve of 3 to 5 MW.

Some comments can be made with regard to these requirements. First, they apply in general for thermal generating units which are more sensible to frequency deviations. Diesel engines, for example, can withstand transitory frequency levels as low as 43 Hz [Rodriguez'09]. Further, all these requirements on generating units might not be satisfied during real disturbances because grid codes are not retroactive and older generating units are excluded from new requirements. Moreover, generating units have to comply with these requirements only if equipment safety is not jeopardized and finally, action of other protection devices (such as overcurrent relays) could trip the generating unit before critical frequency values are reached.

Operation criteria and especially underfrequency operation requirements on generating units define underfrequency load-shedding practices since turbine underfrequency protection and UFLS scheme need to be coordinated. Table 1-1 compares UFLS practices according to the grid codes of Nordel, NGET, EirGrid, HECO and REE system operator. Settings attributed to the NGET coincide with the settings of the NGET power system and do not include settings of the SPT (Scottish Power Transmission) and SHETL (Scottish Hydro-Electric Transmission) systems. Further, EirGrid settings are those of the ESB (Electricity Supply Board) [IEEE'07]. Finally, it should be kept in mind that this is only a sample of possible settings. UCTE recommendations have also been included.

Table 1-1: Underfrequency load-shedding practices (partially taken from [IEEE'07]).

Entity	UFLS scheme							
	Anticipated actions	Step 1	Step 2	Step 3	Step 4	Step 5	Step 6	Step 7	Step 8
UCTE	Quick-start turbines, disconnection pumping units	49Hz 10-20%	48.7Hz 10-15%	48.4Hz 10-15%					
Nordel	Quick-start turbines, HVDC emergency action	48.8Hz 6-10%	48.6Hz 6-10%	48.4Hz 6-10%	48.2Hz 6-10%	48Hz 6-10%			
NGET[1]	Quick-start turbines, disconnection pumping units, interruptible loads	48.8Hz 5%	48.7Hz 15%	48.6Hz 15%	48.5Hz 7.5%	48.4Hz 7.5%	48.2Hz 7.5%	48Hz 5%	47.8Hz 5%
EirGrid[2]	Disconnection pumping units, interruptible loads	48.5Hz 12%	48.4Hz 12%	48.3Hz 12%	48.2Hz 12%				
HECO	Interruptible loads	58.5Hz 5%	58Hz 10%	57.7Hz 10%	57.4Hz 10%	57.2Hz 10%	57.0Hz 5-10%		
REE	Interruptible loads	UF and ROCOF		Frequency thresholds within 50-47Hz					

[1] NGET settings only

[2] ESB settings

It can be inferred from Table 1-1 that load under relief is usually divided into three to six discrete blocks with frequency thresholds in the range of 48 to 49 Hz in the case of larger systems and with frequency thresholds comprised between 47 and 49 Hz for smaller power systems. Further, these discrete blocks correspond to step sizes of 5% to 15% of system demand per step. NGET's UFLS scheme exhibits slightly more steps, but, as in the case of EirGrid's settings, steps can be divided further in substeps. In any case, settings are determined by the system operator. A difference between smaller and larger systems can also be made with respect to anticipated actions. In fact, smaller systems only shed interruptible loads as an anticipated measure, whereas larger systems also dispose of anticipated measures such as disconnection of pumped storage units or connection of quick-start power plants. NGET and EirGrid grid codes plan to manually disconnect demand and to reconnect load shed by the UFLS scheme, if load restoration of load shed by the UFLS is not restored within reasonable a period of time. The purpose of such action is to ensure that a subsequent fall in frequency will again be contained by the operation of the UFLS scheme. Finally, only REE grid code proposes the use of rate of change of frequency (ROCOF) steps due to the small size of the isolated power systems and their inherent sensitivity to large disturbances. Although not presented in Table 1-1, ROCOF relays are also employed by Argentinean system operator CAMMESA [Cammesa'08] and the operator of the central Chilean system CDEC-SIC [CDEC-SIC'08].

Clearly, underfrequency load-shedding practices vary from power system to power system, depending on the characteristics of the system and its operation criteria imposed by the system operator, but most of UFLS schemes exhibit some common characteristics such as step size or number of steps. Differences can be explained by different operation constraints on generating units or the size of the power system.

1-1-4 Increasing decoupled power generation

With increasing intermittent power generation, the impact of intermittent power generation on power-system stability increases as well. For small isolated power systems, typical intermittent energy sources are wind and solar energy. For example, the installed capacity of solar and wind-power generation of the Canary Islands amounts to 271 MW, corresponding to 9.5% of the totally installed capacity [REE'08]. *Decoupled power generation* refers to a particular intermittent power generation, characterized by

mechanical decoupling of the generating unit from the power system through power electronic converters.

The impact of intermittent power generation on power-system stability depends on the wind-turbine and solar technology employed. Wind-turbine technologies can be classified into two categories: variable speed and constant speed wind turbine technologies. Variable speed wind turbines exhibit higher efficiency than constant speed wind turbines. Variable rotor resistance generators, doubly fed asynchronous generators and full-converter units fall in the first category. Conventional induction generators belong to the second category. Most common are nowadays variable speed generators.

Solar-power technologies can be grouped into photovoltaic and solar-thermal technologies [SolarPACES'01]. Photovoltaic power plants generate power by means of solar panels consisting of several solar cells. The photovoltaic effect creates a direct current and thus, inverters are necessary at the point of connection. By contrast, solar-thermal power plants focus a large area of sun light into a concentrated beam to heat a working fluid. The heated working fluid disserves then as a heat source for conventional power generator. To date, in small isolated power systems, photovoltaics are typically used to provide electric power.

The commonly employed solar and wind-power technologies, i.e. doubly fed asynchronous generators and full-converter units as well as photovoltaics, strongly affect frequency stability of small isolated power systems. These solar and wind-power technologies are characterized by a connection to the power system through a stage of power electronic converters and thus, the actual generating unit is mechanically decoupled from the power system. Generation based on these commonly employed solar and wind-power technologies can be referred as *decoupled power generation* [Koczara'04].

As seen before, frequency dynamics depend on the magnitude of the power imbalance, the available spinning reserve and the overall system response. Essentially, two problems arise due to decoupled power generation. First, frequency control is usually limited. In fact, a margin between available intermittent power at any instant and actual delivered power must be maintained to be able participating in frequency control. Usually, this margin, and consequently the reserve, is small[6]. The second problem is concerned with the fact that the commonly used decoupled power generation technology does not contribute to system inertia due to the mechanical decoupling [Rouco'08]. The mechanical decoupling provokes that the power systems does not percept any inertial reaction of these commonly used generators[7].

Both the negligible frequency control and the fact that decoupled power generation can be considered as generation without inertia, have a negative impact on frequency stability. In fact, the initial rate of change of frequency increases with decreasing inertia. Recalling the typical frequency instabilities due to insufficient spinning reserve or due to a huge loss of power generation as depicted in Figure 1-2, decoupled power generation enhances the risk of frequency instability.

---

[6] If spinning reserve is provided, primary frequency control of wind-power generator is generally faster than the primary frequency control of conventional generators.

[7] Some grid operator require wind farms to contribute to primary frequency control [Ackermann'05], but this will be difficult to realize as the energy source (wind) is not directly controllable. Some methods to implement primary frequency control and to emulate inertial response are reported in [Morren'06; Vittal'07].

1-2 OBJECTIVES

The investigation reported in this dissertation focuses on the problem of short-term frequency stability, its associated underlying dynamics and the emergency control actions to be taken to avoid frequency instability. UFLS schemes are a common remedy against frequency instabilities. However, their performance fundamentally depends on their design. UFLS schemes should be both efficient and robust. Efficiency is tantamount to shedding a minimum amount of load, whereas robustness denotes efficiency for a set of operating and contingency scenarios. Efficiency is achieved by using an appropriate optimization algorithm to determine the optimal value of the decision variables, i.e. underfrequency relay and ROCOF relay parameters. Robustness is guaranteed by applying the optimization algorithm to a set of appropriate operating and contingency scenarios. This dissertation deals with a systematic method to design efficient and robust conventional UFLS schemes. The proposed method is applied to real isolated power systems. In addition, designs of UFLS scheme are analyzed considering varying design conditions and taking into account the variability of UFLS step sizes. More precisely, the objectives are:

- A suitable power-system model will be developed which is able to represent the frequency dynamics in small isolated power systems for short-term frequency stability.
- A method based on Data Mining will be proposed to identify representative operating and contingency scenarios, i.e. to find those contingencies which represent best all other possible contingencies. The impact of decoupled power generation is also addressed.
- The efficient tuning of UFLS scheme parameters will be formulated as an optimization problem, which can be resolved by well-known meta-heuristic algorithms.
- The impact of varying design conditions will be addressed by designing different UFLS schemes resulting from a variation of one of these design conditions.
- A method based on Monte-Carlo simulations will be proposed to tackle the problem of changing UFLS step sizes and to design possible backup steps of UFLS schemes.

1-3 OUTLINE

The dissertation contains 7 chapters and 3 appendixes. Chapter 2 reviews the impact of abnormal frequency operation on power-system equipment. Particular attention is paid to distinct turbine types such as steam turbines, combustion turbines and hydraulic turbines, and to turbine underfrequency protection. Thereafter, a survey on conventional underfrequency load-shedding (UFLS) schemes is given outlining the principles, performances criteria and implementation. Finally, the design of conventional UFLS schemes is reviewed and a description on advanced UFLS schemes is given.

In chapter 3, a simple non-linear multi-generator system frequency dynamics (SFD) model is derived. This SFD model is a low-order model which reduces the computational cost with respect to a fully detailed model maintaining the essential frequency dynamics of the original model. A simple but still accurate model can be obtained which allows simulating a power system with a very low computational cost. The non-linear multi-generator SFD model is used to simulate short-term frequency dynamics of small isolated power systems. In addition, this power-system model is used

to study the influence of different model parameters, including the UFLS scheme, on short-term frequency dynamics and on frequency stability.

Chapter 4 addresses the proposed method for the design of efficient and robust conventional UFLS schemes. In particular, a method to select adequate operating and contingency scenarios for the design of robust UFLS schemes is presented. These so-called representative operating and contingency scenario are those scenarios which represent best all other possible scenarios. Furthermore, an optimization-based method for the efficient tuning of the UFLS parameters is outlined. The proposed method for the design of a conventional UFLS scheme comprises then two steps: first, several operating and contingency scenarios, ideally with different degrees of severity, are selected and then, the parameters of the UFLS schemes are tuned such that an objective function is optimized with respect to the previously selected operating and contingency scenarios and to some constraints on system operation and UFLS scheme performance.

In Chapter 5, an extensive analysis of conventional UFLS scheme designs is carried out. In fact, designs of UFLS schemes are based on certain assumptions concerning design conditions and variability of UFLS scheme step sizes. Design conditions influence directly the performance of the resulting UFLS scheme and different design conditions might result in distinct final UFLS scheme designs. Percentaged values of actual step sizes vary from the implemented step sizes due to changing system-operating conditions. Step-size variations can affect negatively UFLS scheme performance since, for example, less load might be shed than necessary to stabilize the system. Monte Carlo simulations are used to simulate step size variations and to address the design of backup steps.

Chapter 6 provides the conclusions of the present dissertation and also highlights its principal contributions. Hints for future research are also given.

Chapter 7 contains the references.

Appendix A resumes the main features of the Matlab toolbox prototype that has been developed in order to simulate, design and analyze UFLS schemes of small isolated power systems under numerous operating and contingency scenarios. The Spanish system operator currently uses the Underfrequency Load-Shedding Scheme Applications (UFLSA) toolbox. The main goal is to be able to simulate fast numerous operating and contingency scenarios and to design and analyze in an automated manner UFLS schemes.

Appendix B presents several frequency protection schemes based on ω–$d\omega/dt$ phase-plane analysis and on the definition of frequency stability boundary in particular. A simple function is derived to describe frequency stability boundary, which can be considered as a separatrix describing a region of frequency stability. Due to their nature, these frequency protection schemes belong to advanced UFLS schemes.

Finally, Appendix C contains block diagrams of commonly used turbine-governor system models of the PSS/E software package model library.

CHAPTER TWO

AUTOMATIC UNDERFREQUENCY LOAD SHEDDING

2-1 INTRODUCTION

Imbalances between power generation and load demand lead to frequency excursions. Frequency decreases, if load demand exceeds power generation, whereas frequency increases, if more active power is generated than consumed. In general, the situation of lack of generation (i.e. load demand exceeds power generation) is more problematic [Anderson'92]. The loss of power generation which instigates an underfrequency condition depends on the power system. In small isolated power systems, the lack of generation is mostly due to generator outages, whereas in large interconnected power systems, the lack of generation is usually due to system separation into islands because of line tripping. Furthermore, small isolated power systems are more sensitive to power imbalances than interconnected power systems mainly because of the reduced number of generating units involved in power generation. To avoid damages of generation and load-side equipment, it is crucial to operate the power system within the established, acceptable frequency range or at least, to prevent longer frequency excursions out of the established range. This is achieved by restoring as fast as possible power equilibrium by the action of automatic underfrequency load-shedding (UFLS) schemes.

Foremost, the impact of abnormal frequency operation on power-system equipment is discussed. Particular attention is paid to underfrequency behavior and protection of distinct turbine types such as steam turbines, combustion turbines and hydraulic turbines. These are the most typical turbine types in small isolated power systems. Thereafter, a survey on conventional UFLS schemes is given outlining the principles, performance criteria and their implementation. UFLS schemes can be considered as the initial turbine underfrequency protection. Finally, the design of conventional UFLS schemes is reviewed and a description of advanced UFLS schemes is given.

2-2 IMPACT OF ABNORMAL FREQUENCY OPERATION ON POWER-SYSTEM EQUIPMENT

Frequency reduction not only affects turbine-governor systems but also generators and transformers [IEEE'87]. Nevertheless, turbine-governor systems are more sensitive to

frequency deviations. Furthermore, the underfrequency condition is more critical than the overfrequency condition.[1] Underfrequency relays are used to protect generating units against low frequency levels because the highest natural frequency of mechanical turbine components is close to synchronous speed. If no additional counter-measure exists, pronounced frequency deviations may cause to trip generating units due to underfrequency protection, which accelerates the frequency decay further. This may lead to a cascading outage of generating units and consequently, to a system blackout.

Subsequently, the impact of abnormal frequency on steam turbines, combustion turbines and hydroelectric turbines is discussed.[2] These turbine systems are the most typical ones in small isolated power systems. Moreover, the impacts on power plant auxiliaries, such as pumps and fans, and on the generator are also shortly described. Finally, the principles of turbine underfrequency protection are outlined.

2-2-1 Turbine system behavior

2-2-1-1 Steam-turbines

Steam turbines comprise several stages of blades: short blades in high-pressure sections and long blades in lower pressure sections. Each blade displays several natural bending modes of oscillations with different natural frequencies. The principal risk in abnormal frequency operation of steam turbines is the vibration and probable resonance of the long blades in the lower pressures sections. Stress due to the blade vibration depends on the magnitude of the exciting forces and the structural characteristics of the blade. Blade vibrations are caused by the steam-flow variations with a fundamental frequency equal to the turbine operating speed and to harmonics (multiples) of this speed. With an increased steam flow, the magnitude of excitation increases as well. This also implies that at low load levels, stress due to blade vibration is relatively small, although there is some danger of high stress during start up.

The blade vibration principally depends on the proximity of the frequency of the excitation to the blade natural frequency and on blade damping. Resonant peak amplitude occurs when a frequency of the exciting force or some multiple of it is equal to the natural frequency of the blade. If the frequency of the exciting force approaches the natural frequency of the blade, the vibratory stress is extremely high and several hundred times greater than during normal operating conditions. The most critical blades are the long blades in the lower pressure sections of the steam turbine, usually the ones in the last three rows of the low pressure section and in some cases, the last row in the intermediate pressure section since it has been found that it is not reasonable to design theses blades to withstand the stress of a resonant condition [Kundur'94]. These blades

---

[1] For the sake of clarity, overfrequency should not be mistaken for overspeed [REE'95]. Overfrequency is a system-related phenomenon and its protection acts within a range of 51 to 52 Hz in a 50 Hz system, whereas overspeed is a turbine-related phenomenon, occurring when the turbine is tripped at full load and depending on the rotor inertia and the response of the governor. Overspeed protection is a mechanical protection situated between 65 and 70 Hz. In this sense, overspeed protection could be considered as a backup protection to the overfrequency protection. For example, if a generating unit is isolated from the power system due to overfrequency, overspeed could occur if turbine speed control fails, and the overspeed protection would trip the turbine.

[2] Since vast majority of technical literature on abnormal frequency operation of turbine-governor systems deals with 60 Hz systems, discussion and graphics are given on the basis of a 60 Hz system. The extension to a 50 Hz system can be easily accomplished.

have their natural frequency tuned so that their vibration modes will not be in resonance at normal frequency operation.

The effect of the natural frequencies of blade oscillation for different rotor speeds is illustrated in the diagram shown in Figure 2-1, known as the Campbell diagram. This diagram shows how turbine speed changes can excite the natural frequency of the blade by means of a variation in steam flow. The heavy, nearly horizontal bands represent the three natural vibration modes of a long, tuned turbine blade. These three modes correspond to a tangential mode, an axial mode and a torsional mode [Akers'68]. The diagonal lines represent the multiples of rotor speed which coincide with the frequencies of the steam-flow variations (e.g. at rated speed of 60 Hz, the second multiple is 120 Hz, the third one 180 Hz, etc.). The intersection of a diagonal line with a vibration mode band is tantamount to a resonant condition. Turbines are designed such that the natural blade frequencies fall between these multiples of rotor speed. If the rotor speed departs from rated speed, the multiples of rotor speed approach one or more of the blade natural frequency with the resulting higher vibratory stresses. The failure mechanism is related to the endurance of the material when subjected to many cycles of high stress vibrations.

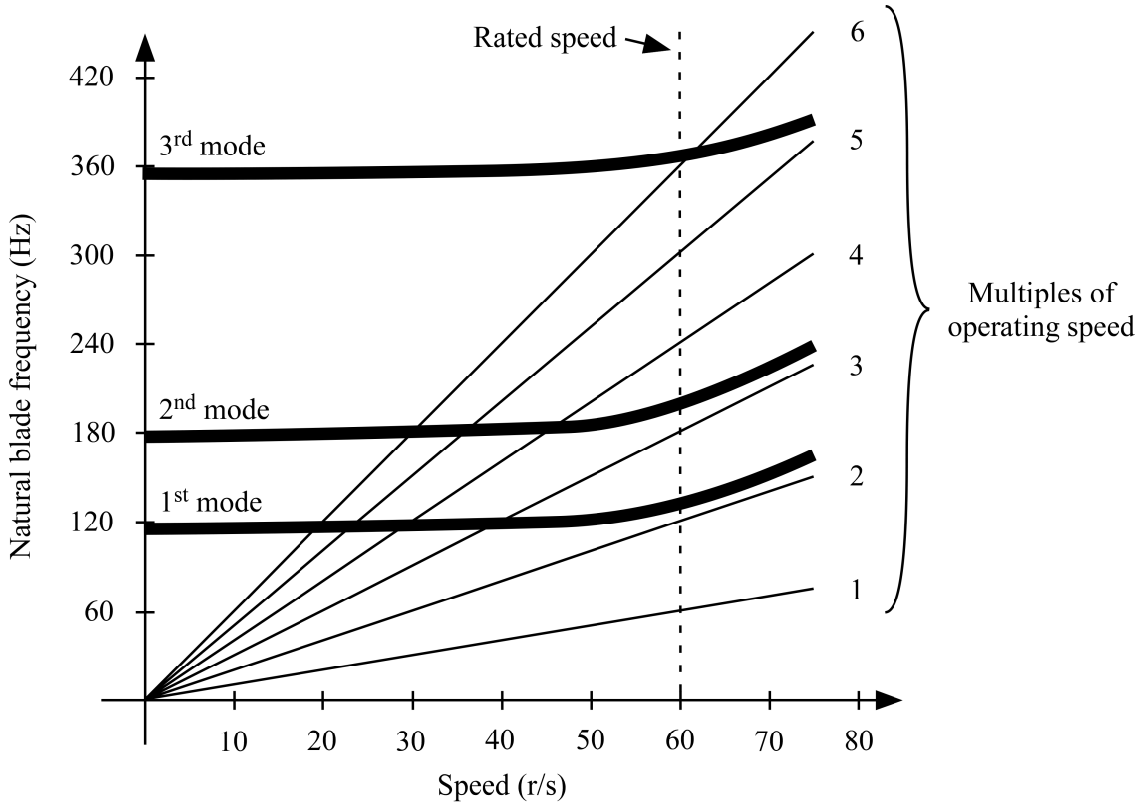

Figure 2-1: Typical Campbell diagram showing blade vibration characteristics [Kundur'94].

Operation at abnormal frequencies is time-restricted. Figure 2-2 schematically depicts the composite steam turbine abnormal-frequency limitations of several turbines built by several manufacturers. Usually, the diversity of turbine designs results in high diversity of abnormal-frequency limitation curves [IEEE'87]. According to Figure 2-2, steam turbines can continuously operate within the band of 59.5 Hz to 60.5 Hz without loss of life due to turbine blade vibrations. In the light gray area, operation of the steam turbine is limited in function of the frequency, whereas operation in the dark gray area is not recommended. For example, steam turbines might be operated at a frequency of

58.5 Hz for several minutes, but if frequency falls below 57 Hz, the generator is tripped within some seconds.

The time-restricted operation at abnormal frequency as shown in Figure 2-2 is due to the fact that the number of cycles of vibration that can be endured decreases with increasing vibratory stress (speed deviation). In other words, the effect of abnormal-frequency operation in a given frequency band is cumulative, but independent of the time accumulated in any other band associated with a vibration mode. During generating unit start up or shut down, blade life will not be significantly affected if proper procedures are followed.

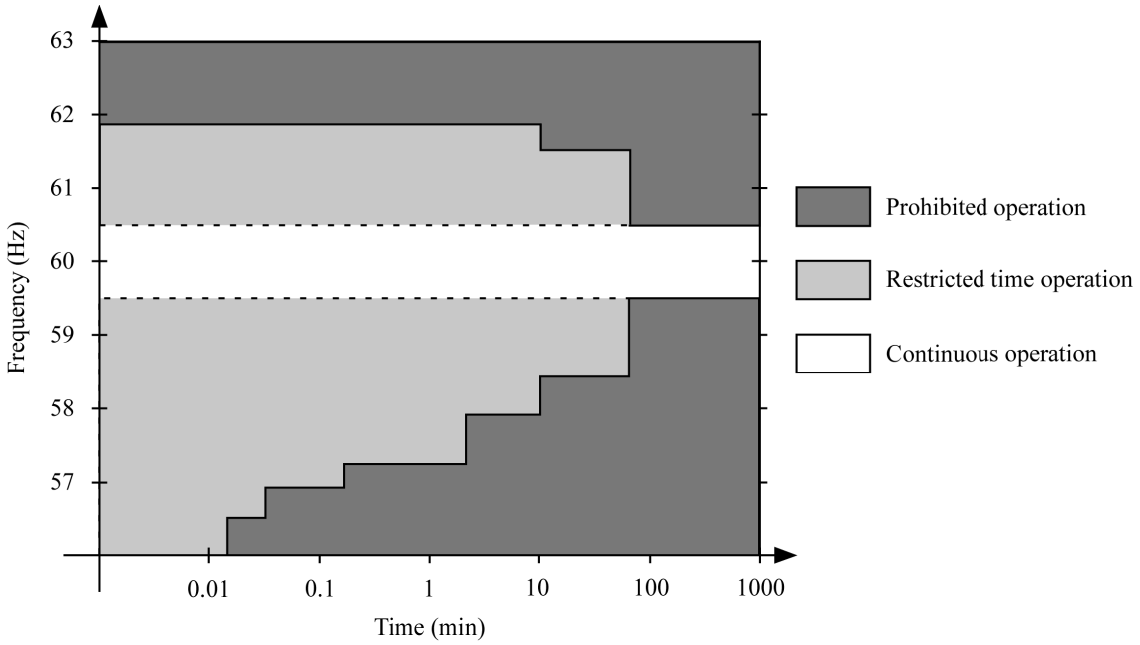

Figure 2-2: Steam turbine partial- or full-load operating limitations during abnormal frequency [IEEE'87; Kundur'94].

2-2-1-2 Combustion turbine

Combustion turbines and steam turbines behave in a similar way during abnormal frequency conditions. Combustion turbines differ from steam turbine primarily in the medium used to drive the turbine and in the fact that they contain both compressor and turbine stages. Inlet air is compressed, mixed with fuel and fed into a combustion chamber. The exhaust gases from the combustion chamber are routed through the turbine blades causing shaft rotation.

Just as in the case of steam turbines, abnormal frequency stresses both turbine blades and compressor airfoils due to vibration. Like the steam turbine, blade and airfoil vibrations are caused by variations of exhaust-gas flow (turbine stage) and variations of the airflow (compressor stage), respectively. However, there are two additional categories of airfoil vibration: flutter and rotating stall [Giampaolo'06]. Flutter denotes the self-excited vibration usually initiated by the airfoil approaching stall. Rotating stall occurs as each blade row approaches its stall limit. In fact, a blade row does not instantly or completely stall, but rather stalled cells are formed. These cells tend to rotate around the flow annulus at about half the rotor speed. Operation in this region is relatively short and usually proceeds into complete stall. Rotating stall can excite the natural frequency of the airfoils.

Stalling can be described as a disrupted or separated airflow on the airfoil shaped compressor blades resulting in a reduction in the air volume beneath the blade. Stalling is then a consequence of a too high angle of attack of the airfoil. The change in air pressure can cause deformation of the airfoils as well as reverse flow in compressor. Some combustion turbine generators have a unique operational control capability that protects the turbine generator during underfrequency conditions. These controls will automatically reduce output when an attempt is made to maintain full output during underfrequency conditions because a combustion turbine may suddenly lose airflow due to stall.

Possible blade vibrations and stalling conditions force the operation at abnormal frequencies to be time-restricted. Figure 2-3 represents the combustion turbine abnormal-frequency limitations [Butler'54; IEEE'87]. According to Figure 2-3, combustion turbines can continuously operate within the band of 58 Hz to 61 Hz without loss of life due to turbine blade vibrations or stalling conditions. In the light gray area, operation of the combustion turbine is restricted, whereas operation in the dark gray area is not recommended. For example, combustion turbines might be operated at a frequency of 64 Hz for several minutes (unlike steam turbines), but if frequency falls below 58 Hz, the generator is tripped within some seconds.

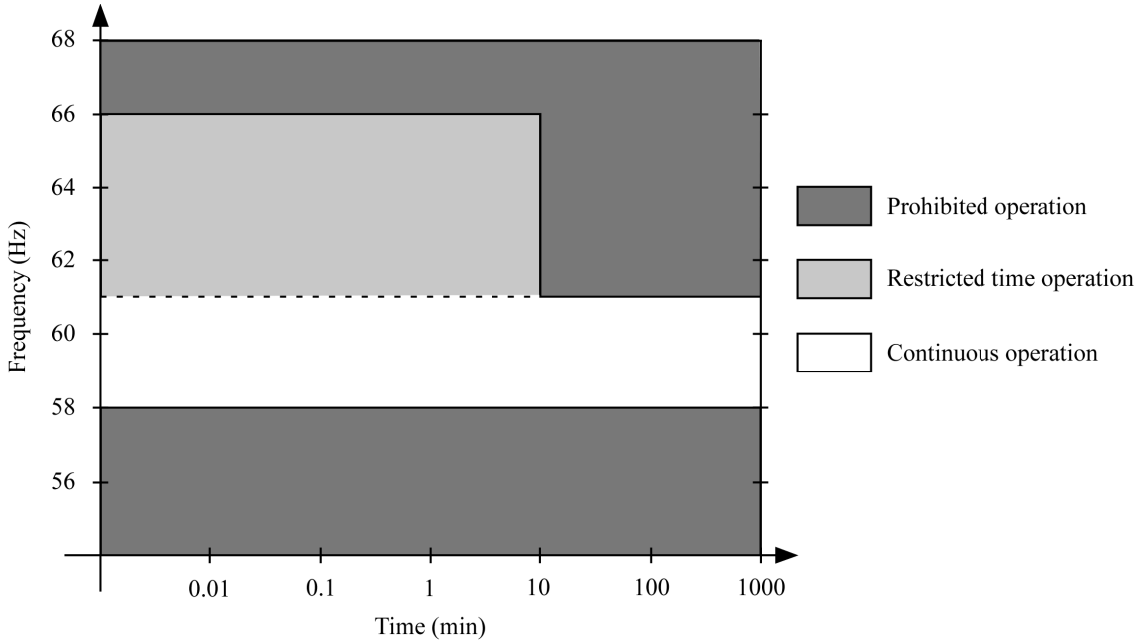

Figure 2-3: Typical combustion turbine operating limitations during abnormal frequency [IEEE'87].

In case of gas turbines and apart from vibratory stresses of turbine blades and compressor airfoils, another critical aspect needs to be considered. During low frequency operation, gas turbine output might be negatively affected by the reduced shaft speed [Kunitomi'01; Kakimoto'03]. In fact, underfrequency conditions affect compressor performance and may cause temperature control to intervene. Temperature control limits the exhaust temperature by reducing the fuel flow as the airflow decreases with shaft speed (reduced compressor performance). This reduces power output in a situation when power output should be increased.[3] By contrast, Diesel engines are less

[3] The Malaysia black-out on August 3, 1996 has been largely affected by the reduced gas turbine power output due to reduced airflow. The initial loss of generation has also been deteriorated by the fact that

sensitive to underfrequency conditions. Experiences on the Canary Islands showed that Diesel engines could withstand transitory frequency levels as low as 51.6 Hz (43 Hz on 50 Hz basis) [Rodriguez'09].

2-2-1-3 Hydraulic turbines

Hydraulic turbines can usually tolerate much larger frequency deviations than steam or combustion turbines. Underfrequency protection of the hydraulic turbine is normally not required. Generally, hydraulic turbine generators are designed to withstand more severe overspeed than steam and combustion turbines, in some cases up to 100% overspeed. This overspeed is caused by the limited closing speed of the gate in case of sudden loss of load. Thus, bucket designs are more rugged than the tapered blade designs found on other turbines. The abnormal frequency capability for continuous operation of a hydraulic turbine is generally outside of the range of 57-63 Hz [IEEE'87].

2-2-2 Behavior of power-plant auxiliaries

The ability of the steam supply system to continue operating during an extended period of underfrequency operation is a function of the margin in capacity of the auxiliary motor drives and shaft driven loads. Some pumps and fans are powered by adjustable speed drives, and can be used to withstand frequency variations. The most limiting auxiliary equipment components of steam power plants are the motor driven boiler feed pumps, circulating water pumps, condensate pumps and boiler fans since a percentage of reduction in frequency (speed) causes major percentage of loss of capacity [Dalziel'59]. Critical frequency, at which the pump and fan performance affects power output, varies from plant to plant depending on its design. Experimental results determined that plan capability starts to decrease for frequencies at 57 Hz. In general, other plant auxiliaries in fossil-fueled power plants have less influence on plant capability [IEEE'87]. For example, induced draft fans can usually operate at frequencies of 54 Hz before plant output is affected [Lokay'68].

The auxiliaries of combustion turbines and hydraulic turbines are, in general, minor loads [IEEE'87]. The output of the auxiliary loads at low frequencies does not affect the performance of theses turbines.

Apart from blade vibration, nuclear power plants are also sensitive to low frequency levels due to the reduced power output of the induction motors that drive the reactor coolant pumps. Reduced coolant flow may be detrimental to equipment and eventually, the reactor might be tripped deteriorating further the underfrequency condition.

Finally, the operating limitations at abnormal frequencies of power plant auxiliaries are less restrictive than the ones of the turbines. In fact, frequency levels for which power output of auxiliaries is affected significantly (below 57 Hz) are prohibitive for the turbine operation (see for example Figure 2-2 and Figure 2-3).

2-2-3 Generator behavior

There are two principal considerations associated with operation of synchronous generators outside of the standard frequency range: accelerated aging of mechanical components and thermal considerations [IEEE'87; IEEE'05]. However, low frequency

---

additional gas turbines tripped out due to temperature limits or flame-out when picking-up the lost generation [CIGRE'99].

operating limits of generators are less restrictive than low frequency operating limits of turbines [IEEE'95].

Low frequency levels coincident with high negative-sequence levels can excite mechanical resonances, particularly double-frequency torsional resonances of rotating components. System negative sequence provides a forcing torque on the generator rotating components at twice the system frequency of quite high magnitude (e.g. at 120 Hz for a 60 Hz system). Although the risk to operate at abnormal frequencies and in presence of a high negative sequence seems unlikely, it is a possible condition which needs to be taken into account in determining the amount of time a unit can operate beyond the continuous operating range.

A decrease in frequency also reduces cooling of the generator due to a reduce speed of rotation; therefore, operation at reduced frequency is only admissible at reduced power output [IEEE'87]. Nevertheless, this is dependent of the power-plant size [Akers'68]. The kilovolt-ampere capability of smaller power plants which have conventional cooled generators is affected by reduced voltage and thus, the kilovolt-ampere output needs to be reduced in proportion to the frequency. However, the kilovolt-ampere capability of larger power plants which have conductor-cooled generators is affected by both reduced voltage and reduced current and thus, the kilovolt-ampere output needs to be reduced in proportion to 1.5 times the reduction in frequency (e.g. 92.5 percent kilovolt-ampere for 95 percent frequency). In addition, the possibility of thermal overload of both the stator and the rotor raises, apart from the reduced cooling, because of increased loading during underfrequency conditions. Problematic is after all an extended underfrequency operation because thermal capability of a generator could be exceeded.

Finally, low frequency levels can damage the cores of both generators and transformers due to overexcitation. Overexcitation occurs whenever the ratio of Volts per Hertz (V/Hz) exceeds design limits of the equipment. However, overexcitation is usually not caused by lack of generation situations[4].

2-2-4 Turbine underfrequency protection

Abnormal frequency conditions can be divided in overfrequency and underfrequency conditions. Overfrequency is mostly due to a sudden increase of generator power or to partial load reduction. Underfrequency is directly related with a loss of power generation. Underfrequency operation of steam and combustion turbines normally poses a more critical problem than overfrequency operation since generation cannot be arbitrarily increased due to turbine-governor system limitations. Furthermore, speed governing or specific operator actions are usually effective enough in reducing the generation in case of overfrequency and thus, to bring frequency back to an acceptable value. To avoid heavy blade vibration stress, underfrequency protections must be implemented.

---

[4] In fact, the majority of overexcitation incidents are caused by generator run-up or run-down, self-excitation, overexcitation control malfunction, or by load shedding in systems supplied by overhead-lines or cables [IEEE'87; IEEE'95]. In general, generators and transformer are equipped with V/Hz relays to protect them from excessive magnetic flux density levels due to overexcitation. Additionally, a V/Hz limiter is implemented within automatic voltage regulators that limits generator field currents in order to hold the generator output voltage to a safe V/Hz value. Obviously, this control feature is only available in the automatic control mode.

Underfrequency protection can be classified into two categories: system-based UFLS schemes and turbine underfrequency protection. The former sheds specific amounts of load to restore frequency and is generally considered as an initial turbine underfrequency protection. The latter trips generating units to limit the possibility of turbine damage in underfrequency conditions and is therefore considered as the last line of protection. The major objective of turbine underfrequency protection is then the protection of equipment from damage and the prevention of accidental tripping if limiting conditions are not reached during the abnormal frequency condition [IEEE'87; IEEE'07].

To satisfy the aforementioned objectives, the design and performance of the turbine underfrequency protection should follow certain criteria [IEEE'87]. The tuning of the protection is based on the turbine abnormal frequency operation limitations. The turbine underfrequency protection needs to be coordinated with other underfrequency protections such as UFLS schemes. Certain redundancy needs to be provided to avoid accidental opening or no-operation of an underfrequency relay. Figure 2-4 illustrates the tuning of a turbine underfrequency protection [Anderson'99]. The system response in terms of frequency following an incident is plotted against the turbine cumulative damage curve and the turbine underfrequency protection. Note that the turbine cumulative damage curve represents the total life of the turbine, not the amount of damage that can be sustained in a single event, whereas the system response in terms of frequency is for only one such event. According to Figure 2-4, the turbine underfrequency protection settings are slightly higher than the turbine abnormal frequency limits (e.g., the abnormal frequency limit is 58 Hz and the protection setting is 58.2 Hz).

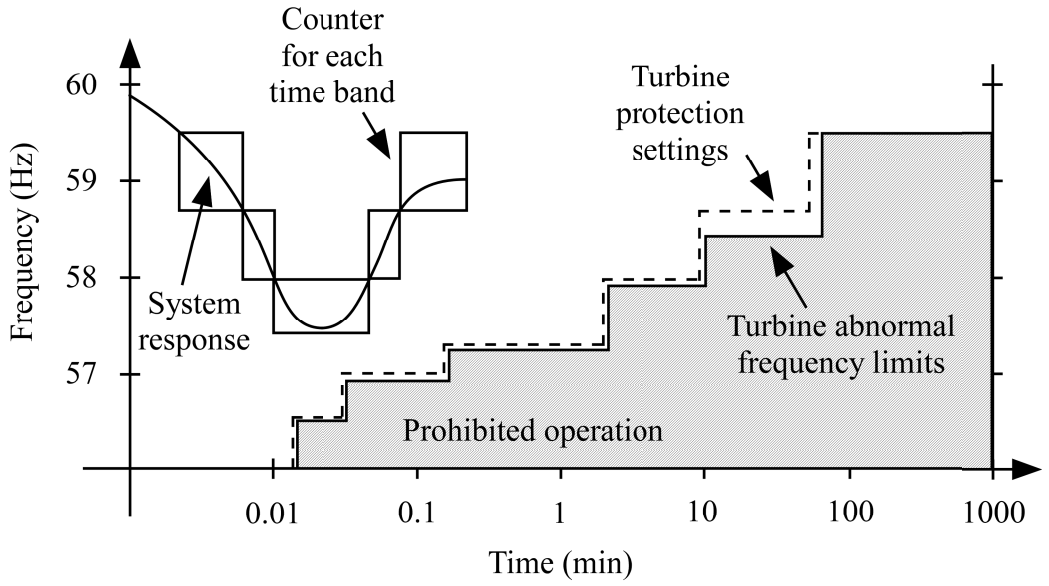

Figure 2-4: Comparison of system response in terms of frequency and turbine underfrequency protection.

The total amount of time the frequency is below the 58.2 Hz setting is about 3 s, whereas the protection setting is set for tripping the unit after about 7 minutes (420 s) totally accumulated in this band. In other words, the single excursion has not even used 1% of the total turbine life. A simple comparison between the system response and the turbine protection will ensure that the unit is not tripped due to exceeding the turbine underfrequency limits for the considered underfrequency excursion.

2-2-5 Summary

Turbine systems are most sensitive to frequency deviations. Albeit abnormal frequencies also affect power-plant auxiliaries and generators, operating limitations on abnormal frequency operation of turbine system are much more restrictive than those of auxiliaries and generators. In general, operation of 60 Hz steam turbines at frequencies below 57 Hz is restricted to some seconds, whereas hydraulic turbines can operate continuously at frequencies below 57 Hz. Operation of combustion turbines and particularly of gas turbines at frequencies below 58 Hz is restricted to some seconds. In a 50 Hz system, critical frequencies of steam and gas turbines are around 47.5 Hz and 48.3 Hz, respectively.

2-3 SURVEY ON UNDERFREQUENCY LOAD SHEDDING (UFLS)

Automatic underfrequency load-shedding (UFLS) schemes are a last-resort tool to protect the power system in case of a severe contingency [Maliszewski'71; Thalassinakis'04]. UFLS schemes provide an initial underfrequency protection for generating units which finally prevents a cascading power outage [IEEE'07]. This implies that both UFLS and turbine underfrequency protection schemes need to be coordinated. They should be simple, quick and effective to avoid possible black-outs [Concordia'95; Delfino'01].

According to the section 1-1-2, there exist different types of automatic UFLS schemes, which can be roughly classified into conventional and advanced UFLS schemes. Conventional schemes can be further differentiated in static and semi-adaptive schemes. Static schemes use only underfrequency relays, whereas semi-adaptive schemes also employ ROCOF relays [Delfino'01; Mohd Zin'04]. Advanced UFLS schemes comprise adaptive and centralized UFLS schemes[5]. Adaptive schemes principally work like their conventional counterpart, but instead of shedding a predefined amount of load at each stage, they determine the quantity of load which needs to be curtailed at each stage. The structure of centralized schemes is completely different to the one of adaptive and conventional UFLS schemes. Unless these schemes, centralized UFLS schemes lack stages and they determine and shed load in function of specific system variables such as frequency, ROCOF, voltage, power generation, etc.

A further distinction can be made with respect to the architecture of conventional and adaptive UFLS schemes [Blackburn'06; IEEE'07]. Their architecture can be local or distributed. In the case of local schemes, one or more underfrequency relays are installed on buses at a distribution substation and for an underfrequency condition, feeder breakers are tripped based on logic incorporated into the circuitry at the substations. By contrast, in the case of a distributed scheme, each feeder is equipped with its own underfrequency relay. Such schemes have grown in popularity with the availability of microprocessor-based relays.

2-3-1 Conventional UFLS schemes

Today, most of the UFLS schemes are conventional (i.e. static and/or semi-adaptive) schemes and are based upon a local or distributed architecture. Although advanced UFLS schemes improve load-shedding performances, their implementation is delayed since they require considerable data and communication facilities operating at high speeds, which is costly [Blackburn'06]. After all, for large utilities, the installation and

[5] Adaptive UFLS schemes are sometimes also called dynamic UFLS schemes.

implementation of advanced UFLS schemes would require big investments. Furthermore, the technical and technological feasibility is questionable for large power systems. Hence, utilities and energy councils such as NERC, UCTE, etc., still recommend and use conventional static and semi-adaptive UFLS schemes to protect power systems against contingencies [IEEE'07; NERC'08].

Static UFLS schemes are characterized by the fact that they only measure the frequency deviation and act according to this frequency deviation. Off-line contingency simulations determine the relay parameters and the amount to be shed. Even though UFLS schemes are very quick and simple to implement, they present disadvantages such as over- or undershedding in presence of contingencies these schemes were not designed for. For example, in case of a large disturbance, underfrequency relays may not shed enough load to stop the frequency drop and hence, to avoid a total blackout. In [Ait-Kheddache'88], the constancy property of the time delay in underfrequency relays is viewed as one of the chief causes of the overshedding or undershedding problem, which can be circumvented by ROCOF relays.

Semi-adaptive UFLS schemes present an improvement with respect to the disadvantages of static UFLS schemes [Delfino'01; Mohd Zin'04]. These schemes also measure the rate of change of frequency (ROCOF). The ROCOF threshold may be implemented in a separate step or in combination with an existing step of the static UFLS scheme. The measurement of the ROCOF enables semi-adaptive UFLS schemes to distinguish between smaller and larger disturbance. In addition, they improve the frequency response due to the fact that they shed loads earlier in case of larger disturbances. As a consequence, nowadays the majority of conventional UFLS schemes are usually a combination of both static and semi-adaptive schemes. However, the problem of overshedding still persists.

The application of ROCOF relays also presents new problems. In fact, both frequency and ROCOF are not uniform, but differ from area to area and even from bus to bus. However, the ROCOF measurement is more delicate since ROCOF is more distorted by local dynamics [Concordia'95]. The ROCOF is strongly affected by inter-machine oscillations. A possible solution is to measure the frequency close to the center of inertia [Terzija'06]. Unfortunately, the center of inertia changes with changing power-system conditions. Furthermore, the computation of the ROCOF is inexact and slow for ROCOF measurements with low frequency oscillations [Novosel'96]. In fact, low inertia values give rise to increased ROCOF oscillations and hence, decrease the computation time. However, increased oscillations lead to higher peak-to-peak values which deteriorate the precision of the ROCOF measurement. These disadvantages can be improved or using an integrated ROCOF value which is less sensitive to the ROCOF oscillations [Li'06] or measuring an average ROCOF value with respect to a time window corresponding to two consecutive threshold crossing times.

2-3-2 Principles of conventional UFLS schemes

Conventional UFLS schemes disconnect a predefined amount of load by means of underfrequency relays to reestablish the power balance between power generation and load demand. The instance of shedding depends on imposed frequency and eventually ROCOF thresholds ($\omega_{thrshld}$, $d\omega/dt_{thrshld}$) as well as intentional time delays (t_{int}). The imposed thresholds and time delay then define a stage (or step). At each stage, some percentage of the total load is shed. This fraction of load is associated to high voltage/medium voltage transformers in case of large systems or to medium voltage feeders in the case of small systems. Once the frequency has fallen below the threshold,

load is shed, if, after the intentional delay has elapsed, the frequency is still below this threshold. This is illustrated in Figure 2-5 where the imposed frequency threshold $\omega_{thrshld}$ of 48.5 Hz is crossed at time 2 s and shedding occurs after the intentional time delay t_{int} of 1 s because frequency is still below 48.5 Hz.

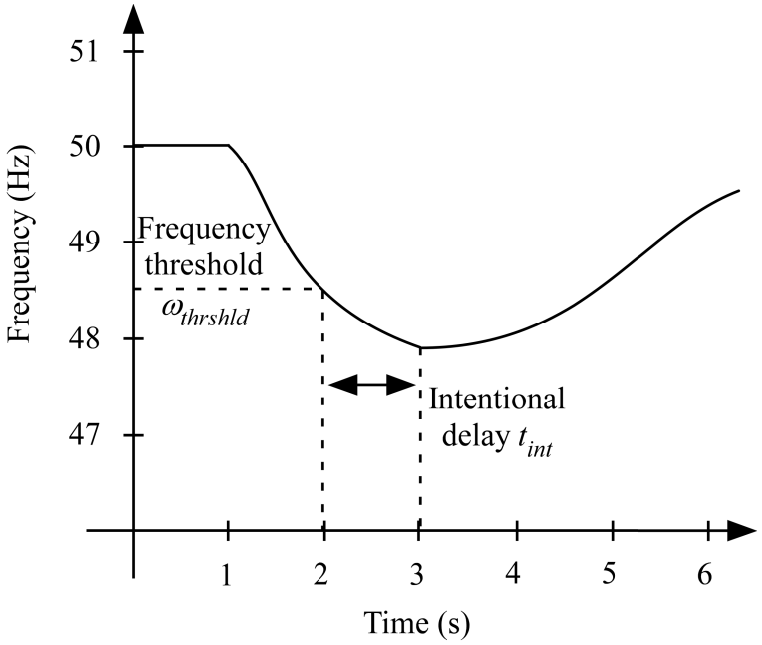

Figure 2-5: Load shedding due to the action of a conventional UFLS scheme.

Two consecutive stages can be differentiated (or coordinated) using different frequency or different intentional time delay settings [Treewittayapoom'90]. Usually, frequency and time coordination have distinct purposes. Frequency coordination is applied to stop frequency declines, whereas time coordination is used to guarantee that frequency restores to an acceptable value [Min'91]. Hence, the performance of an UFLS scheme mainly depends on the following parameters which are tuned in function of a set of disturbances [Maliszewski'71; Concordia'95]:

- Frequency and/or ROCOF thresholds
- Intentional time delay
- Amount of load under relief
- Number of steps and the corresponding step size

The first frequency threshold should not be set too high to avoid unnecessary load shedding during transients or small disturbances. The frequency thresholds should be coordinated to reduce the risk of overshedding [Treewittayapoom'90]. In addition, it is important to coordinate UFLS protection with the turbine underfrequency protection [Anderson'92; Chuvychin'96]. Frequency threshold values typically lie in the range of 49.5 to 48 Hz [IEEE'68; Lokay'68]. ROCOF threshold depends strongly on the power system considered, its inertia, etc. Values range between -1 to -2 Hz/s.

A minimum time delay is normally introduced to override transients. Earlier papers [Maliszewski'71; Concordia'95] recommend to minimize the time delay or at least, to apply them cautiously. Nevertheless, time delays may improve the UFLS performance when correctly adjusted. In fact, an intentional time delay is mostly introduced in order to avoid overshedding in less severe events while raising the frequency set point of the successive (usually the second) stage to start it earlier for more severe events [Treewittayapoom'90].

Since UFLS schemes are an emergency tool, they must be effective and not timid with respect to the amount of shed load [Concordia'95]. A sufficiently large amount of load under relief needs to be considered. The amount of load under relief is variable and depends strongly on the power system under consideration. Isolated power systems use until 80% of the total load demand whereas in interconnected systems 30-50% of the total load is under relief [IEEE'68; Concordia'95]. Loads are normally divided into critical (typically public safety and health, large industrial customer, etc.) and non-critical loads (typically residential, commercial and smaller industrial customers). Due to the priority, non-critical customers should be shed first [Horowitz'71]. In addition, distributed generation is normally tripped under underfrequency conditions and in general, the settings of the underfrequency relay associated to distributed generation are such that tripping occurs before UFLS happens. In this case, additional load should be considered for UFLS to account for the amount of tripped distributed generation [Blackburn'06].

The number of steps and the corresponding step size are also critical with respect to the performance of an UFLS scheme. Normally, three to six steps are implemented [IEEE'68; Anderson'92]. If the number of steps is increased, the risk of overshedding and the frequency overshoot are reduced, but a poorer frequency performance is obtained than with fewer steps. In other words since the step size decreases with increasing step number (the amount of load under relief is constant), less load is shed at each stage and the arrest of frequency decay might be slower than with a smaller number of steps. Furthermore, with an increasing number of steps, also the number of relays increases. However, if the settings of the steps are too close, too many steps could be involved in load shedding, causing possible overshedding because more load is shed than necessary. This makes sense since many smaller steps with very similar settings correspond somehow to one larger step with unique setting. The step size has even more influence on the UFLS performance. Typical values are 5-15% per step [IEEE'68] (see also Table 1-1 in section 1-1-3). If the step size is too large, overshedding occurs for small disturbances, whereas if the step size is too small, undershedding occurs for large disturbances. However, the implemented step size normally differs of the actual step size due to changing power-system conditions. In fact, the predefined step size associated to each step during the design process might considerably vary from the actual step size if for example a customer is offline or consumes a larger amount of energy than expected, etc. To gain some insight in the behavior of the customers and to strengthen the assumption of the step size, a statistical analysis of the historical data of the consumption could be carried out [Sigrist'10a]. To date, the impact of varying step sizes on the performance of UFLS schemes have not been studied.

2-3-3 Criteria for conventional UFLS schemes

The relay parameters are tuned such that the UFLS scheme fulfills some specified performance criteria. These criteria mainly concern frequency levels and the amount of curtailed load and are strongly related to the power system of interest. For example, small isolated power systems are more sensitive to power outages than large interconnected systems and therefore, the relay parameters of the respective UFLS schemes might differ considerably. Typical criteria for an UFLS scheme of a small isolated power system include:

- The minimum possible quantity of load should be shed [Anderson'99].

- The frequency deviation should be as small as possible. The earlier load is shed, the less is the frequency deviation [Anderson'92; Lukic'98].
- The frequency should not stay below a minimum allowable value for more than a certain amount of time. Typically, the frequency should not stay below 47.5 Hz for more than 3 s [IEEE'87; REE'05].
- The frequency overshoot should be less than a maximum allowable value (e.g. 51.5 to 52 Hz).

Additional criteria sometimes reported are:

- The post-transient steady-state frequency value should be higher than predefined value (e.g. 49.5 Hz) [Thompson'94].
- The UFLS scheme should respect the priority of the load [Blackburn'06].
- Load shedding should take place where the disturbance occurs [Prasetijo'94].

Another criterion, which can be taken into account to improve UFLS scheme performance and which has not been reported in the literature, states that no load should be shed once the frequency has passed its minimum value. By virtue of this criterion, unnecessary load shedding should be reduced.

The most important criteria are those with respect to the amount of load to be shed and with respect to minimum and maximum allowable frequency. The amount of shed load should be as small as possible provided that the system does not collapse. Obviously, for any disturbance and if sufficient spinning reserve exists, the maximum amount of load to be shed is lower than or equals the amount of lost power generation. The minimum and maximum allowable frequencies may vary from one system to the other. Large systems usually use a minimum allowable frequency of 48 Hz [UCTE'04]. In either case, older generating units may be more sensitive to frequency variation and disconnect at higher frequencies than foreseen [MITyC'06]. The criterion on the location of load shedding normally applies only for large power systems. The criterion on load shedding after the instant of minimum frequency has not been reported in the literature. However, shedding after the instant of minimum frequency is useless since frequency already starts recovering and in addition, might cause a critical frequency overshoot.[6] Finally, for the design of an UFLS scheme, criteria on minimum and maximum allowable frequency values are usually hard coded, i.e. the UFLS scheme has to fulfill them always, whereas criteria on the instant of load shedding or on the priority might be soft coded.

2-3-4 Implementation of conventional UFLS scheme

Underfrequency load shedding is accomplished by applying underfrequency relays at distribution or transmission stations where major load feeders can be controlled by automatically tripping breakers when frequency relays reach the setting threshold [IEEE'07]. Power system bus stations are often the focus of automatic UFLS schemes because they present access to tripping devices (line and feeder breakers) that supply blocks of load, and they include necessary infrastructure to support frequency-sensing relays. More recently, with the development of digital relays, even partial feeder load shedding or even individual customer load shedding can be performed.

---

[6] Note that shedding after the instant of minimum frequency only is necessary if frequency is unable to exceed the predefined post-transient steady-state frequency. This can be usually accomplished by shedding manually load.

Figure 2-6 illustrates in a simplified way the application of an underfrequency relay to a distribution feeder. The relay measures the frequency of a signal provided by the current (CT) or the voltage transformer (VT) and acts upon a circuit breaker (52) if the frequency is below the threshold. Usually, the voltage signal is preferable to a current signal [Moore'96]. In Figure 2-6 (b), the relay is presented in more detail. In fact, it consists of the underfrequency relay (81U) and the circuit breaker control circuit, formed by the circuit breaker trip coil (52TC) and the circuit breaker auxiliary contacts (52a). During normal operation, the circuit breaker and the auxiliary circuit break contacts are closed. If an underfrequency condition is detected, the underfrequency relay closes its contact that causes current to flow in the circuit breaker trip coil, tripping the circuit breaker main contacts and also the auxiliary contacts.

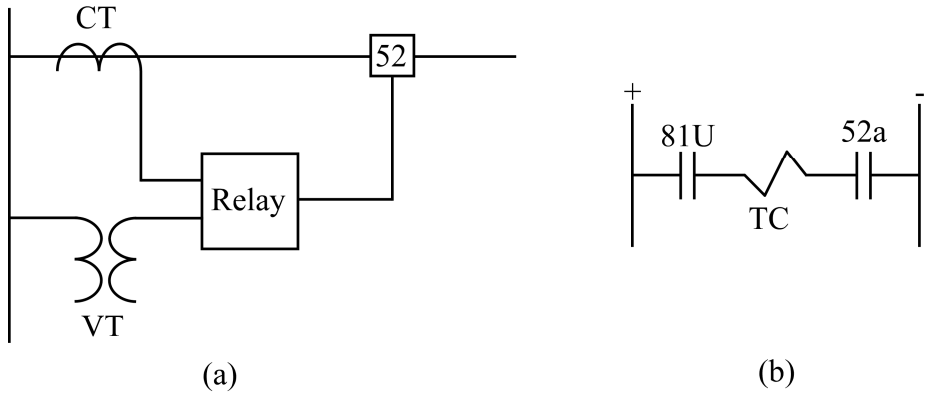

Figure 2-6: Typical relay connection and control logic of an underfrequency relay.

Underfrequency relay performance is normally supervised by some additional input signals such as voltage, current, directional power or rate of change of frequency. These input signals avoid malfunction of the relay. For example, during transient conditions (short-circuit, etc), a rate of change of frequency detector blocks tripping of the underfrequency relay for very fast frequency changes (>10 Hz/s), but permits tripping for typical power system frequency decay rates (<10 Hz/s).

The evolution of underfrequency relays has been described by three generations of equipment designs: electromechanical, solid-state and microprocessor relays [Anderson'99; IEEE'07][7]. Nowadays, after all microprocessor underfrequency relays are used since they are more versatile due to their programmable nature, the capability of self-monitoring, their adaptivity and the forward software compatibility [Anderson'99; Blackburn'06]. Microprocessor relays apply digital signal processing techniques to sampled input signal quantities. The main advantages in digital signal processing are the standards allowing exchanging data between devices of different manufacturers, the large inventory of digital signal processing software and finally, the low cost of memory.

Several frequency estimation and tracking techniques exist for microprocessor-based underfrequency relays. According to the assumption on the signal type, two groups can be identified: non-stationary and quasi-stationary signal-based techniques. The former estimate the instantaneous frequency for example by means of FIR filter

[7] The classification of underfrequency relays may vary in literature. Sometimes solid-state relays are also called static, digital or numerical relays. Similarly, microprocessor relays may be called digital relays. To avoid confusion, microprocessor-based relays are those relays of which the input signal passes through an A/D converter and is thus strictly digital.

orthogonalized input signal components or by an algorithm based on the estimation of a function related to the frequency from three samples of single-phase or three-phase voltage signals [Moore'96; Lopez'08]. Quasi-stationary signal-based techniques are more common and various estimation alternatives exist to measure frequency such as zero-crossing techniques [McLlwaine'86; Morrow'91; Backmutsky'93], least-square techniques [Sachdev'85; Pradhan'05], fast Fourier transformation based leakage techniques [Girgis'82; Ham'85], discrete Fourier transformation based phasor computation techniques [Phadke'83; Dawei'07] or Kalman filter techniques [Girgis'90; Routray'02; Chien-Hung'08].

The principal problem in frequency estimation is the presence of harmonics and noise. With an increasing application of power electronics, the presence of harmonics increases as well, corrupting the purity of the 50 Hz sine wave. The inherent simplicity of zero-crossing techniques cannot be matched by any other technique. However, zero crossing is sensitive to noise and harmonics and thus, the input signal should be filtered to reduce harmonics. Zero crossing in combination with polynomial fitting or with orthogonal components of Fourier series reduces the sensitivity to noise [Begovic'93; Duric'05]. Sliding windows increase the accuracy. Fourier transformations are inherently insensitive to harmonics but vulnerable to noise. The application of polynomial fitting with least squares method smoothes the effect of noise [Begovic'93]. Kalman filter methods seem to be insensitive to noise but not to harmonics which can be reduced by an extended Kalman filter. In general, efficient pre- and postfilters yield to suppress the effects of noise and harmonics, increasing the computation effort [Moore'96; Thomas'01]. Adequate frequency estimation occurs within 50 to 100 ms, depending on the algorithm used [Moore'96; Routray'02; Duric'05]. Thus, operating times of underfrequency relays are about 100 to 200 ms [Blackburn'06].

Several manufacturers offer microprocessor-based relays [Cooper'99; GEIndustrial'02]. Both zero crossing techniques and multiple filter functions are applied to a sampled voltage input signal. Frequency measurement of ABB's SPAF 340 underfrequency relay is based on measuring the time between zero crossings [ABB'04]. Frequency is then calculated as a moving average. Siemens' SIPROTEC 7RW600 relay measures frequency by means of various filter functions [Siemens'97], whereas Attaché's RV-UTF applies measurement techniques based on Fourier transformations [Arteche'06].

2-3-5 Advanced UFLS Schemes

Apart from conventional static and semi-adaptive UFLS schemes, also advanced UFLS schemes can be found in the literature; in particular, adaptive and centralized UFLS schemes. These schemes use additional information to compute the amount of load which needs to be shed. Advanced UFLS schemes adjust their reaction in function of the actual power-system conditions.

2-3-5-1 Adaptive UFLS schemes

Adaptive UFLS schemes use the ROCOF as an additional input signal to compute the load to be shed and to accelerate the load shedding process [Anderson'92; Thompson'94; Lukic'98; You'02; Parniani'06]. In fact, the initial ROCOF is proportional to the amount of lost power generation. Adaptivity refers then to the fact that the amount of load to be shed is computed in function of the lost power. In a further step, the computed amount of load needs to be distributed over the steps of the adaptive UFLS schemes. In general, the first step sheds half of the amount of load, whereas the

other half is distributed over the remaining steps [Anderson'92; Lukic'98]. Another way is to shed one third in the first step and two thirds in the second step [Parniani'06]. A further possibility is to distribute the amount of load uniformly over the steps [Terzija'06]. Moreover, the relay settings could be adaptively adjusted improving the UFLS performances [Chuvychin'96; Terzija'06]. For example, to protect against consecutive disturbances, the relay settings of the steps which did not actuate during the first disturbance, can be adjusted to improve the performance for a possible consecutive disturbance [Chuvychin'96].

In larger power systems, load shedding should take into account the disturbance location [Terzija'06]. In fact, due to the larger extension of the power system, frequency decay is not immediate everywhere throughout the system. Thus, shedding in a location remote to the disturbance might not alter frequency decay. Adaptive UFLS schemes permit to recollect additional information where the disturbance took place. One possibility is to analyze the voltage reduction due to the disturbance [Prasetijo'94]. Another method consists in using information provided by SCADA [Parniani'06].

Adaptive UFLS schemes need modern and sophisticated techniques [Thompson'94; Novosel'96; Parniani'06; Terzija'06]. Only the application of microcomputer-based relays, SCADA and the installation of high-speed communication allow implementing adaptive UFLS schemes. High-speed communication is important to initiate quickly load shedding in presence of a possible power imbalance. Furthermore, high-speed communication plays a central role in the transmission of SCADA data on the system status and the power-system characteristics. Microcomputers permit to implement the frequency and ROCOF measuring and computation algorithms as well as to adjust adaptively the relay settings.

However, adaptive UFLS schemes present several drawbacks. A primary disadvantage is given by the fact that adaptive UFLS schemes are based on the assumption that sophisticated techniques and high-speed communication are available [Apostolov'94]. This is normally not the case. In addition, to compute the amount of load to be shed, certain power-system parameters must be known. In general, these parameters are unknown and consequently, it is difficult to tune and reliably operate adaptive UFLS schemes [Larsson'02]. Finally, the estimation of the amount of lost power generation is based on ROCOF measurements. These measurements, as pointed out earlier, are however distorted, possibly yielding to a wrong estimation.

2-3-5-2 Centralized UFLS schemes

Centralized schemes continuously measure critical system variables such as frequency, real power generation, etc. and, in case of a contingency, act according to the actual power-system condition [Apostolov'94; Larsson'02; Shokooh'05]. A centralized system initiates the load shedding process depending on the received measurements. Measurements are carried out by means of SCADA, WAMS, and PMU etc. Centralized schemes require advanced technologies. For example, a programmable logic controller (PLC) can send specified load-shedding signals to the relays of interest [Rodríguez'05; Shokooh'05]. Underfrequency relays are usually used as backup elements [Mitchell'00b].

Early application of centralized load-shedding schemes shed a specified amount of load immediately after detection of a contingency [Nirenberg'92]. Nowadays, an substantial effort is made to minimize the amount of load to be shed according to the actual power-system condition [De Tuglie'00; Bonian'05; Sanaye-Pasand'06]. Other methods shed load such that the steady-state frequency is higher than a critical steady-

state frequency threshold or such that an uncritical ROCOF threshold is met after load shedding [Larsson'02; Rodríguez'05]. Further studies take into account the difference between power loss and system reserve or between the post-fault generation capability and the maximum amount of power which can be imported through interconnections [Apostolov'94; Shokooh'05]. In general, the feeders and the corresponding relays to shed load are selected by simple iterative methods, if the number of feeders is limited [Larsson'02], or by optimization algorithms, if the number of feeders is large [Apostolov'94; Rodríguez'05].

Centralized UFLS schemes have, apart from the ability to quickly shed an adequate amount of load, several advantages. They are able to include additional constraints on voltage and angular stability, on bus voltage levels and line flows, etc [De Tuglie'00; Bonian'05; Sanaye-Pasand'06]. In addition, load-shedding action could be applied within 0.1 to 0.3 s depending on the measurement techniques applied and the computation time required. Nevertheless, the principal drawback resides in the need for modern and fast communication infrastructure.

2-4 DESIGN OF CONVENTIONAL UFLS SCHEMES

Several methods have been reported in literature to design conventional UFLS schemes, but there exists no generally accepted systematic method for the design of UFLS schemes [Thalassinakis'04]. Power utilities adopt different approaches to this problem, which are mainly based on their experience and the robustness of the system [Concordia'95; Thalassinakis'04] and usually follow typical design criteria on the number of steps, step size, frequency thresholds, etc [IEEE'75; Anderson'92; Concordia'95; Delfino'01]. Principally, two design approaches can be distinguished to date: experimental and optimal designs. Experimental designs employ trial-error procedures or choose the best scheme of a set of candidate schemes. Optimal designs, by contrast, make use of optimization techniques to adjust the parameter settings of the UFLS schemes.

Most of the proposed methods, either experimental or optimal, are based upon simulations of the power system's dynamic behavior. These simulations evaluate the responses of the power system to a set of hypothetical disturbances[8]. In the literature, previous to the papers [Sigrist'08; Sigrist'10b], little attention has been paid to the selection of these hypothetical disturbances. Various models with distinct degrees of complexity have been reported in the literature. However, simplified models are usually employed to reduce computational cost. Recent publications also suggest the use of artificial neural networks (ANNs) to estimate frequency dynamics, avoiding time-consuming simulations [Kottick'96; Mitchell'00b].

2-4-1 Experimental design of conventional UFLS schemes

In [Lokay'68], a trial and error procedure is outlined. The procedure is applied for a hypothetical maximum overload situation and is somehow similar to the one outlined in section 2-2-4. First the amount of load to be shed is estimated and subsequently, the number of steps and the step size. The choice of the number of steps and the step size is

[8] Apart from response-based design methods, there also exist event-base methods [Seyedi'09]. In this case, the decision of shedding load is based on the state of specific elements in the system such as important transmission lines or generators. This method usually requires a communication link to transmit the information to the relays. However, event-based methods are rather applied to restoration problems and their design is addressed by load-flow computations [Subramanian'71; Mostafa'97; Seyedi'06].

still rather arbitrary and mainly depends on the utility's experience. Initially, frequency thresholds are determined such that the difference between two consecutive thresholds is somehow proportional to the step size, with the first step at about 49.5 Hz. Then, coordination between steps is checked one by one considering an overload that would lead the frequency to settling out at the frequency threshold of the following step. This process is repeated until the coordination between each step and between the UFLS scheme and the turbine underfrequency protection is guaranteed. For a different set of initial frequency threshold values, better final results might be obtained. During the design process, time delays are maintained constant. An improved and automated version of this trial and error procedure is described in [Jones'88]. In fact, the major difference consists in calculating the frequency threshold of a given load-shedding step instead of an initial estimation as in [Lokay'68], using the frequency at which the previous step actuated.

In [Concordia'95], the design of UFLS schemes is based upon a screening process. The design consists then in determining the best scheme of a set of manually selected candidate UFLS schemes. Candidate schemes are subjected to low, medium and large generation losses for low, medium high load-demand levels. The performance of each UFLS scheme is evaluated by means of some statistical measures of the minimum frequency deviation, the post-shedding steady-state frequency, etc. No consideration has been given to a possible reduction of the amount of load to be shed. Instead several experiments have been carried out with extending time delays for final stages. During the screening process, a lumped model and simplified grid model are consecutively applied to explore and test various UFLS schemes. A full transient-stability model is finally used to determine and verify the most efficient scheme. The experiments with extended time delays showed that less load could be shed for some scenarios while increasing minimum frequency deviations.

Monte-Carlo simulations have also been applied to the problem of UFLS scheme design [Thalassinakis'04; Shrestha'05]. In [Thalassinakis'04], a linear system frequency dynamics model has been used to represent the power system. Failure events of generating units have been modeled by exponential distributions. The selection of the UFLS scheme is made using computed probabilistic indices. Similar to [Concordia'95], the design consists rather in determining the best UFLS scheme of a set of different candidate schemes than in readjusting the UFLS scheme parameters. The different candidate schemes are created manually by either changing the number of steps or by changing at least one parameter. An improvement over this method consists in the combination of artificial neural networks (ANN) and Monte-Carlo simulations to select the appropriate UFLS scheme [Thalassinakis'06]. This method can be applied to both static and semi-adaptive UFLS schemes. The necessary patterns to train the ANNs are obtained from the Monte-Carlo simulation. These patterns are formed by frequency response and load-shedding indices, which coincide with the typical UFLS design criteria. A large set of possible UFLS scheme candidates is randomly obtained and evaluated by Monte-Carlo simulations, giving rise to the aforementioned indices. The ANNs define then the appropriate setting of the UFLS scheme parameters, i.e. frequency thresholds, ROCOF thresholds, time delays and step size on the base of these patterns. However, the method is restricted to maximally three steps. In [Shrestha'05], a very simple procedure is outlined which combines static UFLS schemes designed for specified outages using the probabilistic indices of these outages. Frequency threshold settings and step sizes correspond then to the weighted average of the settings adjusted for each individual outage, assuming known time delays. Frequency dynamics are modeled only through the load-damping factor. Again, knowing the forced outage rate

of generators (failure probability of generating units), Monte-Carlo simulations are applied to evaluate the performance of the proposed UFLS scheme. Note that for small outages with high probabilities, this procedure might lead to UFLS schemes unable to arrest frequency in case of large outages.

A slightly different approach evaluates the UFLS scheme by means of cost-benefit analysis [Cheng'03]. Again, the design is based upon a screening process. The selected scheme is the one with least total cost including costs due to load shedding and due to available spinning reserve. In other words, the resulting scheme is the one which sheds the lowest amount of load of all candidate schemes and which has the lowest probability of load shedding.

The preceding review of experimental UFLS scheme designs confirms the existence of multiple design approaches adjusting distinct UFLS scheme parameters. Which parameters need to be adjusted also depends whether a static or a semi-adaptive UFLS scheme is considered. A generally accepted, systematic method does not exist. Furthermore, an optimal UFLS scheme performance in terms of the amount of shed load is difficult to guarantee. An attractive alternative to these designs is to optimize existing conventional UFLS schemes. The parameters of the UFLS schemes are tuned such that an objective function is optimized with respect to previously selected operating and contingency scenarios. In the literature, several optimization strategies have been pursued and applied to the design of UFLS schemes (e.g. [Lopes'00; Denis Lee Hau'06]). For the sake of completeness, one must add that the use of optimization strategies for the design of UFLS schemes has been criticized [Concordia'95] arguing that the main objective of an UFLS scheme is to protect and save a power system. However, adequate constraints permit to obtain an optimal UFLS scheme without jeopardizing power system safety.

2-4-2 Optimal design of conventional UFLS schemes

The main objective of an optimal UFLS scheme is to minimize the amount of shed load. Deterministic algorithms such as steepest descent and quasi-Newton methods, have been applied to solve the optimization problem [Jenkins'83; Halevi'93; Denis Lee Hau'06].

In [Jenkins'83] and [Halevi'93], only static UFLS schemes are treated, whereas in [Denis Lee Hau'06] also semi-adaptive UFLS schemes can be implemented. In [Jenkins'83] a simplified second-order linear model of the power system is used. The frequency-dependency of loads has been modeled, too. It is assumed that the frequency thresholds are known and therefore, neglecting time delays, only the amount of load at each step is optimized by means of Newton’s method such that the amount of shed load is minimal. A non-linear, lumped power-system model is used in [Halevi'93] to minimize the amount of shed load and overall frequency deviation. In addition, the optimization algorithm takes into account a set of credible contingencies depending on different operating points and disturbance magnitudes. Further, design criteria have been introduced as constraints to the optimization problem, too. Like in [Jenkins'83], it assumed that the frequency thresholds are known and, even if the application to optimal time delays is stated, only the amount of load at each step has been optimized using the gradient-projection method. Finally, in [Denis Lee Hau'06] an analytical system frequency dynamics model incorporating a UFLS scheme has been presented to derive closed-form expressions of the load-frequency response, including the effect of the UFLS scheme. In contrast to [Jenkins'83] and [Halevi'93], each generator of the power system is modeled by a first-order linear model. It should be also noted that intentional

time delays of the UFLS scheme have been implemented as simple delays assuming that these time delays are small and that a step will actuate once frequency has fallen bellow its threshold. Obviously, this assumption is not always true and a step might not act since frequency has recovered before the time delay has elapsed. The optimization problem includes, like in [Halevi'93], design criteria as constraints and takes into account the possibility of a range of contingencies. In addition, all UFLS scheme parameters, i.e. number of steps, frequency thresholds, time delay and step size, are optimized to minimize both amount of shed load and minimum frequency deviation. Contemplating all UFLS scheme parameters during the design process makes the problem in general more complex, but it allows finding a more efficient solution than when optimizing uniquely the step size.

However, a substantial drawback of deterministic algorithms lies in the fact that they may get caught in local minima. The optimal solution is therefore highly dependent on the initial guess of the decision variables as indicated in [Denis Lee Hau'06]. Furthermore, the assumption of linear generator models is not very realistic. At least, the limitations of the primary reserve need to be taken into account. Similarly, the applicability of a lumped power-system model is questionable for power systems with diverse generation mix. Due to the problem's non-linear (generator models) and discontinuous (UFLS scheme) nature, heuristic algorithms seem to be more adequate [Lopes'99; Denis Lee Hau'06].

In [Lopes'99], the use of genetic algorithms (GA) is discussed. A similar approach is proposed in [Mitchell'00a; Mitchell'00b], where ANNs are combined with GA to identify optimal shedding levels of a simple single-stage UFLS scheme. The ANN is used to estimate the frequency dynamics, whereas a GA should optimize the performance of the UFLS scheme in real time. Solely the step size of the single-stage UFLS scheme is optimized, whereas frequency threshold and time delays remain constant, as in [Jenkins'83] and [Halevi'93]. Finally, in [Martínez'93], the adequate load shedding is also determined via GA for some hypothetical contingencies. The power system is modeled by an equivalent generator. For every hypothetical contingency, an optimal UFLS scheme is designed, ideally in real time, taking into account typical design criteria. Decision variables are the frequency thresholds and the corresponding step sizes. It is however not clear how the UFLS scheme and its impact on the power system are evaluated.

2-4-3 Operating and contingency scenario selection

To design an efficient UFLS scheme, different operating and contingency scenarios need to be considered to guarantee the robustness of the approach. An operating and contingency scenario is defined as a particular disturbance for a particular system operating condition. In general, the tuning is such that the UFLS scheme protects the power system against the maximum disturbance [Lokay'68; Anderson'92; Thompson'94]. However, the design taking into account only the maximum disturbance may cause overshedding for smaller, less critical disturbances. On the contrary, if the scheme has been designed for smaller disturbances, it may not shed sufficient load to avoid a system collapse in the case of a large disturbance. Thus, it is crucial to select credible, appropriate operating and contingency scenarios [Lokay'68; Concordia'95].

In general, many contingency scenarios under many power-system conditions can be considered (line tripping, generation outages, etc). In large interconnected power systems, an underfrequency condition is usually caused by system separation into islands because of line tripping. By contrast, in small isolated power systems, outages of

generating units lead to pronounced frequency deviations since any individual generating unit in-feed presents a substantial portion of the total demand; therefore, only generator outages are usually considered as contingency scenarios for isolated power systems [Concordia'95]. However, it is computationally not very efficient or even impossible to design an UFLS scheme for all possible generator outages and for all power-system conditions.

Traditionally, after a major disturbance, settings of protection devices and control actions are revised and possibly readjusted to enable the system to withstand the same disturbance next time [Jung'02]. The principal drawback of a design based on a worst-case scenario is the possibly poor performance of the UFLS scheme for less severe disturbances. In [Denis Lee Hau'06], four different contingency scenarios of distinct severity have been considered. However, severity alone is not sufficient since other factors such as available spinning reserve, system inertia or generation mix, all dependent on the operating point, influence the system response as well. This can be resolved selecting an appropriate set of possible operating and contingency scenarios since the power system may behave in the same way for different operating and contingency scenarios. A common practice is therefore to determine the system conditions corresponding to different load-demand levels (e.g. minimum and maximum) and to design the UFLS scheme taking into account the outages of the largest, the smallest and eventually a medium-size generator for each of these system conditions [Thompson'94; Concordia'95]. Nevertheless, this kind of scenario selection does not necessarily guarantee a selection of representative scenarios, i.e. those scenarios which resume best the patterns in frequency dynamics due to power imbalances. For example, it is possible that only smaller and very large disturbances, in terms of relative power imbalance, are considered, whereas medium-size disturbances are neglected, decreasing the robustness of the resulting UFLS scheme.

2-4-4 Summary of design methods of conventional UFLS schemes

Table 2-1 shows a summary of the most relevant methods for the design of conventional UFLS scheme described in the literature. Different methods consider different UFLS parameters as decision variables. The mark corresponding to the tuning of the intentional time delays for the method presented in [Denis Lee Hau'06] is between parentheses since this intentional time delay has been simply modeled as a delay, neglecting its time-dependent character. Some methods are based upon trial and error or screening processes, others use different optimization algorithms. Mostly linear SFD or lumped models are used. Interrogation points denote that authors did not clarify what kind of model has been used. However, it can be supposed that an ANN-GA-based method as proposed in [Mitchell'00b] makes use of a detailed power-system model, whereas in [Martínez'93] the reference to an equivalent generator model suggest the use of a lumped model.

Thus, according to the résumé given in Table 2-1 and compared to the dissertation's objectives (see also section 1-2), there exists no design method based upon a non-linear multi-generator SFD model. The basic idea of SFD models is to provide low-order models that retain the essential frequency dynamics of the original systems. Further, no design method makes uses of Simulate Annealing or any other heuristics to tune all UFLS scheme parameters. In fact, a partial, more industry-oriented optimization strategy, which uniquely adjusts frequency and ROCOF thresholds and intentional time delays, as well as a complete optimization strategy, which also adjusts step size, will be pursued. Mostly, the partial strategy is applied since in small power systems, it is difficult to find feeder blocks that finally sum up to a desired step size (i.e., determined

by a complete strategy). It can also be inferred from Table 2-1 that the application of Data Mining techniques to the problem of operating and contingency scenario selection, which has attracted less attention in the literature, is also unique. In addition, the problem of varying design conditions and varying step sizes has not been addressed so far. Finally, the impact of decoupled power generation, either wind or solar power, on the design of UFLS schemes has not been considered.

Table 2-1: Résumé of conventional UFLS scheme designs.

		References									
		[Lokay'68]	[Concordia'95]	[Thalassinakis'04]	[Thalassinakis'06]	[Jenkins'83]	[Halevi'93]	[Denis Lee Hau'06]	[Mitchell'00b]	[Martínez'93]	Dissertation
Model	Linear SFD	**X**		**X**	**X**	**X**		**X**			
	Lumped		**X**				**X**			**?**	
	Detailed		**X**						**?**		
	Non-linear SFD										**X**
Experimental	Trial & error	**X**									
	Screening		**X**	**X**							
	ANN				**X**						
Optimal	Newton					**X**					
	Projected gradient						**X**				
	quasi-Newton							**X**			
	GA								**X**	**X**	
	SA										**X**
Decision variables	$\omega_{thrshld}$	**X**	**X**	**X**	**X**			**X**	**X**	**X**	**X**
	t_{int}		**X**	**X**	**X**			**(X)**			**X**
	$d\omega/dt_{thrshld}$			**X**	**X**			**X**			**X**
	p_{step}	**X**	**X**	**X**	**X**	**X**	**X**	**X**	**X**	**X**	**X**
Disturbances	Maximum	**X**									
	Common practice		**X**								
	Severity							**X**			
	Monte Carlo			**X**	**X**						
	Representative										**X**
Objective	Σpshd					**X**				**X**	
	$\Sigma(\Delta\omega min + pshd)$							**X**	**X**		
	$\Sigma(\int\Delta\omega(t)dt + pshd)$						**X**				

?: not clearly defined

(X): not actual parameter (see section 2-4-2)

2-5 SUMMARY

This chapter has reviewed the impact of abnormal frequency operation on power-system equipment and automatic UFLS schemes. Precisely, the principles, performances criteria and implementation of conventional UFLS schemes have been detailed. Advanced UFLS schemes have also been briefly exposed. Finally, a survey on the design of conventional UFLS scheme has been given.

Abnormal frequency operation not only affects turbine-governor systems but also generators and transformers, but turbine-governor systems are more sensitive to frequency deviations. Furthermore, the underfrequency condition is more critical than the overfrequency condition. This chapter reviewed the impact of underfrequency condition on several, for small isolated power system typical turbine systems. In particular, steam turbines, combustion engines and hydraulic turbines have been considered. The principal problem of underfrequency condition is the excitation of resonant conditions of mechanical components such as turbine blades and compressor airfoils of steam turbines and combustion engines, respectively. Hydraulic generators are far less sensitive to underfrequency conditions. Further problems arise due to reduced output of power-plan auxiliaries such as fans and pumps which reduce the power generation further and may cause thermal overload.

To protect generating units against low frequency levels, underfrequency relays are used. Turbine underfrequency protection trips generating units to limit the possibility of turbine damage in underfrequency conditions and is therefore considered as the last line of protection. The major objective of turbine underfrequency protection is then the protection of equipment from damage and the prevention of accidental tripping if limiting conditions are not reached during the abnormal frequency condition. However, if no additional counter-measure exists, pronounced frequency deviations may then cause to trip generating units due to underfrequency protection, which accelerates the frequency decay further and may result in a system blackout.

UFLS schemes are implemented to avoid black outs. These schemes shed load to restore the power equilibrium and to arrest frequency decay. UFLS can thus be considered as the initial turbine underfrequency protection. UFLS scheme can be grouped in conventional and advanced UFLS schemes. Main attention is paid to conventional UFLS schemes. They principally shed a predefined amount of load at a specified frequency threshold. Some performance criteria such as, for example, minimum and maximum allowable frequency values or criteria on the amount of load to be shed are considered for the design of UFLS schemes. UFLS schemes are implemented, on the majority, by means of microprocessor-based underfrequency and rate of change of frequency relays.

In the literature, several methods have been reported to design conventional UFLS schemes. Some are based on iterative adjusting methods; others apply optimization algorithms to the design of existing UFLS schemes. The main objective of an optimal UFLS scheme is to minimize the amount of shed load taking into account different constraints focusing on the system stability and the UFLS scheme performance. Different types of optimization algorithms such quasi-Newton based algorithms or Genetic Algorithms have been used. However, independent of the design method applied, the tuning of the UFLS parameters is based on a set of hypothetical disturbances. The adequate selection of these disturbances guarantees a robust UFLS scheme. The selection of these disturbances, however, has attracted less attention in the literature. The common practice of disturbance selection does not necessarily guarantee an adequate selection.

Finally, this chapter also reviewed advanced UFLS schemes. Advanced UFLS schemes are grouped into adaptive and centralized schemes. The former maintains the structure of a conventional UFLS scheme but determines the amount of load to be shed adaptively, i.e. in function of the power imbalance which is estimated by the initial rate of change of frequency. Centralized schemes continuously measure critical system variables such as frequency, real power generation, etc. and, in case of a contingency,

act according to the actual power-system condition. Measurements are carried out by means of SCADA, WAMS, and PMU etc. Although advanced UFLS schemes improve load-shedding performances, their implementation is delayed since they require considerable data and communication facilities operating at high speeds, which is costly.

CHAPTER THREE

MODELING AND SIMULATION OF SMALL ISOLATED POWER SYSTEMS

3-1 INTRODUCTION

Power systems are highly complex systems consisting of many individual elements. The interconnections between these elements give rise to a large set of possible dynamic interactions. Normally, power-system dynamics are divided into four groups: wave, electromagnetic, electromechanical and thermodynamic phenomena. Short-term frequency dynamics are generally classified as slower electromechanical phenomena. In fact, rotor dynamics still play an important role in short-term frequency dynamics, but the dynamics associated to the turbine-governor system influence to a much greater extent [Machowski'97].

The classification of power-system dynamics is closely related to the location in the power system where these dynamics originate. The origin of the power-system dynamics in turn influences the modeling detail of the involved elements [Machowski'97]. Short-term frequency dynamics, for example, are mainly affected by the generator rotor and the turbine-governor system and primarily, these elements need to be represented. However, modeling of generating units also depends on other factors such as the problem statement or the time horizon considered. For example, short-term frequency dynamics studies assume lumped turbine-generator inertias, whereas for the analysis of subsynchronous oscillations, a more detailed turbine-generator shaft model must be considered. Or, boiler models, with time constants of hundreds of seconds, are not represented for studies of short-term frequency dynamics with a time range of several seconds, in contrast to long-term frequency dynamics.

In this chapter, a suitable power-system model is obtained to analyze short-term frequency stability in small isolated power systems. This model should be sufficiently simple to reduce computational cost but still accurate enough to reflect short-term frequency dynamics since many simulations need to be run to design a UFLS scheme as will be shown in chapter 4. In section 3-2, it will be shown that for short-term frequency stability analysis, it is possible to represent the generating units by their turbine-governor systems and the power system by a single bus assuming constant loads. At the

same time it will be shown that frequency can be assumed uniform, i.e., inter-machine oscillations can be neglected. In section 3-3, the complexity of the generating unit models is further reduced assuming that the turbine-governor system can be represented by a non-linear first-order or second-order model including generator output limitations. Parameter estimation of these non-linear first-order or second-order models is addressed in section 3-4. These considerations merge into a non-linear multi-generator system frequency dynamics (SFD) model presented in section 3-5. The basic idea of SFD models is to provide low-order models that retain the essential frequency dynamics of the original systems. Finally, section 3-6 outlines the numerical integration method to simulate this power-system model, whereas in section 3-7, the SFD model is used to study the influence of the different model parameters, including the UFLS scheme, on short-term frequency dynamics and on frequency stability. This also includes an analysis of the impact of decoupled power generation on frequency stability. A toolbox based on Matlab has been developed to run the simulations of single and/or multiple outages. In the appendix A, the main features of the prototype of the toolbox are outlined.

3-2 A SIMPLIFIED POWER-SYSTEM MODEL

In this section, it will be shown that for the purpose of short-term frequency dynamics analysis, the power system can be modeled by a simplified model. This model assumes that all generating units and loads are connected to a single bus, neglecting therefore the network. Inter-machine oscillations are also neglected, resulting in uniform frequency. In the case of two isolated power systems connected by a tie line and depending on the disturbance, this assumption reduces the accuracy of the model. Furthermore, generating units are represented by their turbine-governor systems. Finally, loads are voltage and frequency independent and thus constant. In addition, for large and possibly interconnected systems, the large amount of system inertia slows down frequency dynamics and secondary control systems should be considered as well.

The response of a power system to a power imbalance can be described in four stages [Machowski'97]. The transition between these stages is smooth and a real distinction does not exist, but this differentiation helps studying and determining the principal elements participating in frequency dynamics. Figure 3-1 illustrates these four stages.

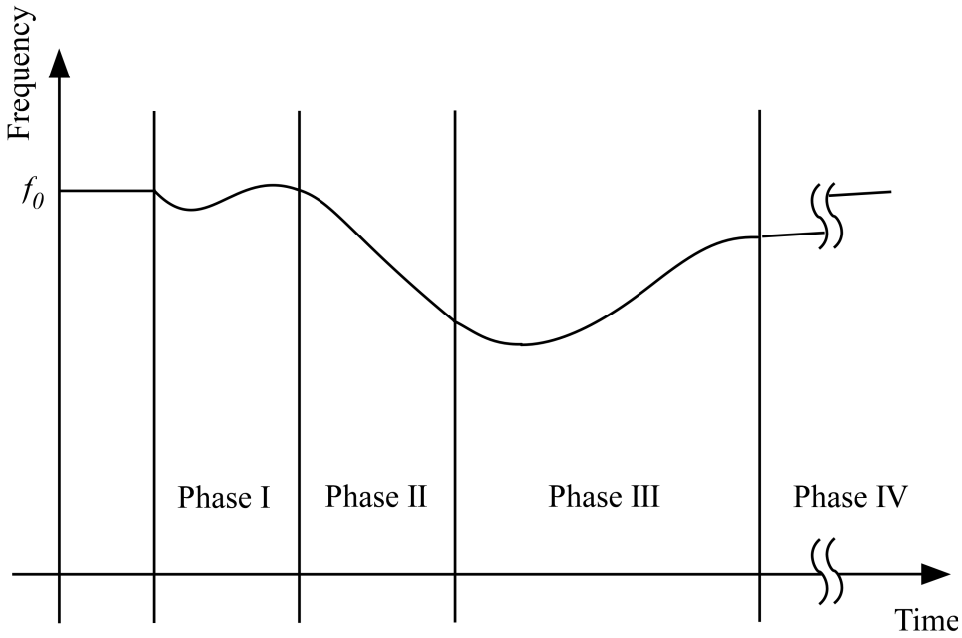

Figure 3-1: Four stages of frequency dynamics.

In the first stage, during the first few seconds, the system's behavior is dominated by rotor swings due to rotor angle oscillations. The share of each generator in meeting the power loss depends on its electrical distance to the disturbance. The following two stages lasting from a few seconds to several seconds consecutively describe the frequency drop (with constant rate of change of frequency) and the action of the turbine-governor system. In fact, it has been tacitly supposed that generators remain in synchronism during the first stage. Thus, after the first stage, the power imbalance instigates an increase or a decrease in frequency depending whether load or generation has been lost. During the second stage, frequency increases or decreases with a constant slope since still no primary frequency control action takes place. The participation of each generator during this stage depends on its inertia. The lower the inertia, the faster is the frequency decay or its increase. Subsequent to the second stage, primary controls of turbine-governor systems intervene and try to balance power generation and load demand. Turbine-governor systems provide a means of controlling power and frequency. The contribution of each generator is basically a function of its governor speed drop, the speediness of the turbine-governor system response and the amount of available spinning reserve. In fact, the amount of available spinning reserve is not unlimited which might have a destabilizing effect on short-term frequency dynamics. Finally, within a time frame of one or several minutes, secondary control action and energy supply system dynamics prevail in frequency dynamics.

Short-term frequency dynamics are affected by the aforementioned first three stages, i.e. by the rotor swings, the inertial response and the turbine-governor system response. Figure 3-2 portrays the functional relationship between the elements involved in short-term frequency dynamics. The principal elements involved are the turbine-governor system, the generator and particularly its inertia and the electrical system including other generators units, loads, etc. Secondary control system and the energy supply system do not intervene in short-term frequency dynamics for being too slow and are therefore neglected [Chan'72; Anderson'99].

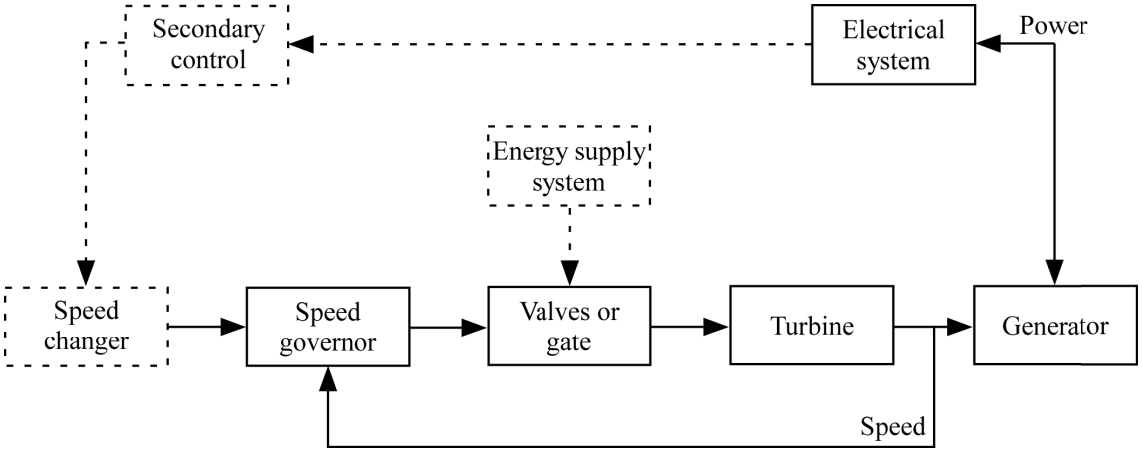

Figure 3-2: Elements involved in short-term frequency dynamics.

As a consequence, it seems reasonable to assume that short-term frequency dynamics are mainly affected by the turbine-governor system and the generating unit's inertia. Consequently, for short-term frequency stability analysis, generators could be represented by their turbine-governor systems. Moreover, when short-term frequency stability phenomena are studied, the models of the excitation system and the synchronous machine can also be neglected since their associated dynamics are usually too fast and therefore, hardly influence the response of the generating unit. Even if voltage is affected by the loss of a generating unit, the response of the excitation systems of the remaining generating units restores voltage in a relative short time to its prefault value (compared to turbine-governor systems) [Elgerd'82]. In addition, as seen in chapter 2, frequency dynamics influence to much lower extent generators, transformers or excitation systems. Finally, for small isolated power systems, it is possible to neglect the transmission network and to assume uniform frequency. Loads can be considered voltage and frequency independent.

3-2-1 Representation of generating units by their turbine-governor systems

The assumption that the generator can be represented by its turbine-governor system is verified by considering for small isolated power systems typical turbine-governor systems. In particular, Diesel engines, gas turbines and steam turbines are analyzed.

For this purpose, generating unit responses to a step at the governor reference are compared with the responses to an equivalent rise in load power. The response to a rise in load power involves the dynamics of the turbine-governor system, the excitation system and the synchronous machine, whereas by applying a step at the governor reference, only dynamics of the turbine-governor system and the rotor are decisive. By comparing the responses to a step at the governor reference and to an equivalent rise in load power, it can be shown that turbine-governor systems mainly affect short-term frequency dynamics. These responses are simulated by means of PSS/E software package. Figure 3-3 shows the test system used to simulate the response to a rise in load power by closing the breaker between buses 2 and 4. The responses to a step at the governor reference are obtained by using GRUN activity of PSS/E.

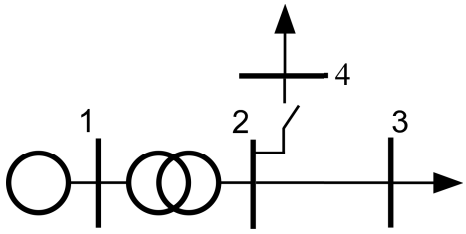

Figure 3-3: Test system used to simulate a rise in load power (bus 4).

For this problem, turbine-governor systems are represented by commonly used standard models from the PSS/E software package model-library [Siemens'05b]. In other words:

- Diesel-based turbine-governor systems are modeled by the DEGOV1 model.
- Gas-based turbine-governor systems are modeled by the GAST2A or the GASTWD model.
- Steam-based turbine-governor systems are modeled by the IEEEG1 model.

The block diagrams of these four turbine-governor system models are shown in the appendix C.

Figure 3-4 shows and compares the simulated responses to a rise in load power and to a step at reference of the turbine-governor system. The simulations have been carried out using PSS/E software package. A low initial power of 0.4 pu has been chosen to avoid interferences with saturation and to ease the comparison. Obviously, for higher initial values, saturation intervenes and distorts the response. Step in load power has been applied at $t = 1\ s$. From Figure 3-4, it can be inferred that there exists only a negligible difference between the model of the full generating unit and the detailed model of the turbine-governor-rotor system. Hence, the generators can be fully represented by the associated turbine-governor system.

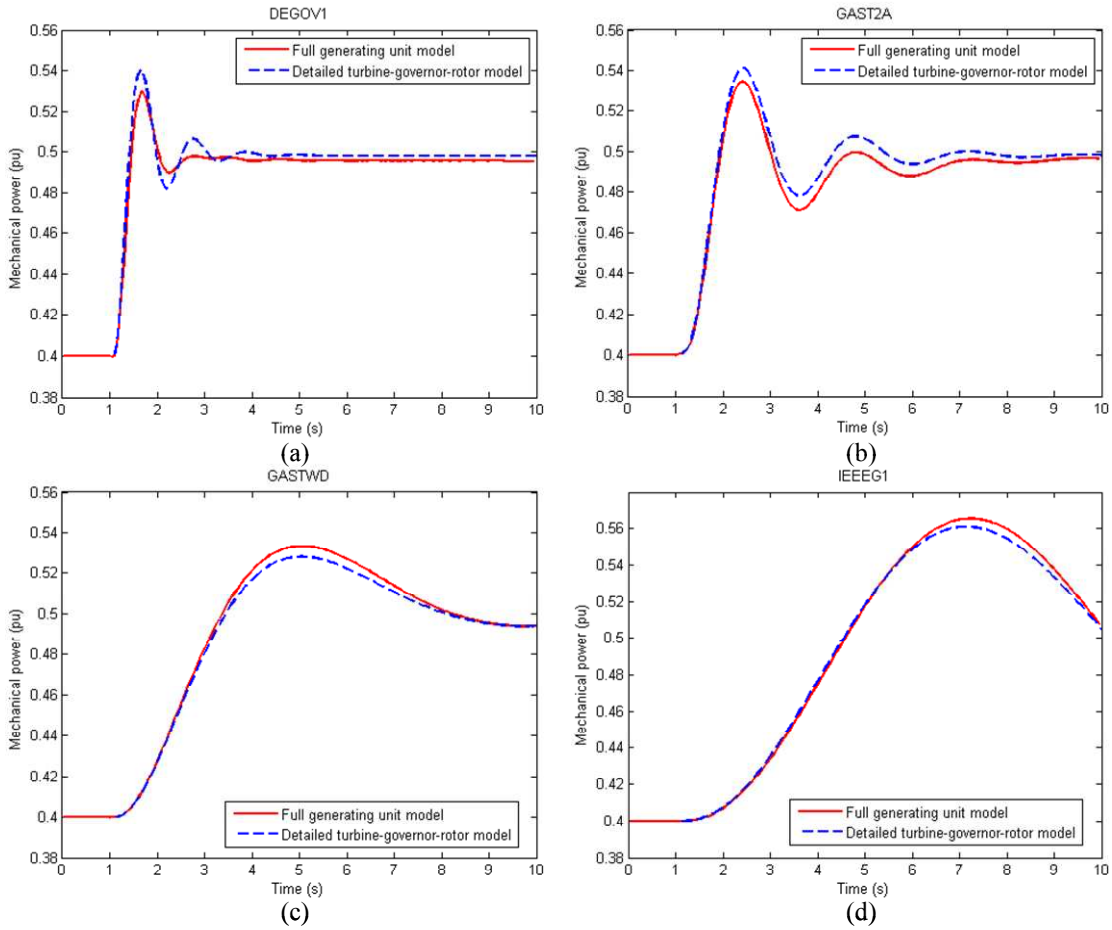

Figure 3-4: Comparison of the responses of (a) a Diesel-based power plant (DEGOV1), (b) a Gas-based power plant (GAST2A), (c) a Gas-based power plant (GASTWD) and (d) a Steam-based power plant (IEEEG1).

3-2-2 Reduction of the transmission network to a single bus and uniform frequency

Figure 3-4 shows that by merely considering the unit response to a step at the governor reference, the generating unit can be approximately modeled by its turbine-governor system. The response of the power system is driven by the response of all connected generating units and depends furthermore on the extension of the network, connected loads, etc. However, in small isolated power systems, the influence of the network on short-term frequency dynamics and especially on inter-machine oscillations is usually negligible. This finally results in a uniform frequency.

Figure 3-5 shows the inter-machine oscillations of the system with transmission network. The outage of a 3.15 MW Diesel generator of the La Palma power system has been simulated. It can be deduced from Figure 3-5 that inter-machine oscillations quickly die out.

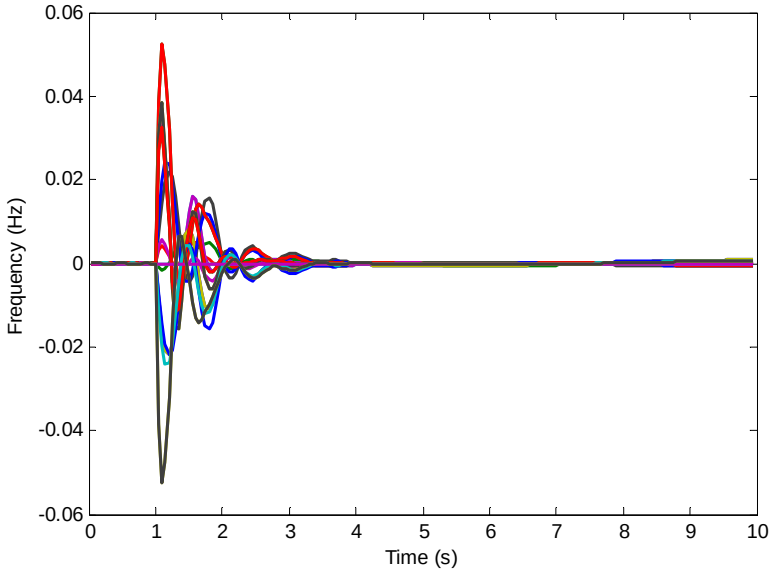

Figure 3-5: Inter-machine oscillations of a system with transmission network.

Figure 3-6 compares the power-system frequency once modeling the network and once omitting the network by concentrating load demand and power generation on a single bus. Frequencies at different buses are shown for the case including the network. It results that that the average frequency does not significantly differ from one case to the other and thus, the network has a negligible impact on the system frequency. Furthermore, without network, the connections between the generators (and the loads) are absolutely rigid and consequently, as shown in Figure 3-6, the oscillations in frequency tend to disappear.

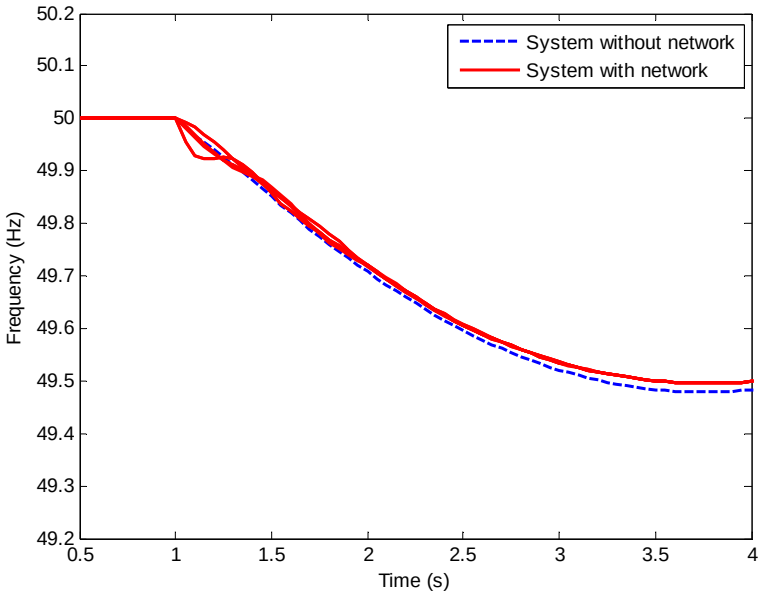

Figure 3-6: Comparison of the frequency variation of a system with and without transmission network.

Neglect of inter-machine oscillations in short-term frequency dynamics by neglecting synchronizing power and transmission performance results in an average or uniform frequency. In fact, frequency dynamics have been simulated using the concept

of uniform frequency (or "dynamic energy balance" [Crevier'75]) to reduce the complexity of the model of a large power system and to eliminate the effect of inter-machine oscillations [Stanton'72]. Inter-machine oscillations are avoided by setting up dynamic models which allow relative movement between generator rotors without representing the transient slow-down-speed-up process associated with oscillatory transfer of kinetic energy from rotor to rotor.[1] Consequently, the center of inertia for the system and the associated frequency of the center of inertia can then be used. Frequency dynamics are described by an aggregate equation of motion of the center of inertia reducing the total number of equations of motion of each generator. The complexity can be further reduced developing dynamic equivalents of different generating units by applying delay or canonical models [Chan'72] or by identifying coherent generating units [Germond'78]. For small isolated power systems, it is verifiable, as seen in Figure 3-6, that short-term frequency dynamics are accurately described by the average system frequency.

3-2-3 Constant power loads

In general, power-system loads are a composite of a variety of electrical devices and depend on voltage and frequency. Voltage dependency can be neglected since voltage varies modestly and is usually restored in a short time. Resistive loads such as lighting and heating are usually frequency independent, whereas motor loads such as fans or pumps depend on frequency due to changes in motor speed. The overall frequency-dependent behavior of loads is described by means of the load-damping factor. The UCTE uses a load-damping factor of 1 [UCTE'04]. However, an accurate value of the load-damping factor is difficult to estimate. Furthermore, the impact of the load variation on short-term frequency dynamics is extremely small compared to the impact of the turbine-governor system [Anderson'99]; therefore, it is reasonable to consider voltage and frequency independent loads [Chan'72; Chuvychin'96].

3-3 A SIMPLIFIED TURBINE-GOVERNOR SYSTEM MODEL

From Figure 3-4, it can be inferred that the generating unit responses to a step at the governor reference resemble the responses of a second-order or third-order closed-loop system. This closed-loop system is actually formed by the lower loop of Figure 3-2 or in other words, by the interaction of the speed-governor and the shaft rotation by means of the equation of motion. A closed-loop second-order model implies a first-order open-loop model since the retroaction, governed by the relationship between angular speed and power described by the equation of motion of a rigid body (inertia), is a first order loop. Similarly, a second-order open-loop model leads to a third-order closed-loop model.

Figure 3-7 shows a block diagram of a turbine-governor system $G(s)$ and its associated backward loop depending on the inertia H_i. If $G(s)$ is a first-order transfer function, the reduced transfer function between $\Delta\omega_{ref}$ and $\Delta p_{m,i}$ is a second-order transfer function. Analogously, if $G(s)$ is a second-order transfer function, the reduced transfer function is a third-order transfer function. As a consequence, first-order and second-order models are studied to represent the distinct turbine-governor systems.

[1] The key feature for eliminating inter-machine oscillations is the assumption that variation of speed of each generating unit with respect to the variation of speed of the center of inertia is zero and therefore, the equation of motion of each generating unit reduces to an energy balance.

Typically, steam-driven turbines can be modeled by first-order transfer functions, whereas gas-driven or diesel-driven combustion turbines might require second-order models [Anderson'90]. In addition, by simplifying the model of the turbine-governor system, the computational cost can be remarkably reduced. However, the model-order reduction also implies a reduction in the accuracy of the model.

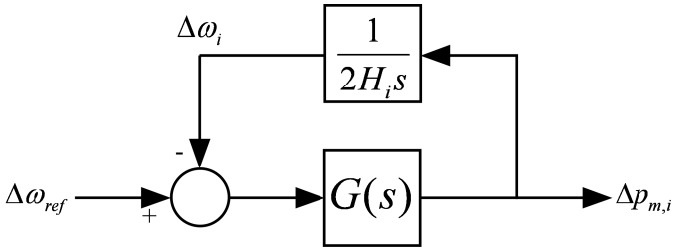

Figure 3-7: Block diagram of the interaction between turbine-governor system and rotor.

Figure 3-8 shows the block diagram of a generic second-order model of a turbine-governor system. With respect to Figure 3-7, the governor reference is constant since there is no secondary control and therefore, frequency deviation is directly fed, with positive sign, into turbine-governor second-order block. This model also includes the generator power-output limitations $\Delta p_{i,min}$ and $\Delta p_{i,max}$. A first-order model can be readily deduced from this generic model.

The parameter K_i represents the gain of the turbine-governor system, which is usually the inverse of the governor droop and is not tunable. The parameters $a_{1,i}$ and $a_{2,i}$ and $b_{1,i}$ and $b_{2,i}$ correspond to the dominant poles and possible zeros of the turbine-governor system. The tunable parameters of the second-order model, i.e. $a_{1,i}$, $a_{2,i}$, $b_{1,i}$ and $b_{2,i}$, are adjusted such that the response of the model resembles as much as possible the response of the complete model of the turbine-governor system. Optionally, these parameters can also be obtained from field tests, i.e. the response of the simplified model is adjusted in order to resemble as much as possible the actual test responses.

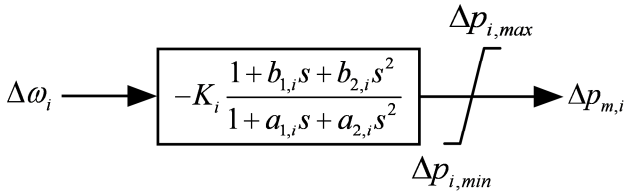

Figure 3-8: Generic second-order model approximation of the turbine-governor system.

3-4 PARAMETER ESTIMATION OF SIMPLIFIED TURBINE-GOVERNOR SYSTEM MODELS

The parameters of the simplified first-order and second-order models, i.e. the time constants corresponding to poles and zeros, are tuned such that responses of the simplified model and of the detailed model of the turbine-governor system are as similar as possible. Five different model types are initially considered:

- a first-order model without zeros (Order 1.0)
- a first-order model with one zero (Order 1.1)
- a second-order model without zeros (Order 2.0)
- a second-order model with one zero (Order 2.1)
- and a second-order model with two zeros (Order 2.2)

These model types seem to be adequate to represent distinct turbine-governor systems. Tuning consists then in minimizing the difference between the simplified model response and the response of the detailed model of the turbine-governor system, which is basically a parameter estimation problem. Well-known algorithms exist for parameter estimation problems [Ljung'87; Bates'88]. The estimation process used here is similar to the one proposed in [Criado'94] and [Rouco'99], where model responses are given by time-domain responses and the model parameters are determined by means of a nonlinear estimation algorithm.

The present parameter estimation problem essentially depends on four factors: the accuracy of the detailed model, the time interval chosen to simulate the simplified and the detailed model, the model structure (open loop or closed loop) and the selection of the simplified model type[2]. Detailed models usually include several non-linearities. However, in many cases the response of the detailed model fits well with the response of a linearized version of the detailed model and thus, the linearized version is used in a first instance to tune the abovementioned parameters [Egido'10][3]. A linearized version of the detailed model maintains the order of the detailed model, but it neglects non-linearities such as saturations, etc. Figure 3-9 (a) shows such a case for a DEGOV1 turbine-governor system. Moreover, this circumvents the need for simulations of the detailed turbine-governor model with programs such as PSS/E. However, in some occasions, the response of the linearized turbine-governor model might not be accurate enough and the detailed model or even field test data must be used. A typical example is the concurrence of a significant delay and a speed-dependent turbine-governor system output. In an underfrequency condition, the turbine output initially decreases (due to the decreasing frequency) before the governor action takes place to increase the output. Figure 3-9 (b) shows an occasion where the response of the linearized version of the detailed model does not coincide with the response of the detailed model of a DEGOV1 turbine-governor system due to a significant delay and the speed-dependent output (see also appendix C). The output of the detailed model initially decreases due to the non-linearity causing a slower response than the one of the linearized version of the DEGOV1 model.

[2] Although the initial guess of the tunable parameters is also relevant, this is minor problem. In fact, if the simulation time and the simplified model to be adjusted are carefully chosen, common curve-fitting algorithms find the most appropriate parameter settings.

[3] Linear models are widely used to describe approximately the behavior of real systems. In fact, many real processes with non-linear dynamics may be adequately modeled over suitable time and spatial scales by linear models [Levine'99]. The ability to approximately reproduce the essential system dynamics allows tuning simplified low-order models using linearized versions of complex models. Furthermore, it is easier to implement linear models (e.g. by means of LTI transfer functions) than their non-linear counterparts. Moreover, the tuning of the simplified model will depend on the output and the step size of the simulation, if non-linearities influence the response of the complete model. Fortunately, this is not usually the case.

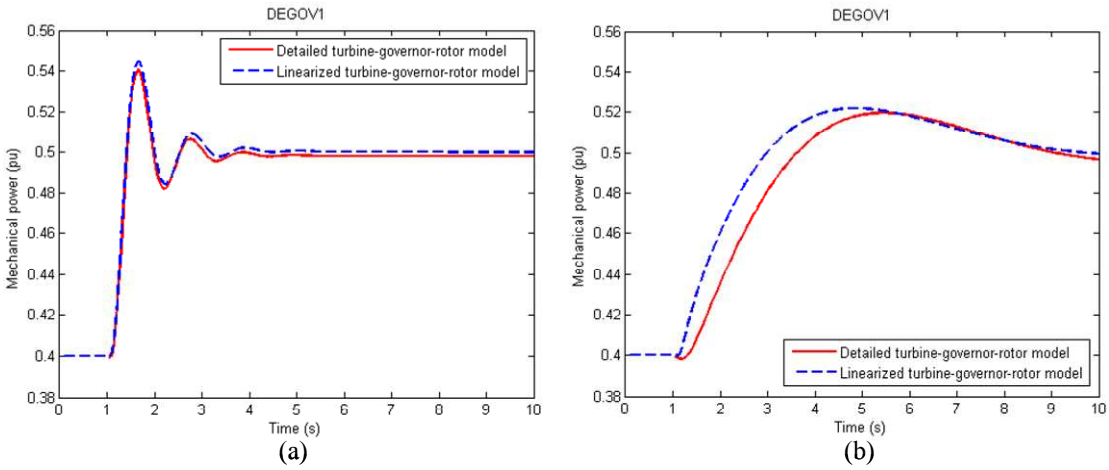

Figure 3-9: Comparison of the detailed and the linearized version of two different DEGOV1 turbine-governor systems.

The parameter estimation procedure is either based on an open-loop or closed-loop structure. An open-loop structure only considers the turbine-governor system $G(s)$, whereas a closed-loop structure also contemplates the feedback loop depending on the rotor dynamics as shown for example in Figure 3-7. The choice of the model structure normally depends on the response the simplified model should be adjusted for. Field tests, for example, can be either carried out with the generating unit online or offline, depending on the signal to be measured and on the test applied [Hannet'93; Pereira'03]. Speed deviations due to changes at the governor reference can only be measured with the generating unit offline [Berube'99], resulting in a closed-loop parameter estimation. By contrast, online tests can be carried out, if active power deviation due to a step at the governor reference is measured as in [Tor'04], requiring an open-loop structure. If parameters of detailed turbine-governor systems are available, both open-loop and closed-loop structure could be used.

In [Egido'10], parameters of several first-order models have been estimated applying a step input to the first-order model and the linearized detailed model and minimizing the difference of the open-loop outputs. A step input seems appropriate, if online measurements to a change at the governor reference are used. Another possibility consists in applying a ramp input since the response of the turbine-governor system and the system frequency could be represented by a ramp during the first few instants after a system-wide disturbance [Rouco'08]. In fact, the impact of primary control on the frequency is still negligible and frequency falls with a constant rate. Based on the open-loop responses to a ramp input, various adjustments have then been realized with different simulation times ranging from one to four seconds. This time range usually comprises points in time when minimum frequency occurs. These points in time are of particular interest for the analysis of short-term frequency dynamics and especially, for the design and analysis of UFLS schemes. As an example, Table 3-1 displays the parameters of the first-order model approximations of an IEEEG1 turbine-governor system using three different simulation time settings (i.e. 1 s, 3 s and 5 s). Figure 3-10 (a) compares the closed-loop responses of the four first-order models with the closed-loop response of the linearized complete IEEEG1 model. Clearly, with increasing simulation time, the accuracy of the first-order model increases as well. This is due to the fact that the considered IEEEG1 turbine-governor system is a rather slow system. For faster turbine-governor systems, shorter simulation time settings lead to more accurate low-order models as in the case of the DEGOV1 model and its first-order

model shown in Figure 3-10 (b) and Table 3-1. In fact, due to the extended simulation time, more weight has been given to post-transient data, distorting the curve-fitting problem.

Table 3-1: Comparison of parameter turnings with different simulation times.

Model	1s		3s		5s	
	K	a_1 (s)	K	a_1 (s)	K	a_1 (s)
IEEEG1	16.66	11.00	16.66	6.90	16.66	6.10
DEGOV1	25.00	0.51	25.00	0.75	25.00	0.92

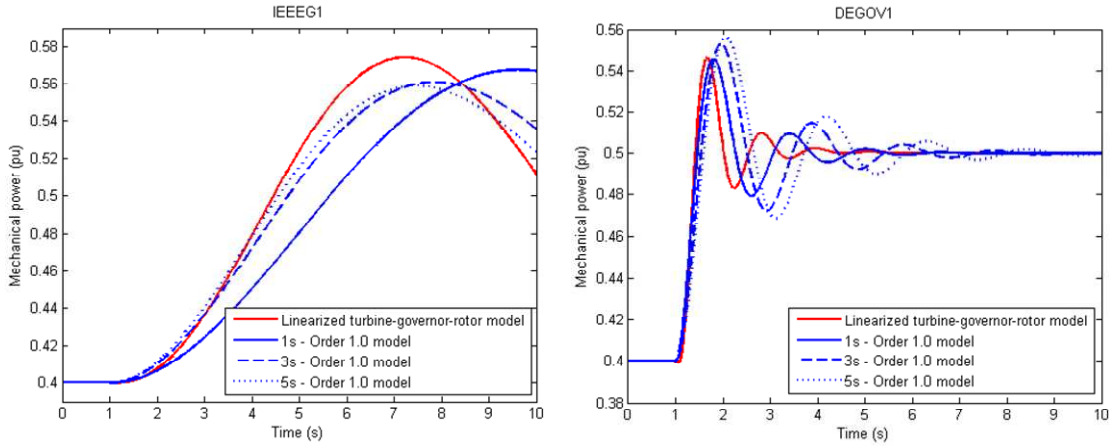

Figure 3-10: Comparison of the responses of (a) the linearized IEEEG1 model with the responses of the simplified models and (b) linearized DEGOV1 model with the responses of the simplified models adjusted using different simulation times to a step of 0.1 pu.

Along with the tuning of simplified models based on open-loop responses to step or ramp inputs, closed-loop responses to step inputs could also be used to adjust the simplified models. The feedback is formed by the interaction of the turbine-governor system and the rotor dynamics as shown in Figure 3-7. With this model structure, the tuning process is still dependent on the simulation time, but to a much lesser extent. For example, too long simulation time led to misleading results in the case of the open-loop adjusted DEGOV1 model because adjustments between detailed and simplified model towards the end of the simulation time outweighed the initial differences. Usually, simulation time settings around three to five seconds lead to good results and allow representing the dynamics of the turbine-governor system. A good estimation for the simulation time is given by twice the point in time of the maximum of the output of the complete turbine-governor system[4]. In addition, the closed-loop structure delivers a more appropriate input in terms of frequency deviation to the turbine-governor system than the ramp input. This could be important since the input should resemble as much as possible those inputs for which the model should be most accurate [Levine'99]. Figure 3-11 compares the closed-loop responses of the simplified models adjusted by means of

[4] It has been found that shorter simulation time settings determined, for example, by the point in time of the maximum of the output of the turbine-governor system yielded to stable simplified open-loop models but to unstable closed-loop models since not the entire dynamics could have been considered. For instance, for a GAST2A turbine-governor system, the following parameters have been obtained (see Figure 3-8): $K = 25$, $b_1 = b_2 = 0$, $a_1 = 0.26$ and $a_2 = 0.14$. The closed-loop model (with $H = 6.5$ s), however, presented the following poles: $p_1 = -1.9009$ and $p_{2,3} = 0.0219 \pm j2.688$. This is clearly an unstable system. A stable result has been obtained by increasing the simulation time.

a closed-loop (CL) structure with the responses of the linearized turbine-governor systems. In addition, the results are compared to the ones obtained when using an open-loop (OL) structure. For both the DEGOV1 and the GASTWD turbine-governor system, the CL-based parameter estimations seem to be more accurate.

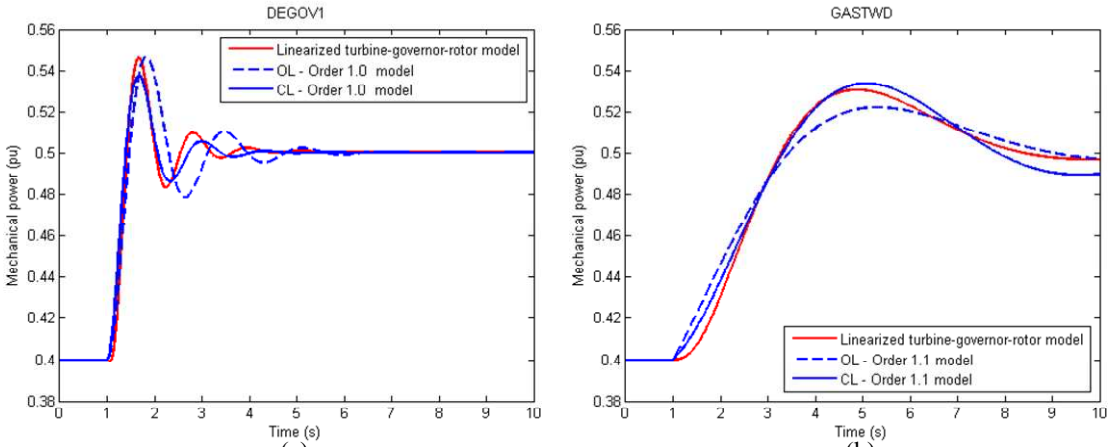

Figure 3-11: Comparison of the responses of (a) the linearized IEEEG1 model with the responses of the simplified models and (b) linearized DEGOV1 model with the responses of the simplified models adjusted using different simulation times to a step of 0.1 pu.

Finally, the parameters of the five different first and second-order model types are estimated by using both OL and CL structures. The most accurate simplified models are then selected and compared. The most accurate model type is the one which minimizes the parameter estimation problem, i.e. which minimizes the difference between the responses of the simplified and the original turbine-governor system model. Figure 3-12 compares the responses of the most accurate simplified models, adjusted by using both OL and CL structures, with the responses of the linearized models of DEGOV1, GASTWD and GAST2A turbine-governor systems.

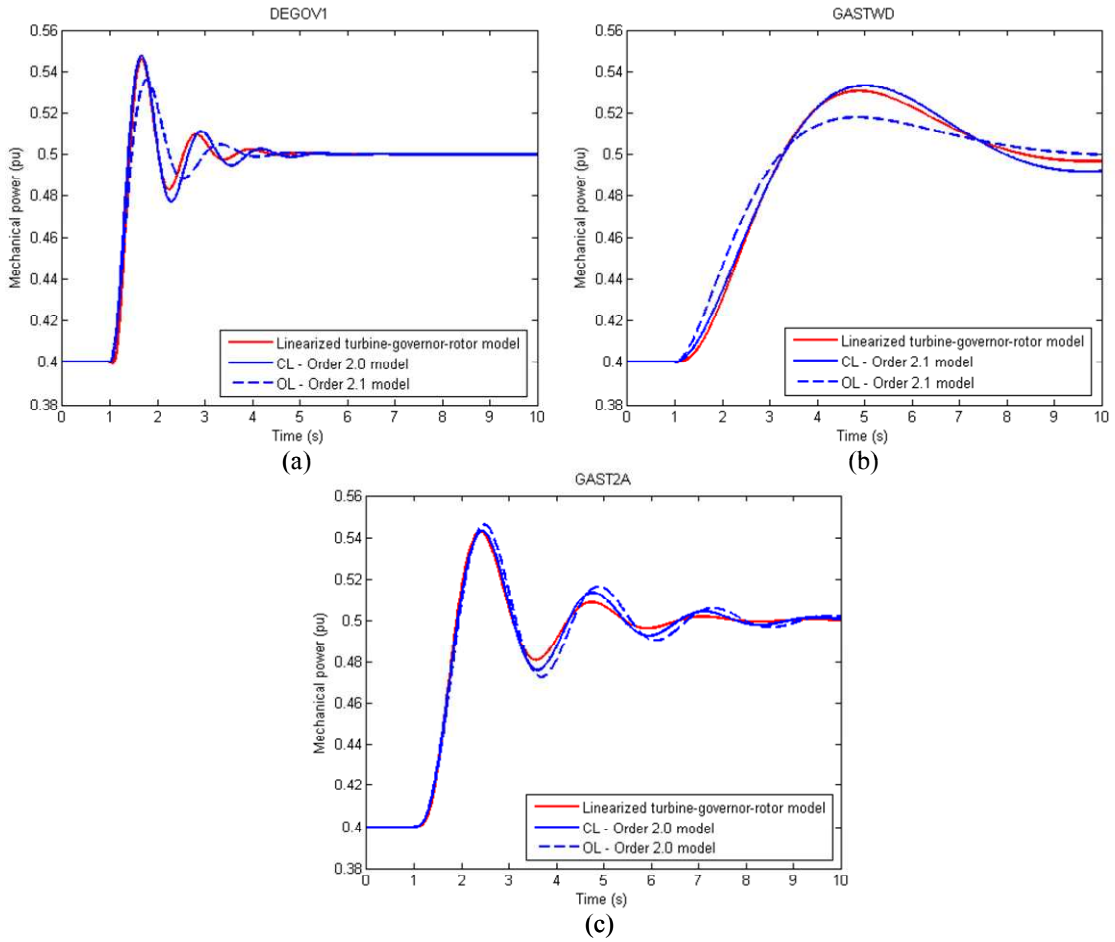

Figure 3-12: Comparison of the responses of (a) the simplified and the linearized DEGOV1 model, (b) the simplified and the linearized GASTWD model and (c) of the simplified and the linearized GAST2A model to a step at the reference of the turbine-governor system.

For the turbine-governor systems shown, the results of the tuning process using either an OL or a CL model structure differ and in general, the adjustment based on a closed-loop model structure seems to be more accurate. Different turbine-governor systems require different models. For example, the GASTWD model of Figure 3-12 (b) seems to be best represented by a second-order model with one zero (CL – Order 2.1), whereas the DEGOV1 model of Figure 3-12 (a) can be modeled by a second-order model without zeros (CL – Order 2.0). The GAST2A model also seems to be best represented by a second-order model without zeros (CL – Order 2.0). It is interesting that in the case of the DEGOV1 model, the open-loop structure yields to a second-order model with one zero, whereas the closed-loop structure gives rise to a second-order model without zeros. By any means, it seems that the simplified model represents the complete turbine-governor system model quite accurately.

3-5 SYSTEM FREQUENCY DYNAMICS (SFD) MODEL

Frequency dynamics are mainly affected by the speed-governor action; therefore, for short-term frequency stability analysis, it is possible to represent the generator by its turbine-governor system. Furthermore, compared to turbine-governor dynamics, excitation and generator transients can be neglected for being much faster. In small isolated power systems, the transmission network has a negligible impact on short-term frequency dynamics and thus, the power-system network can be reduced to a single bus ignoring the dynamics between generating units, i.e. the oscillatory nature of frequency

due to electromechanical inter-machine oscillations. This implies a uniform frequency. Finally, loads are assumed to be voltage and frequency independent. All these considerations merge into the so-called system frequency dynamics (SFD) model [Anderson'90].

3-5-1 Review of SFD models

The principal idea of SFD models is to provide low-order models that retain the essential frequency shape of a system with typical time constants and active turbine-governor systems [IEEE'73; IEEE'91]. An important feature of SFD models is the assumption of uniform frequency.

Several SFD models have been proposed in the technical literature. First SFD models only considered the impact of the load-damping factor on short-term frequency dynamics [New'77]. Thereupon, a simple linear single-bus SFD model has been developed, where the generating units are represented by a single first-order model of the turbine-governor systems [Anderson'90]. This model was based upon the assumption that the generating units are predominantly driven by steam turbines. In [Denis Lee Hau'06], a general linear SFD model is outlined allowing the representation of several first-order models of turbine-governor systems. A similar SFD model is presented in [Egido'10]. However, these SFD models are all linear and do not take into account the generator output limitations. For short-term frequency dynamics in small isolated power systems, it is important to be aware of the finite reserve. In fact, the assumption of a linear model is only valid for small disturbances and is therefore questionable for the design of UFLS scheme of a small isolated power system. In addition, the first-order models of the generating units adopted in [Anderson'90] and [Denis Lee Hau'06] correspond to steam turbines. In general, the generation mix contains also gas-driven and Diesel-driven turbines. Thus, a non-linear SFD model needs to be defined which enables to implement different turbine types. Mainly delays in the response of generating units demand for a higher order model. A first step in this direction is given in [Egido'10] by adjusting the first-order models in function of different turbine-governor systems. Finally and as seen in section 3-3, the order of the simplified model of each generating unit may vary in function of the turbine type and its parameters and therefore, the model adopted to represent a particular generating unit should be the one which represents best the detailed turbine-governor system.

3-5-2 Proposed non-linear multi-generator SFD model

A complete model consists of n generators with n equation of motions and n different turbine-governor models. The equation of motion of the *ith* generator is given by:

$$2H_i\dot{\omega}_i = p_{m,i} - p_{d,i} \tag{3.1}$$

or uniquely considering deviations:

$$2H_i\Delta\dot{\omega}_i = \Delta p_{m,i} - \Delta p_{d,i} \tag{3.2}$$

where H_i is the inertia in (s), $\Delta\omega_i$ the frequency deviation in pu, $\Delta p_{m,i}$ the mechanical power deviation in pu and $\Delta p_{d,i}$ the load power deviation in pu. Equation (3.2) is given on the base of the rating of the *ith* machine $M_{base,i}$. Assuming that the equations are normalized to the size of the isolated power system, the system base, S_{base}, is the sum of the ratings of all generating units. Thus:

$$2H_i\frac{M_{base.i}}{S_{base}}\Delta\dot{\omega}_i = \frac{M_{base.i}}{S_{base}}\left(\Delta p_{m,i} - \Delta p_{d,i}\right) \tag{3.3}$$

with

$$S_{base} = \sum_{i=1}^{n} M_{base.i}$$

Summing the *n* equations of motion yields to:

$$2\sum_{i=1}^{n} H_i \frac{M_{base.i}}{S_{base}} \Delta\dot{\omega}_i = \sum_{i=1}^{n} \frac{M_{base.i}}{S_{base}} \Delta p_{m,i} - \sum_{i=1}^{n} \frac{M_{base.i}}{S_{base}} \Delta p_{d,i} \tag{3.4}$$

At this stage, the equivalent inertia *H* can be defined as:

$$H = \sum_{i=1}^{n} \frac{H_i \cdot M_{base,i}}{S_{base}} \tag{3.5}$$

Combining equation (3.4) and equation (3.5), the uniform frequency deviation is described by the average frequency deviation $\Delta\omega$ given in equation (3.6).

$$2H\Delta\dot{\omega} = \Delta p_{m,tot} - \Delta p_{d,tot} \tag{3.6}$$

where $\Delta p_{m,tot}$ and $\Delta p_{d,tot}$ are the total power generation and total load demand deviation, respectively.

Figure 3-13 details the power-system model proposed to design robust and efficient UFLS schemes of small isolated power systems of *n* generating units. This is a SFD model with equivalent inertia where the whole generation and load demand is assumed to be connected to the same bus. Generators can be represented by a non-linear first or second-order turbine-governor model approximation as shown Figure 3-8. Load is constant in quantity as long as the UFLS scheme does not intervene[5]. The UFLS schemes permits to implement both underfrequency relays and ROCOF relays.

[5] For the sake of completeness, the load-damping factor has been included in the SFD model shown in Figure 3-13 as in [Anderson'90]. The reason for this is to show its negligible impact with respect to the gain of the turbine-governor system in subsequent analysis. Later, the load-damping factor is not contemplated as discussed in section 3-2-3.

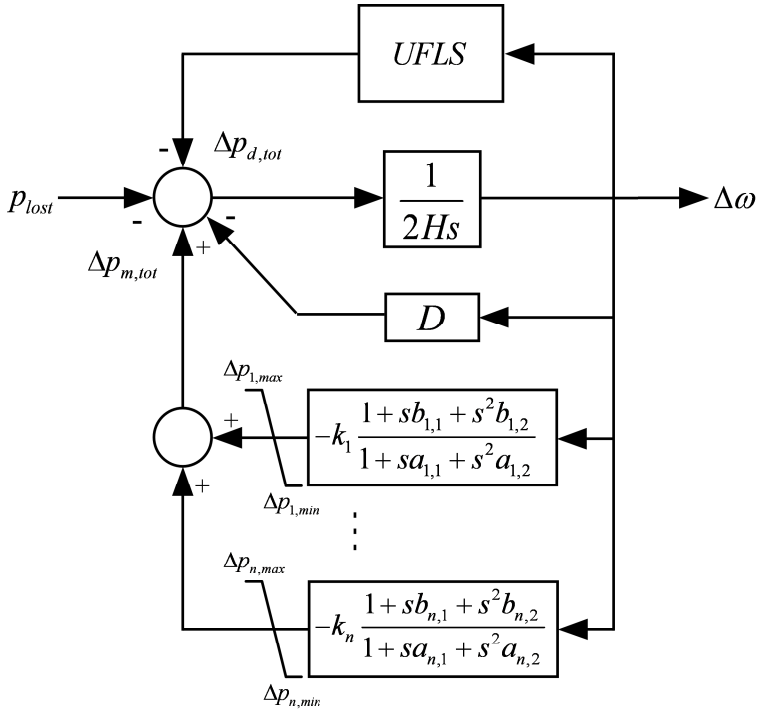

Figure 3-13: Non-linear multi-generator SFD model of a small isolated power system.

Finally, writing the equation of motion of the center of inertia in the base of the system rating S_{base} requires the gain of the first-order or second-order generator model K_i to be expressed according to S_{base}:

$$k_i = \frac{M_{base,i} \cdot K_i}{S_{base}} \tag{3.7}$$

3-5-3 Extension of the SFD model to decoupled power generation

Currently, decoupled power generation essentially suffers from two drawbacks: its limited primary frequency control capacity and its negligible inertial response. Both the lack of primary frequency control and the lack of inertial response have a negative impact on frequency stability. Substituting conventional generation by decoupled power generation further weakens system ability to withstand large disturbances. In fact, the initial rate of change of frequency increases with decreasing inertia. Furthermore, availability of sufficient spinning reserve is critical for system stability. Thus, the smaller the inertia and the smaller the available spinning reserve, the larger are frequency deviations.

The differences between the characteristics of conventional and decoupled power generation and the prevision of an increasing amount of installed capacity of decoupled power generation require contemplating scenarios with different levels of decoupled power generation penetration for the analysis of short-term frequency dynamics. Due to its specific characteristics, decoupled power generation can be represented as a negative load omitting any dynamics. In other words and in terms of the non-linear multi-generator SFD model of Figure 3-13, decoupled power generation is modeled like a generating unit, but with zero inertia H_i and zero gain K_i.

3-6 SIMULATION OF SMALL ISOLATED POWER SYSTEMS

Short-term frequency dynamics are simulated using the non-linear multi-generator SFD model shown in Figure 3-13. Several software packages such as Matlab offer powerful

simulation tools which implement different methods of numerical integration of non-linear differential equations. The system of non-linear differential equations, which can be deduced from Figure 3-13, is non-stiff and thus, well-known numerical integration methods such as Heun's method can be applied[6].

Heun's integration method, also known as Modified Euler's method, is used to numerically solve systems of differential equations. It can be seen as an extension of the Euler method into a two-stage second-order Runge-Kutta method [Kendall'09]. In fact, Heun's method divides the numerical integration into a predictor and a corrector step.

Consider for example the system of differential equations given in equation (3.8)

$$\dot{\mathbf{x}}_s(t) = \mathbf{f}(t, \mathbf{x}_s(t)), \quad \mathbf{x}_s(t_0) = \mathbf{x}_{s,0} \tag{3.8}$$

where $\mathbf{x}_s$ is a vector of state variables and $\mathbf{x}_{s,0}$ its initial values and **f(•)** a vector of functions of time t and $\mathbf{x}_s$. Here, the vector of functions **f(•)** implements the system of non-linear differential equations, describing the SFD model. Heun's method resolves the initial value problem of equation (3.8) as follows

$$\begin{aligned} \tilde{\mathbf{x}}_{s,k+1} &= \mathbf{x}_{s,k} + h \cdot \mathbf{f}(t_k, \mathbf{x}_{s,k}) \\ \mathbf{x}_{s,k+1} &= \mathbf{x}_{s,k} + \frac{h}{2} \cdot \left(\mathbf{f}(t_k, \mathbf{x}_{s,k}) + \mathbf{f}(t_{k+1}, \tilde{\mathbf{x}}_{s,k+1}) \right) \end{aligned} \tag{3.9}$$

where h is the integration step and k is the iteration number. First, a predictor $\tilde{\mathbf{x}}_{s,k}$ is calculated using Euler's method and subsequently the corrector $\mathbf{x}_{s,k}$ is determined by means of an explicit trapezoidal method.

Heun's method is a fixed-step solver, working well for non-stiff problems and with low computational cost. The integration step is usually defined as a fraction of the smallest time constants in order to guarantee accuracy and since Heun's method like other explicit Runge-Kutta methods is not stable for any integration step. If very small time constants are present, variable step-size solver such as the Dormand-Prince method might be more appropriate. However, if UFLS scheme intervene and irrespective of the numerical solver applied, small integration steps are required to determine accurately frequency crossing instants and opening times.

A toolbox based on Matlab has been developed to simulate short-term frequency dynamics. This toolbox makes use of Heun's method. In the appendix A, the main features of the prototype of the toolbox are outlined. Among others, PSS/E software package also applies Heun's numerical integration method to solve non-linear differential equations [Siemens'05a].

Subsequently, Heun's method is applied to simulate the SFD models of two real power systems. Figure 3-14 and Figure 3-15 compare the system frequency obtained by the SFD model with the system frequency obtained by the detailed power-system model. In Figure 3-14, the loss of 66.68 MW (corresponding to 21.9 % of total demand) of the Gran Canaria power system has been simulated, whereas in Figure 3-15 the loss of 2.35 MW (corresponding to 13 % of the total demand) of the La Palma power system has been simulated. Clearly, the response of the SFD model of the Grand Canaria system fits very well the response of the detailed power-system model.

---

[6] A stiff equation is a differential equation for which certain numerical methods for solving the equation are numerically unstable, unless the step size is taken to be extremely small [Kendall'09]. Stiffness is usually associated to some terms in the differential equation that can lead to rapid variations in the solution [Hoffman'01].

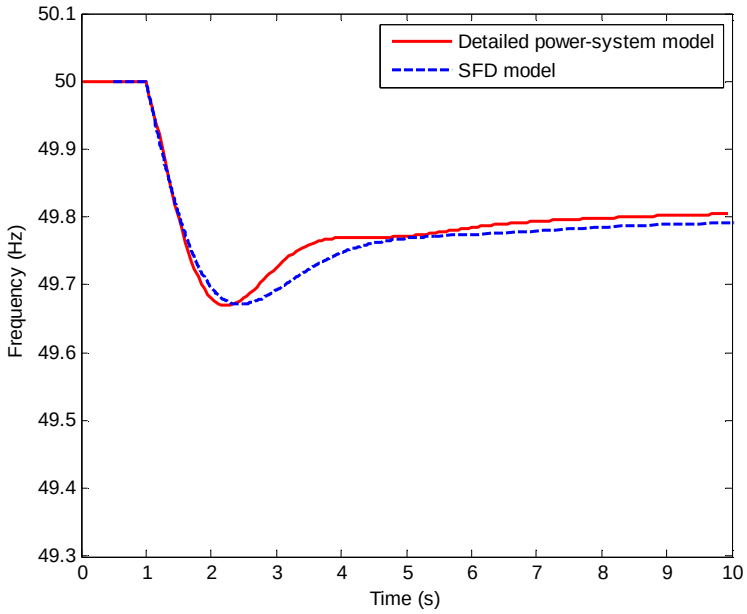

Figure 3-14: Comparison of the responses of the detailed Gran Canaria power-system model and the SFD model.

In case of the La Palma power system, the response of the SFD model, as shown in Figure 3-15, also fits the response of the detailed model satisfactorily. Hence, taking into account the inherent simplicity of the SFD model compared with the detailed power-system model, the results are very satisfactory and encourage the use of SFD models for the design of UFLS schemes.

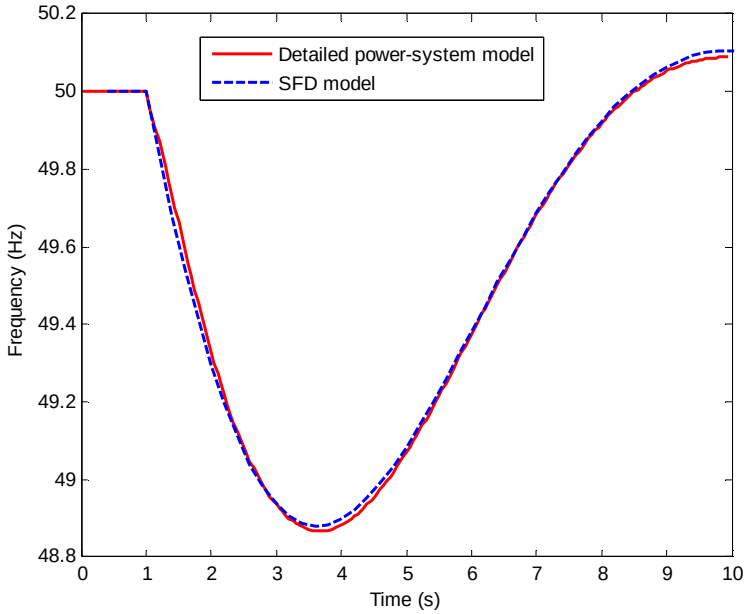

Figure 3-15: Comparison of the responses of the detailed La Palma power-system model and the SFD model.

3-7 SENSITIVITY OF THE MODEL RESPONSE WITH RESPECT TO MODEL PARAMETERS

In this section, the sensitivity of the SFD model response with respect to variation of its model parameters is analyzed. First, the impact of the SFD generator model parameters on the frequency is studied, neglecting the UFLS scheme. In a second step, the impact of the UFLS scheme on the frequency is analyzed. This simple analysis permits to illustrate the influence of generating units and UFLS scheme on short-term frequency dynamics. Finally, the impact of decoupled power generation on frequency stability is studied. These impacts are evaluated by means of system responses in terms of frequency.

3-7-1 Impact of the SFD generator model parameters

Subsequently, the impact of the equivalent inertia, of the generator gains and time constants and the impact of generator output limitations as well as of the load-damping factor on frequency are evaluated. In [Anderson'90], a similar analysis has been carried out with regard to the inertia, generator gain and pole time constant. However, a linear single-generator first-order model has been used there and no attention has been paid therefore to zero time constants or to the generator output limitations. For this purpose, the SFD model of Figure 3-13 is supposed to represent two generating units, with each generating unit represented by a first-order model. An initial power imbalance of 0.15 pu is applied. The load-damping factor is neglected except for the analysis of its impact. Likewise, generator output limitations are also neglected except for the analysis of their impact. Table 3-2 resumes the assumed SFD model parameters.

Table 3-2: SFD model parameters.

Generator	H (s)	K	a_1 (s)	b_1 (s)	Mbase (MW)	Δp_{min}	Δp_{max}
1	3	25	3	0	130	-	-
2	5	25	5	0	70	-	-

The integration step should be defined as a fraction of the smallest time constant of the model formed by the two generators. An appropriate choice for the integration step is 0.1 s.

3-7-1-1 Inertia

By inspecting the non-linear multi-generator SFD model of Figure 3-13 and by applying the final value theorem, the well-known expression for the steady-state frequency deviation can be obtained:

$$\Delta\omega_{ss} = -\frac{\Delta p_d}{\sum_{i=1}^{n} k_i + D} \tag{3.10}$$

where n is the number of generators, D the load-damping factor and k_i the gain of the *ith* generator expressed according to the system base S_{base}. In a similar way, applying the initial value theorem to the derivative of frequency yields to the initial value of the rate of change of frequency [Anderson'90]:

$$\Delta\dot{\omega}_0 = -\frac{\Delta p_d}{2H} = -\frac{\Delta p_d}{2\sum_{i=1}^{n} \frac{H_i \cdot M_{base,i}}{S_{base}}} \tag{3.11}$$

where H_i is the inertia of the *ith* generator and $M_{base,i}$ is its base rating.

Figure 3-16 shows the impact of the inertia on frequency. According to equation (3.11) and to Figure 3-16, the most pronounced effect of increasing H_1 (which increases in turn the equivalent inertia) is to reduce the initial rate of change of frequency, and to delay and reduce the minimum frequency deviation. The equivalent inertia does not affect the final steady-state value of frequency as stated in equation (3.10). Higher inertia values result in a slower drop in frequency, which is logical, and also in a slower recovery. Since the response is slower for higher inertias, the governor has more time to respond and therefore limits the minimum frequency deviation to smaller values.

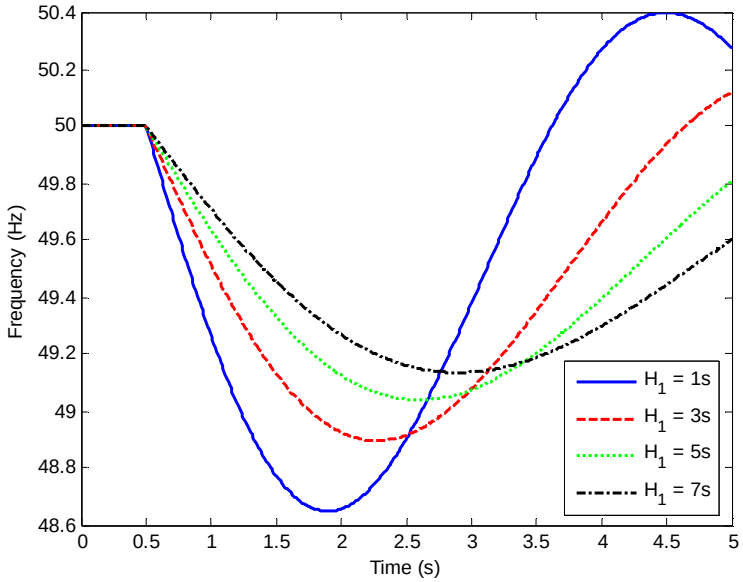

Figure 3-16: The impact of varying the inertia H_1 on frequency.

3-7-1-2 Generator gain and time constants

To show the effect of the generator gain, different K_1 are considered, corresponding to governor droops of 0.04, 0.05, 0.06 and 0.07 pu. In fact, actual observed system responses have sometimes shown the net system regulation to differ from the value of 0.04 or 0.05 pu [Anderson'90]. Figure 3-17 shows the resulting impact on frequency.

As seen in Figure 3-17 and as stated in equation (3.11), the generator gain has absolutely no effect on the initial rate of change of frequency. Even if all governors are at the extreme valve-closing end of the individual backlash limits, as in following a gradual load decrease, a sudden power imbalance would require a rapid change to a valve or gate open condition. However, this cannot occur instantaneously. Higher generator gains shorten the recovery time and reduce the steady-state frequency deviation. In addition, the minimum frequency deviation is also reduced with increasing generator gains.

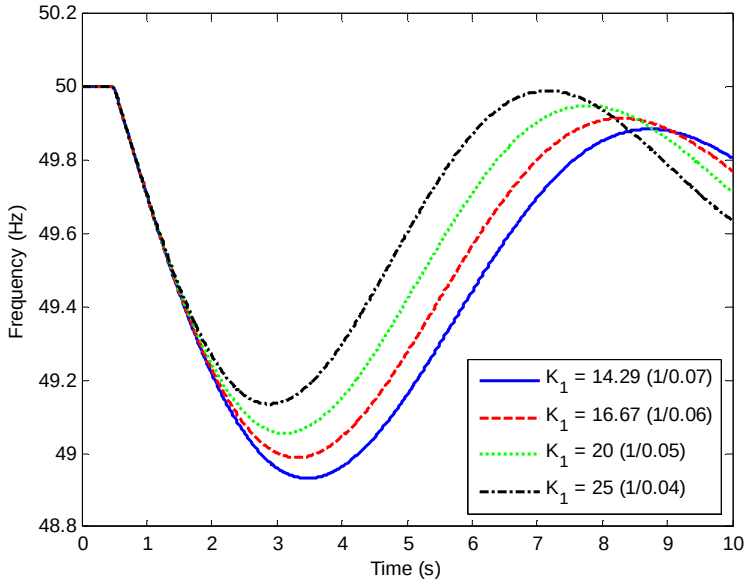

Figure 3-17: The impact of varying the generator gain K_1 on frequency.

Figure 3-18 and Figure 3-19 depict the impact of the generator time constants a_1 and b_1 for different values. The time constants a_1 of 1 s, 3 s, 5 s and 7 s are typical for gas, diesel and steam turbines, respectively. The major effect of the generator time constant a_1 is to produce a lag in the response of the frequency following its initial dip. This lag also increases the minimum frequency deviation and delays the peak values of this maximum in proportion to the size of the time constant. In other words, this parameter has an effect on the response and the total time of exposure to low frequencies. Higher values also cause a larger frequency overshoot as seen in Figure 3-18. Similar conclusions can be drawn for a second-order model.

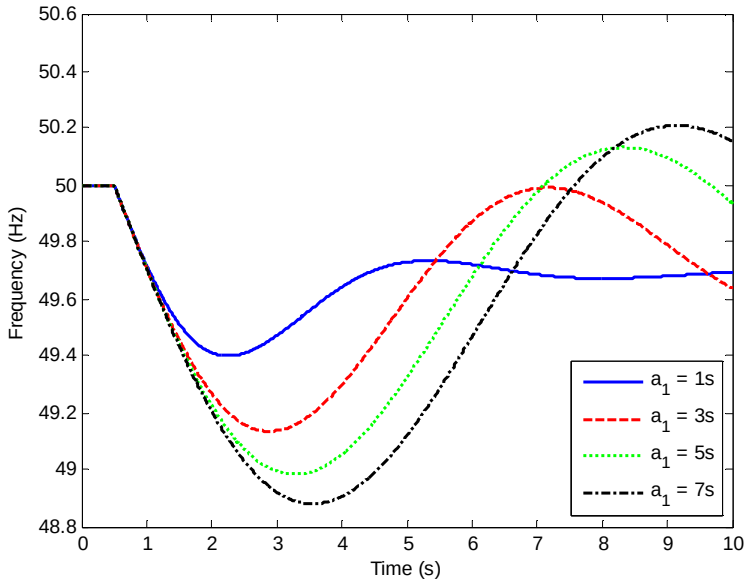

Figure 3-18: The impact of generator time constant a_1 on frequency.

The major effect of the generator time constant b_1 is to accelerate the response of the turbine-governor system and to decrease both the frequency deviation and the peak values of its oscillation in proportion to the size of the time constant. In other words,

this parameter has an effect on the response and the total time of exposure to low frequencies. The accelerated response with higher values of b_1 is due to the fact that this parameter represents the sensitivity of the model to the rate of change of its input, i.e. the frequency. It is interesting that for b_1 larger than a_1, the oscillatory behavior of the response disappears.

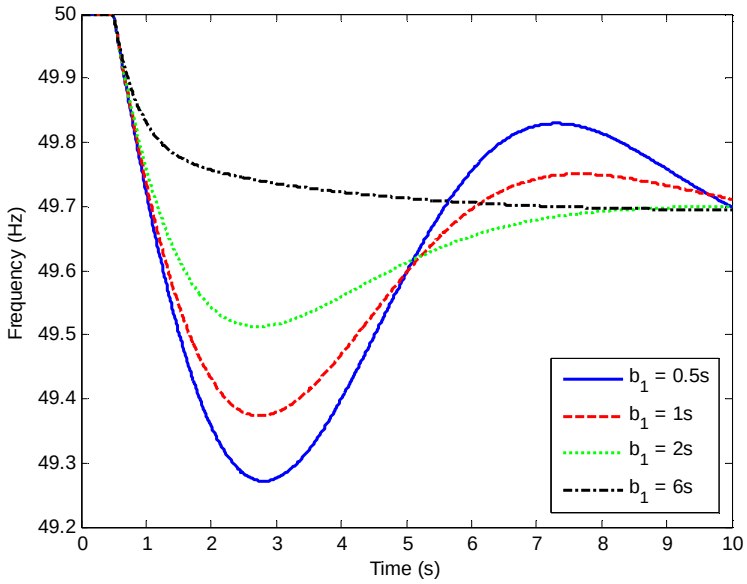

Figure 3-19: The impact of generator time constant b_1 on frequency.

3-7-1-3 Generator output limitations

Previous SFD models omitted generator output limitations for the analysis of short-term frequency dynamics. This assumption is however not valid for small isolated power systems where large disturbances can occur. Usually, spinning reserve is limited and covers for the outage of the largest generating unit. Figure 3-20 shows the impact of finite reserve on frequency. In fact, the generator output limitation Δp_{max} has been set to 0.17 pu and 0.1 pu, which is slightly above and clearly below the amount of lost real power. Furthermore, for the case of 0.17 pu, both uniformly and non-uniformly distributed finite spinning reserve have been considered.

Obviously, the generator output limitation slowed down the frequency recovery. In addition, in the case of non-uniformly distributed reserve, frequency reduced further and gained its minimum value later than in the case of uniformly distributed spinning reserve. Thus, in multi-generator systems, generator output limitations could also retard the overall primary frequency control action if spinning reserve is non-uniformly distributed. Finally, if the amount of spinning reserve is lower than the amount of lost power, frequency decay cannot be arrested and the system goes frequency unstable. This is also illustrated in Figure 3-20. Thus, generator output limitations significantly affect short-term frequency dynamics and frequency stability and must be taken into account in the power-system model of small isolated power systems.

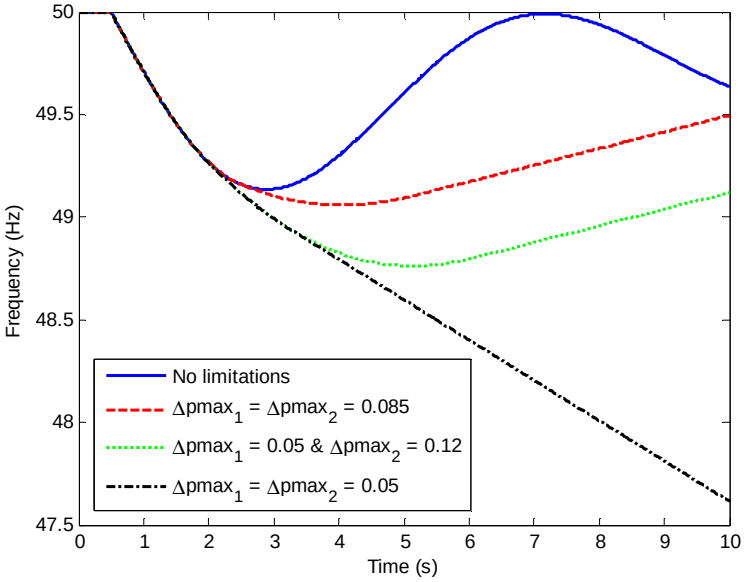

Figure 3-20: The impact of generator output limitations on frequency.

3-7-1-4 Load-damping factor

The effect of the load-damping factor *D* on frequency can be illustrated by plotting the system response for various values of this parameter. Figure 3-21 compares the impact on frequency for three different values. The UCTE, for example, recommends a load-damping factor of 1 [UCTE'04].

Comparing Figure 3-17, which shows the variation of *K*, and Figure 3-21 and taking into account equation (3.10), it results that the effect of varying *D* and *K* is much the same, but *K* plays a much more important role than *D*. Usually, *K* amounts to 25 pu, whereas *D* ranges between 0.5 to 1 pu. Thus, even though the load has a frequency dependent component, it is not nearly as important as the generator gain with respect to the impact on short-term frequency dynamics. Consequently, it is justified to neglect load-damping factor in SFD models as discussed in section 3-2-3.

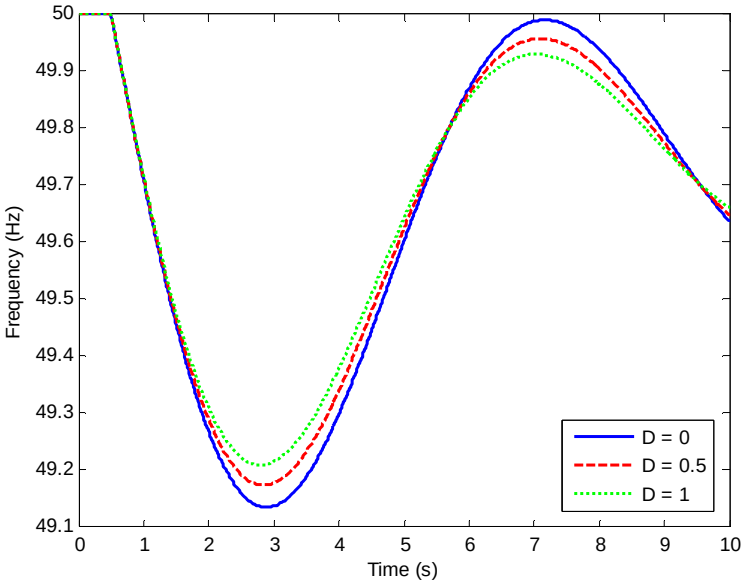

Figure 3-21: The impact of load-damping factor on frequency.

3-7-2 Impact of UFLS schemes

UFLS schemes protect power systems against underfrequency conditions; therefore, the impact of an UFLS scheme on short-term frequency dynamics is evaluated. Again, the SFD model of Figure 3-13 is supposed to represent two generating units, with each generating unit represented by a first-order model as displayed in Table 3-3. A power loss of 0.15 pu is applied. The maximum generator output limitation is lower than the amount of lost real power.

Table 3-3: SFD model parameters.

Generator	H (s)	K	a_1 (s)	b_1 (s)	Mbase (MW)	Δp_{min}	Δp_{max}
1	3	25	3	0	130	-	0.05
2	5	25	5	0	70	-	0.05

Figure 3-20 has shown that for the SFD model defined by Table 3-3, the system turns frequency unstable since there is not enough spinning reserve available to cover the loss of 0.15 pu. Clearly, such an underfrequency condition would lead to a system blackout due to underfrequency turbine tripping. As a consequence, a simple single-stage UFLS scheme is implemented. Table 3-4 displays the parameters of the UFLS scheme. The value of the step size has been chosen such that the step size and the amount of available spinning reserve at least equal to the amount of lost power.

Table 3-4: UFLS scheme parameters.

Stage	Threshold (Hz)	Intentional delay (s)	Delay (s)	Step size (pu)
1	49	0	0	0.08

Again, the integration step could be set to 0.1 s as seen in section 3-7-1. However, due to the UFLS scheme, integration step should be smaller in order to obtain more accurate threshold crossing times, etc. Thus, for the first 5 seconds, where load shedding usually occurs, an integration step of 0.01 s is applied, whereas for the remaining simulation time, the calculated integration step (e.g. 0.1 s) is used.

Figure 3-22 shows the impact of the UFLS scheme on both the frequency and the power imbalance. The amount of 0.08 pu is shed 0.43 s after the contingency occurred. Clearly, the system remains stable. In fact, frequency is far away from the allowable minimum frequency of 47.5 Hz.

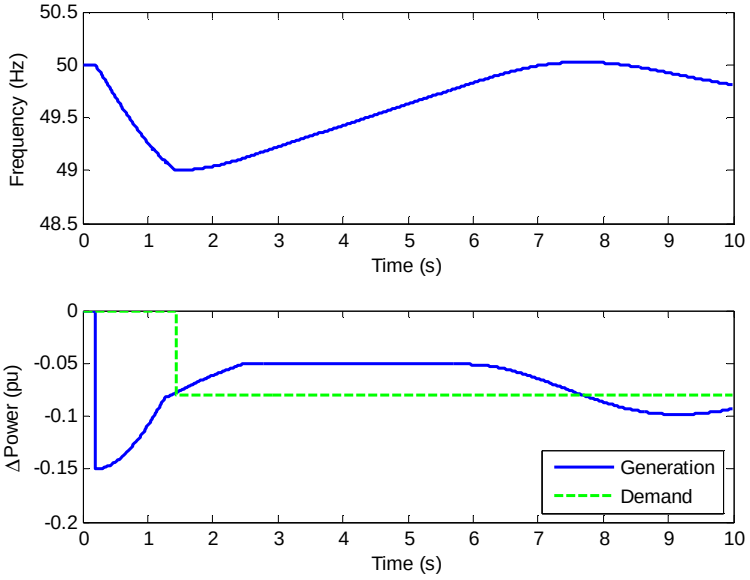

Figure 3-22: The impact of an UFLS scheme on frequency and real power.

Figure 3-23 depicts the effect of the UFLS scheme in the phase plane ω–dω/dt. Initial rate of change of frequency is -1.014 Hz which corresponds with the theoretical amount determined by equation (3.11). Furthermore, the UFLS action at 49 Hz is also clearly observable due to the abrupt change in the rate of change of frequency. Phase-plane analysis can be, as will be seen in appendix B, a powerful tool to study frequency stability.

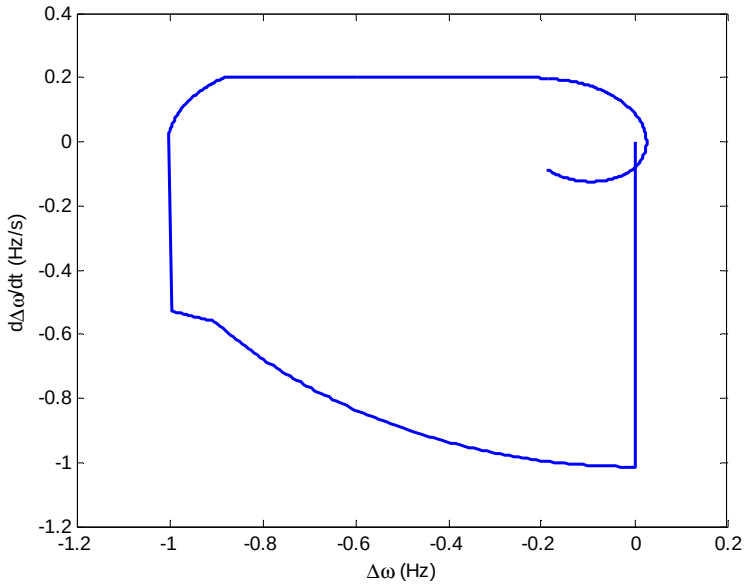

Figure 3-23: Phase-plane representation.

3-7-3 Impact of decoupled power generation

To analyze the impact of decoupled power generation (DPG) penetration on short-term frequency dynamics, consider the power system shown in Figure 3-24, consisting of a conventional generator (CG) and for example, a wind farm represented by an equivalent generator (DPG) [Rouco'08]. This system can be represented by a SFD model, where

the DPG is represented as a generator without inertia and zero gain. Table 3-5 displays the parameters of the SFD model.

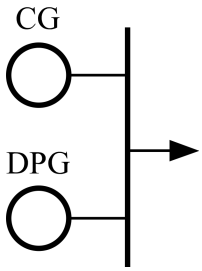

Figure 3-24: Simple power system with decoupled power generation.

Table 3-5: SFD model parameters.

Generator	H (s)	K	a_1 (s)	b_1 (s)	Mbase	Δp_{min}	Δp_{max}
CG	5	25	3	0	100	-	-
DPG	-	-	-	-	100	-	-

According to equation (3.5), the equivalent inertia of the simple power system is 2.5 s. Figure 3-25 shows the impact of the presence of DPG on short-term frequency dynamics and compares the responses with and without decoupled power generation (see Table 3-2). Clearly, the initial rate of change of frequency increases due to reduction of equivalent inertia. Furthermore, primary frequency control capacity is equally affected since the gain is reduced according to equation (3.7) to 12.5 pu. Thus, scenarios with decoupled power generation penetration need to be taken into account for the analysis of short-term frequency dynamics and for the design of UFLS schemes in particular. The proposed SFD model allows including DPG by simply adjusting its parameters.

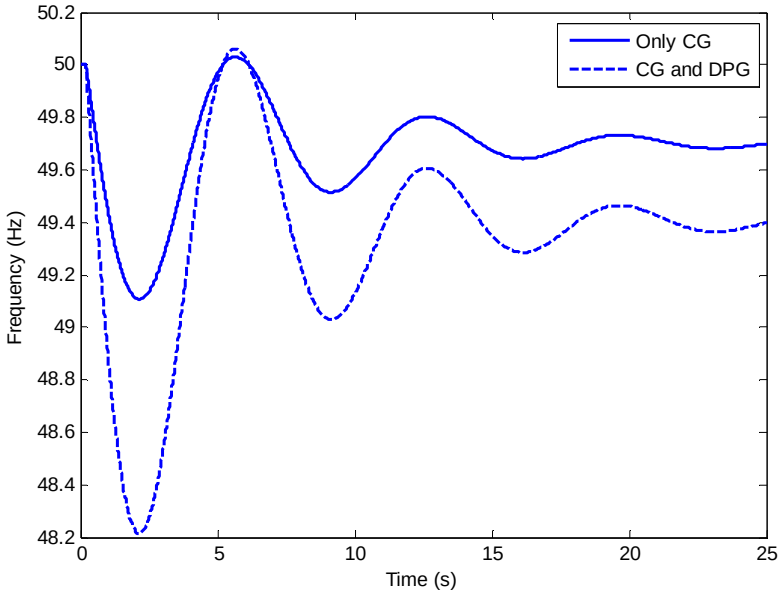

Figure 3-25: The impact of decoupled power generation on frequency.

3-7-4 Summary of the model response sensitivity

The response of the proposed SFD model depends very much on its parameter settings. The impact of these parameter settings has been studied and evaluated by means of SFD model responses in terms of frequency. The following points merit highlighting:

- It has been shown that lower generator model gains (larger droop values) and smaller pole values result in larger frequency deviation. In addition, lower inertia lead to steeper initial rate of change of frequency and to more pronounced frequency oscillations.
- The limit case is given by the actual characteristics of DPG. This kind of generation does not contribute to the system inertia and it does not participate in primary frequency control. Simple substitution of conventional generation by DPG could eventually jeopardize system stability.
- Finally, the impact of limited spinning reserve has also been studied. If available spinning reserve is smaller than the amount of lost generation, the system turns frequency unstable unless load is shed. It has also been shown that non-uniformly distributed spinning reserve could have a negative impact on frequency dynamics.

3-8 PARTIAL CONCLUSIONS

In this chapter, a simple non-linear multi-generator system frequency dynamics (SFD) model has been derived. This SFD model is a low-order model which reduces the computational cost with respect to a fully detailed model maintaining the essential frequency dynamics of the original model. A simple but still accurate model has therefore been obtained which allows simulating a power system with a very low computational cost. The non-linear multi-generator SFD model is used to simulate short-term frequency dynamics of small isolated power systems.

The SFD model is based on the following assumptions: (1) the generating units can be represented by their turbine-governor systems, (2) the network can be neglected and reduced to a single bus, (3) loads are voltage and frequency independent and (4) turbine-governor systems can be represented by non-linear first-order or second-order models. These assumptions have been confirmed for a real power system. The first assumption is a consequence of the fact the short-term frequency dynamics fundamentally depend on the turbine-governor responses, which limit frequency deviations by restoring the power equilibrium. Due to the reduced size of small isolated power systems, the impact of the network on frequency dynamics and frequency dynamics propagation can also be neglected. Neglecting the network implies also neglecting inter-machine oscillations. Frequency is then described by the average system frequency. The third assumption on load modeling can be justified by the fact that voltage dependency is negligible since voltage varies modestly and is usually restored in a short time. Furthermore, frequency dependency can be omitted because the load-damping factor, which describes the frequency dependency of loads, is small compared to the droop of the turbine-governor systems. Thus, the total load connected is constant unless the UFLS scheme does intervene and sheds a fraction of the connected load. Finally, from the shape of the turbine-governor system responses, it can be deduced that they approximately behave like a first-order or second-order models.

Several SFD models have been described. First SFD models only considered the impact of load. A second generation extended the approach on linear single-generator and multi-generator SFD models. However, the assumption of a linear model, neglecting non-linearities such as generator output limitations, is only valid for small power imbalances. For larger imbalances, which are likely to occur in a small isolated power system, non-linearities need to be considered. Further, apart from first-order models, also second-order generator models should be considered. The ability of the proposed non-linear multi-generator SFD model to accurately reproduce short-term

frequency dynamics has been validated comparing the SFD model output with simulations run with PSS/E software package.

The non-linear multi-generator SFD model has been implemented in a toolbox specialized in the analysis of short-term frequency stability (see appendix A for further information on the toolbox). This power-system model is then be used to study the influence of the different model parameters, including the UFLS scheme, on short-term frequency dynamics and on frequency stability. In particular, effects of the inertia, of the parameters of the first-order model approximation of the turbine-governor systems and the effects of the generator output limitations have been analyzed. It has been shown that the inclusion of generator output limitations has a significant impact on short-term frequency dynamics. It has also been shown that the load-damping factor can be neglected. In addition, the positive impact of UFLS scheme on frequency stability has also been illustrated. Finally, decoupled power generation has been studied from a frequency stability point of view. Both the lack of primary frequency control and the lack of inertial response of decoupled power generation require that scenarios with decoupled power generation penetration need to be taken into account for the analysis of short-term frequency dynamics and for the design of UFLS schemes. Decoupled power generation can be included in the proposed SFD model by simply adjusting its parameters.

CHAPTER FOUR

METHOD FOR THE DESIGN OF UFLS SCHEMES

4-1 INTRODUCTION

Today, most of the UFLS schemes are conventional schemes applying underfrequency and rate of change of frequency (ROCOF) relays. Although advanced UFLS schemes improve load-shedding performances, their implementation is delayed since they require considerable data and communication facilities operating at high speeds, which is costly [Blackburn'06]. After all, for large utilities, the installation and implementation of advanced UFLS schemes would require big investments. Furthermore, the technical and technological feasibility is questionable for large power systems. Hence, utilities and energy councils such as NERC, UCTE, etc., still recommend and use conventional UFLS schemes to protect power systems against contingencies [IEEE'87; IEEE'07; NERC'08].

Several methods have been reported in literature to design conventional UFLS schemes, but there exists no systematic, generally accepted method for the design of UFLS schemes [Thalassinakis'04]. Conventional UFLS schemes can be separated into experimental and optimal designs. Experimental designs employ trial-error procedures or choose the best scheme of a set of candidate schemes, whereas optimal designs make use of optimization techniques to determine the settings of the UFLS schemes. Common to all of them is the fact that simulations are indispensable. These simulations evaluate power system responses to a set of hypothetical disturbances. However, no attention has been paid to the selection of these hypothetical disturbances. This chapter focuses thus on a method for the design of robust and efficient UFLS schemes covering both selection of hypothetical disturbances and optimal tuning of UFLS scheme parameters.

This chapter proposes a method for the design of efficient and robust UFLS schemes comprising two tasks: the selection of adequate operating and contingency scenarios and the application of an optimization algorithm. Efficiency is tantamount to shedding a minimum amount of load, whereas robustness denotes efficiency for a set of operating and contingency scenarios. In section 4-2, a method to select adequate operating and contingency scenarios for the design of robust UFLS schemes is presented. This method consists in applying Data Mining techniques to the problem of

representative operating and contingency scenario identification. Then, the adaptive Simulated Annealing optimization algorithm is applied to the optimal tuning of the UFLS parameters. This optimization algorithm should determine the optimal setting of the UFLS parameters and thus, achieve an efficient performance of the UFLS scheme. The formulation of the optimization problem for the design of UFLS schemes is described in more detail in section 4-3. The proposed method for the design of efficient and robust UFLS schemes has been implemented in the Matlab toolbox presented in more detail in the appendix A. Finally, section 4-4 applies the proposed method for the design of UFLS schemes to two real power systems. Chapter 5 discusses the robustness of the designs achieved and provides a sensitivity analysis of the proposed method.

4-2 SELECTION OF OPERATING AND CONTINGENCY SCENARIOS

To design a robust UFLS scheme, different operating and contingency scenarios need to be considered to guarantee the robustness of the approach; therefore, it is crucial to select appropriate operating and contingency scenarios [Lokay'68; Concordia'95]. Operating and contingency scenarios consist in a set of credible disturbances for different operating points, which could be described by their corresponding generation dispatch scenarios. For example, if the scheme has been designed for smaller disturbances, it may not shed sufficient load to avoid a system collapse in the case of a large disturbance. On the contrary, a scheme that has been designed for larger disturbances may shed too much load in cases of smaller disturbances.[1] In small isolated power systems, outages of generating units are usually considered as disturbances because they are likely to occur and they lead to pronounced frequency deviations. Finally, not only N-1 outages have to be considered, but also multiple outages of generators must be assumed, similar to the contingency which led to the Mallorca-Menorca system collapse; therefore, also simultaneous outages of several generators should be taken into account in the selection process of adequate operating and contingency scenarios.

The common practice consists in determining system-operating conditions corresponding to different load-demand levels (e.g. minimum and maximum) and to design the UFLS scheme taking into account the outages of the largest, the smallest and eventually a medium-size generating unit for each of these system conditions. Nevertheless, this kind of scenario selection does not necessarily guarantee a selection of adequate operating and contingency scenarios. Thus, a method based on Data Mining is proposed to identify the representative operating and contingency scenarios, i.e. to find those scenarios which represent best all other possible scenarios, reducing the computational cost and increasing the efficiency of the UFLS scheme design [Sigrist'08]. Figure 4-1 illustrates the method of finding representative operating and contingency scenarios. Two representative operating and contingency scenarios (bold lines) describe in this example two clearly distinct groups of power system responses given in terms of frequency (dashed lines). These representative scenarios are real disturbances given by the outage of a particular generating unit for a particular operating scenario. In fact, this method is based upon the assumption that the power system behaves in a similar way for different disturbances of different operating

[1] The definition of a credible disturbance is somehow vague and strongly depends on the power system and the operator's experience. In connection with UFLS scheme design, a credible disturbance is a possible disturbance that causes a real-power imbalance, that is related with short-term frequency dynamics and that has predictable consequences (e.g., the outage of a generating unit).

conditions. It should be therefore possible to find different patterns in the behavior of the power system.

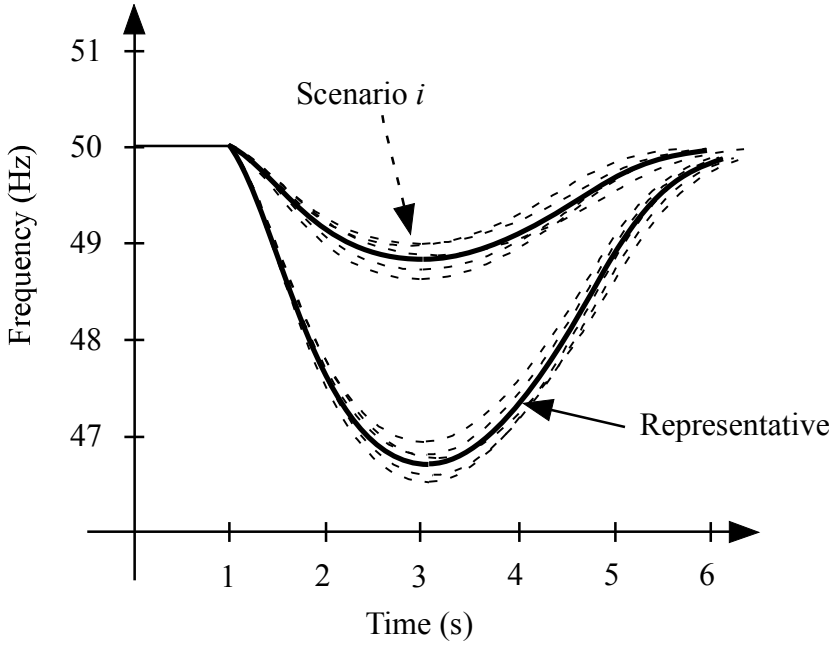

Figure 4-1: Illustration of representative operating and contingency scenarios.

The problem of power-system security assessment presents somehow similarities with the problem of representative operating and contingency scenarios selection. In fact, power-system security assessment is based on contingency analysis determining and classifying contingencies. Contingency analysis is in general only performed on a list of credible contingency cases which are selected by means of so-called contingency selection algorithms [Stott'87]. Contingency selection can be carried out by means of ranking indices, which try to approximately evaluate the load level of transmission lines and transformers after a disturbance, or by dint of contingency screening techniques, which approximate the state of the power system after a contingency by running one or two iterations of a load flow and check for branch overloads and out-of-limit voltages [Gómez-Expósito'08]. Clustering techniques such as artificial neural networks (ANN), Kohonen self-organizing feature maps (KSOM), etc, seem to be well suited to the problem of contingency selection since it is essentially a pattern-recognition problem [Rodrigues'99].

In [Chow'90] an improved Little-Hopfield neural network has been used to classify contingencies since at that time learning algorithms and internal architectures which guaranteed convergence were not available for multiperceptron ANNs. The procedure for classifying contingencies is divided into two stages: the off-line design of the ANN using AC power flows and the on-line classification using real-time measurements. In [Fidalgo'96] and [Mansour'97], multiperceptron feedforward ANNs are used to perform dynamic security evaluation. The ANN carries out contingency screening and ranking. The static and dynamic features were applied as inputs, and the selected outputs were frequency deviation or energy margin and maximum swing angle. In [Niebur'91], KSOM has also been applied to the classification of line-loading patterns after contingencies for power-system static security assessment. KSOM determines similarities of system states in an unsupervised manner. Finally, classification is achieved since KSOM maps secure operating points to a different region of the neural net than insecure operating points. The problem of representative operating and contingency scenarios selection differs from contingency selection as stated by the

contingency analysis by the fact that, instead of approximate power-flow computations, transient power-system simulations are used to quantify contingencies for ranking purposes.

Subsequently, K-Means, Fuzzy C-Means and KSOM algorithms are shortly presented and finally applied to the selection of representative operating and contingency scenarios. These algorithms are very common techniques used in Data Mining [Michie'94; Rojas'96; Hand'01].

4-2-1 Operating and contingency scenarios

An operating and contingency scenario is defined as the outage of a single generator G_i or multiple simultaneous outages of generators $[G_i, G_{i+1}, \ldots]$ for a particular system operating condition. For convenience, a system operating condition will be henceforth described by its corresponding generation dispatch scenario. Thus, representative operating and contingency scenarios are those single or multiple outages of a particular system operating condition which represent all other possible operating and contingency scenarios. In other words, representative scenarios are those scenarios which describe best the patterns in frequency dynamics due to power imbalances.

The non-linearities introduced by the generator-output limitations require a suitable simulation tool to analyze operating and contingency scenarios. Simulations are carried out using the non-linear multi-generator SFD model presented in chapter 3. The operating and contingency scenarios are then given by the corresponding responses of the system frequency to the considered outages:

$$\boldsymbol{\Omega} = \left[\boldsymbol{\omega}_1(t) \quad \ldots \quad \boldsymbol{\omega}_j(t) \quad \ldots \quad \boldsymbol{\omega}_M(t) \right]$$

where $\boldsymbol{\omega}_j(t)$ is the response of the system frequency to *jth* operating and contingency scenario and M is the number of scenarios. The simulation time and the integration step are fixed to ensure that all vectors $\boldsymbol{\omega}_j(t)$ are of the same length. This is important because clustering algorithms employ distance measures (e.g. Euclidean distance) which require vector inputs of equal length.

However, it is not necessary to simulate the SFD model over a longer period since the time window of interest only contains the first few seconds after a contingency. It is during these first seconds the UFLS scheme has to act. Thus, the necessary time window can be reduced, but differences due to slower or faster turbine-governor response or insufficient spinning reserve should still be perceptible [Sigrist'10b]. A solution is to set the simulation time equal to the maximum instant of minimum frequency of all operating and contingency scenarios. Or

$$t_{sim} = \max(t_{\omega min,j}), \quad j = 1, \ldots, M \tag{4.1}$$

where $t_{\omega min,j}$ is the instant of minimum frequency of scenario j. In practice, the instant of minimum frequency is unknown, but it can be estimated. A possible solution is based upon the assumption of a linear SFD model with only one equivalent generator and without generator output limitations. The equivalent generator is represented by a first-order model. In this particular case, the system frequency follows a damped sinusoidal oscillation [Anderson'90]. The oscillation frequency is given by:

$$f_d = \frac{\omega_n}{2\pi}\sqrt{1-\varsigma^2} \tag{4.2}$$

where ω_n is the natural frequency and ς the damping. Equation (4.2) can be rewritten in function of the first-order SFD model parameters as:

$$f_d = \frac{1}{2\pi}\sqrt{\frac{2a_1 K/H - 1}{4a_1^2}} \approx \frac{1}{2\pi}\sqrt{\frac{K}{2Ha_1}} \tag{4.3}$$

Once the oscillation frequency is known, the instant of minimum frequency can be approximated as a quarter of the oscillation period.[2] With typical power system data, the instant of minimum frequency occurs after two to three seconds after the contingency. For example, the smallest K, and the largest a_1 and H could be chosen to calculate, with enough safety margins, the instant of minimum frequency. If second-order generator models were used, either their corresponding first-order generator models could be derived or the parameter a_1 of the second-order model could be employed, being usually the dominant time constant.[3] However, this approximation is based in either case on a linear model. For a non-linear system, the impact of the generator output limitations have to be taken into account and the instant of minimum frequency (i.e., a quarter of the oscillation period) can be estimated by:

$$t_{\omega min} = \frac{k_{lim}(\Delta p_{i,min}, \Delta p_{i,max})}{4 \cdot f_d} \tag{4.4}$$

where k_{lim} is a parameter depending on the generator output limitations $\Delta p_{i,min}$ and $\Delta p_{i,max}$. Thus, according to equation (4.4), the instant of minimum frequency and consequently, the simulation time are determined as a quarter of the oscillation period (the inverse of oscillation frequency) multiplied by a constant k_{lim} taking into account generator output limitations (see also section 3-7-1-3). Experiments showed that k_{lim} ranges between 1 and 2. The integration step is determined as outlined in section 3-7-1.

4-2-2 Data Mining techniques

The identification of representative operating and contingency scenarios can be realized by means of several Data Mining techniques. Data Mining techniques emerged in the early nineties and they allow processing and extracting relevant information from large data bases. Cluster Analysis forms part of Data Mining. Cluster Analysis refers to the partitioning of a data set into clusters, so that the data in each subset ideally share some common trait and differ from the data in other subsets. There exist different methods

---

[2] Note that the simulation time could also be calculated using the methodology outlined in [Egido'10] where the response of a generator i is a linear function in time, i.e. the output is approximated by an average ramp C_i. In this special case, the instant of minimum frequency is given by the quotient of twice the inertia and the sum over all average ramps C_i. Again, the value of the average ramp C_i must be adjusted according to the generator model.

[3] The time constant for a first-order model corresponds to the time need for its associated exponential term to decrease from a value of 1 to a value of 1/e. This definition of time constant is also applicable for undamped ($0 < \varsigma < 1$) and critically damped ($\varsigma = 1$) second-order models and in special occasions even for overdamped second-order models ($\varsigma > 1$) [Cha'00]. With $\varsigma = 0.5a_1/\sqrt{a_2}$ and $\omega_n = 1/\sqrt{a_2}$, the time constant τ_n is defined as:

$$\tau_n = \begin{cases} \dfrac{1}{\varsigma\omega_n}, & \varsigma \le 1 \\ \dfrac{1}{\left(\varsigma - \sqrt{\varsigma^2 - 1}\right)\omega_n}, & \varsigma > 1 \end{cases}$$

based on advanced statistical and modeling techniques such as K-Means, Fuzzy C-Means and KSOM, which are commonly employed.

4-2-2-1 K-Means

The K-Means algorithm attempts to cluster N objects into K_N partitions. The main objective is to find K_N clusters such that the quadratic quantization error (QE) is minimal:

$$\min(QE)$$

with

$$QE = \sum_{c=1}^{K_N} QE_c = \sum_{c=1}^{K_N} \sum_{\substack{e \in Learning\ Set \\ e \in Cluster\ c}} \left\| \mathbf{x}_e - \mathbf{c}_c \right\|^2$$

In general, the Euclidean distance is used as a distance measure between clusters and the input data vectors. The input vectors $\mathbf{x}_e$ belong to the learning set $\mathbf{\Omega}$ and thus, correspond here to the simulated system-frequency responses $\boldsymbol{\omega}_j$ associated to the operating and contingency scenarios. $\mathbf{c}_c$ is the centroid which is computed by averaging the $\boldsymbol{\omega}_j$ associated to the *cth* cluster. The operating and contingency scenario $\boldsymbol{\omega}_j$ closest to the centroid $\mathbf{c}_c$ is then a representative operating and contingency scenario. The number of clusters K_N is a priori unknown and needs to be estimated. Furthermore, K-Means strongly depends on the initial solution due to its inherent gradient-based optimization algorithm to solve QE. Nevertheless, K-Means is a fast algorithm.

4-2-2-2 Fuzzy C-Means

The Fuzzy C-Means algorithm attempts to cluster N objects into C_N partitions. In contrast to the K-Means algorithm, an object can belong to several clusters, with a different degree of membership [Abonyi'07]. The main objective is to find C_N clusters minimizing the Fuzzy C-Means objective function:

$$\min(J)$$

with

$$J = \sum_{e=1}^{N} \sum_{c=1}^{C_N} u_{ec}^m \left\| \mathbf{x}_e - \mathbf{c}_c \right\|^2$$

where m is any real number greater than 1, u_{ec} is the degree of membership of $\mathbf{x}_e$ in the cluster c. The degree of membership is determined by

$$u_{ec} = \frac{1}{\sum_{k=1}^{C_N} \left(\left\| \mathbf{x}_e - \mathbf{c}_c \right\| / \left\| \mathbf{x}_e - \mathbf{c}_k \right\| \right)^{2/(m-1)}}, \ \forall e, \ \forall c \text{ and } m > 1$$

Note that for m approaching 1, Fuzzy C-Means reduces to K-Means. The input vectors $\mathbf{x}_e$ correspond here to the simulated system-frequency responses $\boldsymbol{\omega}_j$ from the learning set $\mathbf{\Omega}$. $\mathbf{c}_c$ is the centroid which is the weighted mean of $\boldsymbol{\omega}_j$, where the weights are the membership degrees. The operating and contingency scenario $\boldsymbol{\omega}_j$ closest to the centroid $\mathbf{c}_c$ is then a representative operating and contingency scenario. The number of clusters C_N is a priori unknown as in the case of K-Means algorithm. The inconvenience with regard to the minimization problem is minor than in the case of K-Means since fuzzy logic allows an input vector belonging to several clusters, improving global

performance of the algorithm. However, in the absence of overlapping partitions, K-Means and Fuzzy C-Means show similar performances.

4-2-2-3 Kohonen Self-Organizing Maps (KSOM)

KSOM learns to classify input vectors according to how they are grouped in the input space [Niebur'91]. The Kohonen network is an array of S neurons. For each simulated system-frequency response $\boldsymbol{\omega}_j$ randomly chosen form the learning set $\boldsymbol{\Omega}$, the KSOM algorithm identifies a winning neuron by an appropriate distance measure such as the Euclidean distance. The winning neuron and all neurons within a certain neighborhood are then updated according to the Kohonen-rule [Rojas'96]. As more and more input vectors are presented, the winning neurons and their neighboring neurons shift towards these vectors and learn vectors similar to each other. That is, the neurons learn to recognize similar profiles within the system-frequency responses of the learning set $\boldsymbol{\Omega}$. The operating and contingency scenario $\boldsymbol{\omega}_j$ closest to a winning neuron is then a representative operating and contingency scenario. However, just as for K-Means, the number of neurons S is a priori unknown and needs to be estimated. Furthermore, the KSOM algorithm is computationally heavier than K-Means. By contrast, it is less sensitive to the initial solution [Michie'94].

4-2-3 Application example

To illustrate the process of operating and contingency scenarios selection, K-Means, Fuzzy C-Means and KSOM algorithms are applied to the clustering of all possible operating and contingency scenarios of the La Palma power system. The La Palma power system is a very small system and consists of eleven generators. Table 4-1 summarizes the generator model parameters. These parameters have been obtained by applying the parameter estimation procedure discussed in section 3-3 and using a closed-loop model structure.

Table 4-1: Parameters of the generator models of the La Palma power system.

Generator	H (s)	K	b1 (s)	b2 (s)	a1 (s)	a2 (s)	Pmin (MW)	Pmax (MW)
G11	1.75	20	1.44	0	18.6	3.98	2.5	4
G12	1.75	20	1.44	0	18.6	3.98	2.5	4
G13	1.75	20	1.44	0	18.6	3.98	2.5	4
G14	1.73	20	1.44	0	18.6	3.98	3	4.5
G15	2.16	20	1.32	0	18.4	2.7	3.5	7
G16	1.88	20	1.43	0	18.7	3.85	3.5	7
G17	2.1	20	1.32	0	18.3	2.71	7	12
G18	6.5	21.25	0.89	0	5.66	3.48	0	22.8
G19	2.1	20	1.32	0	18.3	2.71	7	12
G20	2.1	20	1.32	0	18.3	2.71	7	12
G21	2.1	20	1.32	0	18.3	2.71	7	12

Table 4-2 displays the different generation dispatch scenarios of the La Palma power system without considering decoupled power generation (DPG).

Table 4-2: Generation dispatch scenarios of the La Palma power system without decoupled power generation.

S. O. C.	G11	G12	G13	G14	G15	G16	G17	G18	G19	G20	G21	$P_{G_{tot}} = P_{D_{tot}}$
1	2.35	0	2.35	0	3.29	3.69	10.41	0	0	0	0	22.09
2	0	0	2.35	0	3.29	4.26	9.26	0	0	0	0	19.16
3	0	0	2.35	0	3.29	3.29	9.55	0	0	0	0	18.48
4	0	0	2.35	0	3.29	3.69	8.96	0	0	0	0	18.29
5	0	0	2.35	0	3.29	3.29	9.35	0	0	0	0	18.28
6	0	0	2.35	0	3.29	3.29	9.61	0	0	0	0	18.54
7	2.35	0	2.35	0	3.29	3.29	10.02	0	0	0	0	21.3
8	2.53	0	2.53	0	5.84	5.84	0	0	6.63	4	0	27.37
9	2.35	0	2.35	2.82	4.92	4.92	0	0	6.63	6.7	0	30.69
10	2.41	0	2.41	2.82	5.59	5.59	0	0	6.63	6.7	0	32.15
11	2.46	0	2.46	2.82	5.69	5.69	0	0	6.63	6.7	0	32.45
12	2.49	0	2.49	2.82	5.77	5.77	0	0	6.63	6.7	0	32.67
13	2.58	0	2.58	2.82	5.96	5.96	0	0	6.63	6.7	0	33.23
14	2.4	0	2.4	2.82	5.56	5.56	0	0	6.63	6.7	0	32.07
15	2.35	2.35	2.35	2.82	5.12	5.12	0	0	6.63	4	0	30.74
16	2.35	2.35	2.35	2.82	4.74	4.74	0	0	6.63	4	0	29.98
17	2.35	2.35	2.35	2.82	4.22	4.22	0	0	6.63	4	0	28.94
18	2.35	2.35	2.35	0	3.29	3.29	9.21	0	6.63	0	0	29.47
19	2.35	2.35	2.35	0	3.29	3.29	8.68	0	6.63	0	0	28.94
20	2.35	2.35	2.35	0	3.29	3.29	9.35	0	6.63	0	0	29.61
21	2.35	2.35	2.35	0	3.71	3.71	11.38	0	6.63	0	0	32.48
22	2.35	2.35	2.35	0	3.58	3.58	11.38	4.85	6.63	0	0	37.07
23	2.35	2.35	2.35	0	3.63	3.63	11.38	0	6.63	0	0	32.32
24	2.35	2.35	2.35	0	3.29	3.29	6.63	0	6.63	0	0	26.89
25	0	0	2.35	0	3.29	3.29	9.16	0	0	0	0	18.09
26	2.35	2.35	2.35	0	3.58	3.58	11.38	4.85	6.66	0	0	37.1

The installed capacity of solar and wind-power generation of the Canary Islands amounts to 271 MW, corresponding to 9.5% of the totally installed capacity [REE'08]. For example, on the La Palma island, 5.58 MW of wind power and 0.09 MW of solar power have been installed to date [MITyC'09]. On average, about 5 to 10% of the total demand is covered by solar and wind-power generation [REE'09], which corresponds to an average use of 40% of the installed capacity. Table 4-3 shows the generation dispatch scenarios with 40% of the total installed capacity of DPG in the La Palma power system. To accommodate actual demand coverage by DPG, conventional generation is substituted by DGP. In other words, generating unit G13 of Table 4-2 is substituted by 40% of the installed DPG and the remaining generation of G13 is added to generating unit G15 due to technical minimum of G13. Obviously, solar power is not available at night.

Table 4-3: Generation dispatch scenarios of the La Palma power system with 40% of the total installed capacity of decoupled power generation.

S. O. C.	G11	G12	G13	G14	G15	G16	G17	G18	G19	G20	G21	DPG	$P_{G_{tot}} = P_{D_{tot}}$
1	2.35	0	0	0	3.41	3.69	10.41	0	0	0	0	2.23	22.09
2	0	0	0	0	3.41	4.26	9.26	0	0	0	0	2.23	19.16
3	0	0	0	0	3.41	3.29	9.55	0	0	0	0	2.23	18.48
4	0	0	0	0	3.41	3.69	8.96	0	0	0	0	2.23	18.29
5	0	0	0	0	3.41	3.29	9.35	0	0	0	0	2.23	18.28
6	0	0	0	0	3.41	3.29	9.61	0	0	0	0	2.23	18.54
7	2.35	0	0	0	3.41	3.29	10.02	0	0	0	0	2.23	21.3
8	2.53	0	0	0	6.1	5.84	0	0	6.63	4	0	2.27	27.37
9	2.35	0	0	2.82	5	4.92	0	0	6.63	6.7	0	2.27	30.69
10	2.41	0	0	2.82	5.73	5.59	0	0	6.63	6.7	0	2.27	32.15
11	2.46	0	0	2.82	5.88	5.69	0	0	6.63	6.7	0	2.27	32.45
12	2.49	0	0	2.82	5.99	5.77	0	0	6.63	6.7	0	2.27	32.67
13	2.58	0	0	2.82	6.27	5.96	0	0	6.63	6.7	0	2.27	33.23
14	2.4	0	0	2.82	5.69	5.56	0	0	6.63	6.7	0	2.27	32.07
15	2.35	2.35	0	2.82	5.2	5.12	0	0	6.63	4	0	2.27	30.74
16	2.35	2.35	0	2.82	4.82	4.74	0	0	6.63	4	0	2.27	29.98
17	2.35	2.35	0	2.82	4.3	4.22	0	0	6.63	4	0	2.27	28.94
18	2.35	2.35	0	0	3.37	3.29	9.21	0	6.63	0	0	2.27	29.47
19	2.35	2.35	0	0	3.37	3.29	8.68	0	6.63	0	0	2.27	28.94
20	2.35	2.35	0	0	3.41	3.29	9.35	0	6.63	0	0	2.23	29.61
21	2.35	2.35	0	0	3.83	3.71	11.38	0	6.63	0	0	2.23	32.48
22	2.35	2.35	0	0	3.7	3.58	11.38	4.85	6.63	0	0	2.23	37.07
23	2.35	2.35	0	0	3.75	3.63	11.38	0	6.63	0	0	2.23	32.32
24	2.35	2.35	0	0	3.41	3.29	6.63	0	6.63	0	0	2.23	26.89
25	0	0	0	0	3.41	3.29	9.16	0	0	0	0	2.23	18.09
26	2.35	2.35	0	0	3.7	3.58	11.38	4.85	6.66	0	0	2.23	37.1

To select representative operating and contingency scenarios, all possible scenarios are considered, i.e. all possible individual generator outages for all possible generation dispatch scenarios according to Table 4-3[4]. Figure 4-2 shows the response of the SFD model to all possible operating and contingency scenarios of the La Palma power system.

[4] It could also be possible to determine representative operating and contingency scenarios taking into account actual probabilities of the operating scenarios, i.e., the generation dispatch scenarios, and failure rates of the generating units. However, some operating and contingency scenarios could be missed. This might be critical after all in cases where improbable but severe operating and contingency scenarios are not taken into account. Finally, UFLS schemes are used to protect a power system, including worst-case scenarios with a small probability to occur.

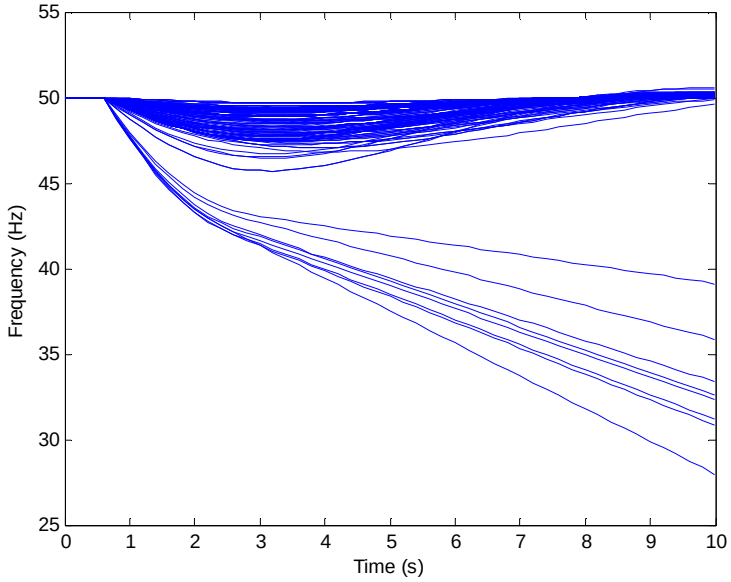

Figure 4-2: SFD model response to all possible operating and contingency scenarios of the La Palma power system.

Clearly, the responses of the SFD model follow some certain patterns. According to (4.4) and with $K = 20$, $a_1 = 18.3\ s$ and $H = 3\ s$, the maximum instant of minimum frequency occurs after about 3.5 seconds after the contingency. Thus, the simulation time for the clustering process is set to 4 s (the additional 0.5 s comes from the fact that the outage occurs at 0.5 s).

Clustering techniques depend on the number of clusters to be formed; therefore, first the number of clusters needs to be decided. A common way to determine the number of clusters is to iteratively apply the K-Means or Fuzzy C-Means algorithm. Figure 4-3 plots the number of clusters against the quadratic quantization error and the Fuzzy C-Means objective function. It can be inferred that four clusters seem to be sufficient. In what follows, the scenarios are grouped according to four clusters.

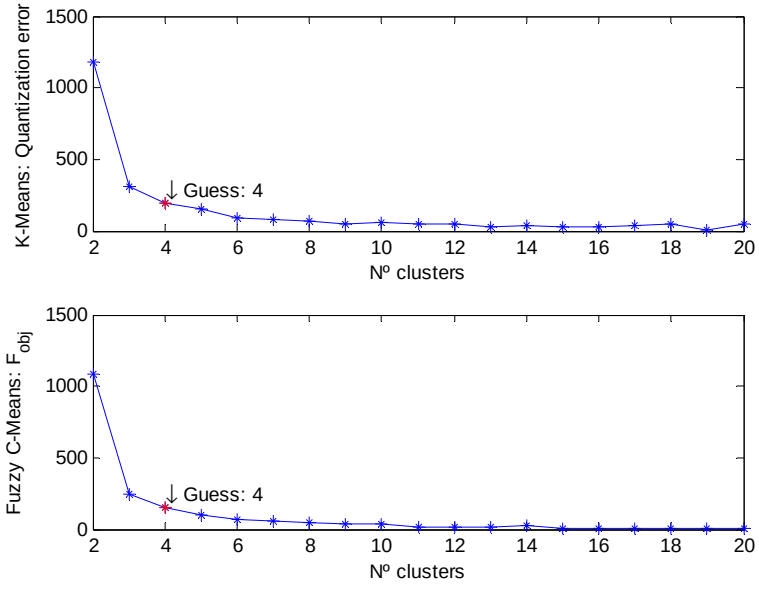

Figure 4-3: Determination of the number of clusters using the K-Means and the Fuzzy C-Means algorithm.

Figure 4-4 shows the results obtained applying K-Means algorithm. It also indicates by the number of vectors or NVR the amount of operating and contingency scenarios belonging to a specific cluster. Figure 4-4 reveals that cluster 3 and cluster 4 of the K-Means algorithm cover the scenarios with smallest and largest frequency deviations, respectively. Furthermore, it can be inferred from clusters 2 and 3 that their respective scenarios seem to have different inherent oscillation frequencies, e.g. the instant of minimum frequency in cluster 3 occurs later than in cluster 2. Finally, outstanding scenarios can be detected in cluster 1. These scenarios have been added to cluster 1 because they are closest to cluster 1 and because there are possibly not enough similar scenarios to lower the cluster. If the scenarios were grouped according to five clusters, these scenarios would form a separate cluster.

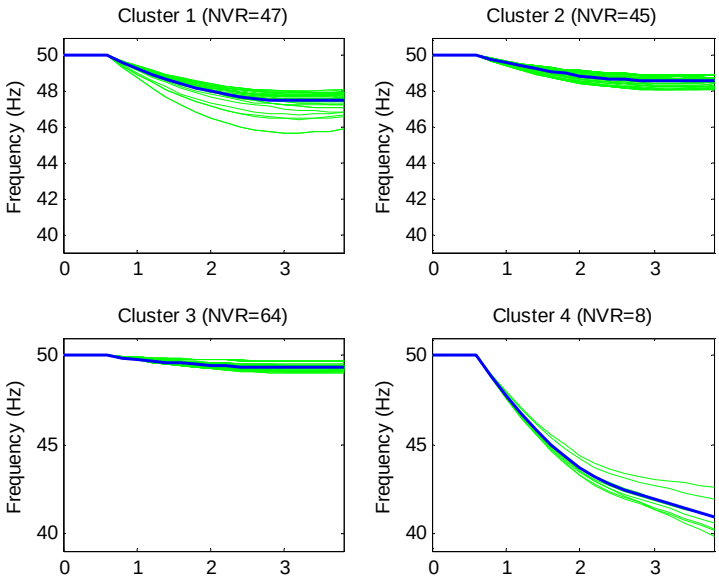

Figure 4-4: Representation of the four clusters formed by K-Means and the associated scenarios.

Table 4-4 and Figure 4-5 give some additional information on the K-Means clusters, showing the distribution of the clusters and the allocation of the scenarios to the four clusters. Remember that representative scenarios are finally described by real disturbances given by the outage of a particular generating unit for a particular operating scenario that are closest to the cluster. As seen from Table 4-4, most of the scenarios belong to cluster 3 (49.4%). Furthermore, it is interesting to note that cluster 4 comprises only the scenarios due to the outages of generator G17 which, if connected, provides more than one third of the total demand (see also Table 4-3), whereas DPG outages are grouped within cluster 3.

Table 4-4: Number of generator outages associated to the K-Means clusters.

Cluster	Occurence (%)	G11	G12	G13	G14	G15	G16	G17	G18	G19	G20	G21	DPG
1	23.2					7	3	6		16	6		
2	22.6					13	16	2	2		4		
3	49.4	20	11		9	6	7			2			26
4	4.9							8					

Figure 4-5 (a) compares the principal component analysis (PCA) of the six clusters and of all possible operating and contingency scenarios[5]. PCA is a useful tool to visualize data distributions. According to the two-dimensional space describe by the first and second PCA components, the distribution of the clusters seems to reflect well the distribution of all possible operating and contingency scenarios. The silhouette plot in Figure 4-5 (b) confirms this[6]. Note that the silhouette plot is able to detect the outstanding scenarios in cluster 1 which have clearly lower and inclusively negative silhouette values. It will be shown in chapter 5 that an additional cluster, which covers these outstanding scenarios, does not significantly improve the UFLS scheme design.

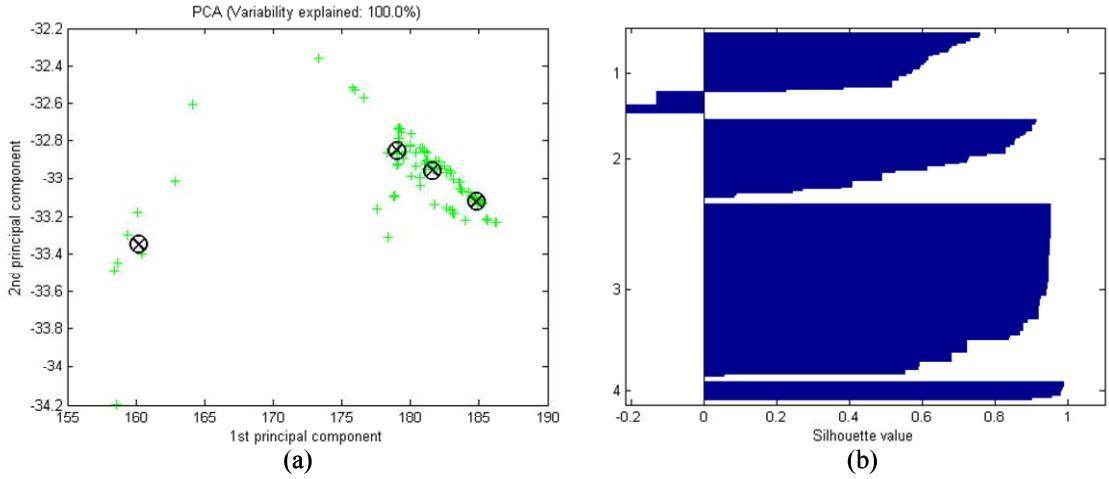

Figure 4-5: (a) Principal component analysis and (b) silhouette plot of the six clusters formed by K-Means and their associated scenarios.

Figure 4-6 compares the clusters obtained by applying different clustering algorithms. From Figure 4-6 it is readily identifiable that not only the K-Means and Fuzzy C-Means algorithms but also KSOM algorithm yielded to nearly the same results, i.e. extremely similar clusters have been identified. The most perceptible differences can be detected for the last cluster, covering scenarios with the largest frequency deviations, and for the second cluster. However, the differences are small shortly after the

[5] PCA is mathematically defined as an orthogonal linear transformation that transforms the data to a new coordinate system such that the greatest variance by any projection of the data comes to lie on the first coordinate (called the first principal component), the second greatest variance on the second coordinate, and so on [Hand'01].

[6] The silhouette plot displays a measure of how close each point in one cluster is to points in the neighboring clusters [Kaufmann'90]. This measure ranges from +1, indicating points that are very distant from neighboring clusters, through 0, indicating points that are not distinctly in one cluster or another, to -1, indicating points that are probably assigned to the wrong cluster. Thus, the more rectangular and the closer to +1 the silhouette of a particular cluster is, the better describes this cluster its associated scenarios.

contingency and increase only after about five seconds in the case of the last cluster. A potential UFLS scheme would have acted during the first two seconds.

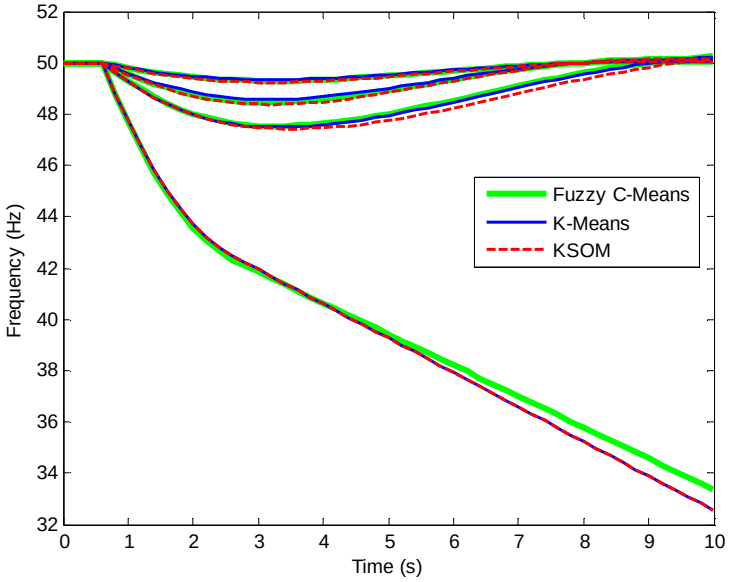

Figure 4-6: Comparison of clusters obtained by K-Means, Fuzzy C-Means and KSOM.

In view of these results, different Data Mining techniques yield to similar results. This is mainly due to the fact that problem posed by the application example seems to be well conditioned in terms of a clear definition of a minimum of the optimization problem inherent to the clustering algorithms. Similar conclusions could have been drawn for other systems. However, the computational cost of different clustering algorithms differs: KSOM is computationally heavier than the Fuzzy C-Means or K-Means; therefore, it is preferable to use Fuzzy C-Means or K-Means with regard to the computational cost. However, KSOM have the advantage that it does not get stuck in a local minimum as it might happen in the case of K-Means or Fuzzy C-Means. The performance of Fuzzy C-Means and K-Means are similar, but Fuzzy C-Means is an improvement over K-Means if the data set is not clearly subdivided into underlying partitions (when clusters overlap). Finally, it must be mentioned that these algorithms define the membership of a particular operating and contingency scenario to a cluster in function of a distance measure. In general, the more operating and contingency scenarios are close to a potential centroid, the more it is possible that they form a cluster. This has a negative impact on a few but clearly distinct operating and contingency scenarios. These scenarios might be grouped into a “wrong” cluster, even if they intuitively form an own cluster. This might be a drawback in cases where extremely severe operating and contingency scenarios were grouped into a cluster describing a less severe scenario.

Finally, Figure 4-7 compares the proposed approach of representative scenario identification with the common practice of manual scenario selection. Generation dispatch scenarios 25 and 26 from Table 4-3 have been chosen (valley and peak demand) and the outages of the largest and the smallest generator for each of these system conditions have been simulated. The representative scenarios correspond to the scenarios obtained by means of the K-Means algorithm. It can be seen from Figure 4-7 that the proposed approach of representative scenario identification covers a wider range of system responses than the common practice of scenario selection. As a consequence, an UFLS scheme designed with operating and contingency scenarios

which have been selected by means of clustering might be more robust than the same UFLS scheme designed with operating and contingency scenarios selected via the common practice.

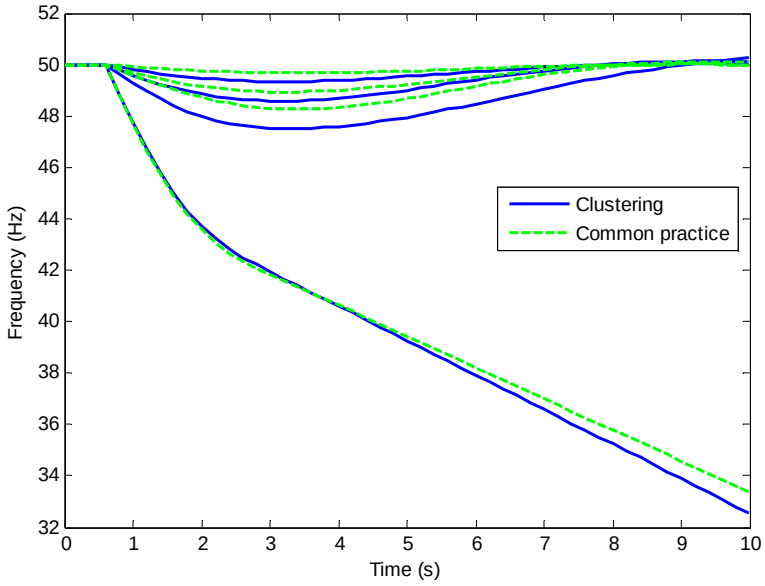

Figure 4-7: Comparison between (a) representative scenarios (continuous line) and (b) scenarios selected manually (dashed line).

4-3 OPTIMIZATION OF UFLS SCHEMES

The efficiency of the UFLS scheme depends on the tuning of the UFLS scheme parameters. Tuning of the UFLS parameters is carried out in function of the selected scenarios. The problem of UFLS tuning can be stated as an optimization problem.

In the literature and as presented in chapter 2, several optimization strategies have been pursued and applied to the design of UFLS schemes (e.g. [Lopes'00; Denis Lee Hau'06]). These strategies include among others steepest descent and quasi-Newton methods such as Sequential Quadratic Programming (SQP) as well as meta-heuristics such as Genetic Algorithms. A substantial drawback of gradient and Hessian-based algorithms lies in the fact that they get caught in local minima. The optimal solution is therefore highly dependent on the initial guess of the decision variables. Furthermore, these algorithms have been created for continuous problems. The optimization of an UFLS scheme, as will be seen later, is a highly discontinuous problem due to step-like behavior of the UFLS scheme. For discontinuous problems, it is difficult to define gradients or even Hessians. Thus, due to the problem's non-linear (generator models) and discontinuous (UFLS) nature, heuristic algorithms seem to be more adequate to optimize an UFLS scheme [Lopes'99; Denis Lee Hau'06]. Several candidate heuristic algorithms exist such as Simulate Annealing (SA), Genetic Algorithms (GA), Tabu Search, Particle Swarm Optimization (PSO), Pattern Search, etc., but most common are SA and GA. Henceforth, adaptive Simulated Annealing algorithm will be used in order to optimize real UFLS schemes. Adaptive Simulated Annealing is an effective optimization algorithm [Ingber'93] that can be easily implemented and that showed good performance in terms of computational effort and optimal solutions found and in

comparison with GA and Patter Search when applied to a simple UFLS scheme design[7]. In addition, this optimization algorithm has not been applied to the design of UFLS schemes so far. In Chapter 5, designs obtained by adaptive Simulated Annealing are compared with GA-based and SQP-based designs.

Equation (4.5) gives a generic formulation of an optimization problem:

$$\begin{aligned} &\underset{\mathrm{x}}{\text{minimize}}\, f(\mathbf{x}_d) \quad \text{s.t.} \\ &lb \le \mathbf{x}_d \le ub \\ &h_l(\mathbf{x}_d) = 0, \quad l = 1,...,m_e \\ &g_l(\mathbf{x}_d) \le 0, \quad l = m_e + 1,...,m_t \end{aligned} \tag{4.5}$$

where $\mathbf{x}_d$ are the decision variables bounded above and below by ub and lb, $f(\bullet)$ is the objective function, $h_l(\bullet)$ and $g_l(\bullet)$ are the equality and inequality constraints, respectively, and m_e and m_t are the number of equality constraints and the total number of constraints, respectively. The decision variables are in the case of UFLS scheme optimization the parameters of the underfrequency and eventually, the ROCOF relays. In particular:

- The frequency threshold $\omega_{thrshld,uf}$ and the intentional time delay $t_{int,uf}$ of the underfrequency relays.
- The frequency threshold $\omega_{thrshld,rocof}$, the ROCOF threshold $d\omega/dt|_{thrshld}$ and the intentional time delay $t_{int,rocof}$ of the ROCOF relays.

This selection of the underfrequency and ROCOF relay parameters as decision variables is tantamount to a partial, more industry-oriented optimization of the UFLS scheme.

In fact, in most optimization strategies applied to the design of UFLS schemes, the step size of each UFLS stage, $p_{step,uf}$ or $p_{step,rocof}$, respectively, has been considered as a decision variable, too [Halevi'93; Martínez'93; Lopes'99; Denis Lee Hau'06]. However, for rather small power systems it does not make sense to adjust the step size. De facto, the step size is usually defined by the utility and also depends on the feeders connected to the relays defined by a particular stage and on the priority of the associated loads; therefore, in smaller power systems such as the La Palma power system, it will be difficult to find feeder blocks which finally sum up to the desired step size. Nevertheless, even if the step size is not a decision variable for rather small power systems, step size of a stage can be varied since it is possible to combine adjacent stages without compromising the priority constraint. Another possibility could consist in relaxing priority of stages which allows rearranging stages, similar to a somehow rough step size optimization. By contrast, in case of bigger systems such as the Gran Canaria power system, it is possible to adjust the step size since feeder blocks are usually a small fraction of the total load under relief and thus, can be readily grouped to sum up to the desired step size. In either case, it is supposed that the implementable step size coincides with actual step size, neglecting thus step-size variations. The latter is studied in more detail in chapter 5.

The efficiency of the UFLS scheme firstly depends of the tuning of the relay parameters and ultimately, on the objective function and constraints imposed to the

[7] Note that since heuristics usually depend on their algorithm parameter settings and because not all existing heuristic algorithms have been tested, this is not equivalent to say that adaptive Simulated Annealing is the best algorithm.

optimization problem. Subsequently, the objective function, the constraints and the applied optimization algorithm are described in more detail.

4-3-1 Objective function

The principal objective of an UFLS scheme is to protect a power system against instability by curtailing a minimum amount of load. Equation (4.6) formulates a possible objective function complying with the principal objective:

$$f_1(\mathbf{x}_d) = \sum_{j=1}^{M} \alpha_{f,j} p_{shd,j}(\mathbf{x}_d) \tag{4.6}$$

where $\alpha_{f,j}$ is a weighting factor, $p_{shd,j}$ the amount of shed load in pu for the *jth* contingency and M is the total number of contingencies. For example, the weighting factor $\alpha_{f,j}$ could be inversely proportional to the amount of lost power generation in pu. This is,

$$\alpha_{f,j} = \frac{p_{loss,max} - p_{loss,min}}{p_{loss,j}}$$

This way, load shedding for smaller outages outweighs load shedding for larger outages, which finally should reduce or even avoid load shedding for smaller outages. It could be also possible to determine the weighting factor $\alpha_{f,j}$ according to the number of operating and contingency scenarios (NVR in Figure 4-4) associated to each representative scenario, trying to reduce, if possible, the amount of shed load for representative scenarios with a larger number of associated operating and contingency scenarios.[8] Figure 4-8 shows the shape of the objective function f_1 in case of a very simple UFLS scheme with only one stage and where only the frequency threshold is optimized, i.e. the decision variable $\mathbf{x}_d$ contains only the frequency threshold. Clearly, the objective function f_1 is discontinuous. Furthermore, the definition of gradients of this objective function would be useless.

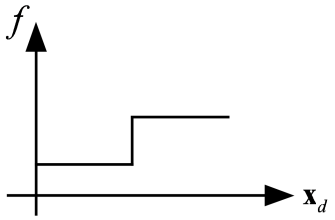

Figure 4-8: Shape of the objective function f_1.

Another possible and more generic formulation of the objective function is given by equation (4.7). The composite objective function f_2 adds to the objective function f_1 a term related with the minimum frequency of each contingency j:

$$f_2(\mathbf{x}_d) = \sum_{j=1}^{M} \alpha_{f,j} p_{shd,j}(\mathbf{x}_d) + \sum_{j=1}^{M} \beta_{f,j} \Delta\omega_{min,j}(\mathbf{x}_d) \tag{4.7}$$

[8] The weighting factor does not necessarily influence the final solution. In fact, the settings of UFLS scheme parameters are not independent of the considered operating and contingency scenarios. For example, although less load could be shed for one scenario, in presence of a second, worse scenario, the amount of load shed in the first scenario must be increased in order to be able to comply with constraints in the second scenario.

where $\alpha_{f,j}$ and $\beta_{f,j}$ are weighting factors. Again, the weighting factors could be inversely proportional to the amount of lost power generation in pu. In this case, $\alpha_{f,j}$ should be arranged in ascending order, from the smallest to the largest loss, and $\beta_{f,j}$ in descending order. In addition, $\beta_{f,j}$ could be multiplied by the equivalent gain k_{eq} of the generators to obtain numerically comparable measures. Mathematically, this can be expressed as follows:

$$\alpha_{f,j} = \frac{p_{loss,max} - p_{loss,min}}{p_{loss,j}}$$

$$\boldsymbol{\beta}_f = \begin{bmatrix} 0 & \cdots & 0 & k_{eq,M} \\ \vdots & & k_{eq,M-1} & 0 \\ 0 & \iddots & & \vdots \\ k_{eq,1} & 0 & \cdots & 0 \end{bmatrix} \boldsymbol{\alpha}_f$$

This way, for example, the minimum frequency deviation outweighs the amount of shed load for larger outages. In other words, the amount of lost load is less important than the minimum frequency deviation. Another possibility is to choose both $\alpha_{f,j}$ and $\beta_{f,j}$ equal to unity [Denis Lee Hau'06], enabling the definition and use of gradients. In this case, the minimum frequency related term simply smoothes the objective function. Figure 4-9 shows the shape of the objective function f_2 in case of a very simple UFLS scheme with only on stage and where only frequency threshold is optimized. The objective function f_2 is still discontinuous, but the effect of the term related with the minimum frequency appears clearly.

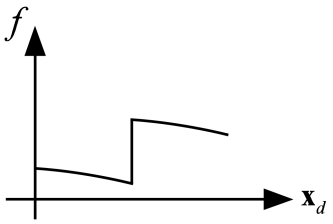

Figure 4-9: Shape of the objective function f_2

Finally, two other possible formulations of the objective function are given by equations (4.8) and (4.9). Again, $\alpha_{f,j}$, $\beta_{f,j}$, $\gamma_{f,j}$ and $\delta_{f,j}$ are weighting factors of the composite objective functions f_3 and f_4.

$$f_3(\mathbf{x}_d) = \sum_{j=1}^{M} \alpha_{f,j} p_{shd,j}(\mathbf{x}_d) + \sum_{j=1}^{M} \gamma_{f,j} \int \frac{1}{2} \Delta\omega_j(\mathbf{x}_d, t)^2 dt \tag{4.8}$$

$$f_4(x) = \sum_{j=1}^{M} \beta_{f,j} \Delta\omega_{min,j}(\mathbf{x}_d) + \sum_{j=1}^{M} \delta_{f,j} \Delta\omega_{ss,j}(\mathbf{x}_d) \tag{4.9}$$

The objective function f_3 [Halevi'93] is similar to the one stated in equation (4.7), but instead of adding a term related to the minimum frequency, the integral of the frequency deviation is added. The difference between the objective functions f_2 and f_3 is then that f_3 attempts to minimize, apart from the amount of shed load, the overall frequency deviation and not only the term related to the minimum frequency. The objective function f_4 is rather exotic since it does not include the amount of shed load, but instead the post-contingency steady-state frequency deviation.

Subsequently, the objective function f_1 given in equation (4.6) is used with a weighting factor $\alpha_{f,j}$ equal to unity. This is justified by the fact that the principal

objective of the UFLS design process is to minimize the amount of shed load. Power-system stability can be guaranteed by adequately implementing some specific constraints such as minimum and maximum allowable frequencies, etc. As long as frequency deviations stay within the established range and comply with the constraints on minimum and maximum allowable frequencies, there is little reason to shed more load in order to reduce frequency deviations and therefore, the objective function does not need to include frequency deviations. Note that objective functions including a frequency-related term might lead to more conservative UFLS scheme designs in the sense that these schemes will shed more load while reducing frequency deviations. The impact of varying the objective function is studied in chapter 5.

4-3-2 Constraints

According to the criteria outlined in chapter 2, the constraints can be divided into two principal categories. The first one contains the constraints imposed by the power system, whereas the second category covers the constraints with respect to the performance of the UFLS scheme. Here, the constraints of the first category are:

- The minimum and maximum allowable frequency values.

In general, the constraint of minimum allowable frequency is accompanied by a maximum time delay during which the frequency can stay below the minimum allowable frequency. Typical values for small isolated power systems are 47.5 Hz during maximum 3 s [REE'05]. The maximum allowable frequency varies between 51.5 and 52 Hz.

The constraints with respect to the performance of the UFLS scheme used here are:

- The UFLS scheme should not act once the frequency has passed its minimum value (or short instant of shedding).
- The UFLS scheme should respect the priority of loads (or short priority).
- The amount of shed load must be lower than or at most equal to the amount of lost real power (or short amount of shed load).

These constraints can be mathematically formulated as inequality constraints $g_l(\mathbf{x}_d) \leq 0$, for $l = m_e+1,\ldots,m_t$, where m_e is the number of equality constraints, m_t the total number of constraints and $\mathbf{x}_d$ is a vector containing the decision variables, i.e.:

$$\mathbf{x}_d = \begin{bmatrix} \omega_{thrshld,uf} \\ \omega_{thrshld,rocof} \\ d\omega/dt_{thrshld} \\ t_{int,uf} \\ t_{int,rocof} \\ p_{step,uf} \\ p_{step,rocof} \end{bmatrix}$$

These decision variables are the frequency thresholds, the intentional time delays and the step sizes of underfrequency and ROCOF stages. Functions $g_1(\bullet)$ and $g_2(\bullet)$ in equation (4.10) describe the constraints of the first category, confining frequency deviation within minimum and maximum allowable frequency values, $\Delta\omega_{min,allowable}$ y $\Delta\omega_{max,allowable}$. Note that the constraint on minimum allowable frequency is usually accompanied by a maximum time delay $t_{max,j}$ during which the frequency of the *jth*

operating and contingency scenario (of totally M scenarios) can stay below the minimum allowable frequency.

$$\begin{aligned} g_1(\mathbf{x}_d, t) &= \Delta\omega_{min,allowable} - \Delta\omega_{min,j}(\mathbf{x}_d) \quad \text{for} \quad t < t_{max,j}, \quad j = 1,...,M \\ g_2(\mathbf{x}_d) &= \Delta\omega_{max,j}(\mathbf{x}_d) - \Delta\omega_{max,allowable} \end{aligned} \tag{4.10}$$

Functions $g_3(\bullet)$, $g_4(\bullet)$ y $g_5(\bullet)$ in equation (4.11) implement the constraints associated to the second category. Constraint $g_3(\bullet)$ restricts the instant of shedding $t_{shd,j}$ of the *jth* operating and contingency scenario to the instant of minimum frequency $t_{\omega min,j}$. Function $g_4(\bullet)$ controls the priority by imposing a minimum difference of σ_ω Hz between the frequency thresholds $\omega_{thrshld}$ of two consecutive stages. A comment must be made with respect to this implementation. In fact, this constraint causes that there is a difference of σ_ω Hz between each stage of the UFLS scheme and thus, only indirectly controls the criterion on priority of the loads[9]. During the optimization process, the constraint on priority is evaluated. Nonetheless, it might be desirable to impose a certain difference of σ_ω Hz between adjacent stages. Finally, constraint $g_5(\bullet)$ limits the amount of shed load $p_{shd,j}$ to the amount of lost generation $p_{loss,j}$.

$$g_3(\mathbf{x}_d) = t_{shd,j}(\mathbf{x}_d) - t_{\omega min,j}(\mathbf{x}_d) \quad \text{for} \quad j = 1,...,M$$

$$g_4(\mathbf{x}_d) = \left[\begin{array}{ccccc|ccc|ccc|ccc|ccc|ccc} -1 & 1 & \cdots & & & 0 & & \cdots & & 0 & 0 & \cdots & 0 & \cdots & \cdots & \cdots & 0 & \cdots & 0 \\ 0 & 0 & \vdots & & & 0 & & \vdots & & 0 & & & & & & & & & \\ 0 & 0 & 0 & -1 & 1 & 0 & & \cdots & & 0 & & \vdots & & \vdots & \vdots & \vdots & & \vdots & \\ 0 & & \cdots & & & -1 & 1 & \cdots & & & & \vdots & & \vdots & \vdots & \vdots & & \vdots & \\ 0 & & \vdots & & & 0 & 0 & \vdots & & & & & & & & & & & \\ 0 & & \cdots & & & 0 & 0 & 0 & -1 & 1 & 0 & \cdots & 0 & \cdots & \cdots & \cdots & 0 & \cdots & 0 \end{array}\right] \mathbf{x} - \left[\begin{array}{c} \sigma_\omega \\ \\ \vdots \\ \vdots \\ \\ \sigma_\omega \end{array}\right]$$

$$g_5(\mathbf{x}_d) = p_{shd,j}(\mathbf{x}_d) - p_{loss,j}$$

(4.11)

Finally, the decision variables are bounded above and below as indicated in equation (4.12). The range of the frequency threshold of the underfrequency relays $\omega_{thrshld,uf}$ is typically between 47 and 49 Hz, whereas the range of the frequency threshold of the ROCOF relays $\omega_{thrshld,rocof}$ varies between 49.3 to 49.8 Hz. The ROCOF threshold $d\omega/dt|_{thrshld}$ depends on the power system and ranges usually between -0.5 Hz/s and -2.5 Hz/s. The intentional time delays $t_{int,uf}$ and $t_{int,rocof}$ vary typically between 0 and 0.5 to 1 s. The step size varies normally between 10 and 15% of the load demand [REE'95]. In [Denis Lee Hau'06], the step size $p_{step,uf}$ ranges between 5 and 20% for underfrequency steps, whereas for ROCOF steps, the step size $p_{step,rocof}$ may vary between 0 and 50% of the total load demand.

[9] Priority is guaranteed for the cases where the intentional time delay is very small and frequency thresholds are used to differentiate the UFLS stages. In these cases, there exists no overlapping of UFLS stages. However, time delays are not always very short and thus, the (i+1)*th* stage may act without the *ith* stages acts.

$$\begin{bmatrix} \omega_{thrshld,uf,min} \\ \omega_{thrshld,rocof,min} \\ d\omega/dt_{thrshld,min} \\ t_{int,uf,min} \\ t_{int,rocof,min} \\ p_{step,uf,min} \\ p_{step,rocof,min} \end{bmatrix} \leq \mathbf{x} \leq \begin{bmatrix} \omega_{thrshld,uf,max} \\ \omega_{thrshld,rocof,max} \\ d\omega/dt_{thrshld,max} \\ t_{int,uf,max} \\ t_{int,rocof,max} \\ p_{step,uf,max} \\ p_{step,rocof,max} \end{bmatrix} \tag{4.12}$$

4-3-3 Solution by Simulated Annealing

The Simulated Annealing algorithm was independently introduced and applied to an optimization problem by Kirkpatrick [Kirkpatrick'83] and Cerny [Cerny'85]. Simulated Annealing is a heuristic method suited to solve complex optimization problems of combinatorial nature. Typical examples are the travelling salesman or the component placement problem [Kirkpatrick'83; Dowsland'03].

This classical algorithm relates the annealing of a material, i.e. finding its minimum energy state, to the solution of an optimization problem. If a liquid material anneals too fast, it solidifies in a suboptimal energy state. In contrast, a slow annealing process guarantees an optimal solidification (minimum energy state). Mathematically, this has been described by the Metropolis algorithm which simulates the energy variations of a system of particles with decreasing temperature, until a minimum energy state is reached [Metropolis'53].

At a certain temperature τ, a new possible solution (i.e. the configuration Γ) is retained with a probability following a Boltzmann distribution, even if its associated energy state is worse than the one obtained by the previous configuration. If the energy state of the new solution is lower than the energy state of the previous solution, the new solution is automatically accepted. The classical Simulated Annealing algorithm tends to find minimum energy states with progressively decreasing temperatures. Figure 4-10 summarizes the Simulated Annealing algorithm.

1. define τ_0, Γ_0
2. set $\tau_0 \rightarrow \tau_{k=1}, \Gamma_0 \rightarrow \Gamma_{actual}$
3. while $T_0 > T_{min}$ or not Stop Criterion
4. while not Equilibrium
5. create $\Gamma_{disturbed}$
6. $E_1 = E(\Gamma_{actual})$
7. $E_2 = E(\Gamma_{disturbed})$
8. $\Delta E = E_1 - E_2$
9. if $\Delta E < 0$
10. $\Gamma_{disturbed} \rightarrow \Gamma_{actual}$
11. else
12. if $e^{-\Delta E/\tau k} >$ Random
13. $\Gamma_{disturbed} \rightarrow \Gamma_{actual}$
14. end
15. end
16. end
17. $\tau_k \rightarrow \tau_{k+1}$
18. end

} Metropolis

Figure 4-10: Classical Simulated Annealing algorithm.

The algorithm starts with an initial configuration of the variables Γ_0, commonly random, and an initial temperature τ_0 (lines 1 and 2). For a given temperature τ_k at iteration k, the energy states of the current and the disturbed configuration are calculated and compared (lines 5-8). If the energy of the disturbed configuration is lower than the energy of the current configuration, the disturbed configuration is accepted (lines 9 and 10). In the contrary case, the disturbed configuration is accepted with a probability from a Boltzmann distribution (lines 12 and 13). This is repeated until the energy equilibrium has been reached. Then the temperature is lowered (line 17). With lower temperature, fewer configurations which deteriorate the solution are accepted. The algorithm stops when the temperature has fallen below a certain minimum or when another stop criterion has been fulfilled (e.g. relative improvement of the objective function over a certain number of iterations).

In an optimization problem, the temperature loses its physical meaning and only acts as a control parameter. The initial temperature τ_0 should be sufficiently high to accept most of all disturbed configurations and to guarantee somehow the independence of the initial solution [Kirkpatrick'83; White'84; Dowsland'03]. In [Johnson'89], it is suggested that the initial temperature is such that the initial acceptance probability is about 40%. Clearly, if the initial temperature is set to the standard deviation of the objective function, then the initial acceptance probability is about 40% [White'84]. It is however also possible to iteratively determine the initial temperature in order to obtain a desired initial acceptance probability as proposed in [Kirkpatrick'83].

The condition of the energy equilibrium can be implemented using an iteration loop. For example, in [Johnson'89] the number of iterations L is determined by multiplying the expected neighborhood size by a constant and after L iterations, the best solution and its associated configuration are considered as the state of energy

equilibrium.[10] The condition of energy equilibrium can be avoided using the so-called adaptive Simulated Annealing algorithm [Ingber'89; Ingber'93] presented hereafter.

The disturbed configuration can be obtained in various ways by changing one or several elements of the current configuration. In either case, the neighborhoods must be defined such that any point in the finite search space is reachable from any other point through traversals of neighboring points. Thus, the generation probability to create a disturbed configuration from the current configuration must be bigger than zero and the sum of all generation probabilities from a given current configuration must equal to one. Several generation functions have been reported:

- Randomly pick an element of the current configuration and randomly select a value within the element's bounds [Brooks'95]
- Add a Boltzmann-distributed perturbation to the current configuration [Szu'87]
- Add a Cauchy-distributed perturbation to the current configuration [Szu'87; Wah'99]
- Add a Gaussian-distributed perturbation to the current configuration [Wah'99]
- Add an uniform random variable to the current configuration [Guo'05]

Commonly, to confine the neighborhood, generation functions or some of their parameters depend on the temperature or on the rate of accepted and rejected configurations [Ingber'93; Wah'99].

Nonetheless, most important to Simulated Annealing is the choice of the cooling (annealing) schedule [Dowsland'03]. An infinitely slow cooling scheme guarantees the convergence to the global optimum. However, the convergence is only guaranteed for an infinitely slow cooling which is not realistic. In [Hajek'88], it was shown that a cooling schedule following an inverse logarithmic function multiplied by the maximum depth guarantees asymptotic convergence to the global optimum. However, the value of the maximum depth to escape local optima is in practice unknown. Thus, several cooling schedules have been proposed in the literature:

- geometric (exponential) [Kirkpatrick'83; Ingber'93]: $\tau_{k+1} = a_\tau \tau_k$
- reciprocal [Szu'87]: $\tau_k = \tau_0 / k$
- rational [Lundy'86]: $\tau_{k+1} = \tau_k / (1 + b_\tau \tau_k)$

In general, the geometric cooling schedule is used, with a_τ taking values between 0.8 and 0.97.

It is interesting to see that in function of the neighborhood function and the cooling schedule, different Simulated Annealing algorithms can be identified. If a inverse logarithmic cooling schedule and a Boltzmann-distributed neighborhood were used, the classical Simulated Annealing is obtained, whereas if a reciprocal cooling schedule and a Cauchy-distributed neighborhood were used, Fast Simulated Annealing is obtained [Szu'87]. If a geometric cooling schedule and a specific, shrinkable uniform neighborhood distribution were employed, one obtains the Adaptive Simulated Annealing algorithm. This algorithm is used throughout this dissertation for the optimization of UFLS schemes due to its good performance. It has also been

[10] From any given state s, there are a set of states, say N, where transitions from s are allowed, i.e. these states must be reachable through traversals of neighboring states. N is then set of neighbors of s. If only one element of a configuration can be changed, then the neighborhood size coincides with the number of decision variables.

implemented by Matlab. Adaptive Simulated Annealing includes also Reannealing which periodically rescales the temperature in function of the sensitivity of the objective with respect to the configuration [Ingber'89]. Reannealing attempts to stretch out the range over which the relatively insensitive configuration elements are being searched.

Finally, the energy state is equivalent to the objective function value. A penalty term needs to be added to the objective function to handle the constraints with Adaptive Simulated Annealing. Equation (4.13) describes the energy function.

$$E(\mathbf{x}_d) = f(\mathbf{x}_d) + \phi(g_l(\mathbf{x}_d)), \quad l = m_e + 1, ..., m_t \tag{4.13}$$

where $f(\bullet)$ is the objective function and $\Phi(\bullet)$ is the penalty term associated to the constraints. The simplest implementation of a penalty function consists in death penalties, i.e., rejecting all infeasible solutions. Barrier functions offer another possibility. This means, if a solution is infeasible, i.e. some constraints are violated, a sufficiently large constant is added to the objective function. Such simple penalty functions define therefore a very restrictive feasibility region. A more sophisticated penalty function determines the degree of constraint violation and takes into account the importance of the constraint. The degree of violation can be either the number of constraint violation or the amount of constraint violation, or both [Yeniay'05]. Usually, constraints can be divided into soft and hard. Hard constraints need to be fulfilled always (e.g. the minimum allowable frequency), whereas soft constraints can be violated in a certain degree. Thus, the penalty function should strongly penalize the violation of the minimum allowable frequency constraints but not the constraints corresponding to the latest shedding instant, for example. Good results have also been obtained by including temperature dependent penalty functions [Stern'92]. In [Wah'99], the constrained Simulated Annealing algorithm is presented which includes Lagrange multiplier in the search space and increases their values accepting lower values similar to the Metropolis criterion. However, due to the Simulated Annealing's property to accept from time to time worse solutions, relatively simple penalty function formulations lead to feasible, satisfactory results [Zabinsky'03].

Subsequently, the adaptive Simulated Annealing algorithm is applied to optimization of UFLS scheme designs. Adaptive Simulated Annealing is shown in Figure 4-11.

1. define τ_0, Γ_0
2. set $\tau_0 \rightarrow \tau_{k=1}, \Gamma_0 \rightarrow \Gamma_{actual}$
3. while not Stall
4. $\quad \Gamma_{disturbed} = \Gamma_{actual} + \text{Range}_{\Gamma} \cdot \text{sign}(u - 0.5)\, \tau_k[(1 + 1/\tau_k)^{|2u-1|} - 1]$
5. $\quad E_1 = f(\Gamma_{actual}) + \Phi(g_l(\Gamma_{actual}))$
6. $\quad E_2 = f(\Gamma_{disturbed}) + \Phi(g_l(\Gamma_{disturbed}))$
7. $\quad \Delta E = E_1 - E_2$
8. $\quad$ if $\Delta E < 0$
9. $\quad\quad \Gamma_{actual} = \Gamma_{disturbed}$
10. $\quad$ else
11. $\quad\quad$ if $e^{-\Delta E/\tau k} >$ Random
12. $\quad\quad\quad \Gamma_{actual} = \Gamma_{disturbed}$
13. $\quad\quad$ end
14. $\quad$ end
15. $\quad \tau_{k+1} = a_\tau \tau_k$
16. $\quad$ if ReannealInterval
17. $\quad\quad \tau_{k+1} = \text{Reanneal}(\Delta E)$
18. $\quad$ end
19. end

Metropolis

Figure 4-11: Adaptive Simulated Annealing algorithm.

The working principle is similar to the one of the classical Simulated Annealing summarized in Figure 4-10. The initial temperature τ_0 is determined by the value of the energy function of the initial configuration. The initial solution (or configuration) Γ_0 is given by settings of the existing UFLS scheme. The stop criterion *Stall* corresponds to the satisfaction of the relative improvement of the objective function over a certain number of iterations (line 3). This iteration number depends on the number of decision variables. In line 4, a shrinkable, temperature-dependent uniform neighborhood distribution is used to create the disturbed configuration (u is a uniformly distributed random variable). $Range_{\Gamma}$ is the range of the decision variables (see section 4-3-2). Again, the Metropolis algorithm is applied to accept or reject a new configuration $\Gamma_{disturbed}$. The temperature at iteration k, τ_k, is lowered according to a geometric cooling scheme (line 15). Line 16-18 show the mechanism of Reannealing, activated after a certain number of disturbed configurations *ReannealInterval* have been accepted (typically 100). Constraints are implemented via penalty functions depending on the degree of constraint violation and taking into account the importance of the constraint. In its most generic formulation, the penalty function is:

$$\phi(\mathbf{x}_d) = \mu \sum_{l=m_e+1}^{m_t} d_l \left(C_{1,l} + C_{2,l} g_l(\mathbf{x}_d) \right) \tag{4.14}$$

where d_l indicates whether the constraint l is active (i.e. 1) or not (i.e. 0), whereas $C_{1,l}$ and $C_{2,l}$ are penalty constants and μ an iteration dependent factor. These constants also ensure that the importance of the constraint is taken into account. In fact, $C_{1,l}$ is chosen such that the sum of soft-constraint violations (e.g., instant of shedding) is always inferior to the sum of hard-constraint violations (e.g., minimum allowable frequency). Equation (4.14) resembles the co-evolutionary penalty function described by [Coello'99]. If penalty constant $C_{2,l}$ is set to 0, a penalty function uniquely depending on

the number of constraint violations is obtained, similar to the one used in [Kuri-Morales'02] and in [Skiena'98] for Simulated Annealing.

4-3-4 Application example

As an example, the optimization of the La Palma UFLS scheme is shown. According to the common practice of operating and contingency scenarios selection, generation dispatch scenarios 25 and 26 of Table 4-3 have been chosen, corresponding to valley and peak load-demand levels, and the outages of the largest and the smallest generator for each system operating condition, i.e., generation dispatch scenario, will be simulated. In particular, the outages of generators DPG and G17 for generation dispatch scenario 25 and the outages of DPG and G17 for generation dispatch scenario 26 are considered. Table 4-5 gives some additional information on the selected operating and contingency scenarios.

Table 4-5: Operating and contingency scenarios of the La Palma power system according to the common practice.

Scenario	Generator	Pdem (MW)	Ploss (MW) (%)
25	G17	18.09	9.16 (50.6)
25	DPG	18.09	2.23 (12.3)
26	G17	37.1	11.38 (30.7)
26	DPG	37.1	2.23 (6.0)

Table 4-6 details the existing UFLS scheme of the La Palma power system. This UFLS scheme will be optimized taking into account the following constraints:

- $\omega < 48$ Hz for maximum 2 s
- $\omega > 47$ Hz and $\omega \leq 52$ Hz
- Instant of shedding, i.e. no shedding after the instant of minimum frequency
- Priority, i.e. maintaining the priority associated to each stage
- The amount of shed load [MW] < the amount of loss power generation [MW]

Constraints imposed on minimum allowable frequency are more restrictive than those described in section 2-3-3 (e.g. $\omega < 47.5$ Hz for maximum 3 s). This leads to a more conservative scheme and gives therefore a certain safety margin. Further, more restrictive constraints might also benefit UFLS scheme performance in the case of assumed step sizes do not correspond with actual step size due to feeder-load variation, feeder outages or breaker failures. The latter is studied in more detail in chapter 5.

Table 4-6: Existing UFLS scheme of the La Palma power system.

Underfrequency relays					
Stage	ω (Hz)	t_{int} (s)	t_{opn} (s)	Step size (%)	Cumulative (%)
1	48.81	0.6	0.2	7.1	7.1
2	48.81	0.9	0.2	0.6	7.7
3	48.66	1.3	0.2	14.5	22.2
4	48.66	1.8	0.2	3.6	25.8
5	48.66	2.3	0.2	7.3	33.1
6	48.00	1.2	0.2	13.6	46.7
7	48.00	1.7	0.2	12.5	59.2
8	47.00	1.8	0.2	4.2	63.4
9	47.00	2.1	0.2	15.1	78.5
10	47.00	2.4	0.2	20.5	99

ROCOF relays						
Stage	ω (Hz)	dω/dt (Hz/s)	t_{int} (s)	t_{opn} (s)	Step size (%)	Cumulative (%)
1	49.50	-1.8	0.1	0.2	7.1	7.1
2	49.50	-1.8	0.1	0.2	0.6	7.7
3	49.50	-1.8	0.1	0.2	14.5	22.2
4	49.50	-1.8	0.1	0.2	3.6	25.8

A partial, more industry-oriented optimization strategy is applied. In other words, the decision variables are the parameters of the underfrequency and ROCOF relays; in particular, the frequency thresholds, ROCOF thresholds and the intentional time delays. The UFLS scheme parameters are bounded above and below as follows:

- 47 Hz ≤ Frequency threshold of the underfrequency relays ≤ 49 Hz
- 49.3 Hz ≤ Frequency threshold of the ROCOF relays ≤ 49.8 Hz
- -1.5 Hz/s ≥ ROCOF threshold of the ROCOF relays ≥ -2.5 Hz/s
- 0 s ≤ Intentional time delay for both relay types ≤ 0.5 s

The step sizes of the underfrequency and ROCOF steps have not been considered here as decision variables and therefore, the step sizes of the existing UFLS scheme have been used. This coincides with a partial, more industrial-oriented strategy. In fact, the step size is usually defined by the utility and also depends on the feeders connected to the relays defined by a particular stage and on the priority of the associated loads; therefore, in smaller power systems such as the La Palma power system, it will be difficult to find feeder blocks which finally sum up to the desired step size. In chapter 5, the inclusion of step sizes as decision variables is studied, i.e., a complete optimization strategy is pursued.

The optimization is carried out using the adaptive Simulated Annealing algorithm discussed in section 4-3-3 and shown in Figure 4-11. Parameter a_τ of the cooling scheme is set to 0.95, the interval of Reannealing is set 100 and parameter μ of the penalty function has been assumed constant and set to 1. These are typical values for the adaptive Simulated Annealing algorithm. The initial temperature τ_0 is determined by the value of the energy function of the initial configuration, i.e., the settings of the existing UFLS scheme. Assuming that the constraint on the instant of shedding is less important than the constraint on priority which, in turn, is less important than the constraints on allowable frequencies and amount of shed load, the penalty constant $C_{1,l}$ for the constraint on the instant of shedding is set to 1, $C_{1,l}$ related to the constraint on priority is set to 5 and $C_{1,l}$ associated to the constraints on allowable frequencies and amount of shed load is set to 25. In other words, the algorithm prefers that for the four considered operating and contingency scenarios, constraints on instant of shedding and priority are violated instead of constraints on allowable frequencies or the amount of shed load. $C_{2,l}$

is adapted during the adaptive Simulated Annealing such that the amount of constraint violation is taken into account but without distorting the importance of the constraint imposed by $C_{1,1}$. These setting have been experimentally determined and led to satisfactory results.

Table 4-7 shows the optimized UFLS scheme (adjusted steps in red bold). The number of stages optimized depends on the maximum amount of lost power generation. For, example, the outage of generator G17 for the generation dispatch scenario 25 implies a lost of 50.6 % of power generation. Thus, using the first six stages of the UFLS scheme in Table 4-6, the system can be stabilized and consequently, the first six stages have been optimized. This indicated by red bold characters. It can be inferred from Table 4-7 that the optimization algorithm lowered the frequency threshold values and decreased the values of the intentional time delays. Note that the new ROCOF threshold is close to the original one, although a bit lower. Remaining steps (7 to 10) could be used as backup steps in case of step-size variations or non-responding turbine-governor systems (see chapter 5).

Table 4-7: Optimized UFLS scheme of the La Palma power system.

Underfrequency relays					
Stage	ω (Hz)	t_{int} (s)	t_{opn} (s)	Step size (%)	Cumulative (%)
1	**48.20**	**0.49**	**0.2**	**7.1**	**7.1**
2	**48.08**	**0.21**	**0.2**	**0.6**	**7.7**
3	**47.98**	**0.23**	**0.2**	**14.5**	**22.2**
4	**47.81**	**0.5**	**0.2**	**3.6**	**25.8**
5	**47.60**	**0.15**	**0.2**	**7.3**	**33.1**
6	**47.44**	**0**	**0.2**	**13.6**	**46.7**
7	48.00	1.7	0.2	12.5	59.2
8	47.00	1.8	0.2	4.2	63.4
9	47.00	2.1	0.2	15.1	78.5
10	47.00	2.4	0.2	20.5	99

ROCOF relays						
Stage	ω (Hz)	dω/dt (Hz/s)	t_{int} (s)	t_{opn} (s)	Step size (%)	Cumulative (%)
1	**49.55**	**-2.1**	**0.05**	**0.2**	**7.1**	**7.1**
2	**49.55**	**-2.1**	**0.05**	**0.2**	**0.6**	**7.7**
3	**49.55**	**-2.1**	**0.05**	**0.2**	**14.5**	**22.2**
4	**49.55**	**-2.1**	**0.05**	**0.2**	**3.6**	**25.8**

Figure 4-12 and Table 4-8 compare the two UFLS schemes. Figure 4-12 shows the impact on system frequency of both, the existing and the optimized UFLS scheme. From Figure 4-12, one can see that the minimum and maximum frequency deviations clearly exceed the minimum and maximum allowable frequency deviations in case of the existing UFLS scheme. Frequency overshoot also indicates overshedding. In the case of the optimized UFLS scheme, frequency is confined within the allowable frequency range.

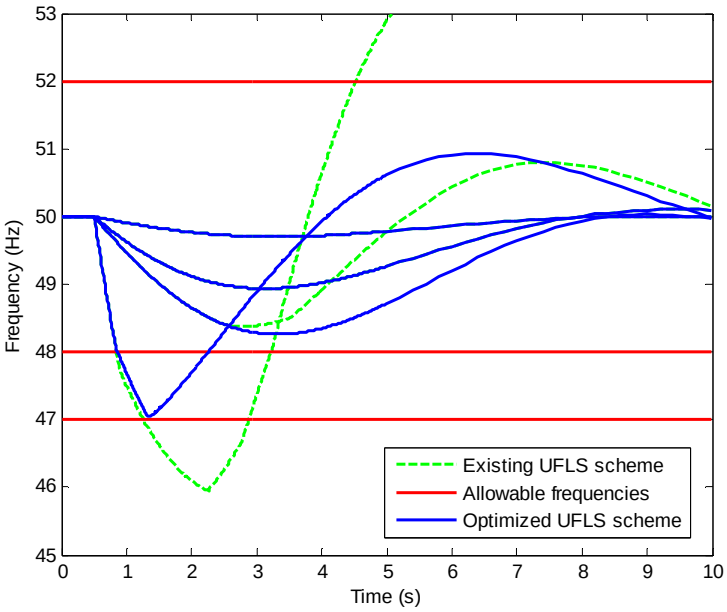

Figure 4-12: Comparison of the SFD model responses of the existing and the optimized UFLS scheme of the La Palma power system.

Table 4-8 provides some additional information on the performance of both the existing and the optimized UFLS scheme. Table 4-8 indicates whether the UFLS scheme satisfies the constraints on its performance (state) and in addition, provides a cause in case of constraint violation. For example, it can be inferred that the existing UFLS scheme sheds too much load for the first contingency (error state with cause 2). Furthermore, load is shed after the frequency has passed its minimum. Overshedding is also the reason for the large frequency overshoot and the resulting frequency instability since generators can not lower their output to the new demand level. Finally, it can be seen from Table 4-8 that the optimized UFLS scheme sheds less amount of load than the existing UFLS scheme and that no constraint on its performance is violated. Thus, the existing UFLS scheme has been successfully improved with respect to considered operating and contingency scenarios.

Table 4-8: Comparison of the performance of the existing and the optimized UFLS scheme of the La Palma power system.

		Existing UFLS scheme						Optimized UFLS scheme					
Scenario	Generator (MW)	ωmin (Hz)	ωmax (Hz)	#Relays	Pshed (MW)	State	Cause	ωmin (Hz)	ωmax (Hz)	#Relays	Pshed (MW)	State	Cause
25	9.16 (50.6)	45.95	57.96	11	10.71	error	2,3	47.06	50.93	10	8.45	correct	
25	2.23 (12.3)	48.94	50.1	0	0	correct		48.94	50.1	0	0	correct	
26	11.38 (30.7)	48.37	50.8	3	8.24	error	3	48.26	50.03	0	0	correct	
26	2.23 (6.0)	49.7	50.01	0	0	correct		49.7	50.01	0	0	correct	

1 priority
2 overshedding
3 late shedding

To come to full circle, both, the existing and the optimized UFLS scheme are applied to all possible operating and contingency scenarios. Figure 4-13 compares the performances of both UFLS schemes. According to Figure 4-13, the amount of shed load has been remarkably reduced after implementing the optimized UFLS scheme. This is also reflected in the lower number of relays which opened. In addition, fewer errors (e.g. overshedding, priority, etc.) occurred thanks to the optimized UFLS scheme. It is however interesting that the total minimum frequency deviations remained more or less constant. This is mainly due to the fact that the optimized UFLS scheme, in contrast to the existing UFLS scheme, does not act for less severe outages (the majority of

outages as seen in section 4-2-3) and consequently, accepts frequency to deviate in such cases without shedding.

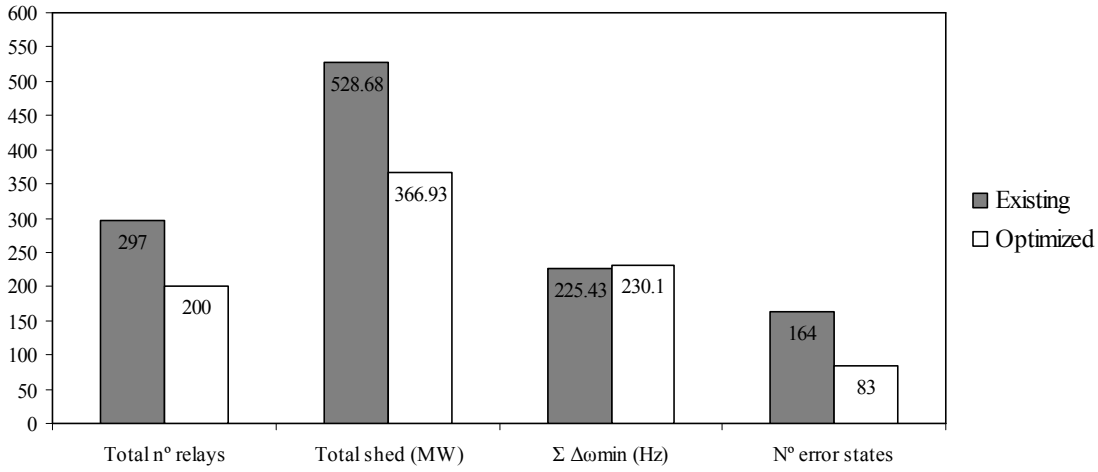

Figure 4-13: Comparison of the existing and optimized UFLS scheme of the La Palma power system.

Finally, Figure 4-14 and Figure 4-15 show the responses of the power system to all possible operating and contingency scenarios. Figure 4-14 depicts the effect of the existing UFLS scheme on system frequency, whereas Figure 4-15 exhibits the effect of the optimized UFLS scheme. It can be inferred that the existing UFLS scheme exhibits a much worse performance with respect to the minimum and maximum allowable frequencies than to optimized scheme. In fact, it is likely that the power system turns unstable in the case of the existing UFLS scheme.

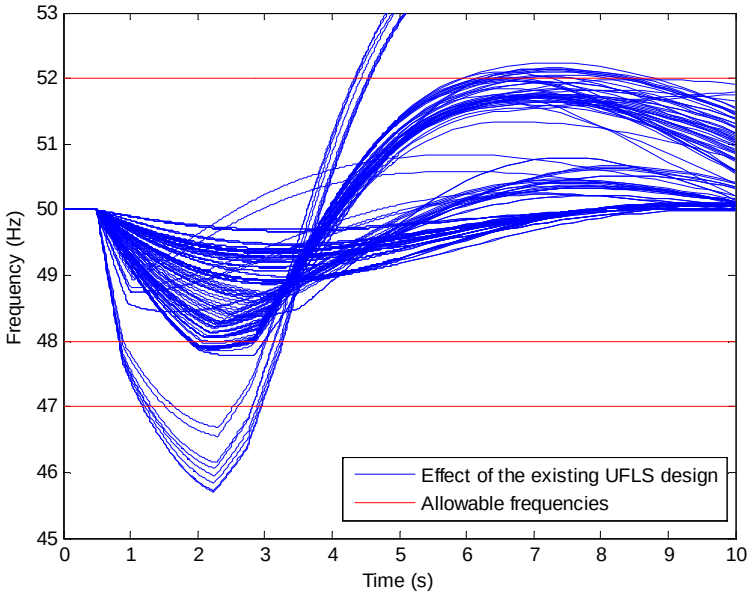

Figure 4-14: Responses of the power system to all possible outages for all operating conditions with the existing UFLS scheme of the La Palma power system.

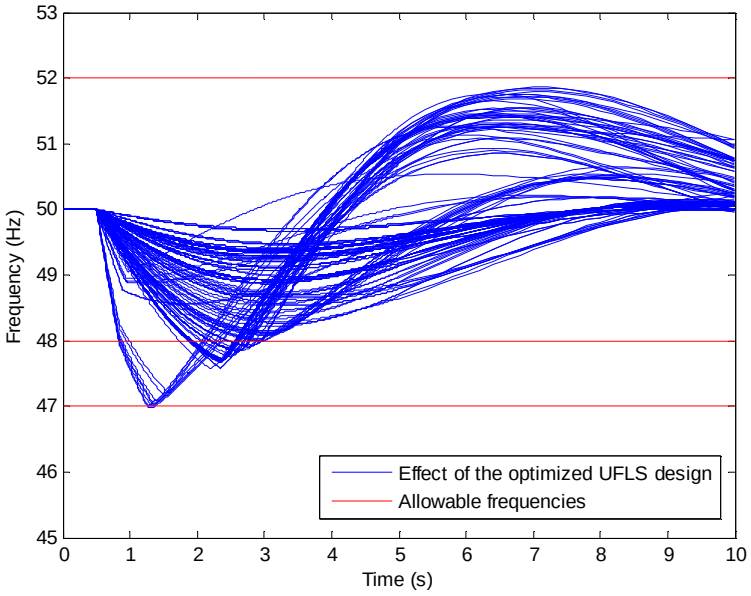

Figure 4-15: Responses of the power system to all possible outages for all operating conditions with the optimized UFLS scheme of the La Palma power system.

4-4 APPLICATION OF THE DESIGN METHOD TO REAL POWER SYSTEMS WITH PENETRATION OF DECOUPLED POWER GENERATION

The proposed method for the design of UFLS schemes is applied to the power systems of the La Palma and the Gran Canaria islands. La Palma and Gran Canaria power systems are isolated systems of different size. La Palma has peak demand of about 35 MW compared to the 530 MW peak demand of the Gran Canaria power system. Briefly, the proposed method consists in optimal tuning of the UFLS scheme parameters based upon operating and contingency scenarios which have been selected by means of clustering techniques. The objective is to minimize the amount of shed load as described by equation (4.6) with respect to specified constraints. In what follows, first, UFLS schemes are designed using the Matlab toolbox presented in more detail in the appendix A. Afterwards, these designs are validated using more sophisticated power-system simulation software such as PSS/E.

4-4-1 La Palma power system

Table 4-1 and Table 4-3 contain the SFD model parameters and the generation dispatch scenarios of the La Palma system with 40% of the installed capacity of decoupled power generation, covering around 10% of the total demand. Table 4-6 shows the existing UFLS scheme of the La Palma power system. To show the superior robustness of the proposed method of UFLS scheme design, the proposed UFLS scheme will also be compared with the optimized UFLS scheme obtained in section 4-3-4 using the common practice of scenario selection (see Table 4-7).

In a first step, the representative operating and contingency scenarios are determined. The number of clusters is set to four according to the results obtained in section 4-2-3. This also eases the comparison with the optimized UFLS scheme. Figure 4-16 compares the operating and contingency scenarios selected by applying the common practice (see section 4-3-4) and the clustering-based method. Clearly, the clustering-based method covers a wider range of possible system responses. Table 4-9

gives some additional information on the representative operating and contingency scenarios.

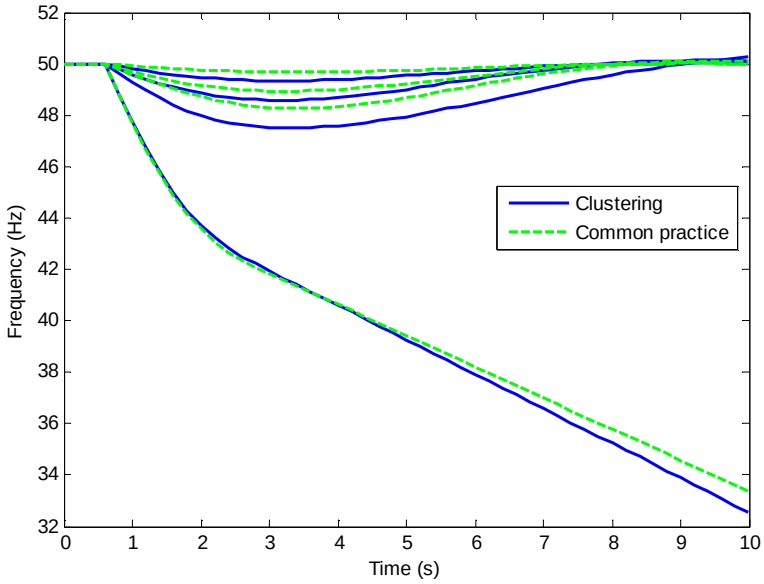

Figure 4-16: Comparison of the operating and contingency scenarios selection applying the common practice and the clustering-based method.

Table 4-9: Representative operating and contingency scenarios of the La Palma power system.

Scenario	Generator	Pdem (MW)	Ploss (MW) (%)
10	G20	32.15	6.7 (20.8)
4	G17	18.29	8.96 (49.0)
16	G16	29.98	4.74 (15.8)
15	G11	30.74	2.35 (7.6)

Again, the existing UFLS scheme of the La Palma power system of Table 4-6 will be optimized taking into account the following constraints:

- $\omega < 48$ Hz for maximum 2 s
- $\omega > 47$ Hz and $\omega \leq 52$ Hz
- Instant of shedding, i.e. no shedding after the instant of minimum frequency
- Priority, i.e. maintaining the priority associated to each stage
- The amount of shed load [MW] < the amount of loss power generation [MW]

Constraints imposed on minimum allowable frequency are more restrictive than those described in section 2-3-3 (e.g. $\omega < 47.5$ Hz for maximum 3 s). This leads to a more conservative scheme and gives therefore a certain safety margin. Further, more restrictive constraints might also benefit UFLS scheme performance in the case of assumed step sizes do not correspond with actual step size due to feeder-load variation, feeder outages or breaker failures. The latter is studied in more detail in chapter 5.

Like in section 4-3-4, a partial, more industry-oriented optimization strategy is applied, tuning frequency thresholds, ROCOF thresholds and intentional time delays of underfrequency and ROCOF relays. The UFLS scheme parameters are bounded above and below as follows:

- 47 Hz ≤ Frequency threshold of the underfrequency relays ≤ 49 Hz
- 49.3 Hz ≤ Frequency threshold of the ROCOF relays ≤ 49.8 Hz

- -1.5 Hz/s ≥ ROCOF threshold of the ROCOF relays ≥ -2.5 Hz/s
- 0 s ≤ Intentional time delay for both relay types ≤ 0.5 s

Again, the step sizes of the underfrequency and ROCOF steps have not been considered as a decision variable and therefore, the step sizes of the existing UFLS scheme have been used. In chapter 5, the inclusion of step sizes as decision variables is studied. Table 4-10 shows the proposed UFLS scheme (adjusted steps in red bold characters). The number of stages optimized depends on the maximum amount of lost power generation. As indicated in section 4-3-4, the first six stages have been optimized. With respect to the existing UFLS scheme shown in Table 4-6, frequency thresholds of the underfrequency relays have been lowered, whereas frequency thresholds of the ROCOF relays have been slightly increased and their time delays have been lowered. The latter allows a faster UFLS scheme intervention. Note that the new ROCOF threshold is lower than the one of the solely optimized UFLS scheme (see Table 4-7). The same value as in Table 4-7 could be used without worsening the results. In fact, the adaptive Simulated Annealing algorithm is not able to distinguish these two ROCOF threshold settings since they give rise to the same objective function value. In addition, intentional time delays of the underfrequency steps are smaller and the first frequency threshold is slightly higher, whereas frequency thresholds of steps 2 to 6 are lower. Remaining steps (7 to 10) could be anew used as backup steps in case of step-size variations or non-responding turbine-governor systems (see chapter 5).

Table 4-10: Proposed UFLS scheme of the La Palma power system.

Underfrequency relays					
Stage	ω (Hz)	t_{int} (s)	t_{opn} (s)	Step size (%)	Cumulative (%)
1	**48.32**	**0.03**	**0.2**	**7.1**	**7.1**
2	**47.95**	**0.22**	**0.2**	**0.6**	**7.7**
3	**47.83**	**0.01**	**0.2**	**14.5**	**22.2**
4	**47.69**	**0.11**	**0.2**	**3.6**	**25.8**
5	**47.58**	**0.05**	**0.2**	**7.3**	**33.1**
6	**47.34**	**0.01**	**0.2**	**13.6**	**46.7**
7	48.00	1.7	0.2	12.5	59.2
8	47.00	1.8	0.2	4.2	63.4
9	47.00	2.1	0.2	15.1	78.5
10	47.00	2.4	0.2	20.5	99

ROCOF relays						
Stage	ω (Hz)	dω/dt (Hz/s)	t_{int} (s)	t_{opn} (s)	Step size (%)	Cumulative (%)
1	**49.54**	**-2.4**	**0.04**	**0.2**	**7.1**	**7.1**
2	**49.54**	**-2.4**	**0.04**	**0.2**	**0.6**	**7.7**
3	**49.54**	**-2.4**	**0.04**	**0.2**	**14.5**	**22.2**
4	**49.54**	**-2.4**	**0.04**	**0.2**	**3.6**	**25.8**

Figure 4-17 plots the SFD model responses for the four representative operating and contingency scenarios after implementing the proposed UFLS scheme. Note that the UFLS scheme only acts for the last two operating and contingency scenarios of Table 4-9 due to their higher relative power losses.

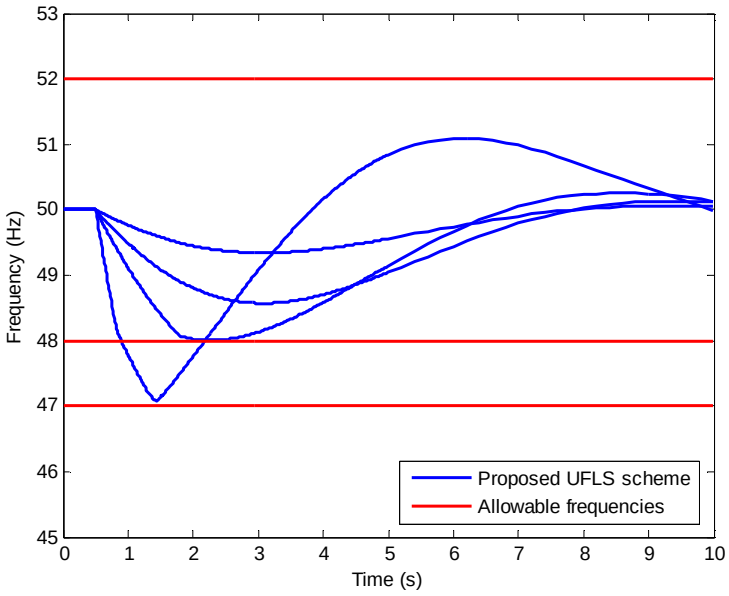

Figure 4-17: Performances of the proposed UFLS scheme of the La Palma power system.

To demonstrate the superior robustness of the proposed UFLS scheme, both the optimized UFLS scheme and the proposed UFLS scheme have been consecutively applied to the all possible outages of all system-operating conditions, i.e., all generation dispatch scenarios. Remember that the optimized scheme has been obtained using scenarios determined by the common practice, whereas the proposed scheme is the result of the application of the optimization to representative operating and contingency scenarios.

Figure 4-18 summarizes and compares the performances of both UFLS schemes. Three important characteristics with respect to the robustness of the proposed design can be deduced from Figure 4-18. First, the number of errors (occasions of poor performance) is remarkably reduced in the case of the proposed scheme. Frequency deviations have also been reduced which is indicated by the lower sum of minimum frequency deviations (corresponding to minimum frequencies). Finally, the amount of shed load has been significantly reduced thanks to the proposed design. This can also be deduced from the total number of relays which have opened.

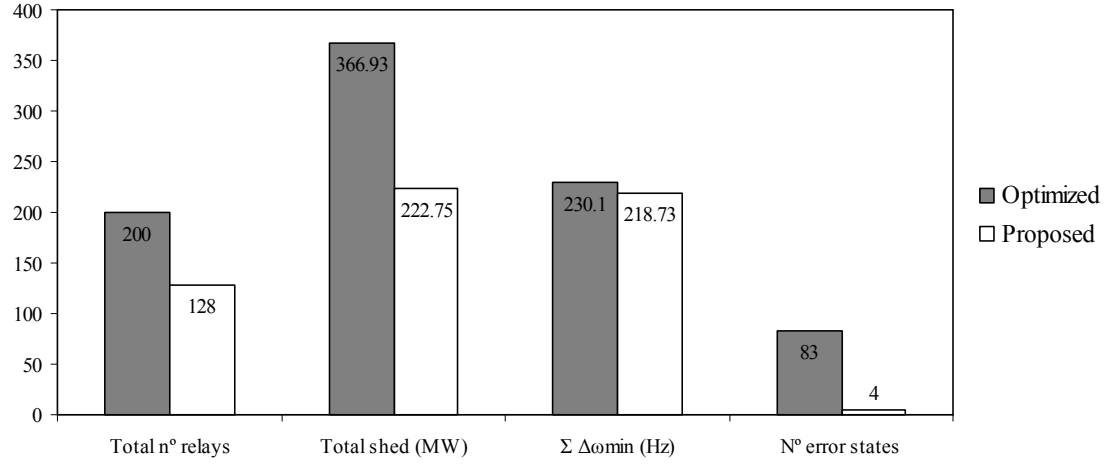

Figure 4-18: Comparison of the optimized and the proposed UFLS scheme of the La Palma power system.

Figure 4-19 and Figure 4-20 confirm some of the findings illustrated in Figure 4-18. Figure 4-19 depicts the impact of the optimized UFLS scheme on system frequency, whereas Figure 4-20 shows the effect of the proposed UFLS scheme. The lower amount of shed load occasioned by the proposed scheme is tantamount to reduced overfrequency. The slightly lower total frequency deviation is also observable comparing Figure 4-19 and Figure 4-20. Note, however, that frequency falls slightly below the 47 Hz–0 s restriction in the case of the proposed UFLS scheme. In view of these results, it can be concluded that the proposed design guarantees a robust and efficient UFLS scheme.

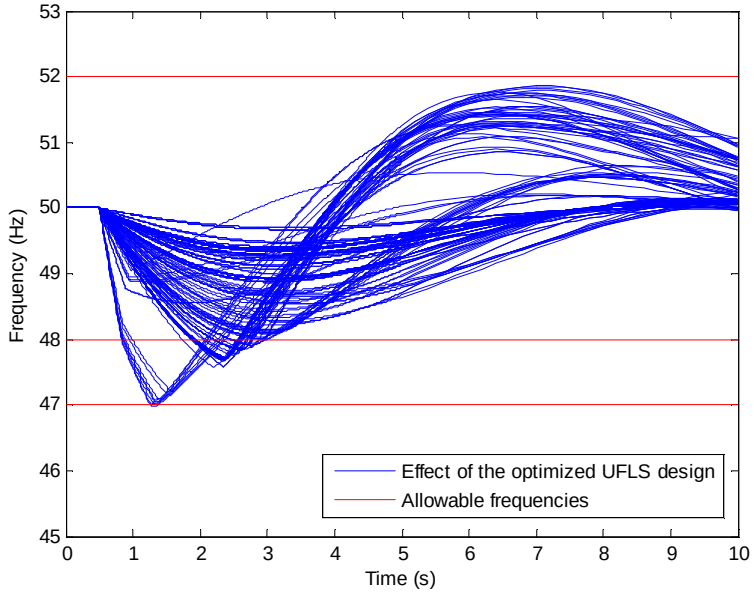

Figure 4-19: Responses of the La Palma power system to all possible outages for all operating conditions with the optimized UFLS scheme of the La Palma power system.

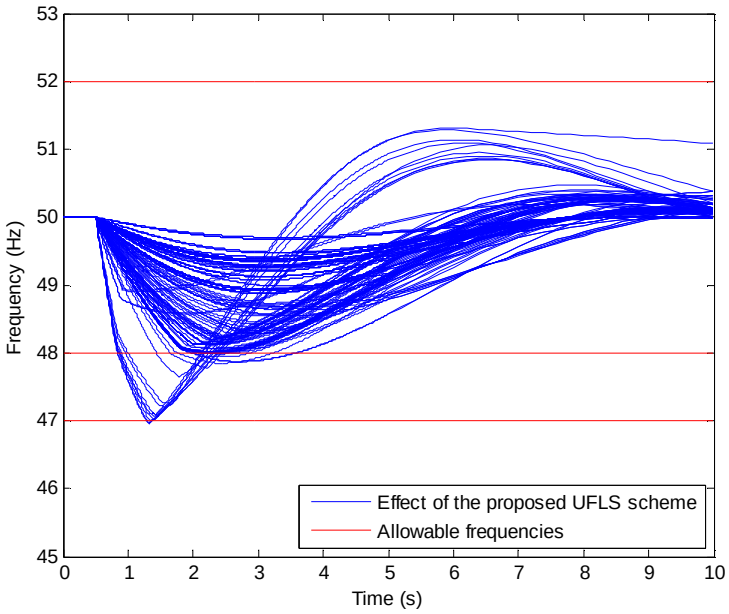

Figure 4-20: Responses of the La Palma power system to all possible outages for all operating conditions with the proposed UFLS scheme of the La Palma power system.

Finally, the proposed UFLS scheme is validated using more sophisticated power-system simulation software such as PSS/E software package. Consider the plausible and severe outage of generating unit G17 for the valley load-demand level corresponding to generation dispatch scenario 25 in Table 4-2. The outage of G17 is equivalent to a loss of 50.6% of the total load demand. Figure 4-21 compares frequency once simulated with the original PSS/E model and once simulated using the SFD model. It can be inferred from Figure 4-21 that both simulations coincide satisfactorily. In fact, the maximum difference in frequency is about 0.1 Hz. In either case, the same quantity of load has been shed corresponding to the actuation of the ROCOF and the first underfrequency stage. Thus, the presented proposed method is able to design realistic UFLS schemes.

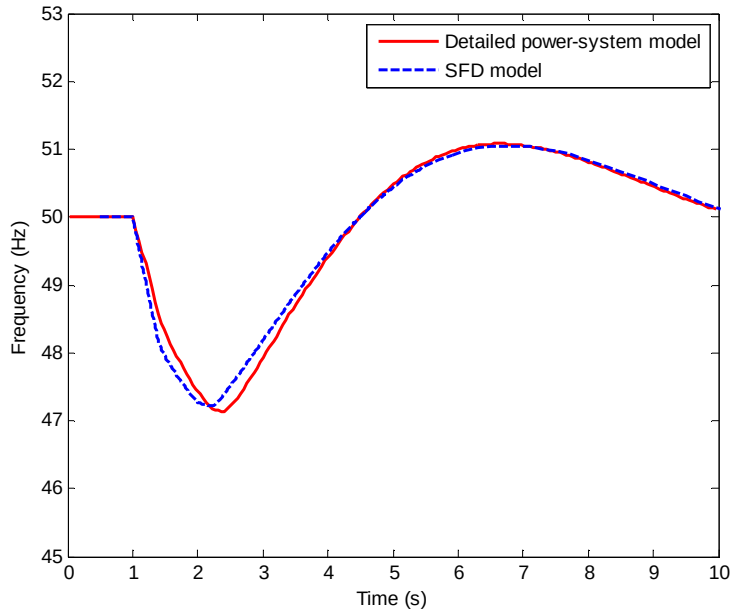

Figure 4-21: Comparison between frequency simulated with PSS/E and frequency simulated with SFD model of the La Palma power system.

4-4-2 Gran Canaria power system

Analogously to the preceding section, the proposed method for the design of UFLS schemes is now applied to the Gran Canaria power system. The Gran Canaria system is another isolated power system, but it is much bigger than the La Palma power system. Table 4-11 contains the SFD model parameters Gran Canaria power system.

Table 4-11: Parameters of the generator models of the Gran Canaria power system.

Generator	H (s)	K	b1 (s)	b2 (s)	a1 (s)	a2 (s)	Pmin (MW)	Pmax (MW)
G1	5.6	16.7	0	0	5.35	1.75	27.8	74.2
G2	5.6	16.7	0	0	5.35	1.75	27.8	74.2
G3	5.1	20.2	0	0	0.43	0.1	3.2	67.6
G4	5.1	20.2	0	0	0.43	0.1	3.2	67.6
G5	5.1	16.7	0	0	5.35	1.75	3.2	67.6
G6	5.0	34.1	2.39	0	3.99	1.87	5.8	32.3
G7	5.0	35.2	2.66	0	4.32	2.08	5.8	32.3
G8	5.1	20.2	0	0	0.43	0.1	9.7	68.7
G9	5.1	20.2	0	0	0.43	0.1	9.7	68.7
G10	3.0	16.7	1.09	0	5.99	5.47	13.5	28.0
G11	3.0	16.7	1.09	0	5.99	5.47	13.6	37.3
G12	3.0	16.7	1.09	0	5.99	5.47	13.6	37.3
G13	4.0	16.7	1.12	0	6.06	5.64	26.6	55.6
G14	4.0	16.7	1.12	0	6.06	5.64	26.6	55.6
G15	1.5	25.0	0	0	0.35	0	4.6	11.3
G16	1.5	25.0	0	0	0.35	0	4.6	11.3
G17	1.5	25.0	0	0	0.35	0	4.6	11.3
G18	1.5	25.0	0	0	0.35	0	14.1	20.5
G19	1.5	25.0	0	0	0.35	0	14.1	20.5
G20	5.0	39.9	2.51	0	4.02	1.95	5.8	21.6
G21	5.0	32.0	2.25	0	3.85	1.75	5.8	32.3
G22	5.0	32.0	2.25	0	3.85	1.75	5.8	32.3

Table 4-12 displays the generation dispatch scenarios of the Gran Canaria system with a decoupled power generation (DPG) penetration corresponding to a 40% of the

installed capacity of DPG, covering about 10% of the total demand. On the Gran Canaria island, 103.47 MW of wind power and 21.33 MW of solar power have been installed [MITyC'09]. The corresponding amount of DPG has been simply added to typical generation dispatch scenarios without DPG.

Table 4-12: Generation dispatch scenarios of the Gran Canaria power system with 40% of the total installed capacity of decoupled power generation.

S. O. C.	G1	G2	G3	G4	G5	G6	G7	G8	G9	G10	G11	G12	G13	G14	G15	G16	G17	G18	G19	G20	G21	G22	DPG	$P_{G_{tot}} = P_{D_{tot}}$
1	38	38	54.6	54.6	54.6	10	10	0	0	0.0	13.6	0.0	27	27	0	0	0	19	19	0	0	0	41	406.1
2	28	28	51.1	51.1	51.1	10	10	0	0	0.0	13.6	0.0	27	27	0	0	0	18	18	0	0	0	41	373.0
3	28	28	48.2	48.2	48.2	10	10	0	0	0	13.6	0.0	27	27	0	0	0	14	14	0	0	0	41	355.8
4	28	28	45.6	45.6	45.6	10	10	0	0	0	13.6	0.0	27	27	0	0	0	14	14	0	0	0	41	348.2
5	28	28	44.8	44.8	44.8	0	0	10	10	0	13.6	0.0	27	27	0	0	0	14	14	0	0	0	41	345.6
6	28	28	47.4	47.4	47.4	0	0	10	10	0	13.6	0.0	27	27	0	0	0	14	14	0	0	0	41	353.5
7	31	31	54.5	54.5	54.5	0	0	10	10	0	14	0	27	27	0	0	0	19	19	0	0	0	41	390.0
8	54	54	54.7	54.7	54.7	0	0	9.7	10	0	14	0	27	27	0	0	0	19	19	0	0	0	50	445.4
9	53	53	54.7	54.7	54.7	0	0	9.7	9.7	0	14	0	51	51	0	0	0	19	19	0	0	0	49.9	491.6
10	70	70	55.0	55.0	55.0	0	0	9.7	9.7	0	14	0	51	51	0	0	0	19	19	0	0	0	49.9	527.6
11	70	70	64.0	64.0	64.0	0	0	9.7	9.7	0	14	0	51	51	0	0	0	19	19	0	0	0	49.9	554.6
12	70	70	65.3	65.3	65.3	0	0	9.7	9.7	0	18	0	51	51	0	0	0	19	19	0	0	0	49.9	563.2
13	70	70	65.3	65.3	65.3	0	0	9.7	9.7	0	25	0	51	51	0	0	0	19	19	0	0	0	49.9	570.0
14	70	70	65.3	65.3	65.3	0	0	9.7	9.7	0	23	0	51	51	0	0	0	19	19	0	0	0	49.9	568.2
15	70	70	63.0	63.0	63.0	0	0	9.7	9.7	0	14	0	51	51	0	0	0	19	19	0	0	0	49.9	551.7
16	70	70	55.6	55.6	55.6	0	0	9.7	9.7	0	14	0	51	51	0	0	0	19	19	0	0	0	49.9	529.3
17	68	68	54.8	54.8	54.8	0	0	9.7	9.7	0	14	0	51	51	0	0	0	19	19	0	0	0	49.9	522.2
18	69	69	54.8	54.8	54.8	0	0	9.7	9.7	0	14	0	51	51	0	0	0	19	19	0	0	0	49.9	525.0
19	69	69	54.8	54.8	54.8	0	0	9.7	9.7	0	14	0	51	51	0	0	0	19	19	0	0	0	49.9	524.0
20	70	70	56.6	56.6	56.6	0	0	9.7	9.7	0	14	0	51	51	0	0	0	19	19	0	0	0	41.4	523.8
21	70	70	64.5	64.5	64.5	0	0	9.7	9.7	0	14	0	45	45	0	0	0	19	19	0	0	0	41.4	536.2
22	70	70	65.3	65.3	65.3	0	0	9.7	9.7	0	33	0	51	51	0	0	0	19	19	0	0	0	41.4	569.5
23	70	70	64.4	64.4	64.4	0	0	9.7	10	0	14	0	36	36	0	0	0	19	19	0	0	0	41	517.4
24	65	65	54.8	54.8	54.8	0	0	10	10	0	14	0	27	27	0	0	0	19	19	0	0	0	41	458.9

In a first step, the representative operating and contingency scenarios are determined. The size of the power systems requires that not only individual but also multiple outages must be considered. Multiple outages are defined as those simultaneous outages of generating units for which the total loss of generation is equal to or exceeds a specified minimum threshold [Sigrist'10b]. For example, this threshold could be set to 40% of the totally generated power. In this case, a possible multiple

outage could be the simultaneous outages of generating units G3, G4 and G5 of Table 4-12. Similar values of this threshold are used in the literature to represent a maximum overload (e.g. 100% corresponding to a total loss of generation of 50%) [Lokay'68]. According to (4.4) and with $K = 16.7$, $a_1 = 6\ s$ and $H = 5.6\ s$ and taking into account a generation output limitation factor of two, the maximum instant of minimum frequency occurs after about 6.5 seconds after the contingency. Thus, the simulation time for the clustering process is set to 7 s (the additional 0.5 s originates from the fact that the outage occurs at 0.5 s).

To determine the number of clusters, K-Means or Fuzzy C-Means algorithm are again iteratively applied. Figure 4-22 plots the number of clusters against the quadratic quantization error and the Fuzzy C-Means objective function. It can be inferred that four to five clusters seem to be sufficient. In what follows, the scenarios are grouped according to four clusters.

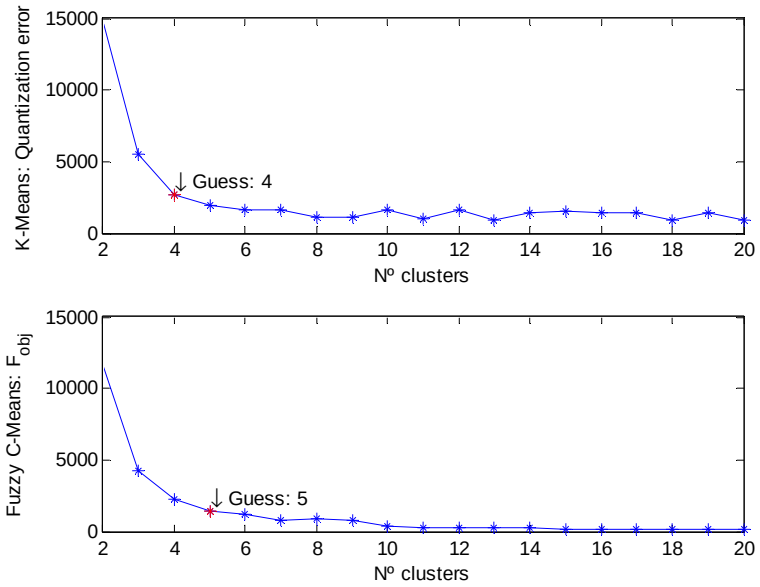

Figure 4-22: Determination of the number of clusters using the K-Means and the Fuzzy C-Means algorithm.

Figure 4-23 shows the results obtained applying K-Means algorithm. Figure 4-23 reveals that cluster 1 and cluster 3 of the K-Means algorithm cover the scenarios with smallest and largest frequency deviations, respectively.

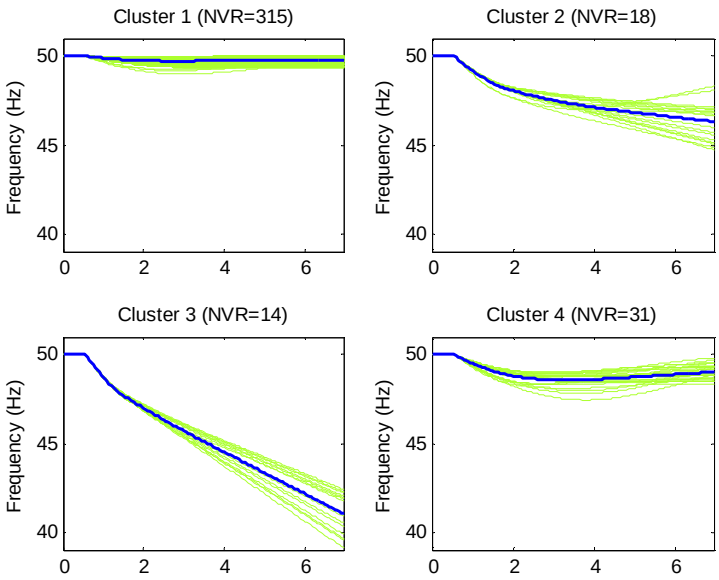

Figure 4-23: Representation of the four clusters formed by K-Means and the associated scenarios.

Figure 4-24 (a) compares the principal component analysis (PCA) of the four clusters and of all possible operating and contingency scenarios. According to the two-dimensional space describe by the first and second PCA components, the distribution of the clusters seems to reflect well the distribution of all possible operating and contingency scenarios. The silhouette plot in Figure 4-24 (b) confirms this. Note that the silhouette plot detects an outstanding scenario in cluster 4 due to a slightly negative silhouette value.

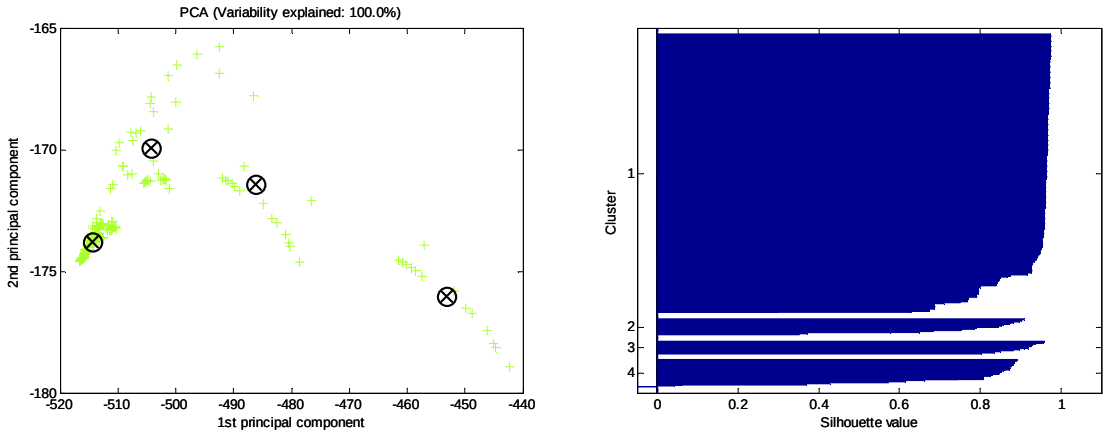

Figure 4-24: (a) Principal component analysis and (b) silhouette plot of the six clusters formed by K-Means and their associated scenarios.

Table 4-13 gives some additional information on the representative operating and contingency scenarios. Clearly, multiple outages have been considered which are also responsible for low frequency levels.

Table 4-13: Representative operating and contingency scenarios of the Gran Canaria power system.

Scenario	Generator	Pdem (MW)	Ploss (MW) (%)
21	G1-G4	536.21	269.47 (50.3)
23	G1, G2	517.42	140.48 (27.2)
10	DPG	527.65	49.92 (9.5)
21	G1-G3	536.21	204.97 (38.2)

In a second step, the existing UFLS scheme of the Gran Canaria power system of Table 4-14 will be optimized taking into account the following constraints:

- $\omega < 48$ Hz for maximum 2 s,
- $\omega > 47$ Hz and $\omega \leq 52$ Hz
- Instant of shedding, i.e. no shedding after the instant of minimum frequency
- Priority, i.e. maintaining the priority associated to each stage
- The amount of shed load [MW] < the amount of loss power generation [MW]

Again a partial, more industry-oriented optimization strategy is applied, tuning frequency thresholds, ROCOF thresholds and intentional time delays of underfrequency and ROCOF relays. The UFLS scheme parameters are bounded above and below as follows:

- 47 Hz ≤ Frequency threshold of the underfrequency relays ≤ 49 Hz
- 49.3 Hz ≤ Frequency threshold of the ROCOF relays ≤ 49.8 Hz
- -0.5 Hz/s ≤ ROCOF threshold of the ROCOF relays ≤ -1.5 Hz/s
- 0 s ≤ Intentional time delay for both relay types ≤ 0.5 s

Likewise, the step sizes of the underfrequency and ROCOF steps have not been considered as a decision variable and therefore, the step sizes of the existing UFLS scheme have been used. The number of stages to be adjusted depends on the maximum amount of lost power generation. Since maximum outage corresponds to a 50% of total generation, the first ten stages have been initially considered. Table 4-15 shows the proposed UFLS scheme (adjusted stages in red bold characters). With respect to the existing UFLS scheme shown in Table 4-14, frequency thresholds of the underfrequency relays have been lowered, whereas frequency thresholds of the ROCOF relays have been increased. ROCOF threshold has been reduced since with its original setting of -0.8 Hz/s more load would be shed. The latter allows a faster UFLS scheme intervention.

Table 4-14: Existing UFLS scheme of the Gran Canaria power system.

Underfrequency relays						
Stage	Feeders	ω (Hz)	t_{int} (s)	t_{opn} (s)	Step size (%)	Cumulative (%)
1	1001 - 1007	49.00	0.1	0.2	3.43	3.43
2	1008 - 1015	48.92	0.15	0.2	5.27	8.70
3	1016 - 1023	48.85	0.2	0.2	5.03	13.73
4	1024 - 1030	48.79	0.3	0.2	5.68	19.41
5	1031 - 1035	48.72	0.4	0.2	4.17	23.58
6	1036 - 1047	48.66	0.5	0.2	9.95	33.53
7	1048 - 1053	48.60	0.6	0.2	5.46	38.99
8	1054 - 1058	48.55	0.7	0.2	3.05	42.04
9	1059 - 1066	48.50	0.8	0.2	4.07	46.11
10	1067 - 1074	48.35	0.9	0.2	5.89	52.00
11	1075 - 1090	48	1	0.2	10.34	62.34

ROCOF relays							
Stage	Feeders	ω (Hz)	dω/dt (Hz/s)	t_{int} (s)	t_{opn} (s)	Step size (%)	Cumulative (%)
1	1008, 1010, 1022 - 1030,1034, 1035	49.30	-0.8	0.15	0.2	9.97	9.97

Table 4-15: Proposed UFLS scheme of the Gran Canaria power system.

Underfrequency relays						
Stage	Feeders	ω (Hz)	t_{int} (s)	t_{opn} (s)	Step size (%)	Cumulative (%)
1	**1001 - 1007**	**48.66**	**0.08**	**0.2**	**3.43**	**3.43**
2	**1008 - 1015**	**48.28**	**0.08**	**0.2**	**5.27**	**8.70**
3	**1016 - 1023**	**48.17**	**0.26**	**0.2**	**5.03**	**13.73**
4	**1024 - 1030**	**48.05**	**0.04**	**0.2**	**5.68**	**19.41**
5	**1031 - 1035**	**47.92**	**0**	**0.2**	**4.17**	**23.58**
6	1036 - 1047	48.66	0.5	0.2	9.95	33.53
7	1048 - 1053	48.60	0.6	0.2	5.46	38.99
8	1054 - 1058	48.55	0.7	0.2	3.05	42.04
9	1059 - 1066	48.50	0.8	0.2	4.07	46.11
10	1067 - 1074	48.35	0.9	0.2	5.89	52.00
11	1075 - 1090	48	1	0.2	10.34	62.34

ROCOF relays							
Stage	Feeders	ω (Hz)	dω/dt (Hz/s)	t_{int} (s)	t_{opn} (s)	Step size (%)	Cumulative (%)
1	**1008, 1010, 1022 - 1030,1034, 1035**	**49.48**	**-1.4**	**0.08**	**0.2**	**9.97**	**9.97**

Figure 4-25 plots the SFD model responses for the four representative operating and contingency scenarios in presence of the original and the proposed UFLS scheme. Both the existing and the proposed UFLS scheme comply with constraints on minimum and maximum allowable frequencies. From Figure 4-25, it can be deduced that the proposed UFLS scheme only acts for the first and the last operating and contingency scenario of Table 4-13, whereas the existing UFLS scheme acts for the first, the second and the last operating and contingency scenario. Table 4-16 gives some additional information on the performance of the considered UFLS schemes. Clearly, the proposed UFLS scheme sheds much less load. Furthermore, no performance error appeared as in contrast to the existing scheme where late shedding and overshedding occurred. However, steady-state frequencies are close to or below 49 Hz, although it is true that system operators could manually shed load in such situation. To improve the steady-state frequency value, an additional constraint on allowable minimum frequency could

be implemented (e.g. $\omega < 49$ Hz for maximum 5 s) or different objective function could be used which includes a term related to frequency deviations. Figure 4-25 also shows the result of imposing the 49 Hz-5 s constraint on the UFLS design. Clearly, frequency recovers 49 Hz for the four representative operating and contingency scenarios.

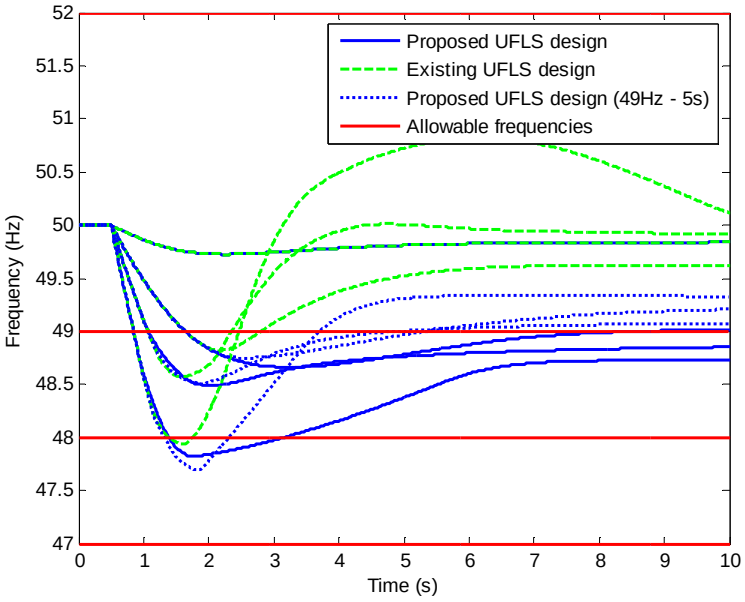

Figure 4-25: Comparison of the SFD model responses of the existing and the proposed UFLS scheme of the Gran Canaria power system.

Table 4-16: Comparison of the performance of the existing and the proposed UFLS scheme of the Gran Canaria power system.

		Existing UFLS scheme						Proposed UFLS scheme					
Scenario	Generator (MW)	ωmin (Hz)	ωmax (Hz)	#Relays	Pshed (MW)	State	Cause	ωmin (Hz)	ωmax (Hz)	#Relays	Pshed (MW)	State	Cause
536.208	269.47 (50.3)	47.94	50.82	87	278.92	error	2,3	47.82	50	48	126.48	correct	
517.418	140.48 (27.2)	48.82	50	23	71.05	error	3	48.66	50	0	0	correct	
527.65	49.92 (9.5)	49.73	50	0	0	error	3	49.73	50	0	0	correct	
536.208	204.97 (38.2)	48.57	50.01	60	179.85	correct		48.49	50	20	71.87	correct	

1 priority
2 overshedding
3 late shedding

As in the case of the La Palma power system, both the existing UFLS scheme and the proposed UFLS scheme have been consecutively applied to all possible outages for all system operating conditions, i.e., all generation dispatch scenarios. Figure 4-26 and Figure 4-27 show the effect of the UFLS schemes on frequency. Clearly, the number of sustained low-frequency scenarios increased with the proposed UFLS scheme. This is an indication of reduced load-shedding activities. However, low steady-state frequency values, as mentioned earlier, are possibly not acceptable. Figure 4-28 shows the result of applying an additional 49 Hz-5 s constraint on the UFLS design. Clearly, steady-state frequency deviations have been reduced with respect to the initial proposed design (i.e. post-transient steady-state frequencies are around 49 Hz), at the expense of increased amount of shed load.

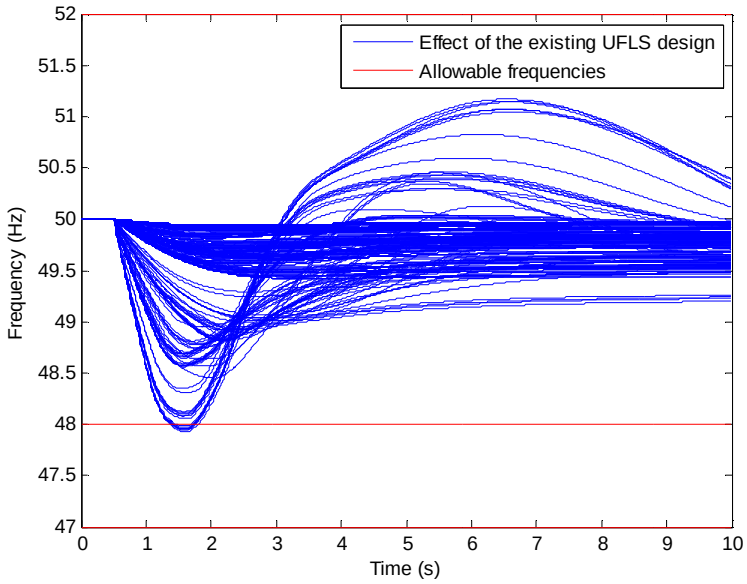

Figure 4-26: Responses of the Gran Canaria power system to all possible outages for all operating conditions with the existing UFLS scheme.

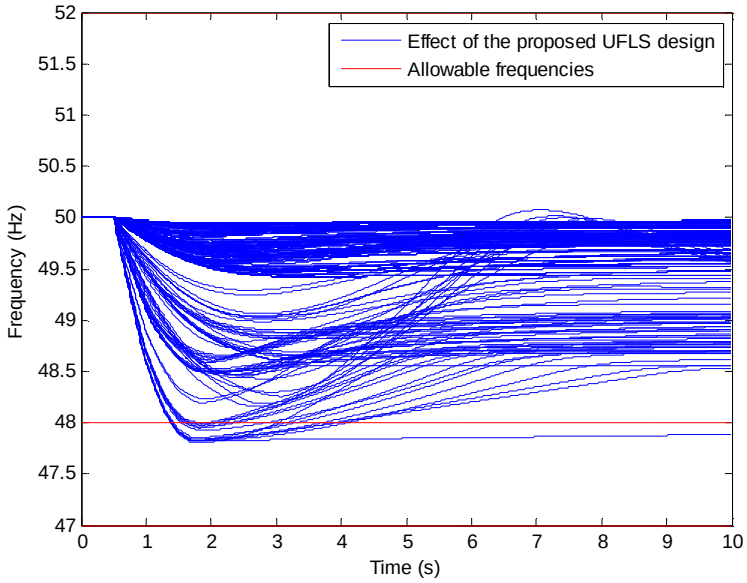

Figure 4-27: Responses of the Gran Canaria power system to all possible outages for all operating conditions with the proposed UFLS scheme.

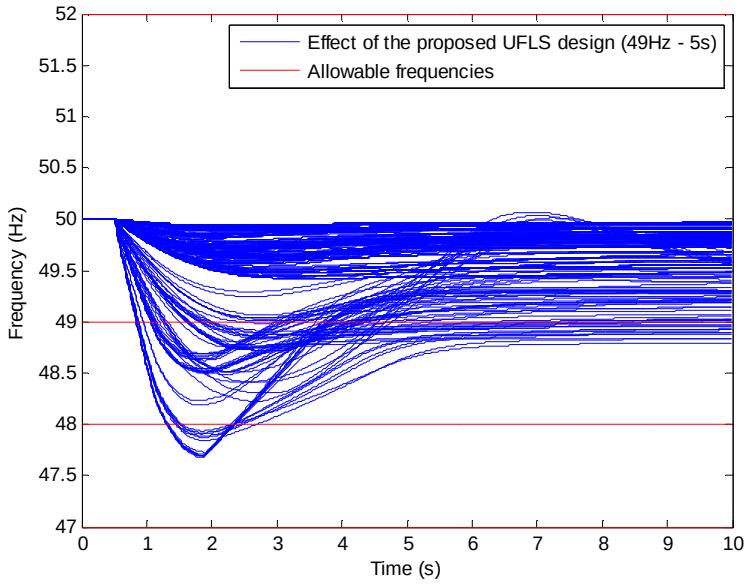

Figure 4-28: Responses of the Gran Canaria power system to all possible outages for all operating conditions with the proposed UFLS scheme with an additional 49 Hz–5 s constraint.

Figure 4-29 graphically compares the performance of the existing and the proposed UFLS scheme as well as the proposed UFLS scheme with an additional 49 Hz–5 s constraint. It can be inferred from Figure 4-29 that the proposed UFLS schemes remarkably reduce the amount of shed load, without affecting total minimum frequency deviation (sum of minimum frequencies). The reduced amount of shed load caused then sustained low-frequency scenarios of Figure 4-27. Figure 4-29 also confirms the fact that the addition of the 49 Hz–5 s constraint increased the amount of shed load.

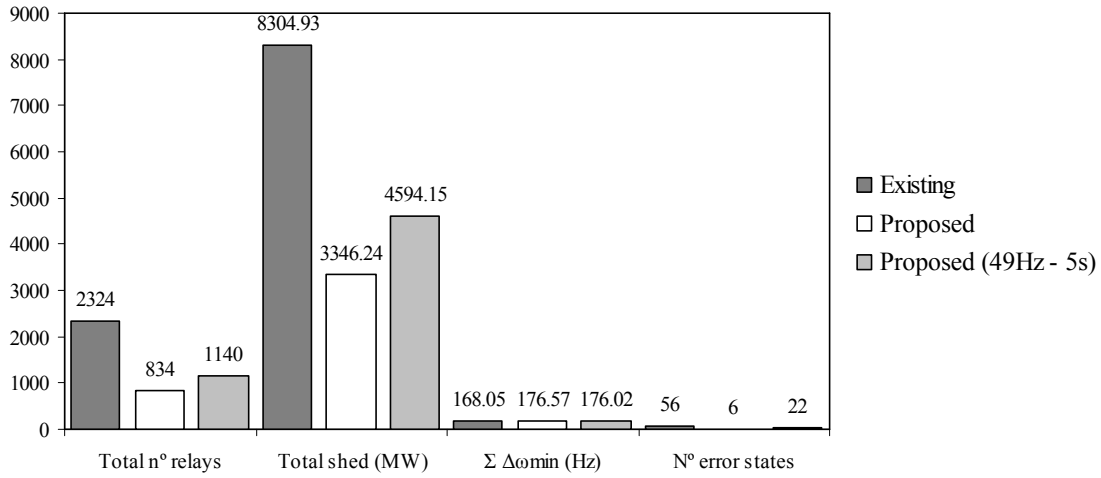

Figure 4-29: Comparison of the optimized and the proposed UFLS schemes of the Gran Canaria power system.

Finally, the initially proposed UFLS scheme is validated using more sophisticated power-system simulation software such as PSS/E software package. Consider the plausible and severe outage of generating units G3, G4 and G5 for the valley load-demand level corresponding to generation dispatch scenario 8 in Table 4-12. The outage of G3, G4 and G5 is equivalent to a loss of 40.7% of the total load demand. Figure 4-30 compares frequency once simulated with the original PSS/E model and once simulated

using the SFD model. It can be inferred from Figure 4-30 that both simulations coincide satisfactorily. In fact, the maximum difference in frequency is about 0.1 Hz. In either case, the same quantity of load has been shed corresponding to the actuation the first underfrequency stage. Thus, the presented proposed method is able to design realistic UFLS schemes.

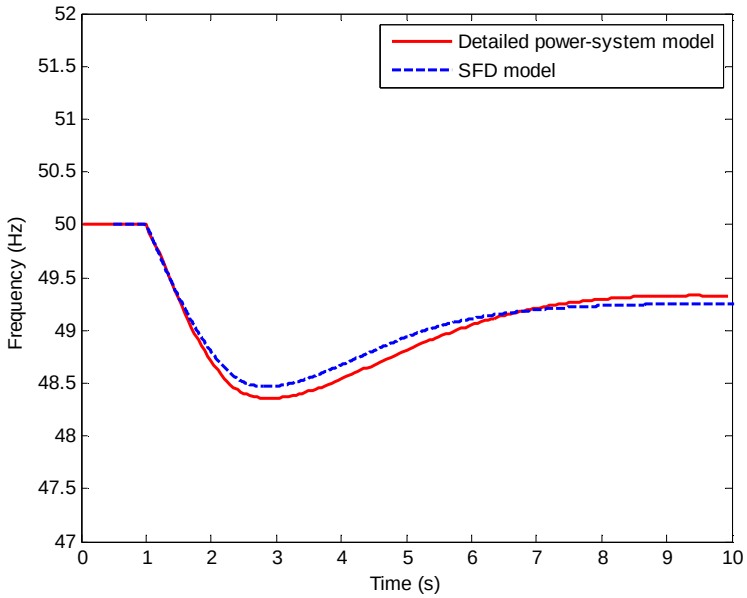

Figure 4-30: Comparison between frequency simulated with PSS/E and frequency simulated with SFD model of the Gran Canaria power system.

4-5 PARTIAL CONCLUSIONS

A method for the design of robust and efficient UFLS schemes of small isolated power system has been elaborated. To guarantee a robust UFLS scheme design, adequate operating and contingency scenarios need to be selected. Efficiency of the UFLS scheme can be achieved by applying an optimization algorithm to tune the parameters of the UFLS scheme. The proposed method for the design of efficient and robust UFLS schemes comprises thus two tasks: the selection of adequate operating and contingency scenarios and the tuning of the UFLS parameters by means of an optimization algorithm. The proposed method has been implemented in the Matlab toolbox presented in the appendix A. Finally, the proposed method has been applied to the design of the UFLS schemes of the La Palma and the Gran Canaria power systems.

A method based on Data Mining has been proposed to identify and select representative operating and contingency scenarios. Representative operating and contingency scenarios are those scenarios which represent best all other operating and contingency scenarios. Several Data Mining techniques such as K-Means, Fuzzy C-Means and KSOM have been presented and applied to the problem of representative scenario selection. It has been shown that by means of Data Mining, representative operating and contingency scenarios can be found. The resulting representative operating and contingency scenarios describe well the patterns among all possible operating and contingency scenarios. Furthermore, the application to the La Palma and the Gran Canaria power system showed that different Data Mining techniques yield to similar results. Finally, the method based on Data Mining has been compared with the common practice of scenario selection. Compared with the common practice of scenario

selection, representative operating and contingency scenarios cover a wider range of possible system responses than the manually selected scenarios.

The optimal tuning of UFLS scheme parameters has been accomplished by means of adaptive Simulated Annealing algorithm. Simulated Annealing is a well-known meta-heuristic optimization algorithm. The main objective of the optimization stage is to minimize the amount of shed load without jeopardizing the system stability. As an application example, the existing UFLS scheme of the La Palma power system has been optimized and compared with the existing scheme. A partial, more industry-oriented optimization strategy has been applied, tuning frequency thresholds, ROCOF thresholds and intentional time delays of underfrequency and ROCOF relays. Optimization constraints include restrictions on priority of loads, the instant of shedding and the amount of shed load as well as on the minimum and maximum allowable frequencies. It has been found that the application of Simulated Annealing yielded to a more efficient UFLS scheme with behalf to the existing UFLS scheme of the La Palma power system. In fact, the optimized UFLS scheme sheds less load and exhibits better performances with respect to imposed constraints such as minimum and maximum allowable frequencies, load priority or unnecessary late shedding. Sensitivity with respect to imposed design constraints is studied in chapter 5.

Finally, the proposed method for the design of UFLS schemes has been successfully applied to both the La Palma and the Gran Canaria power systems. In other words, the optimization stage is based upon representative operating and contingency scenarios determined by Data Mining techniques. Again, a partial, more industry-oriented optimization strategy has been applied, tuning frequency thresholds, ROCOF thresholds and intentional time delays of underfrequency and ROCOF relays. It has been shown that the proposed UFLS scheme is more robust and efficient than the solely optimized UFLS scheme of the La Palma power system, based on operating and contingency scenarios determined by the common practice. Analogously, the proposed UFLS schemes of the La Palma and the Gran Canaria power systems improved remarkably the performance with respect to the existing UFLS schemes in terms of shed load. It has also been found that additional design criteria could be necessary to avoid low steady-state frequencies if these are unacceptably low. Simulations in PSS/E confirmed the feasibility of the proposed method for the design of robust and efficient UFLS schemes.

CHAPTER FIVE

ANALYSIS OF UFLS SCHEME DESIGNS

5-1 INTRODUCTION

Several methods, either experimental or optimal, have been reported in literature to design conventional UFLS schemes. The proposed method for the design of UFLS schemes combines the efficiency of optimization-based methods with the robustness of representative operating and contingency scenarios selection. However, irrespective of the method employed, the design of UFLS scheme is based upon certain design conditions and assumptions on power-system behavior.

Design conditions directly influence the performance of the resulting UFLS scheme. In the case of the proposed method for the design of UFLS schemes in chapter 4, these conditions can be differentiated in those which influence the selection of operating and contingency scenarios and those which affect constraints imposed to the tuning procedure, i.e. the adaptive Simulated Annealing optimization algorithm. Imposing a minimum allowable frequency value implies, for example, that generating units are supposed to withstand such frequencies. Variations of design conditions might lead to distinct final UFLS scheme designs.

In chapter 3, some assumptions on power-system behavior have been already used to elaborate an adequate power-system model. Inter alia, it has been shown for example that short-term frequency dynamics are mainly affected by turbine-governor and rotor dynamics or that small isolated power system can be represented by a single-bus model. Another assumption made is that of voltage and frequency-independent loads. The latter merges into the classical hypothesis of invariant (relative to load-demand) UFLS scheme step sizes. In other words, it is tacitly supposed that the step size is known and its percentaged value remains constant, independent of system operating conditions. In reality, however, the percentaged values of actual step sizes vary from the implemented step sizes due to feeder-load variations, feeder outages or breaker failures. Step-size variations can negatively affect UFLS scheme performance.

In this chapter, the impact on the UFLS scheme of both variations of design conditions and step sizes are analyzed. In a first step, various different design conditions affecting either the selection of operating and contingency scenarios or the formulation

of the optimization problem are studied. Some of these modified design conditions coincide also with UFLS scheme designs proposed in the literature and thus, they allow comparing the proposed method with other methods. In a second step, the impact of step-size variation on UFLS scheme performance is addressed. For this purpose, the variation of step size has to be quantified. Finally, the analysis of step-size variations also provides a mean to adjust possible backup stages of UFLS schemes. Backup steps are those steps of an UFLS scheme which have not been adjusted when applying the proposed method for the design of robust and efficient UFLS schemes.

5-2 IMPACT OF VARYING DESIGN CONDITIONS

The proposed method for the design of robust and efficient UFLS schemes consists in consecutively applying two clearly distinct tasks: first, representative operating and contingency scenarios are selected by means of clustering techniques and subsequently, the parameters of the UFLS schemes are tuned such that an objective function is optimized with respect to the previously selected operating and contingency scenarios. Robustness depends therefore on the way of selecting representative operating and contingency scenarios, whereas efficiency depends very much on the formulation of the optimization problem applied to the design of UFLS schemes. A change in a condition for one of these steps (e.g. the number of representative operating and contingency scenarios) might (but not necessarily has to) result in a different UFLS scheme design. For example, if the number of representative operating and contingency scenarios is cautiously chosen, an additional scenario should not significantly alter the result. By contrast, if the objective function is significantly changed, the resulting UFLS scheme design should have a corresponding effect on operating and contingency scenarios.

A first distinction among design conditions can be realized with respect to the step of the proposed method they affect (i.e. selection of operating and contingency scenarios or optimal tuning of UFLS scheme parameters). A further distinction can be made according to the formulation of the optimization problem. By this means, five different groups of design conditions can be identified and analyzed. These groups describe the five design conditions defined by:

- Operating and contingency scenarios
- Optimization constraints
- Objective functions
- Optimization algorithms
- Decision variables

Clearly, the first group belongs to the problem of operating and contingency scenario selection, whereas the remaining groups belong to the formulation of the optimization problem.

In what follows, different UFLS scheme designs resulting from a variation of one of these design conditions are analyzed and compared to the base case. One can anticipate that most of the resulting designs correspond with an intuitive solution of a gedankenexperiment. The base case is given by the proposed UFLS scheme in chapter 4. Only the case of La Palma is presented as an example since the power system's reduced size allows a simple interpretation and explanation of the results. However, most of the findings are directly applicable to larger systems such as the Grand Canaria power system.

5-2-1 Base case

The UFLS scheme of the Palma power system has been designed for the operating and contingency scenarios displayed in Table 5-1. System operating conditions, i.e., generation dispatch scenarios, with 40% of the total installed capacity of decoupled power generation have been contemplated. In this case, about 10% of the total demand is covered by decoupled power generation.

Table 5-1: Representative operating and contingency scenarios of the La Palma power system.

Scenario	Generator	Pdem (MW)	Ploss (MW) (%)
10	G20	32.15	6.7 (20.8)
4	G17	18.29	8.96 (49.0)
16	G16	29.98	4.74 (15.8)
15	G11	30.74	2.35 (7.6)

The existing UFLS scheme of the La Palma power system has been optimized taking into account the following constraints:

- $\omega < 48$ Hz for maximum 2 s
- $\omega > 47$ Hz and $\omega \leq 52$ Hz
- Instant of shedding
- Priority
- The amount of shed load [MW] < the amount of loss power generation [MW]

The optimization has been realized by means of adaptive Simulated Annealing. The following UFLS scheme parameters have been considered as decision variables:

- Frequency threshold of the underfrequency relays
- Frequency threshold of the ROCOF relays
- ROCOF threshold of the ROCOF
- Intentional time delay for both relay types

The step sizes of the underfrequency and ROCOF steps have not been considered as a decision variable in the base case. This corresponds to a partial, more industry-oriented optimization formulation. The objective function is given by:

$$f(\mathbf{x}_d) = \sum_{j=1}^{M} p_{shd,j}(\mathbf{x}_d) \tag{5.1}$$

where M is the number of operating and contingency scenarios considered, $p_{shd,j}$ the amount of shed load in the *jth* scenario and $\mathbf{x}_d$ a vector containing the decision variables. The proposed design based upon these constraints and decision variables and the aforementioned representative operating and contingency scenarios as well as upon the objective function given by equation (5.1), is referred to as base case.

5-2-2 Impact of operating and contingency scenarios

Three different cases are analyzed and compared with the base case outlined in section 5-2-1. The first one, which has already been shown in section 4-4-1, corresponds to the case where the operating and contingency scenarios are determined by the common practice. In the second case, five (instead of four) representative operating and contingency scenarios are contemplated. Finally, the third case corresponds to the case where the UFLS scheme is designed with representative operating and contingency scenarios defined for generation dispatch scenarios without decoupled power generation

(DPG). This final case is interesting because it helps assessing the impact of DPG on the design of UFLS schemes.

Figure 5-1 compares the selected operating and contingency scenarios of the case with an additional fifth operating and contingency scenario with the selected operating and contingency scenarios of the base case of the La Palma power system. It can be deduced that an additional representative scenario allows covering an even wider frequency range.

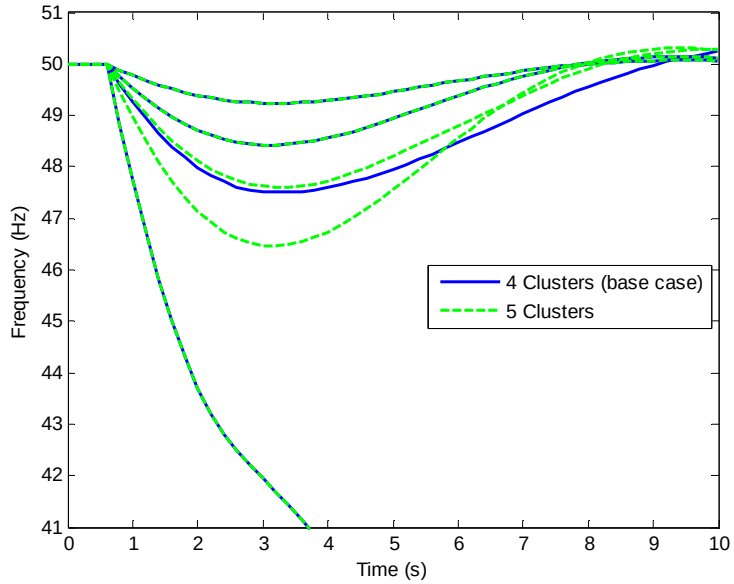

Figure 5-1: SFD model response to all possible operating and contingency scenarios of the La Palma power system.

DPG exhibits two drawbacks with regard to short-term frequency stability: its limited primary frequency control capacity and its negligible inertial response. Figure 5-2 (a) shows the response of the SFD to all possible operating and contingency scenarios of the La Palma power system. In addition, Figure 5-2 (a) compares the SFD model responses to all possible operating and contingency scenarios in the cases with a 40% of the totally installed capacity of DPG, covering about 10% of the total demand, and without decoupled power generation. Readily, system performance worsened with respect to underfrequency levels and to frequency decay rates. Figure 5-2 (b) compares the selected operating and contingency scenarios of the case without DPG with the selected operating and contingency scenarios of the base case of the La Palma power system. It can be deduced that neglecting DPG leads to less severe representative scenarios in terms of frequency. Inclusion or disregard of DPG could therefore have an impact on the UFLS scheme design, requiring a probable revision of an UFLS scheme designed without contemplating DPG.

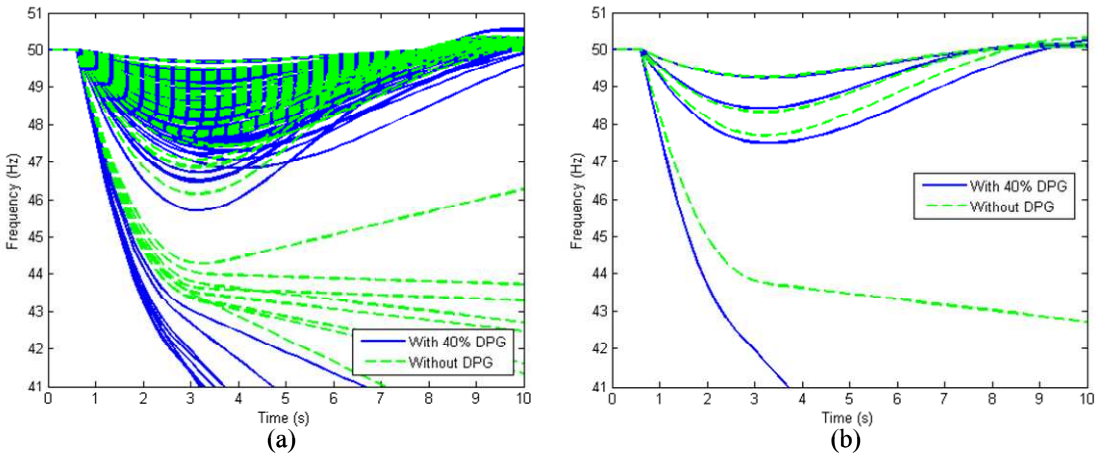

Figure 5-2: Comparison of different selections of operating and contingency scenarios.

The impact of an additional representative operating and contingency scenario and the impact of a set of less severe representative scenarios are shown in group 1 of Table 5-2. Figure 5-3 graphically summarizes some of the findings displayed in Table 5-2. Table 5-2 and Figure 5-3 display the results of the three cases when applied to all possible operating and contingency scenarios for generation dispatch scenarios with 40% of the total installed capacity of decoupled power generation. Compared with the base case and recalling the results from section 4-4-1, a design based on the common practice of scenario selection (case 1a) leads to worse results with relation to minimum frequency deviation, the amount of shed load and the number of error states indicating overshedding, late shedding, low frequency, etc. However, the effect of considering an additional representative scenario (case 1b) is negligible compared with the results of the base case. In fact, the slight differences are mainly caused by the objective function give in equation (5.1), which is a flat function, giving rise to different optimal solutions with equal objective function values (see also section 5-2-4). The same is true (except for the number of errors) for a UFLS scheme designed taking into account representative scenarios without decoupled power generation (case 1c). This is an interesting result since one expected a worse performance of the UFLS scheme designed without DPG when applied to operating and contingency scenarios with DPG.

Table 5-2: Performance of the proposed UFLS scheme for different selections of operating and contingency scenarios.

		UFLS performance				
Group	Case	Simulations	Σ Δωmin (Hz)	Nº Relays	Total shed (MW)	Nº error states
	Original	164	225.43	297	528.68	164
	Base case	164	218.73	128	222.75	4
	a) Common practice	164	230.10	200	366.93	83
1	b) Additional cluster	164	221.59	141	220.29	18
	c) No DPG	164	224.11	129	226.86	22

DPG: Decoupled power generation

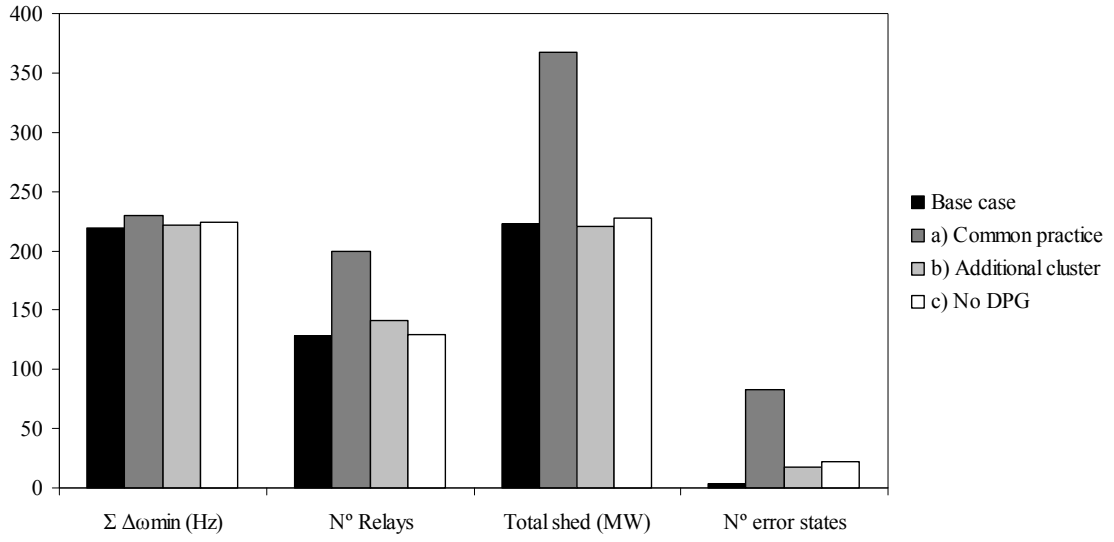

Figure 5-3: Comparison of the performance of different UFLS scheme designs.

A reason for the similar performance in terms of shed load and total frequency deviation of the base case design and the design without DPG could be the relatively low degree of DPG penetration. The use of 40% of the installed DPG capacity covers about 10% of total load demand. Another reason can be found by dint of Figure 5-2 (b). In fact, the difference between the representative operating and contingency is biggest for the scenarios with lowest frequency. It seems that this difference has little impact on the amount of shed load since the worst scenario in the case without DPG seems to be severe enough to prepare the UFLS scheme for even worse scenarios (such as in the case with 40% of the installed DPG capacity). However, the number of error states is distinct. The difference is mainly due to more low and high frequency errors in the case without DPG. This can be also inferred from Figure 5-4, which compares the impact of the base case design and the design without DPG on disturbances causing frequency to fall below 48 Hz. It can be seen that lower and higher frequencies as well as extended low frequency operation occur in the case without DPG.

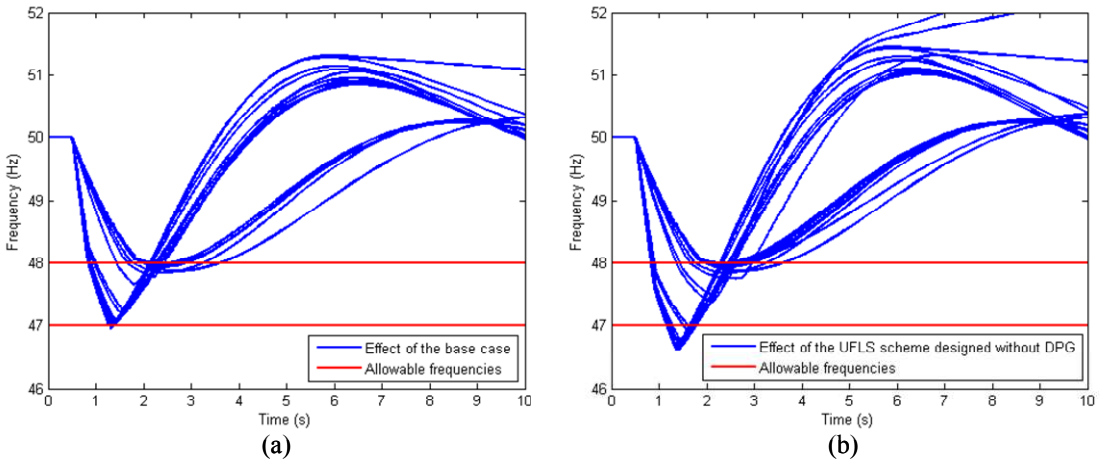

Figure 5-4: Comparison of the performance of (a) the base case design and (b) the design without DPG for disturbances causing frequency to fall below 48 Hz.

In order to check the performance of a UFLS scheme in presence of DPG, the base case design has been applied to operating and contingency scenarios with different degrees of DPG generation. In fact, another 7 MW of DPG are projected to be installed in the La Palma power system [CEIyC'09]. The considered cases include then no DPG, 40% and 80% of the currently installed capacity and 40% and 80% of the projected installed capacity. This allows studying operating and contingency scenarios with a DPG penetration varying between 0 and 40% of total load demand. Figure 5-5 shows the performance of the base case design in terms of average amount of shed load per disturbance and the number of error states. A clearly increasing tendency of the average amount of shed load and the number of error states can be deduced. The lower number of errors for the DPG penetration corresponding to 40% of currently installed capacity with respect to the case without DPG can be explained by the fact the UFLS scheme has been designed for this degree of DPG generation.

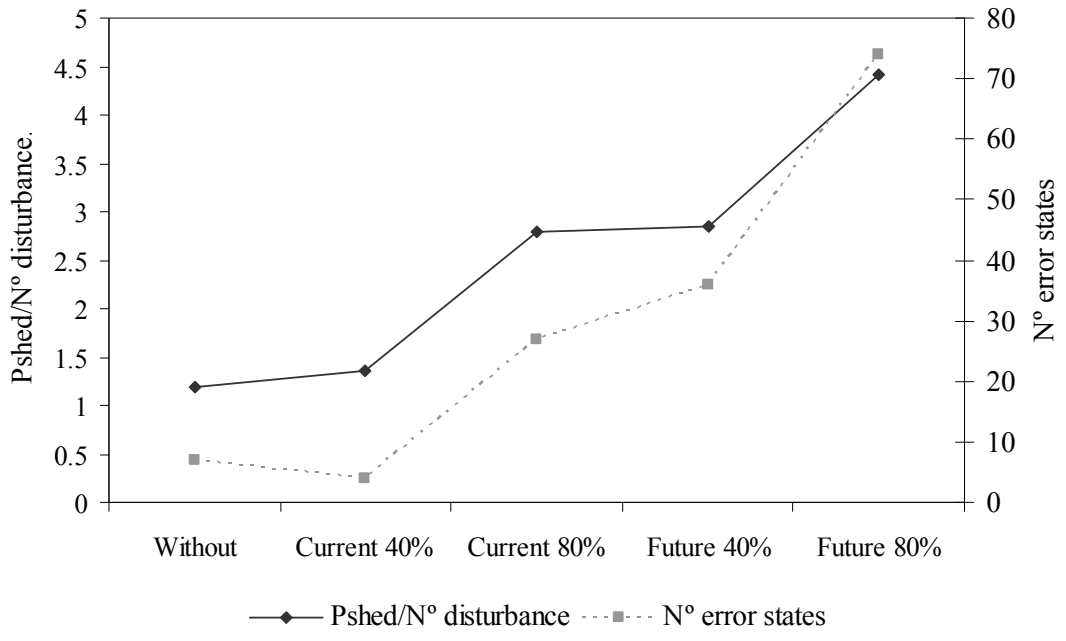

Figure 5-5: Performance of the proposed UFLS scheme for operating and contingency scenarios with increasing DPG penetration.

A consolidated view indicates that an UFLS scheme designed with scenarios which were determined by the common practice is less robust than UFLS scheme designed according to the proposed method. Further and after all, for higher degrees of DPG penetration, DPG should be contemplated when designing UFLS schemes. It seems that a significant change in the generation structure of a power system might require, at least, a review of the implemented UFLS scheme. Finally, if the number of representative operating and contingency scenarios is cautiously chosen, an additional scenario does not alter significantly the result.

5-2-3 Varying optimization constraints

Three different cases are considered to address the impact of a variation in the optimization constraints. In particular, a relaxation on the allowable minimum frequency and the possibility of rearranging the steps are considered. In fact, the omission of the constraint on the priority should intuitively lead to more efficient UFLS scheme designs since this corresponds somehow to a rough optimization of the step size. In other words, by enabling the optimization algorithm to rearrange the stages, a more adequate amount of load can be shed in each step of the final design. The relaxation on the allowable minimum frequency by allowing frequency to stay below 47.5 Hz for maximum 3 s could also result in a lower amount of shed load since the constraint is less restrictive.

Within group 2 in Table 5-3, the impact of changing one of these optimization constraints on the UFLS scheme design is shown, by applying the obtained UFLS schemes to all possible operating and contingency scenarios. Figure 5-6 graphically summarizes some findings of Table 5-3. It can be readily deduced that omitting priority (case 2c) remarkably reduces the amount of shed load as expected. However, the relaxation on the allowable minimum frequency (case 2a) did not improve with relation to the amount of shed load unless the minimum frequency threshold value permitted for the design of underfrequency relays $\omega_{thrshld,uf,min}$ has been lowered from 47 Hz (base case) to 46 Hz (case 2b). In the latter case, the amount of load has been reduced even further compared with the case where steps can be rearranged, at expense of an increased frequency deviation. By relaxing the constraint on allowable minimum frequency by applying the 47.5 Hz–3 s constraint, one accepts very low minimum frequencies (e.g. 46 Hz or less) although power-system responses finally comply with the imposed constraint. This enhances the risk of tripping generating units by their underfrequency protection.

Table 5-3: Performance of the proposed UFLS scheme for different formulations of the optimization problem.

		UFLS performance				
Group	Case	Simulations	Σ Δωmin (Hz)	Nº Relays	Total shed (MW)	Nº error states
	Original	164	225.43	297	528.68	164
	Base case	164	218.73	128	222.75	4
	a) 47.5Hz - 3s	164	234.07	126	219.76	3
2	b) 47.5Hz - 3s (ωuf>46Hz)	164	246.07	67	100.49	6
	c) No priority	164	217.98	121	187.02	10

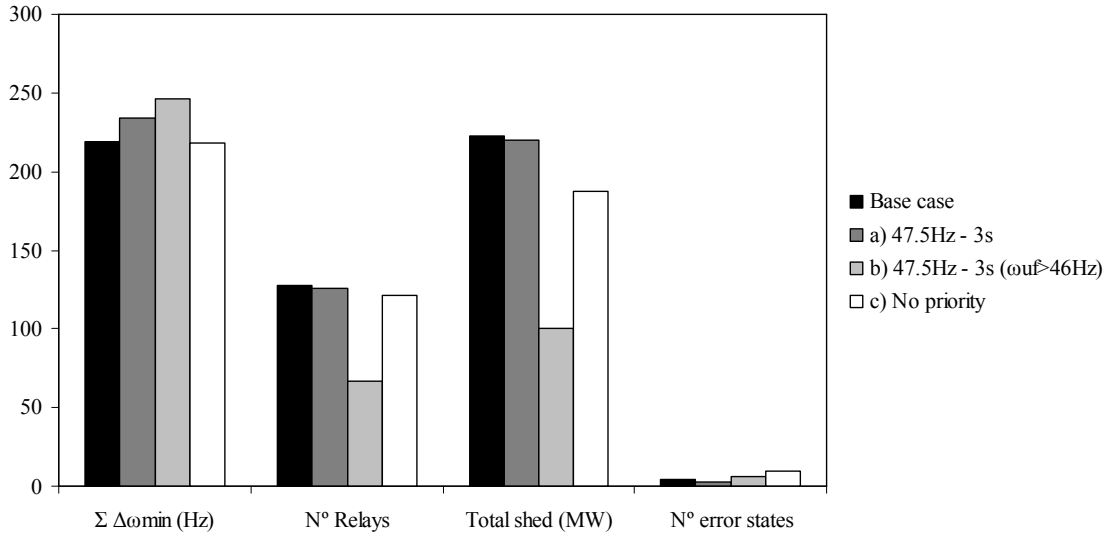

Figure 5-6: Comparison of the performance of different UFLS scheme designs.

5-2-4 Varying objective function formulations

In a next step, three different formulations of the objective function have been analyzed. The contemplated objective functions also include a term related to the minimum frequency deviation. This way, the impact of a composite objective function on the design of UFLS scheme can be observed. In particular, three cases are considered. First, a composite objective function with weights equal to unity is tested. This objective function has been used in [Denis Lee Hau'06]. Thereupon, an objective function with a more heavily weighted frequency term is used, where the weighting coefficient associated to the frequency-dependent term is equal to the equivalent gain k_{eq} of an operating and contingency scenario (here 20). Intuitively, both formulations should influence the result of the UFLS scheme design such that frequency deviation reduce, albeit the latter to a much greater extent. Finally, an objective function similar to the base case formulation is contemplated but with weighting coefficients proportional to the number of operating and contingency scenarios associated to each representative operating and contingency scenario (see also section 4-3-1). This way, less load could be shed for representative scenarios with a larger number of associated operating and contingency scenarios.

Group 3 in Table 5-4 comprehends the results of applying UFLS schemes designed using one of these objective function formulations to all possible operating and contingency scenarios. Figure 5-7 graphically summarizes some findings of Table 5-4. It can be readily deduced that by including a term related to the minimum frequency deviation (case 3a), frequency deviations are reduced at the expense of an increased amount of shed load. This is even truer for the more heavily weighted case (case 3b).

Similar results have been obtained by a slightly more extensive study presented in [Halevi'93]. Finally, weighting the amount of shed in a scenario by the number of operating and contingency scenarios associated to this scenario (case 3c) did not improve the results with respect to the base case design. This can be explained by the fact that the settings of UFLS scheme parameters are not independent of the considered operating and contingency scenarios and that, for example, the amount of shed load in less severe scenarios needs to be increased to guarantee stability for a more severe scenario.

Table 5-4: Performance of the proposed UFLS scheme for different formulations of the optimization problem.

	UFLS performance				
Case	Simulations	Σ Δωmin (Hz)	Nº Relays	Total shed (MW)	Nº error states
Original	164	225.43	297	528.68	164
Base case	164	218.73	128	222.75	4
a) fobj = Σ(Δωmin + pshd)	164	209.02	177	239.03	16
b) fobj = Σ(keq·Δωmin + pshd)	164	188.83	217	318.96	8
c) fobj = Σ ncont·pshd	164	220.44	129	226.95	7

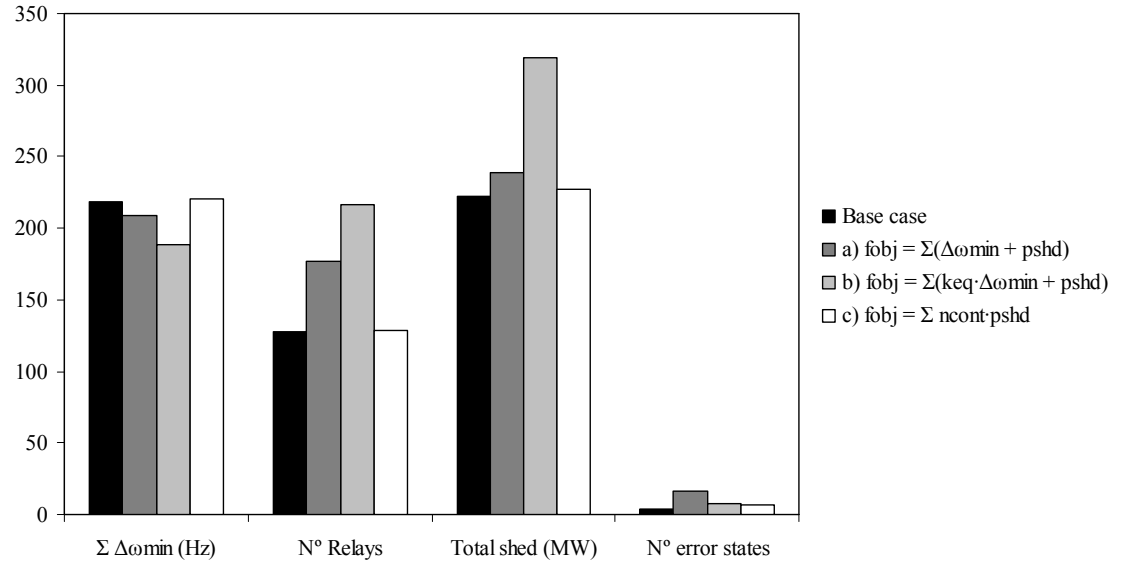

Figure 5-7: Comparison of the performance of different UFLS scheme designs.

A final remark for the slightly weighted case can be made. Due to its step-like nature, the objective function used for the base case is a very flat function, which could generate different optimal solutions with equal final objective function values. Since differences between slightly weighted case (case 3a) and base case are not too large and since the slightly weighted objective function is an uneven function, this objective function is a promising candidate to reduce the set of optimal solutions. Figure 5-8 shows a boxplot for repeated designs using either the base case configuration or a slightly weighted objective function (weights equal to unity). In other words, adaptive Simulated Annealing has been applied several times using either the base case configuration or the modified slightly weighted objective function (case 3a). The considered values, i.e. ΣΔfmin and ΣΔpshd for all possible operating and contingency scenarios, have been normalized by the mean values of the base case in order to be able to compare them. From Figure 5-8, it can be inferred that variations in results of ΣΔfmin and ΣΔpshd have been clearly reduced in the case of repeated designs using a slightly weighted objective function.

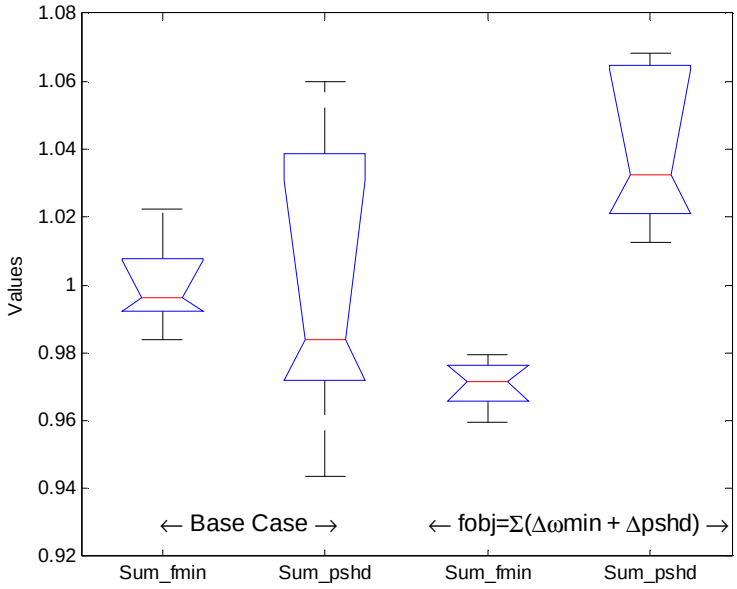

Figure 5-8: Performance comparisons for repeated designs using either the base case configuration or a slightly weighted objective function.

5-2-5 Varying optimization algorithms

A further analysis has been carried out with respect to the optimization algorithm applied to the problem of designing efficient UFLS schemes. A large amount of possible candidate algorithms exist: Sequential quadratic programming (SQP), Genetic Algorithm (GA), Pattern Search, Particle Swarm Optimization, etc [Zabinsky'03; Enrique'09]. Within this group, gradient or Hessian-based algorithms seem to be less appropriate since the present problem is highly discontinuous due to the step-like nature of UFLS schemes, unless the step size (complete optimization) is considered as a decision variable. Heuristics algorithms are thus preferable.

Genetic Algorithm has been finally chosen, as suggested in [Martínez'93; Lopes'99]. If algorithm parameters are properly chosen, similar results should be found. Genetic operators and parameters correspond to those recommended in [Lopes'99; Lopes'00]. As shown in the fourth group in Table 5-5 and in Figure 5-9, the design obtained by applying GA has a similar (although slightly worse) impact on all possible operating and contingency scenarios in terms of minimum frequency deviations and amount of shed load as the base case. In other words, a different heuristic algorithm leads to similar results with similar computation times.

Table 5-5: Performance of the proposed UFLS scheme for different formulations of the optimization problem.

		UFLS performance				
Group	Case	Simulations	Σ Δωmin (Hz)	Nº Relays	Total shed (MW)	Nº error states
	Original	164	225.43	297	528.68	164
	Base case	164	218.73	128	222.75	4
4	GA optimized	164	218.25	128	224.77	6

GA: Genetic algorithm

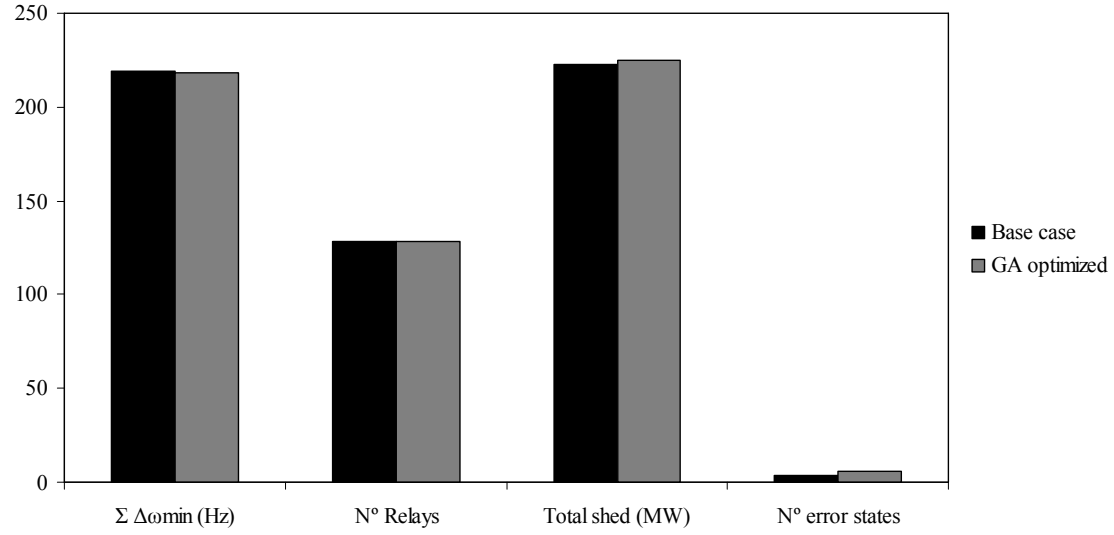

Figure 5-9: Comparison of the performance of different UFLS schemes designs.

5-2-6 Varying decision variables

Three different cases are analyzed to study a variation in the decision variables. In fact, only partial, industry-oriented optimization strategies have been pursued so far, i.e. the step size has not been considered a decision variable. The principal reason was that for rather small power systems it does not make sense to adjust the step size. In fact, the step size is usually defined by the utility and also depends on the feeders connected to the relays defined by a particular stage and on the priority of the associated loads; therefore, in smaller power systems such as the La Palma power system, it will be difficult to find feeder blocks which finally sum up to the desired step size.

Hereupon, complete optimization is studied, i.e. the optimization of all possible UFLS scheme parameters including frequency and ROCOF thresholds, intentional time delays and step sizes. It has been supposed that underfrequency and ROCOF steps are decoupled (i.e. no feeder is equipped simultaneously with an underfrequency and a ROCOF relay). Three cases are considered. First, sequential quadratic programming (SQP) is applied to the problem of optimal tuning of all UFLS scheme parameters. This corresponds to the method presented in [Denis Lee Hau'06]. In a further step, Simulated Annealing (SA) is used. Finally, a partial optimization based on GA is applied. In this case and as proposed in [Martínez'93], only frequency thresholds and step sizes are taken into account. The involvement of the step size should reduce the amount of shed load.

Within group 5 in Table 5-6, the impact of involving the step size as a decision variable is shown, by applying the obtained UFLS schemes to all possible operating and contingency scenarios. These results are also graphically presented in Figure 5-10. It can be readily deduced that the complete optimization based on SQP (case 5a) yielded

to a design which predominantly reduces minimum frequency deviation. In fact, the results resemble those obtained for the case of weighting heavily the frequency-related term in the composite objective formulation in group 3. This results is however not surprising since SQP depends strongly on the initial guess of the decision variables which coincides with the parameters of the currently installed UFLS scheme. This has also been stated in [Denis Lee Hau'06]. By lowering initially frequency thresholds for example, results can be improved.

Table 5-6: Performance of the proposed UFLS scheme for different formulations of the optimization problem.

	UFLS performance				
Case	Simulations	Σ Δωmin (Hz)	Nº Relays	Total shed (MW)	Nº error states
Original	164	225.43	297	528.68	164
Base case	164	218.73	128	222.75	4
a) Complete optimization (SQP)	164	187.65	272	340.34	32
b) Complete optimization (SA)	164	220.25	83	167.05	10
c) ωthrshld - pstep (GA)	164	217.7	85	198.16	7

GA: Genetic algorithm
SA: Simulated Annealing
SQP: Sequential quadratic programming

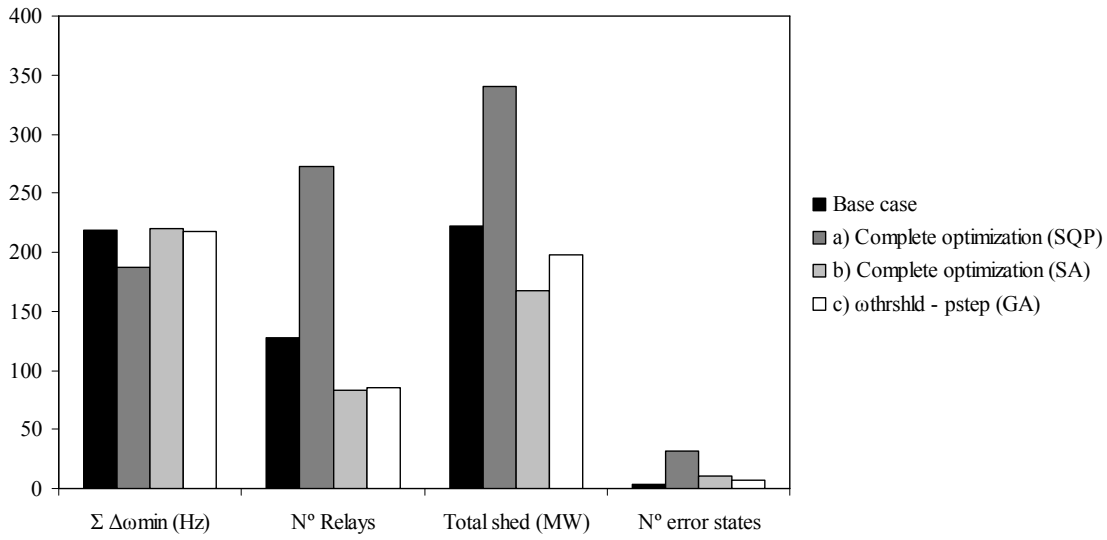

Figure 5-10: Comparison of the performance of different UFLS scheme designs.

By contrast, complete optimization based on SA (case 5b) achieved much better results with respect to amount of shed load. In fact, the design halved the amount of shed load compared with previously obtained design based on SQP, but at the expense of increased minimum frequency deviations. At that time, it is noteworthy that UFLS scheme design obtained through a SA-based complete optimization has similar impact on all possible operating and contingency scenarios than the UFLS scheme designed without considering the priority constraint (see also case 2c in section 5-2-3). This is insofar an interesting finding since it shows that for smaller isolated power systems, where complete optimization is theoretically feasible but less practical, relaxing the constraint on priority leads to very efficient UFLS schemes with a performance similar to SA-based, completely optimized UFLS scheme.

Finally, Table 5-6 and Figure 5-10 also display the results for the case where only frequency thresholds and step size are considered as decision variables (case 5c). This

case corresponds to a design proposed in [Martínez'93]. It can be inferred that this GA-based, partial optimization is slightly less efficient than the SA-based complete optimization. Different algorithm parameters than those suggested in [Lopes'99; Lopes'00], including typical values for crossover and mutation probabilities, did not significantly improve the result with respect to SA-based complete optimization.

5-2-7 Summary of design condition variations

Several variations of design conditions, corresponding either to the problem of operating and contingency scenario selection or to the formulation of the optimization problem, have been studied. In particular, different selections of operating and contingency scenarios and different choices of optimization constraints, objective functions and optimization algorithms as well as different choices of decision variables have been considered.

The resulting UFLS scheme designs of some of these variations and their impact on power system and UFLS scheme performance are of practical interest for system utilities and operators. For the sake of brevity, only the most remarkable ones of these design condition variations are restated; in particular,

- The selection of operating and contingency scenarios using the common practice (case 1a)
- The disregard of decoupled power generation for the design of UFLS schemes (case 1c)
- The omission of load priority for the design of UFLS schemes (case 2c)
- The inclusion of the step size as an additional decision variable (case 5b)

Figure 5-11 compares the performance of the four design condition variations with the performance of the base case. Most significant differences between these cases can be found in the total amount of shed load. More load has been shed in comparison to the base case when applying the common practice to selection of operating and contingency scenarios. Neglect of decoupled power generation worsened after all the number of error states. Further and after all for higher degrees of DPG penetration, DPG should be contemplated when designing UFLS schemes. It seems that a significant change in the generation structure requires reviewing UFLS scheme designs. Moreover, clustering-based selection of operating and contingency scenarios leads to more robust UFLS schemes. By contrast, the amount of shed load has been reduced with regard to the base case by omitting load priority or by considering the step size as an additional decision variable. A comparison of cases 2c and 5b in Figure 5-11 leads to the conclusion that the omission of load priority in small power systems approaches well the solution obtained by including the step size in the optimization process. This is insofar relevant since in small power systems it is difficult to find feeder blocks which finally sum up the step size determined by the optimization algorithm.

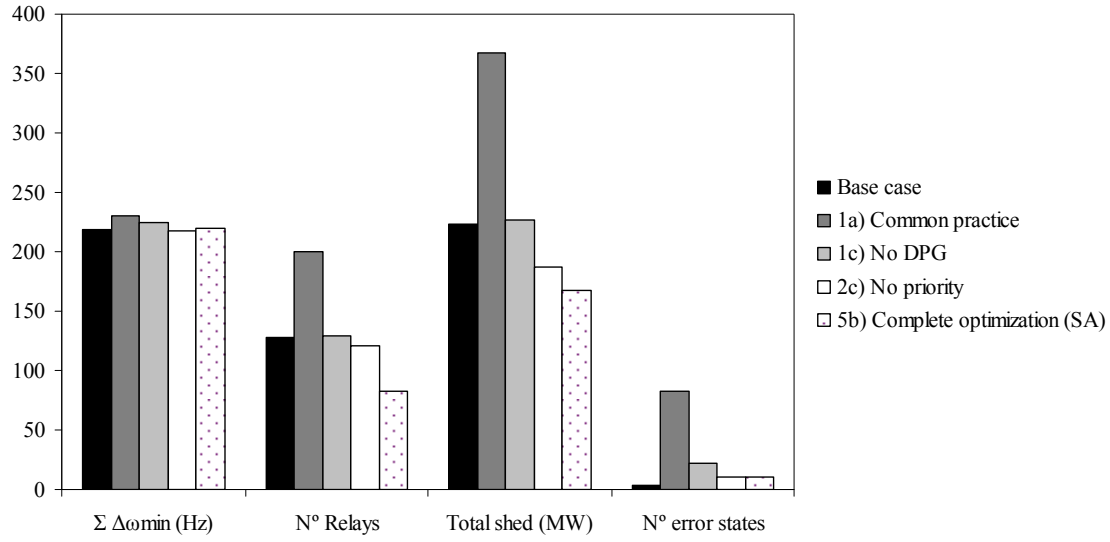

Figure 5-11: Comparison of the performance of different UFLS scheme designs.

5-3 IMPACT OF STEP SIZE VARIATIONS

The step size is critical to the performance of UFLS schemes. Usually, UFLS scheme designs assume an invariant and known percentaged value for the step size or as in the case of optimized step sizes, they suppose that the adjusted step size is both realizable and its percentaged value invariant. Typical values are within 7-15% of load demand per step [IEEE'68].

The implemented step size normally differs of the actual step size due to a number of reasons. First, the predefined step size associated to each step during the design process might vary considerably from the actual step size if, for example, a customer is offline or consumes a larger amount of energy than expected, etc. A statistical analysis of the consumption is usually carried out to gain some insight in the behavior of customers and to strengthen the assumption of the step size [Sigrist'10a]. Apart from rather random changes, this demand variation depends also on daily and seasonal factors and on the customer type. Another reason for differences between implemented and actual step size is given by the fact that feeders might also be disconnected, i.e. out of operation, due to maintenance operations, etc. Finally, actual amount of shed load might differ due to breaker failures [UCTE'06]. However, this last reason is less probable because of the reliability of currently used underfrequency and ROCOF relays. Briefly, differences between implemented and actual step size can be explained by the following causes:

- Variation of feeder load
- Feeders outage
- Breaker failures

In what follows, causes for step-size variations are further explained and their impact on the performance of an UFLS schemes are analyzed. It will be shown that these variations can be modeled using statistical distributions. In a next step, the design of backup steps of UFLS schemes is addressed. These steps should guarantee system stability when implemented step size and actual step size significantly differ due to feeder-load variation, disconnected feeders or breaker failures. In other words, if regular steps, adjusted according to the proposed method for the design of robust and efficient

UFLS schemes, fail to arrest frequency decay, backup steps enter the load-shedding process trying to save the power system.

5-3-1 Causes for step-size variations

Feeder-load variation and its impact, and in particular changing daily load profiles of residential, commercial and industrial costumers, is easiest explained graphically. Figure 5-12 and Figure 5-13 show different load-demand variations during 24 hours. Figure 5-12 illustrates daily load curve corresponding to the peak demand of Spanish power system in 1997 [REE'98]. Although the whole system demand is represented and no insight is gained into demand of particular distribution feeders, it can be inferred that demand of distinct customer groups (residential, commercial or industrial) differently evolves over the course of the day. Consider, for example, the points in time corresponding to valley and peak demand (indicated by dashed lines). Clearly, the proportion of residential and interruptible industrial users with respect to the whole demand significantly varies. If step sizes were determined according to peak demand proportions, appreciable differences could be expected for valley load-demand levels.

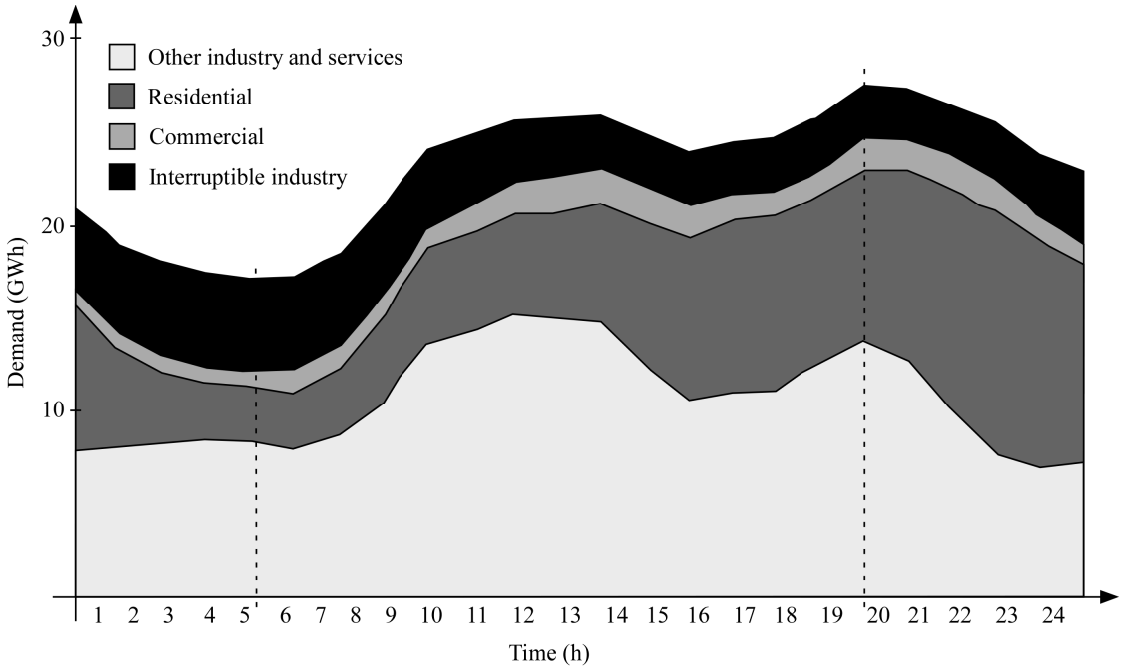

Figure 5-12: Daily load curve of 1997 peak load-demand level [REE'98].

Figure 5-13 gives some more insight into seasonal variations and different customer groups on distribution level. Typical summer and winter load curves of the Canary Islands are compared in Figure 5-13 (a) [REE'09]. A shift in peak demand can be observed. Figure 5-13 (b) shows daily load profiles of industrial and residential customers on distribution level. In addition, weekday and weekend load profiles are compared. More extensive research on load profile determination and classification can be found in [Jardini'00] and [Gerbec'02]. It is clear from Figure 5-13 (b) that different customers exhibit different load profiles with, for example, different peak load-demand instants. Another interesting observation can be made comparing weekday and weekend load profiles. The considered industrial customer has a significantly distinct consumption during weekdays and weekends. Again, this variation in demand due to different customer groups or due to daily or seasonal variations might result in different demand proportions and consequently in different percentaged values of step sizes than foreseen.

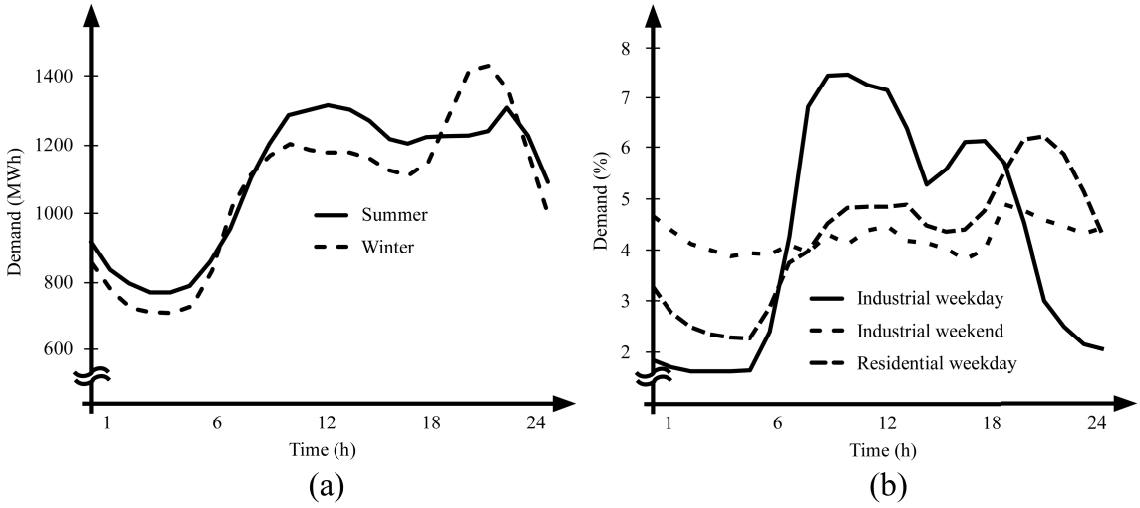

Figure 5-13: (a) Seasonal demand variation and (b) load profile of different customer groups.

5-3-2 UFLS scheme performance in presence of varying step sizes

It has been shown that different customer types and seasonal and daily load variations could cause differences between implemented and actual percentaged values of step sizes of UFLS schemes. The question arises how these variations can be modeled.

A literature review shows that research is principally focused on the application of known statistical distributions, although it is well known that customer level load does not generally follow a known distribution function [Seppala'95]. Some loads even lack any regular distribution. However, according to [Seppala'95], loads are usually distributed around a mean and in many cases the distribution has a bell shape. Thus, a large variety of distribution functions satisfying the latter observation have been studied and applied to actual load data, among others Weibull, beta, log-normal and normal distributions. In [Ghosh'97], it is concluded that using appropriate parameters, the beta function could be a possible candidate for describing load demands because of its flexibility to adapt to the skewness in distribution. Log-normal distributions are proposed in [Seppala'95]. Finally, comparing several distribution functions, it has been shown that for symmetrically distributed load, normal as well as log-normal or beta distributions accurately describe load variation, whereas for asymmetrically distributed load, beta or log-normal distributions are preferable [Ghosh'97; Neimane'01]. Nevertheless, the most common technique to model loads is through normal distribution [Singh'10]. By invoking the Central Limit Theorem (see e.g. [von Lanzenhauer'74]), normal distributions have been applied to total load demand variations or to feeder-level variations for feeders containing a large group of different customers [Leite da Silva'90]. Examples of actual load data and associated probability density functions are shown in Figure 5-14. These data have been obtained by measurements at a medium-voltage substation. Thus, normal distribution is chosen here to model variations of the step size.[1]

[1] Independent of the distribution function chosen, it must be noted that different distribution functions may describe different periods during a day [Seppala'95]. The same is also true for different customer types. But modeling each feeder by a different distribution functions would complicate the problem far behind its objectives.

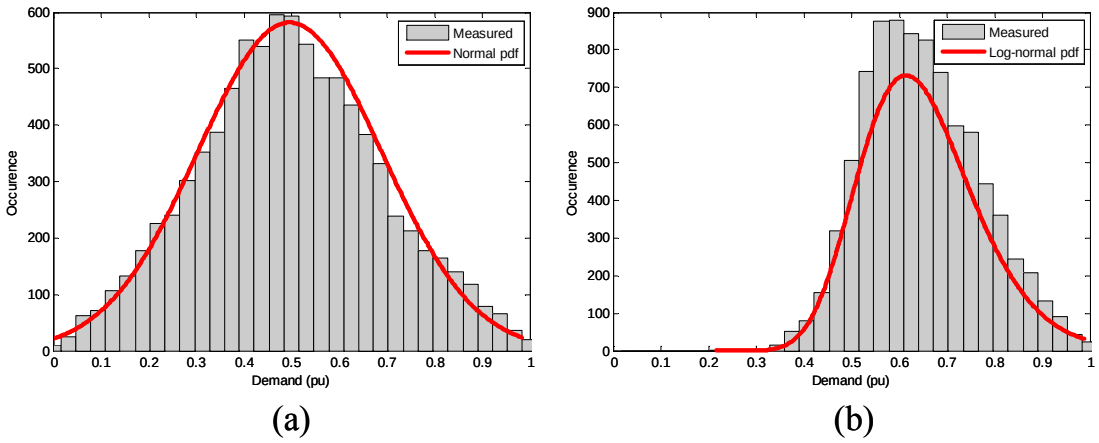

Figure 5-14: Histogram and corresponding density function of actual load data.

The normal distribution only describes the variations due to demand variations. Feeders out of operation or breaker failures are not included. These events could be easily modeled by means of a Bernoulli distribution, i.e. according to the event the step size corresponds with a certain probability to its actual value or is zero. The total variation of the step sizes is therefore described by the simultaneous occurrence of two random variables corresponding to a normal distribution and a Bernoulli distribution, which is equivalent to multiplying these two random variables [Rubinstein'08].

Denote $g_a(\bullet)$ the normal probability density function and $b_e(\bullet)$ the Bernoulli probability density function given by

$$b_e(y) = p\delta_{dirac}(y) + (1-p)\delta_{dirac}(y-1)$$

where p is the failure probability. Then step sizes greater than zero are described by the normal probability density function $g_a(\bullet)$ multiplied by $(1\text{-}p)$, whereas zero step sizes correspond to the sum of the failure probability density $p\delta_{dirac}(0)$ and the value of zero step size of the probability density function $g_a(\bullet)$, i.e. $g_a(0)$, multiplied by $(1\text{-}p)$. The corresponding probability density function $gb(\bullet)$ can be finally written as follows:

$$gb(y) = \begin{cases} p + (1-p)g_a(0), & y = 0 \\ (1-p)g_a(y), & 0 < y \le 1 \end{cases} \tag{5.2}$$

Figure 5-15 illustrates the probability density function given in equation (5.2). Two comments can be made with respect to probability density function $gb(\bullet)$. First, for small values of p, the probability function could be approximated by the normal probability density function. Second, for rather worst-case-like step-size variations, a uniform distribution function could be used, attaching great significance to larger demand variations.

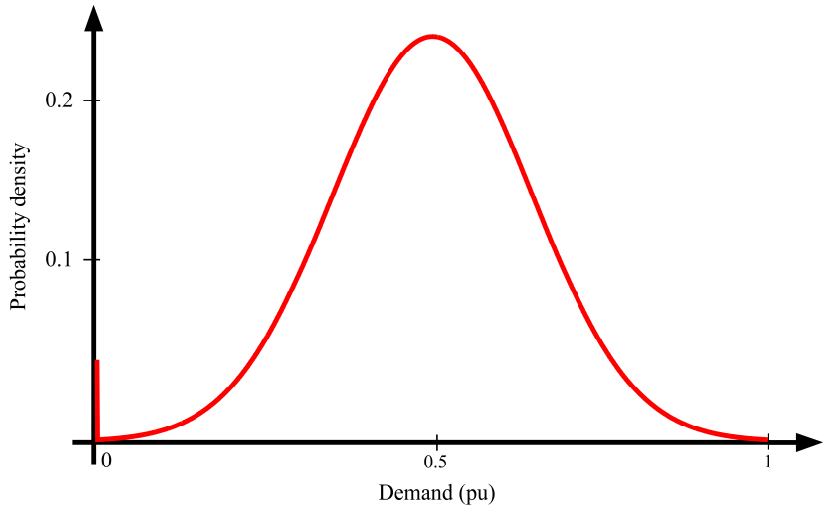

Figure 5-15: Illustration of the probability density function of equation (5.2).

Figure 5-16 and Figure 5-17 show the impact of step-size variation on the representative operating and contingency scenarios (only scenarios with load-shedding activity, corresponding to the first two rows of Table 5-1, are shown) and compare it to the case with constant step sizes. The probability density function of equation (5.2) has been used to model step-size variation. The failure probability of the Bernoulli distribution is set to 0.01, whereas the normal distribution has a mean and a standard deviation of 0.5 and 0.1, respectively. In addition, a minimum available amount of sheddable load is imposed[2]. A realistic value is 60%. Thousand Monte-Carlo simulations have been run.

Figure 5-16 (b) shows the impact of varying step sizes on the performance of the original La Palma UFLS scheme, whereas Figure 5-17 (b) shows the impact on the performance of the proposed UFLS scheme. Clearly, frequency falls in both cases below the minimum allowable frequency of 47 Hz imposed for design (see also 4-4-1), but to a much lesser extent in the case of the proposed design. Furthermore, strong frequency overshoots can be observed for both the original and the proposed UFLS scheme, indicating overshedding. By comparing Figure 5-16 (a) and Figure 5-16 (b) as well as Figure 5-17 (a) and Figure 5-17 (b), it seems that step-size variations affect more the original UFLS scheme design than the proposed UFLS scheme.

[2] It is unrealistic consider situations where, for example, only 10% of total amount of sheddable load is available. Furthermore, in such a case, it would be impossible to protect the power system against collapse. Note that this value is used to limit the overall reduction of available amount of sheddable load, but not the reduction of a single step (which can be unavailable).

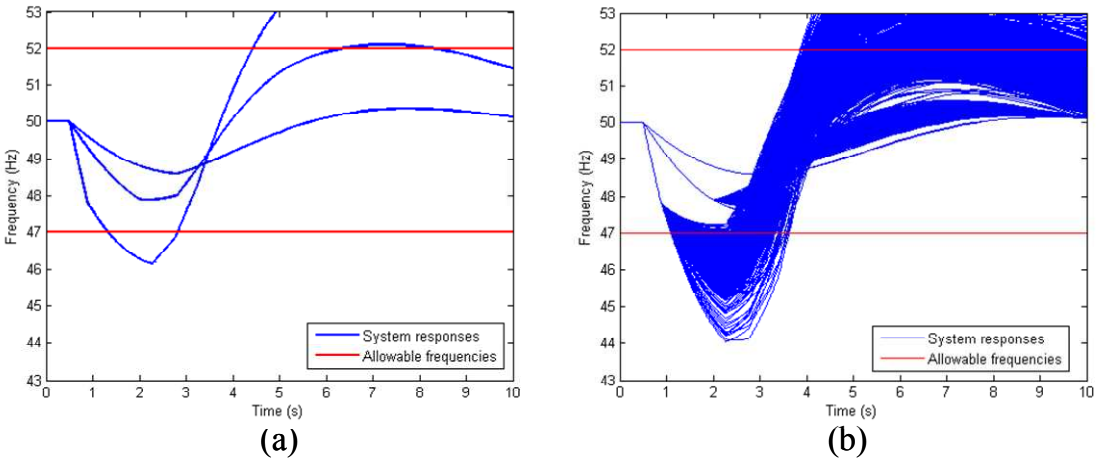

Figure 5-16: System responses in presence of (a) constant step sizes and (b) varying step sizes with the original La Palma UFLS scheme.

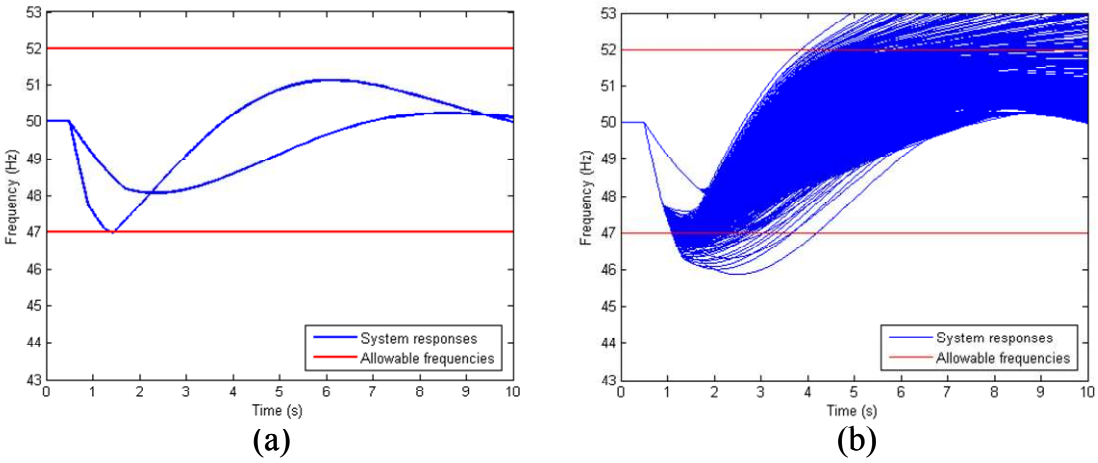

Figure 5-17: responses in presence of (a) constant step sizes and (b) varying step sizes with the proposed La Palma UFLS scheme.

Figure 5-18 compares the performance of the original and proposed UFLS scheme in presence of step-size variations. Accumulated minimum frequency deviations, accumulated time that frequency is below 47 Hz and total amount of shed load of all Monte-Carlo simulations are shown. Figure 5-18 confirms that the power system with the original UFLS scheme suffers larger frequency deviations, with longer frequency operation below 47 Hz and shedding more load than the system with the proposed UFLS scheme. Nevertheless, extended operation below 47 Hz put the power system at risk and should be avoided. The use of properly designed backup steps should reduce the impact of varying step sizes by minimizing operation at dangerously low frequency levels.

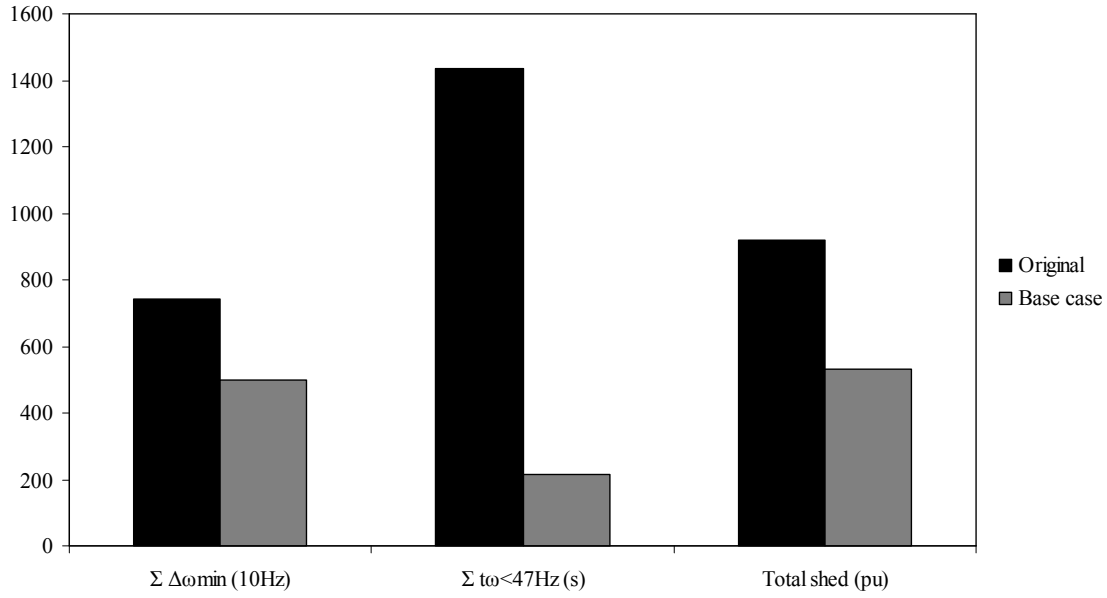

Figure 5-18: Comparison of the performances of the original and the proposed UFLS scheme in presence of step-size variations.

5-3-3 Design of backup steps of UFLS schemes

For the design UFLS schemes, it has been supposed that the percentaged values of step sizes are invariant. However, actual step size usually differs from the implemented one due to variations of feeder load, feeder outages or due to breaker failures. These variations of the step size, simulated by a statistical distribution, can have a jeopardizing impact on system stability. Focus is here on the impact of reduced step sizes. Reduced step sizes will put the power system at risk since less load might be shed than necessary and since frequency deviations increase, allowing the design of backup steps.[3] Backup steps of UFLS schemes should reduce the vulnerability of the power system in such cases. Backup steps are those steps of an UFLS scheme which have not been adjusted since unnecessary when applying the proposed method for the design of robust and efficient UFLS schemes.

Although backup steps are only considered to address the problem of step-size variations, other phenomena such as non-responding or only partially responding turbine-governor systems or consecutive outages of generating units might require the presence of backup steps. In [Chuvychin'96], the problem of consecutive outages has been discussed. The case of partially responding turbine-governor system could occur in steam turbines of combined cycle power plants. In fact, if a gas turbine of the combined cycle power plant is lost, the steam turbine is initially able to provide primary frequency control, but it will reduce or cease generating power after a certain time due to reduced heat ducted to the waste heat boiler. Thus, backup steps are used for a variety of events and disturbances involving different dynamics, which are not considered during the design of UFLS schemes. Their objective is to support the UFLS scheme in such cases and to guarantee system integrity, and minimizing the amount of shed load is not

[3] The impact of increased step size, causing overshedding and possibly high overfrequency, is indirectly taken into account. In fact, such cases can also arise due to step-size reduction since an additional UFLS scheme stage could enter the load-shedding process, causing overshedding and overfrequency.

paramount anymore. For example, consecutive outages of generating units could also occur in a power system, but during design process for UFLS scheme, one does not know when these outages actually occur and which dynamics cause consecutive generating units to trip, complicating the design process.

The need of backup steps has been already recognized in [El-Banhawy'91; Mak'91], but a general method for their design has not been presented so far. According to the characteristics of the power system, one can distinguish between time coordinated or frequency coordinated backup steps [Mak'91; Hsu'97]. Time coordinated backup steps have frequency threshold within the range of frequency of regular UFLS steps but with larger delays (around 5 up to 20 s) and therefore, they can also be considered as restoration steps in the case frequency settles at low frequency values. Frequency coordinated backup steps, by contrast, have lower frequency values than regular UFLS steps and short delays and they actuate if frequency falls below foreseen values.

The proposed method for the design of UFLS backup steps consists in two consecutive tasks. First, several combinations of different backup steps settings are heuristically designed, based on simplified variations of UFLS scheme step sizes. In a second step, the proposed designs are validated and evaluated using a Monte-Carlo simulation approach. Monte-Carlo simulations have been already used to design UFLS schemes in a screening-like manner [Thalassinakis'04]. This screening-based design method is adopted to design UFLS backup steps. The principal difference is that in [Thalassinakis'04] exponential distributions in time have been used to model generator outages, whereas here a distribution function is used that models step-size variations.

5-3-3-1 Propositions of backup-step settings

Analogous to the proposed method for the design of robust and efficient UFLS schemes, the heuristic design of backup steps of UFLS schemes is exclusively applied to representative operating and contingency scenarios. Moreover, only scenarios with load-shedding activity, corresponding to the first two rows of Table 5-1 of the La Palma power system, are taken into account. This makes sense since variations of step sizes only affect these scenarios. If, however, other problems arise such as turbine-governor inactivity, at least all representative operating and contingency scenarios must be contemplated. In either case, design of backup steps is based upon simplified step-size variations which are modeled by variations of 0.1, 0.3 and 0.5 pu and applied equally to all step sizes. A variation of 0.5 pu signifies thus a reduction of 50% of all step sizes. These values correspond to slight, medium and heavy variations of step sizes, but other values could be chosen, if considered more appropriate. Thus, different settings of backup steps are heuristically determined according to the considered operating and contingency scenarios with load-shedding activity and the equally applied step-size variations of 0.1, 0.3 and 0.5 pu.

Table 5-7 displays a selection of reasonable propositions for backup-step settings for the La Palma UFLS scheme. These five propositions have been heuristically determined. Stages 7 to 10 have been adjusted since stages 1 to 6 have been designed using the proposed method as shown in section 4-4-1. Two groups can be readily distinguished. Propositions V1, V2 and V3 switched stages 7 and 8 by imposing a higher threshold frequency to stage 8, trying to reduce the amount of shed load for operating and contingency scenarios of which frequency falls only slightly below the minimum allowable frequency of 47 Hz. In fact, minimum allowable frequencies have been modeled by two constraints, 48 Hz–3 s and 47 Hz–0 s, being the latter the more critical constraint. Propositions V4 and V5 maintain the initial order of backup steps.

Within each group, propositions vary due to different time or frequency coordination among backup steps. For example, the first two steps of V2 are identical to the ones of V1, but the following steps are time-coordinated steps at 47 Hz instead of frequency-coordinated steps like in V1. The intentional time delays of backup steps 9 and 10 are typical values and are similar to the ones of the existing UFLS scheme (see Table 4-6). By contrast, proposition V3 has closer frequency thresholds than V1, but identical intentional time delays; therefore, V3 should faster arrest frequency decays, at the expense of possible overshedding. Similar remarks apply to propositions V4 and V5.

Table 5-7: Propositions of different backup-step settings for the La Palma UFLS scheme.

UFLS backup steps											
Stage	V1		V2		V3		V4		V5		Step size (%)
	ω (Hz)	t_{int} (s)	ω (Hz)	t_{int} (s)	ω (Hz)	t_{int} (s)	ω (Hz)	t_{int} (s)	ω (Hz)	t_{int} (s)	
7	46.5	0.1	46.5	0.1	46.8	0.1	46.8	0.1	46.8	0.1	12.5
8	47	0.1	47	0.1	47	0.1	46.6	0.1	46.5	0.1	4.2
9	46	0.1	47	1.5	46.4	0.1	46.4	0.1	47	1.5	15.1
10	45	0.1	47	2.5	45	0.1	47	2.5	47	2.5	20.5

t_{opn} = 0.2s

5-3-3-2 Evaluation of the proposed backup-step settings

Backup-step settings V1 to V5 have been determined using representative operating and contingency scenarios with load-shedding activity and assuming that step-size variations are equally applied to all step sizes. Subsequently, these backup-step settings are applied again to the representative operating and contingency scenarios, but this time step-size variations are modeled by the probability density function of equation (5.2), which is shown in Figure 5-15. The failure probability is set to 0.01, whereas mean and standard deviation are 0.5 and 0.1, respectively. Again, an overall minimum available amount of sheddable load of 60% is imposed, and thousand Monte-Carlo simulations are performed.

Figure 5-19 illustrates the effect of backup-step propositions of Table 5-7 on representative operating and contingency scenarios with load-shedding activity and in presence of step-size variations. The same random step-size variations have been applied to test the five backup-step propositions.

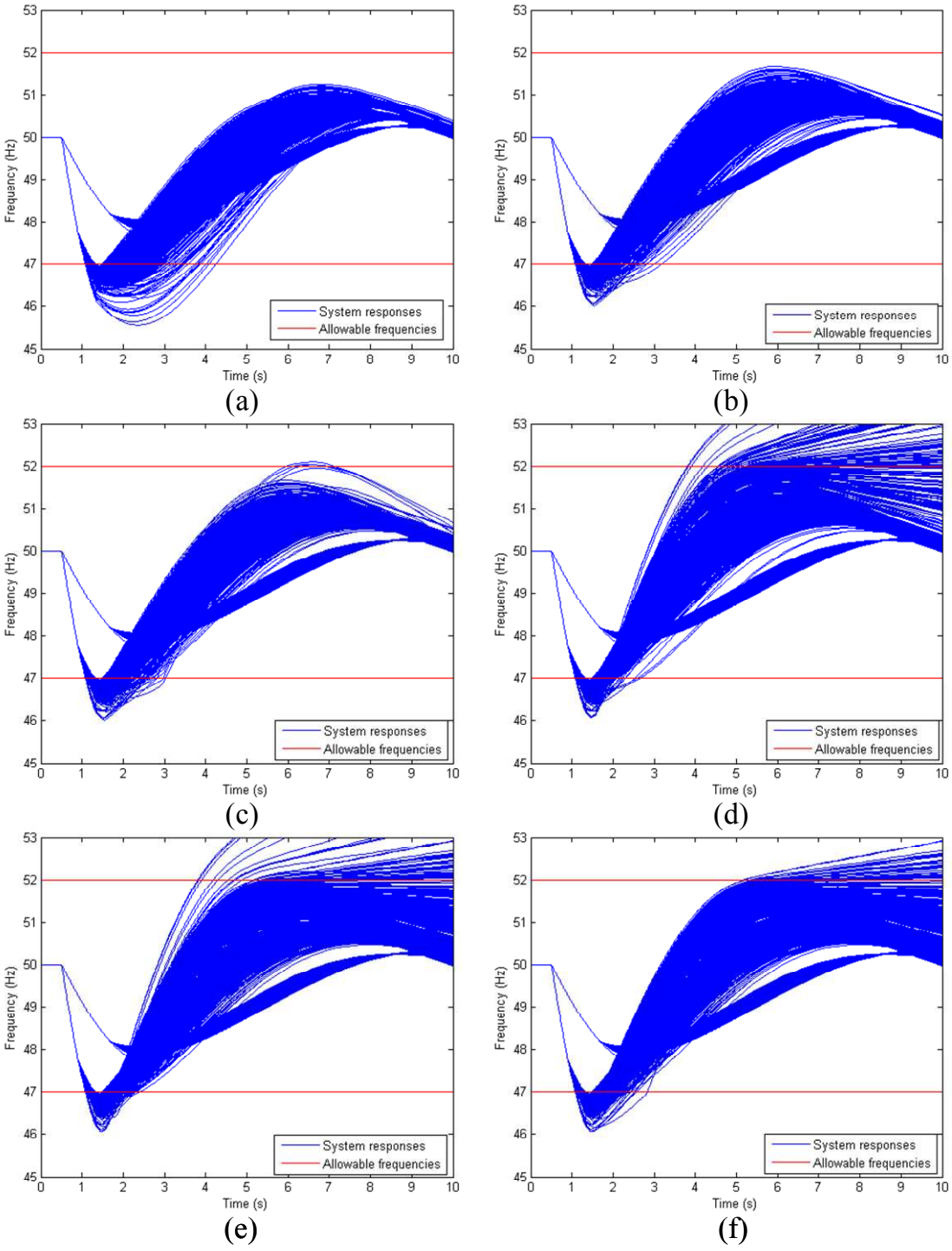

Figure 5-19: Power-system responses (a) without and (b) to (f) with backup-steps settings V1 to V5 of proposed La Palma UFLS scheme.

Two principal observations can be inferred from Figure 5-19. First, uncertainty induced by step-size variations reduces the efficiency of UFLS schemes in terms of frequency deviation reduction. Second, two groups can be identified, according to low frequency operation and overfrequency, which seem to be mutually exclusive. Proposition V1 of Figure 5-19 (a), for example, completely avoids overfrequency conditions, whereas sustained operation below 47 Hz is hardly restricted (frequency is below 47 Hz up to 2 s). Proposition V2 improves the latter only slightly. By contrast, proposition V5 clearly limits operation below 47 Hz, but at the expense of

overfrequency conditions due to overshedding. Similar interpretations apply to propositions V3 and V4. In either case, comparing Figure 5-19 with Figure 5-16 (original La Palma UFLS scheme) and Figure 5-17 (proposed UFLS scheme), backup steps readily increased minimum system-frequency values. Overshedding as caused by V5 could be reduced by splitting the larger blocks of stages 7 and 9 into smaller ones. However, in cases of smaller power systems like the La Palma system, this might not be possible due to fixed block size.

Figure 5-20 gives some additional insight into the performance of the backup-step propositions V1 to V5. Figure 5-20 (a) represents the accumulated time that frequency is below 47 Hz for each proposition, and Figure 5-20 (b) shows the number backup-step interventions as a percentage of the totally performed Monte-Carlo simulations. Figure 5-20 (c) depicts the mean amount of shed load per backup-step intervention (total amount of shed load due to backup-step intervention divided by the number of backup-step interventions), whereas Figure 5-20 (d) shows the total difference between the amount of lost generation and shed load due to backup step intervention. A cero value means that no overshedding occurred due to backup-steps (e.g. propositions V1 and V2).

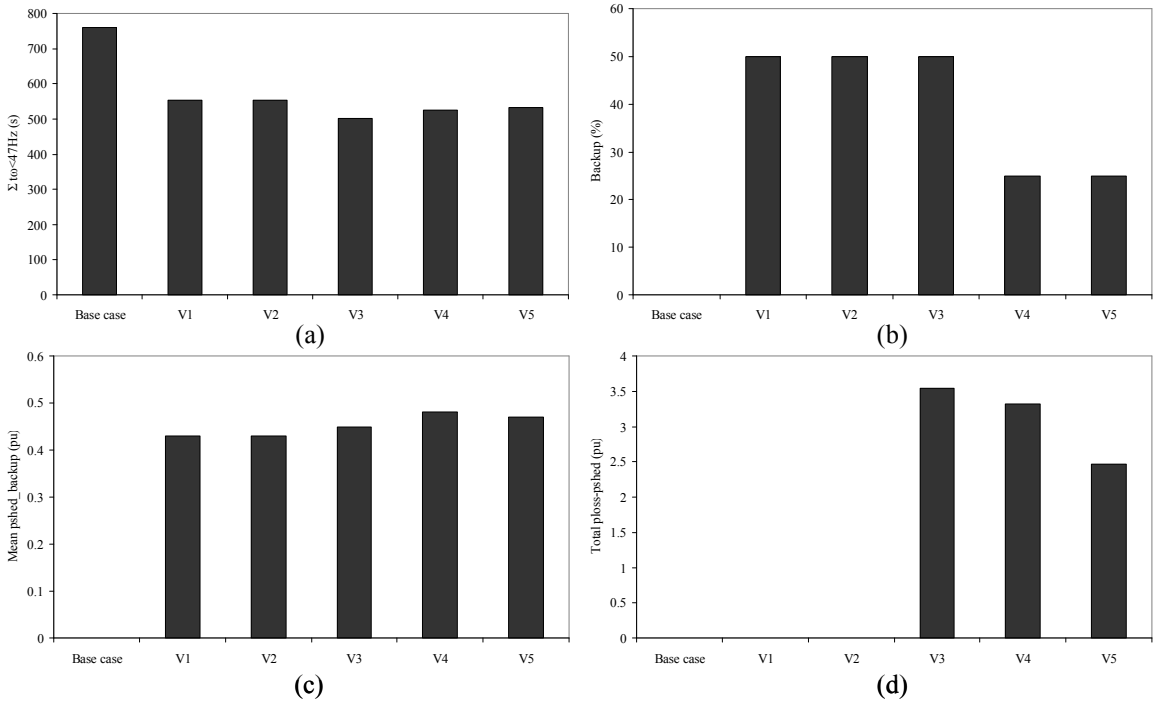

Figure 5-20: Comparison of the performance of the proposed backup settings V1 to V5: (a) accumulated time that frequency is below 47 Hz, (b) percentage of backup-step intervention, (c) mean amount of shed load per backup-step intervention and (d) total difference between the amount of lost generation and shed load due to backup-step intervention.

According to Figure 5-20, propositions V1 and V2 allow longer low-frequency operation and shed less load than proposition V4 and V5, although backup-steps intervene more times. A reduction in the amount of shed load has therefore been obtained by switching stages 7 and 8. Proposition V3 is somehow a mix since it reduces low-frequency operation with regard to V4 and V5, but intervenes more times than these two propositions. Apart from propositions V1 and V2, proposition V5 causes the smallest amount of overshedding due to backup-steps intervention. This is also reflected by the overfrequency situations shown in Figure 5-19. The performance of proposition V4 lies in between the performances of proposition V3 and V5. Note that the high

proportion of backup-step interventions of propositions V1 to V3 is caused by two factors: first, only two operating and contingency scenarios are considered and second, frequency threshold of the first backup step of propositions V1 to V3 is set to 47 Hz. This number will significantly reduce when applying to all possible operating and contingency scenarios (see section 5-3-3-3).

Irrespective the strategy adopted for backup-step settings, both sustained low frequency operation and overfrequency conditions jeopardize system integrity. Depending on power-system characteristics such as the resistance of generating units against low frequency operation, one strategy prevails over the other. For example, if turbines were able to withstand low frequencies (e.g. 47 Hz for two seconds), permissive backup-step settings, such as proposition V1, could be implemented. Nevertheless, if turbines were sensitive to frequency deviations, propositions such as V5 should be implemented to quickly restore frequency to acceptable, safe values.

5-3-3-3 Application of backup-step settings to all possible operating and contingency scenarios

Finally, backup-step design propositions of Table 5-7 are evaluated by means of Monte-Carlo simulations applied to all possible operating and contingency scenarios. Again, only the impact of step-size reductions is analyzed. Step-size variations are modeled by a probability density function with failure probability equal to 0.01, mean of 0.5 and standard deviation of 0.1. As in the previous section and in order to reduce computational effort, only operating and contingency scenarios with load-shedding activity are evaluated. Due to the large amount of operating and contingency scenarios, only 200 Monte-Carlo simulations are performed, resulting in around 14000 simulations.

Figure 5-21 shows the effect of different backup-step settings on all possible operating and contingency scenarios with load-shedding activity.

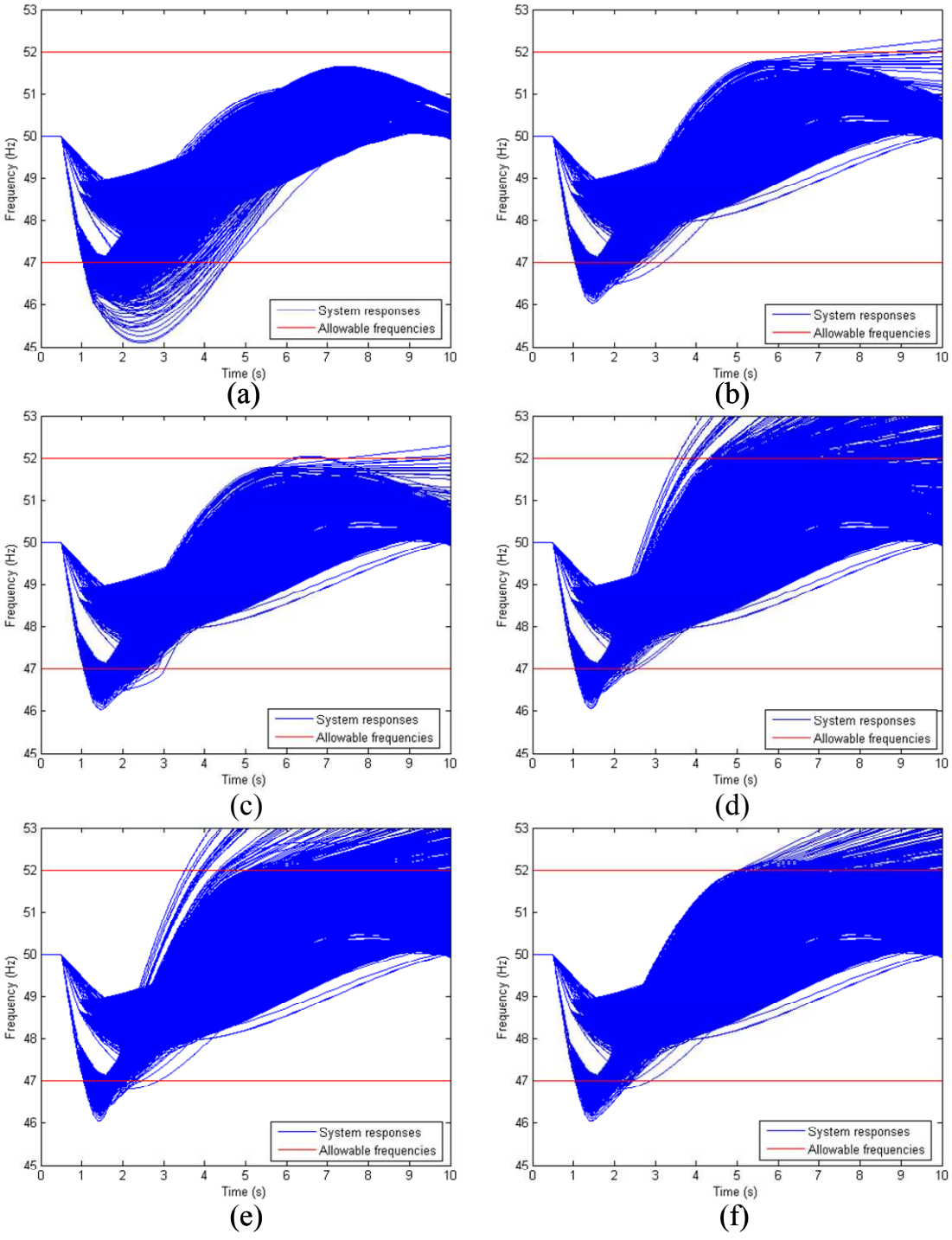

Figure 5-21: Power-system responses (a) without and (b) to (f) with backup-steps settings V1 to V5 of the proposed La Palma UFLS scheme.

Again, two clearly differentiable groups can be identified with regard to sustained underfrequency or overfrequency conditions. Design proposition V1 and V2 accept sustained low frequency operations in order to reduce overfrequency and consequently, overshedding. By contrast, backup-step designs V3 to V5 clearly reduce sustained low frequency operation, at the expense of overfrequency and overshedding. Note anew that proposition V3 exhibits more overfrequency situations than V4 and V5 and that propositions V1 and V2 only cause a few overfrequency situations. Another interesting observation comparing Figure 5-21 with Figure 5-19 can be made with respect to the

benefits of representative operating and contingency scenarios. In fact, it seems that, after all, worst-case scenarios fit quite well with those described by representative scenarios. System responses to intermediate scenarios are more scattered since their associated clusters contain a wider range of operating and contingency scenarios.

Figure 5-22 gives some additional insight into the performance of the backup-step propositions V1 to V5. Figure 5-22 (a) represents the accumulated time that frequency is below 47 Hz for each proposition, and Figure 5-22 (b) shows the percentage of backup-step intervention with regard to the performed simulations. Figure 5-22 (c) depicts the mean amount of shed load per backup-step intervention, whereas Figure 5-20 (d) shows the total difference between the amount of lost generation and shed load due to backup step intervention.

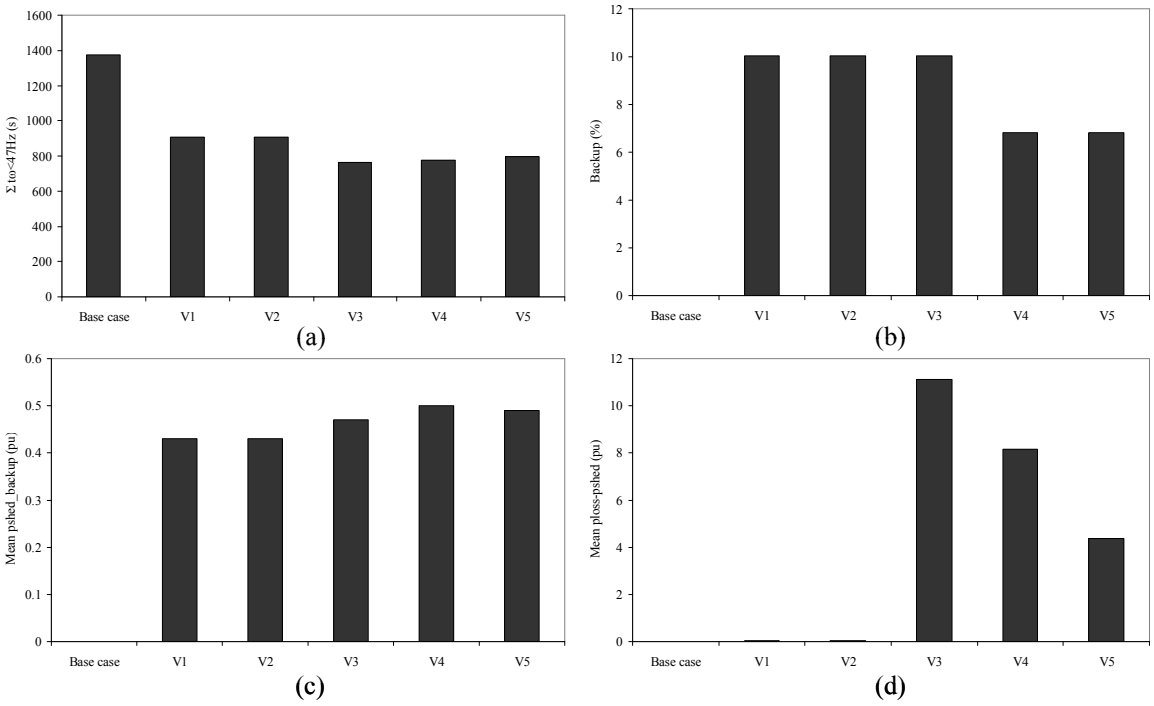

Figure 5-22: Comparison of the performance of the proposed backup settings V1 to V5: (a) accumulated time that frequency is below 47 Hz, (b) percentage of backup-step intervention, (c) mean amount of shed load per backup-step intervention and (d) total difference between the amount of lost generation and shed load due to backup-step intervention.

Anew, propositions V1 and V2 allow longer low-frequency operation and shed less load than proposition V4 and V5, although backup-steps intervene more times. By contrast, proposition V3 reduces low-frequency operation, but still intervenes more times than propositions V4 and V5. Among the propositions V3 to V5, proposition V5 causes the smallest amount of overshedding due to backup-steps intervention, but with slightly longer low-frequency operations than V3. The performance of V4 is somehow in between the performances of propositions V3 and V5. Note that in only 10% (V1 to V3) or 6% (V4 and V5) of all simulations backup-steps are required. This reduction with respect to the results show in Figure 5-20 is mainly due to the fact much more operating and contingency scenarios are considered here. In general, similar conclusions to those obtained by using representative operating and contingency scenarios can be made, reaffirming the utility of representative operating and contingency scenarios.

5-4 PARTIAL CONCLUSIONS

The design of UFLS schemes is based on certain assumptions concerning design conditions and variability of UFLS scheme step sizes. Design conditions directly influence the performance of the resulting UFLS scheme and different design conditions might result in distinct final UFLS scheme designs. Percentaged values of actual step sizes vary from the implemented step sizes due to changing system-operating conditions. Step-size variations can negatively affect UFLS scheme performance. This chapter extensively studied the impact of varying design conditions and varying step sizes.

Design conditions have been classified into five groups according to the step of the proposed method for the design of UFLS scheme they affect. These groups include the selection of operating and contingency scenarios and different choices of optimization constraints, of objective functions, of optimization algorithms as well as different choices of decision variables. Different UFLS scheme designs resulting from a variation of one of these design conditions have been analyzed and compared to the base case, which corresponds to the proposed UFLS scheme of the La Palma power system. Some of these modified design conditions coincided also with UFLS scheme designs proposed in the literature and thus, they allowed comparing the proposed method with other methods. The following results have been obtained:

- Operating and contingency scenario selection: Three different cases have been studied: operating and contingency scenarios determined by the common practice, determination of five (instead of four) representative operating and contingency scenarios and finally, representative operating and contingency scenarios defined for system operating conditions without decoupled power generation. The UFLS scheme designed with scenarios which were determined by the common practice is less robust than the UFLS scheme designed according to the proposed method. Neglecting decoupled power generation worsened after all the number of error states related to low and high frequency operation in comparison to a scheme designed with decoupled power generation. Further and after all, for higher degrees of DPG penetration, DPG should be contemplated when designing UFLS schemes. It seems that a significant change in the generation structure requires reviewing UFLS schemes. Finally, if the number of representative operating and contingency scenarios is cautiously chosen, an additional scenario does not alter significantly the result.
- Variation of the optimization constraints: In particular, relaxations on the allowable minimum frequency and the possibility of rearranging the steps have been considered. Omitting priority remarkably reduced the amount of shed load as expected. However, the relaxation on the allowable minimum frequency did not improve with relation to the amount of shed load unless the minimum frequency threshold value permitted for the design of underfrequency relays has been lowered from 47 Hz (base case) to 46 Hz. In the latter case, the amount of load has been reduced even further compared with the case where steps can be rearranged. However, less restrictive constraints on minimum allowable frequencies entail lower minimum frequencies.
- Variation of the objective function: The contemplated objective functions include a term related to the minimum frequency deviation. First, a composite objective function with weights equal to unity has been tested and thereupon, an objective function with a more heavily weighted frequency term has been used. It could be concluded that by including a term related to the minimum frequency deviation,

frequency deviations are reduced at the expense of an increased amount of shed load. This was even truer for the more heavily weighted case.

- Variation of the optimization algorithm: Genetic Algorithm has been chosen since it has been already applied in the literature to partial optimization of UFLS schemes. The design obtained by applying GA had a similar impact on all possible operating and contingency scenarios in terms of minimum frequency deviations and amount of shed load as the base case. In other words, a different heuristic algorithm led to similar results with similar computation times.
- Variation of the decision variables: First, sequential quadratic programming (SQP) has been applied to the problem of optimal tuning of all UFLS scheme parameters, i.e. frequency and ROCOF thresholds, intentional time delays and step sizes. Step sizes have not been considered as a decision variable in the base case. In a further step, adaptive Simulated Annealing (SA) algorithm has been used and finally, a partial optimization based on GA has been applied. In this case, only frequency thresholds and step sizes have been taken into account. The complete optimization based on SQP yielded to a design which predominantly reduced minimum frequency deviation at the expense of increased amount of shed load. By contrast, complete optimization based on SA achieved much better results with respect to amount of shed load. In fact, the design halved the amount of shed load compared with previously obtained design based on SQP, but at the expense of increased minimum frequency deviations. It has also been shown that for smaller isolated power systems, where complete optimization is theoretically feasible but less practical, relaxing the constraint on priority led to very efficient UFLS schemes with a performance similar to SA-based, completely optimized UFLS scheme. Finally, the GA-based, partial optimization is slightly less efficient than the case base and the SA-based complete optimization.

Most of these findings are applicable to larger isolated systems such as the Gran Canaria power system. In fact, similar conclusions could be drawn with respect to the selection of operating and contingency according to the common practice, an increasing amount of decoupled power generation, the relaxation of optimization constraints or with regard to the addition of a term related to the minimum frequency to the objective function. A difference might be found when pursuing a complete optimization strategy and with reference to its applicability. In fact, in larger systems, the step size determined by the complete optimization strategy is usually implementable.

Actual step size usually differs from the implemented one due to variations of feeder load, feeder outages or due to breaker failures. These variations of the step size, which can be modeled by a statistical distribution of load, can have a jeopardizing impact on system stability, justifying the implementation of backup steps. Backup steps are those steps of an UFLS scheme which have not been adjusted since unnecessary when applying the proposed method for the design of robust and efficient UFLS schemes. A probability density function has been derived to describe the variation of percentaged values of step sizes. This probability density function is based on two probability functions: (i) a normal distribution is used to model feeder-load variation and (ii) a Bernoulli distribution is used to model feeder outages or breaker failures. In addition, a method for the design of UFLS backup steps has been proposed which designs first heuristically several combinations of different backup steps settings, based on simplified variations of UFLS scheme step sizes, and in a second step, the proposed designs are tested and evaluated using a Monte-Carlo simulation approach.

It has been shown in a first step that step-size variations and step-size reduction in particular have a jeopardizing impact on the power system, causing very low frequency levels and frequency instabilities. As a direct consequence, different backup-step designs with different frequency threshold and time delay settings have been heuristically determined. Monte-Carlo simulation showed that one backup-step strategy could prevail over the other, depending on power-system characteristics such as the resistance of generating units against low frequency operation, and that a unique, optimal setting does not exist in this sense. Nonetheless, backup steps increased minimum system-frequency values with respect to the case without backup steps. Another interesting result obtained by extensive Monte-Carlo simulations is that representative operating and contingency scenarios gave a good insight into power-system behavior under uncertainty introduced by step-size variation. This is especially true for rather worst-case operating and contingency scenarios.

CHAPTER SIX

CONCLUSIONS, CONTRIBUTIONS AND FURTHER WORK

6-1 CONCLUSIONS

This dissertation has addressed the problem of designing robust and efficient underfrequency load-shedding (UFLS) schemes of small isolated power systems. UFLS schemes are a well-established remedy against frequency instabilities.

Frequency stability is a major issue for small isolated power systems. In small isolated power systems, frequency instability occurs in the form of continuous frequency decay or of sustained frequency swings leading to tripping of generating units. Main reasons for the continuous frequency decay are insufficient spinning reserve or the loss of a major generating unit. However, the ultimate reason for frequency instability comes from the fact that generating units are equipped with underfrequency protection devices which trip the generating units in case of underfrequency conditions. The main problem of underfrequency frequency operation is the excitation of resonant conditions of mechanical components such as turbine blades and compressor airfoils of steam turbines and combustion engines. Further problems arise due to reduced output of power-plan auxiliaries such as fans and pumps which reduce the power generation further and may cause thermal overload. Thus, if additional counter-measures, such as UFLS, fail, underfrequency protection devices trip the generating units and the power system collapses due to frequency instability. In addition, decoupled power generation enhances the risk of frequency instability due to its negligible frequency-control capabilities and the absence of inertial response. Decoupled power generation refers to those solar and wind-power generating units which are mechanically decoupled form the power system through power electronic converters.

UFLS schemes are implemented to avoid system collapses. These schemes trip loads to restore the power equilibrium and to arrest frequency decay. UFLS schemes can be grouped in conventional and advanced schemes. This dissertation is concerned with conventional UFLS schemes which trips predefined amounts of load at specified frequency thresholds.

The design of such UFLS scheme is usually based on the evaluation of the responses of the power system to a set of contingencies. These evaluations in turn are realized by means of simulations of a model of the power system of interest. A simple but still accurate model has been developed to simulate frequency dynamics of a power system. This so-called non-linear multi-generator system frequency dynamics (SFD) model is a low-order model which reduces the computational cost with respect to a fully detailed model maintaining the essential frequency dynamics of the original model. The proposed SFD model assumes that generating units can be represented by their turbine-governor systems, that the network can be neglected and reduced to a single bus, that loads are voltage and frequency independent and that finally, turbine-governor systems can be represented by non-linear first-order or second order models. Comparison with more detailed power-system models and analysis of SFD model parameters gave rise to the following conclusions:

- Comparisons of simulations based on the proposed non-linear multi-generator SFD model with simulations of much more detailed models run with PSS/E software package have shown that this non-linear multi-generator SFD model is able to accurately reproduce short-term frequency dynamics of real power systems.
- It has been shown that the inclusion of generator output limitations, giving rise to the non-linearities in the SFD model, have a significant impact on short-term frequency dynamics and on frequency stability in particular.
- It has also been shown that the presence of decoupled power generation in small isolated power system needs to be taken into account when studying frequency stability.

Several methods have been reported in literature to design conventional UFLS schemes, but there exists no generally accepted method for the design of UFLS schemes. These methods are mostly based on simulations of a set of operating and contingency scenarios. However, these operating and contingency scenarios are usually determined by the common practice of scenario selection, which does not necessarily guarantee robustness of the designed UFLS scheme. Furthermore, these design methods do not guarantee an optimal performance of the UFLS scheme in terms of shed load. This thesis has developed a method to design robust and efficient UFLS schemes of small isolated power systems. Efficiency is tantamount to shedding a minimum amount of load, whereas robustness denotes efficiency for a set of operating and contingency scenarios. The developed method for the design of robust and efficient UFLS schemes uses the proposed SFD model to perform simulations.

To guarantee a robust UFLS scheme design, adequate operating and contingency scenarios need to be selected. A method based on Data Mining has been proposed to identify and select representative operating and contingency scenarios. Several Data Mining techniques such as K-Means, Fuzzy C-Means and KSOM have been applied to the problem of representative scenario selection. Representative operating and contingency scenarios are those scenarios which represent best all other operating and contingency scenarios. Efficiency of the UFLS scheme can be achieved by applying an optimization algorithm to tune the parameters of the UFLS scheme, corresponding with the tunable parameters of the underfrequency and the rate of change of frequency (ROCOF) relays. This has been referred to as a partial, more industry-oriented optimization strategy since only frequency thresholds, ROCOF thresholds and intentional time delays have been optimized, assuming constant step sizes. The main objective of the optimization stage is to minimize the amount of shed load without

jeopardizing the system stability. Optimization constraints include restrictions on the priority of loads, the instant of shedding and the amount of shed load as well as on the minimum and maximum allowable frequencies. In this dissertation, the use of the adaptive Simulated Annealing algorithm has been suggested to optimally tune UFLS scheme parameters.

The proposed method for the design of efficient and robust UFLS schemes comprises thus two tasks: the selection of adequate operating and contingency scenarios by means of Data Mining techniques and the optimal tuning of the UFLS parameters by means of an optimization algorithm. To confirm the feasibility of the approach, the proposed method has been applied to the design of the UFLS schemes of the La Palma and the Gran Canaria power system. In addition, the proposed UFLS scheme has been compared to a simply optimized UFLS scheme which uses operating and contingency scenarios determined by the common practice of scenario selection. The following results have been obtained with regard to the selection of operating and contingency scenarios:

- It has been shown that by means of Data Mining, representative operating and contingency scenarios can be found. The resulting representative operating and contingency scenarios describe well the patterns among all possible operating and contingency scenarios.
- The application to the La Palma power system showed that different Data Mining techniques yield to similar results.
- The method based on Data Mining has been compared with the common practice of scenario selection. Compared with the common practice of scenario selection, representative operating and contingency scenarios cover a wider range of possible system responses than the manually selected scenarios.
- Furthermore, it has been shown that decoupled power generation has a significant impact on the final selection of representative operating and contingency scenarios.

The use of adaptive Simulated Annealing in combination with representative operating and contingency scenarios gave rise to the following results:

- The application of adaptive Simulated Annealing yields to a more efficient UFLS scheme with behalf to the existing UFLS scheme. In fact, the resulting UFLS scheme sheds less load and exhibits better performances with respect to imposed constraints such as minimum and maximum allowable frequencies, load priority or unnecessary late shedding.
- The proposed UFLS scheme has been compared with the simply optimized UFLS scheme which uses operating and contingency scenarios determined by the common practice of scenario selection. It has been shown that the proposed UFLS scheme is more robust and efficient than the simply optimized UFLS scheme. The superior robustness is mainly due to a more adequate selection of operating and contingency scenarios, i.e. using a wider range of possible system responses.

Like all design methods, the proposed method for the design of robust and efficient UFLS schemes is based upon certain assumptions concerning design conditions and variability of UFLS scheme step sizes. Thus, the impact of changing design conditions and varying step sizes has also been extensively studied.

The analysis of changing design conditions is addressed by designing different UFLS schemes resulting from a variation of one of the design conditions. These design

conditions can be roughly classified into those affecting the selection of operating and contingency scenarios and those affecting the formulation of the optimization problem. The following results have been obtained with regard to variations of design conditions:

- It has been shown that scenarios determined by the common practice yield to less robust UFLS schemes. Further, inclusion of decoupled power generation is crucial for the design of UFLS schemes in small isolated power systems. Finally, if the number of representative operating and contingency scenarios is cautiously chosen, an additional scenario does not alter significantly the result.
- Relaxation on constraints on priority and minimum allowable frequencies has reduced the amount of shed load by accepting larger frequency deviation for the latter. It has also been shown that by including a term related to the minimum frequency deviation, frequency deviations are reduced at the expense of an increased amount of shed load.
- Further, designs obtained by different optimization algorithms such as Genetic Algorithm led to similar results in terms of minimum frequency deviations and amount of shed load as the base case. Finally, Sequential Quadratic Programming applied to complete optimization, which considers also the step size as a decision variable, yielded to designs which predominantly reduced minimum frequency deviation at the expense of an increased amount of shed load. By contrast, complete optimization based on adaptive Simulated Annealing achieved much better results with respect to amount of shed load, accepting by contrast larger frequency deviations. It has also been shown that for smaller isolated power systems, where complete optimization is theoretically feasible but less practical, relaxing the constraint on priority led to very efficient UFLS schemes with a performance similar to the completely optimized UFLS scheme.

In order to address step-size variations and step-size reduction in particular, a method for the design of UFLS backup steps has been proposed which first designs several combinations of different backup steps settings heuristically, based on simplified variations of UFLS scheme step sizes, and in a second step, the proposed designs are validated using a Monte-Carlo simulation approach. Monte-Carlo simulations make use of a probability density function, modeling step-size variation as combination of feeder-load variation and feeder outages and breaker failures. Finally, the following results have been obtained with respect to the analysis of varying step sizes and the design of possible backup steps of UFLS schemes:

- It has been shown that step-size variations and especially step-size reduction have a jeopardizing impact on the power system, causing very low frequency levels and frequency instabilities.
- It has been concluded from the Monte-Carlo simulations applied to the La Palma power system that the heuristically designed backup-step setting can be classified into two mutually exclusive groups, according to low frequency operation or overfrequency operation. Further, depending on power-system characteristics such as the resistance of generating units against low frequency operation, it has been found that one strategy could prevail over the other and that a unique, optimal setting does not exist in this sense. In either case, backup steps have increased minimum system-frequency values with regard to the UFLS scheme without backup steps.

In conclusion, a method for the design of efficient and robust UFLS schemes has been elaborated and successfully applied to real power systems. This, in turn, exhibited the

utility of the developed non-linear multi-generator SFD model. Ultimately, the analysis of varying design conditions and varying step sizes gave some more insight into the performance of UFLS schemes, especially under unpredictable circumstances.

6-2 CONTRIBUTIONS

This section aims at clarifying the contributions of the present dissertation. Main contributions can be grouped with regard to five topics coinciding with the principal research lines of this dissertation: (i) modeling of small isolated power systems, (ii) proposed method for the design of UFLS schemes, (iii) analysis of UFLS schemes, (iv) implementation and applicability of the proposed methods and finally, (v) phase-plane analysis of frequency dynamics.

- A novel non-linear multi-generator system frequency dynamics (SFD) model has been derived. Several SFD models have been described. First SFD models only considered the impact of load. A second generation extended the approach on linear single-generator and multi-generator SFD models. However, the assumption of a linear model, neglecting non-linearities such as generator output limitations, is only valid for small power imbalances. For larger imbalances, which are likely to occur in a small isolated power system, non-linearities need to be considered. Further, apart from first-order models, also second-order generator models should be considered. Thus, this dissertation elaborated a SFD model that includes generator output limitations and that allows representing generating units by a generic second-order model. In addition, the proposed SFD model is also able to easily include decoupled power generation. Finally, the present dissertation also developed a method to adjust the parameters of the generic second-order model using either data from more detailed dynamic models or measurement data obtained by field tests.
- A method for the design of robust and efficient UFLS schemes of small isolated power system has been elaborated. To guarantee a robust UFLS scheme design, adequate operating and contingency scenarios need to be selected. Efficiency of the UFLS scheme can be achieved by applying an optimization algorithm to tune the parameters of the UFLS scheme. A method based on Data Mining has been proposed to identify and select representative operating and contingency scenarios. Representative operating and contingency scenarios are those scenarios which represent best all other operating and contingency scenarios. Several Data Mining techniques such as K-Means, Fuzzy C-Means and KSOM have been implemented and applied to the problem of representative scenario selection. The optimal tuning of UFLS scheme parameters has been accomplished by means of adaptive Simulated Annealing algorithm. The main objective of the optimization stage is to minimize the amount of shed load without jeopardizing the system stability. Both a partial, more industry-oriented optimization strategy, tuning frequency thresholds, ROCOF thresholds and intentional time delays, and complete optimization, including step size to the aforementioned parameters, have been realized. Optimization constraints include restrictions on the priority of loads, the instant of shedding and the amount of shed load as well as on the minimum and maximum allowable frequencies. The proposed method for the design of robust and efficient UFLS schemes has been implemented and applied to two real power systems, taking into account decoupled power generation.

- Designs of UFLS schemes are based on certain assumptions concerning design conditions and variability of UFLS scheme step sizes. This dissertation extensively studied the impact of varying design conditions and varying step sizes. Some of the modified design conditions coincided also with UFLS scheme designs proposed in the literature and thus, they allowed comparing the proposed method with other methods. Variations of the step size, simulated by a statistical distribution, can have a jeopardizing impact on system stability, justifying the implementation of backup steps. In order to address step-size variations and step-size reduction in particular, a method for the design of UFLS backup steps has been proposed which first designs several combinations of different backup steps settings heuristically, based on simplified variations of UFLS scheme step sizes, and in a second step, the proposed designs are evaluated using a Monte-Carlo simulation approach. Monte-Carlo simulations make use of a probability density function, modeling step-size variation as a combination of feeder-load variation and feeder outages and breaker failures.
- Within the abovementioned research lines, a toolbox prototype has been created which allows both simulating and designing UFLS schemes under numerous operating and contingency scenarios. The Underfrequency Load-Shedding Scheme Applications (UFLSA) toolbox is also currently used by the Spanish system operator. UFLSA toolbox has not been conceived to replace other transient simulation programs such as PSS/E. The main goal is to be able to simulate fast numerous operating and contingency scenarios and to design and analyze in an automated manner UFLS schemes.
- An expression describing the frequency stability boundary in the ω–dω/dt phase plane has been derived in the appendix B. This expression is based on the idea of "breaking the loop" [Egido'10], which allows summing power outputs of *n* generators without creating a *(n+1)th*-order system. It has been shown by creating a simple Lyapunov function that this frequency stability boundary is a separatrix, describing thus a region of frequency stability and helping assessing frequency stability. Some implementations making use of the definition of frequency stability boundary have also been proposed.

6-3 PUBLICATIONS

Partial aspects of these contributions culminate in a number of already published journal and conference papers; in particular:

[Sigrist'08]

Sigrist, L., I. Egido, et al. (2008). Representative contingency identification using data mining. Electrical and Electronics Engineers in Israel, 2008. IEEEI 2008. IEEE 25th Convention of.

[Sigrist'10a]

Sigrist, L., I. Egido, et al. (2010a). Ajuste de las protecciones de frecuencia de los clientes interrumpibles de los sistemas eléctricos canarios. CIGRÉ España - Jornada Técnica de Gestión de la Demanda. ETSII UPM (Madrid).

[Sigrist'10b]

Sigrist, L., I. Egido, et al. (2010b). "Representative Operating and Contingency Scenarios for the Design of UFLS Schemes." IEEE Transactions on Power Systems 25(2): 906.

The original idea of applying clustering algorithm to the problem of selecting adequate operating and contingency scenarios is first described in [Sigrist'08]. The subsequent paper [Sigrist'10b] elaborates further this topic, discussing in more detail the impact of non-linearities and multiple outages. In addition, a comparison is made for real power system with the common practice of scenario selection.

Publication [Sigrist'10a] dealt with a particular facet of the problem of varying step sizes. In fact, the determination of step sizes is realized by means of statistical analyses of actual customer data or, as in this case, forecast of load demand of interruptible customers.

Papers under progress tackle the problems of both designing robust and efficient UFLS schemes and assessing the impact of varying step sizes on the design of possible backup steps.

6-4 SUGGESTIONS FOR FURTHER WORK

Through the course of this dissertation, some interesting issues have been identified as subjects for further research. Most relevant untreated aspects are subsequently presented:

- The non-linear multi-generator SFD model derived in chapter 3 showed in general very satisfactory results in comparison with more detailed power-system models such as provided by PSS/E software package. However, small isolated power systems can also appear as two subsystems connected by a rather weak tie line as it is the case of the Lanzarote-Fuerteventura power system. In this particular case, the tie line could be represented by a synchronizing torque coefficient [Kundur'94]. Obviously, if the contingency consist in tie line opening, the proposed SFD is valid.
- Although the presented SFD model takes into account the fact of finite spinning reserve, which translates into generator output limitations, other non-linear limitations such as rate limits have been neglected. These rate limiters model finite speed of valve or gate closing or opening and could be of interest in steam or hydraulic turbines with rather slow servomotors. In addition, valve opening and closing rates may differ, giving rise to different turbine-governor system representations according to whether valves open or close. For example, overspeed can be limited by adding an “auxiliary governor”, increasing the gain of the control loop in such occasions [Kundur'94].
- Irrespective of the SFD model finally adopted, it is of crucial interest to validate the SFD model and its parameters with actual measurement data. These data can be either obtained by field tests applied to involved generating units or by records of power-system incidents. The former allows identifying generator model parameters by applying reference or load changes, whereas the later permits to validate overall performance of the propose non-linear multi-generator SFD model, including UFLS scheme performance.
- The selection of representative operating and contingency scenarios has been applied to small isolated power system only. Contingencies have been defined as single or multiple outages of generating units. It could be interesting to apply this approach to larger systems or even interconnected systems. Instead of generating unit outages, numerous islanding situations, where part of the generating and transmission equipment is lost, could be considered as contingencies. An islanded system could be simulated with the present SFD model [Anderson'90].

- It has been shown that step-size variations have a negative impact on frequency stability of small isolated power systems and on the performance of UFLS schemes. Instead of contemplating step-size variations and designing backup steps after applying the proposed method for the design of robust and efficient UFLS schemes, the optimization stage of the proposed method could take into account slight step-size variations in order to efficiently tune frequency thresholds, ROCOF thresholds and intentional time delays. In addition, governor inactivity could also be contemplated since a non-responding governor is tantamount to reducing the available spinning reserve.
- The expression of the frequency stability boundary has been obtained assuming a simplified version of the generator model. In fact, an isochronous-like governor formulation has been applied. For first-order models (or even second-order models), the first integral approach is not feasible anymore to construct a Lyapunov function. A possible Lyapunov candidate could be constructed by applying Popov's criterion and Kalman's procedure. Finally, it would be interesting to refine further possible applications and implementations of the frequency stability boundary.

CHAPTER SEVEN

REFERENCES

[ABB'04]
ABB (2004). "SPAF 340 C Frequency Relay."

[Abonyi'07]
Abonyi, J. and B. Feil (2007). Cluster Analysis for Data Mining and System Identification. Basel, Birkhäuser.

[Ackermann'05]
Ackermann, T., Ed. (2005). Wind Power in Power Systems. Chichester, John Wiley & Sons, Ltd.

[Ait-Kheddache'88]
Ait-Kheddache, A. and S. Ebron (1988). Optimal load shedding methodologies in power systems. Southeastcon '88., IEEE Conference Proceedings.

[Akers'68]
Akers, H. T., J. Dickinson, et al. (1968). "Operation and Protection of Large Steam Turbine Generators Under Abnormal Conditions." IEEE Transactions on Power Apparatus and Systems **PAS-87**(4): 1180.

[Anderson'99]
Anderson, P. M. (1999). Power system protection. Piscataway, NJ, IEEE Press.

[Anderson'77]
Anderson, P. M. and A. A. Fouad (1977). Power system control and stability. Ames (IA), Iowa State University Press.

[Anderson'90]
Anderson, P. M. and M. Mirheydar (1990). "A low-order system frequency response model." Power Systems, IEEE Transactions on **5**(3): 720.

[Anderson'92]
Anderson, P. M. and M. Mirheydar (1992). "An adaptive method for setting underfrequency load shedding relays." IEEE Transactions on Power Systems **7**(2): 647.

[Antoine'92]
Antoine, J. P. and M. Stubbe (1992). EUROSTAG, software for the simulation of power system dynamics. Its application to the study of a voltage collapse

scenario. Interactive Graphic Power System Analysis Programs, IEE Colloquium on.

[Apostolov'94]
Apostolov, A. P., D. Novosel, et al. (1994). Intelligent protection and control during power system disturbance. Proceedings of the American Power Conference, Chicago, IL.

[Arteche'06]
Arteche (2006). "Voltage protection relay RV-UTF."

[Backmutsky'93]
Backmutsky, V., D. Kottick, et al. (1993). Comparison of Methods and Algorithms for Accurate Frequency Trend Estimation Following Emergency Transients in Power Systems. Athens Power Tech, 1993. APT 93. Proceedings. Joint International Power Conference.

[Bates'88]
Bates, D. M. and D. G. Watts (1988). Nonlinear Regression and Its Applications. New York, Wiley.

[Begovic'93]
Begovic, M. M., P. M. Djuric, et al. (1993). "Frequency tracking in power networks in the presence of harmonics." Power Delivery, IEEE Transactions on **8**(2): 480.

[Berube'99]
Berube, G. R. and L. M. Hajagos (1999). Modeling based on field tests of turbine/governor systems. Power Engineering Society 1999 Winter Meeting, IEEE.

[Blackburn'06]
Blackburn, J. L. and T. J. Damin (2006). Protective Relaying. Principles & Applications. Boca Rata, FL, CRC Press.

[Bonian'05]
Bonian, S., X. Xiaorong, et al. (2005). WAMS-based load shedding for systems suffering power deficit. Dalian, China, IEEE.

[Brooks'95]
Brooks, S. P. and B. J. T. Morgan (1995). "Optimization using simulated annealing." The Statistician **44**(2): 241-257.

[Butler'54]
Butler, O. D. and C. J. Swenson (1954). "Effect of Low Frequency and Low Voltage on Thermal Plant Capability and Load Relief During Power System Emergencies; Effect of Reduced Voltage and/or Frequency Upon Steam Plant Auxiliaries." Power Apparatus and Systems, Part III. Transactions of the American Institute of Electrical Engineers **73**(2): 1628.

[Cammesa'08]
Cammesa (2008). Los procedimientos - Anexos PT 4: Anexos "A" a "H".

[CDEC-SIC'08]
CDEC-SIC, Dirección de Operación (2008). Estudio Esquemas de Desconexión Automáticos de Carga 2008-2009.

[CEIyC'09]
CEIyC, Consejería de Empleo, Industria y Comercio (2009). ORDEN de 26 de mayo de 2009, por la que se resuelve, para el sistema eléctrico de La Palma, el concurso público para la asignación de potencia en la modalidad de nuevos parques eólicos destinados a verter toda la energía en los sistemas eléctricos

insulares canarios, convocado por Orden de 27 de abril de 2007. Boletín Oficial de Canarias.

[Cerny'85]
Cerny, V. (1985). "A Thermodynamical Approach to the Travelling Salesman Problem: An Efficient Simulation Algorithm." J. Optim. Theory Appl. **45**: 41-51.

[CIGRE'99]
CIGRE, Task Force 38-02-14 (1999). Large frequency disturbances: analysis and modeling needs. Power Engineering Society 1999 Winter Meeting, IEEE.

[Coello'99]
Coello, C. A. C. (1999). Self-adaptive penalties for GA-based optimization. Evolutionary Computation, 1999. CEC 99. Proceedings of the 1999 Congress on, Washington, DC, USA.

[Concordia'95]
Concordia, C., L. H. Fink, et al. (1995). "Load shedding on an isolated system." IEEE Transactions on Power Systems **10**(3): 1467.

[Cooper'99]
Cooper (1999). UFD14 and UFD34 Frequency/Load Sheddin Relays.

[Cote'01]
Cote, P. and M. Lacroix (2001). Benefits of special protection systems in competitive market. pica 200. International Conference on Power Industry Computer Applications, Sydney, NSW, Australia, IEEE.

[Crevier'75]
Crevier, D. and F. C. Schweppe (1975). "The use of Laplace transforms in the simulation of power system frequency transients." power apparatus and systems, ieee transactions on **94**(2): 236.

[Criado'94]
Criado, R., M. Gutiérrez, et al. (1994). Identification of Excitation System Models For Power System Stability Studies. CIGRÉ Session 1994, Paris.

[Cha'00]
Cha, P. D., J. J. Rosenberg, et al. (2000). Fundamentals of Modeling and Analyzing Engineering Systems. Cambridge, Cambridge University Press.

[Chan'72]
Chan, M. L., R. D. Dunlop, et al. (1972). "Dynamic Equivalents for Average System Frequency Behavior Following Major Distribances." power apparatus and systems, ieee transactions on **PAS-91**(4): 1637.

[Cheng'03]
Cheng, C. P. and C. Shine (2003). Under-frequency load shedding scheme design based on cost-benefit analysis. 6th International Conference on Advances in Power System Control, Operation and Management. Proceedings. APSCOM 2003. Stevenage, UK, IEE. **Vol.2:** 514.

[Chien-Hung'08]
Chien-Hung, H., L. Chien-Hsing, et al. (2008). "Frequency Estimation of Distorted Power System Signals Using a Robust Algorithm." Power Delivery, IEEE Transactions on **23**(1): 41.

[Chow'90]
Chow, J., R. Fischl, et al. (1990). An improved Hopfield model for power system contingency classification. Circuits and Systems, 1990., IEEE International Symposium on.

[Chuvychin'96]

Chuvychin, V. N., N. S. Gurov, et al. (1996). "An adaptive approach to load shedding and spinning reserve control during underfrequency conditions." IEEE Transactions on Power Systems **11**(4): 1805.

[Dalziel'59]
Dalziel, C. F. and E. W. Steinback (1959). "Underfrequency Protection of Power Systems for System Relief Load Shedding-System Splitting." Power Apparatus and Systems, Part III. Transactions of the American Institute of Electrical Engineers **78**(4): 1227.

[Dawei'07]
Dawei, F. and V. Centeno (2007). "Phasor-Based Synchronized Frequency Measurement in Power Systems." Power Delivery, IEEE Transactions on **22**(4): 2010.

[De Tuglie'00]
De Tuglie, E., M. Dicorato, et al. (2000). "A corrective control for angle and voltage stability enhancement on the transient time-scale." IEEE Transactions on Power Systems **15**(4): 1345.

[Delfino'01]
Delfino, B., S. Massucco, et al. (2001). Implementation and comparison of different under frequency load-shedding schemes. 2001 Power Engineering Society Summer Meeting, Piscataway, NJ, IEEE.

[Denis Lee Hau'06]
Denis Lee Hau, A. (2006). "A General-Order System Frequency Response Model Incorporating Load Shedding: Analytic Modeling and Applications." IEEE Transactions on Power Systems **21**(2): 709.

[Dowsland'03]
Dowsland, K. A. and B. A. Díaz (2003). "Heuristic Design and Fundamentals of Simulated Annealing." Revista Iberoamericana de Inteligencia Artificial **19**: 93-102.

[Duric'05]
Duric, M. B. and Z. R. Durisic (2005). Frequency measurement in power networks in the presence of harmonics using fourier and zero crossing technique. Power Tech, 2005 IEEE Russia.

[Egido'10]
Egido, I., F. Fernández, et al. (2010). "Maximum frequency deviation calculation in small isolated power systems." IEEE Transactions on Power Systems **24**(4): 1731 - 1738.

[EirGrid'09]
EirGrid (2009). EirGrid Grid Code.

[El-Banhawy'91]
El-Banhawy, M. H., M. H. El-Banhawy, et al. (1991). Development of optimal emergency control strategies for Abu Dhabi power system. Power System Monitoring and Control, 1991., Third International Conference on.

[Elgerd'82]
Elgerd, O. I. (1982). Electric energy systems theory. An introduction. New York.

[Elkateb'89]
Elkateb, M. M. and M. M. Elkateb (1989). Analytical techniques for load-shedding assessment. Safeguarding Industrial Plant During Power System Disturbances, IEE Colloquium on.

[Endesa'09]

Endesa (2009). Endesa08 Informe de sostenibilidad.

[Enrique'09]
Enrique, A., B. Christian, et al. (2009). Optimization Techniques for Solving Complex Problems, Wiley Publishing.

[EPRI'79]
EPRI (1979). Report No. EL-596. Mid-term Simulation of Electric Power Systems.

[Fidalgo'96]
Fidalgo, J. N., J. A. Pecas Lopes, et al. (1996). "Neural networks applied to preventive control measures for the dynamic security of isolated power systems with renewables." Power Systems, IEEE Transactions on **11**(4): 1811.

[GEIndustrial'02]
GEIndustrial (2002). MIV M Familiy Voltage/Frequency Relay.

[Gerbec'02]
Gerbec, D., S. Gasperic, et al. (2002). An approach to customers daily load profile determination. Power Engineering Society Summer Meeting, 2002 IEEE.

[Germond'78]
Germond, A. J. and R. Podmore (1978). "Dynamic Aggregation of Generating Unit Models." power apparatus and systems, ieee transactions on **PAS-97**(4): 1060.

[Ghosh'97]
Ghosh, A. K., D. L. Lubkeman, et al. (1997). "Distribution circuit state estimation using a probabilistic approach." Power Systems, IEEE Transactions on **12**(1): 45.

[Giampaolo'06]
Giampaolo, A. (2006). Gas turbine handbook: Principles and practices. Lilburn, GA, The Fairmon Press, Inc.

[Girgis'82]
Girgis, A. A. and F. M. Ham (1982). "A New FFT-Based Digital Frequency Relay for Load Shedding." power apparatus and systems, ieee transactions on **PAS-101**(2): 433.

[Girgis'90]
Girgis, A. A. P., W.L. (1990). "Adaptive estimation of power system frequency deviation and itsrate of change for calculating sudden power system overloads." Power Delivery, IEEE Transactions on **5**(2): 585-594.

[Gómez-Expósito'08]
Gómez-Expósito, A., A. J. Conejo, et al., Eds. (2008). Electric Energy Systems: Analysis and Operation. Boca Raton (FL, USA), CRC Press.

[Guo'05]
Guo, J. Q. and L. Zheng (2005). "A modified simulated annealing algorithm for estimating solute transport parameters in streams from tracer experiment data." Environmental Modelling & Software **20**(6): 811.

[Hain'97]
Hain, Y. and I. Schweitzer (1997). "Analysis of the power blackout of June 8, 1995 in the Israel Electric Corporation." Power Systems, IEEE Transactions on **12**(4): 1752.

[Hajek'88]
Hajek, B. (1988). "Cooling Schedule For Optimal Annealing." Math. Oper. Res. **13**(2): 311-329.

[Halevi'93]

Halevi, Y. and D. Kottick (1993). "Optimization of load shedding system." IEEE Transactions on Energy Conversion **8**(2): 207.

[Ham'85]
Ham, F. M. and A. A. Girgis (1985). "Measurement of Power Frequency Fluctuations Using the FFT." Industrial Electronics, IEEE Transactions on **IE-32**(3): 199.

[Hand'01]
Hand, D., H. Mannila, et al. (2001). Principles of Data Mining. Boston, MA, MIT Press.

[Hannet'93]
Hannet, L. N. and A. Khan (1993). "Combustion Turbine Dynamic Model Validation from Tests." Power Systems, IEEE Transactions on **8**(1): 152.

[HECO'08]
HECO (2008). Integrated Resouce Plan. available at www.heco.com.

[Hoffman'01]
Hoffman, J. D. (2001). Numerical Methods for Engineers and Scientists, 2nd Edition. New York, Marcel Dekker.

[Horne'04]
Horne, J., D. Flynn, et al. (2004). Frequency stability issues for islanded power systems. Power Systems Conference and Exposition, 2004. IEEE PES.

[Horowitz'71]
Horowitz, S. H., S. H. Horowitz, et al. (1971). "Frequency Actuated Load Shedding and Restoration Part II: An Implementation." IEEE Transactions on Power Apparatus and Systems **PAS-90**(4): 1460.

[Hsu'97]
Hsu, C. T., C. S. Chen, et al. (1997). "The load-shedding scheme design for an integrated steelmaking cogeneration facility." Industry Applications, IEEE Transactions on **33**(3): 586.

[IEEE'68]
IEEE (1968). "Survey of Underfrequency Relay Tripping of Load Under Emergency Conditions." IEEE Transactions on Power Apparatus and Systems **PAS-87**(5): 1362.

[IEEE'75]
IEEE (1975). "A status report on methods used for system preservation during underfrequency conditions." power apparatus and systems, ieee transactions on **94**(2): 360.

[IEEE'87]
IEEE (1987). "IEEE guide for abnormal frequency protection for power generating plants." ANSI/IEEE Std C37.106-1987.

[IEEE'91]
IEEE (1991). "Dynamic models for fossil fueled steam units in power system studies." Power Systems, IEEE Transactions on **6**(2): 753.

[IEEE'95]
IEEE (1995). "IEEE Tutorial on the Protection of Synchronous Generators." TP 102.

[IEEE'05]
IEEE (2005). "IEEE Standard for Cylindrical-Rotor 50 Hz and 60 Hz Synchronous Generators Rated 10 MVA and Above." IEEE Std C50.13™-2005 (Revision of ANSI C50.13-1989).

[IEEE'07]

IEEE (2007). "IEEE Guide for the Application of Protective Relays Used for Abnormal Frequency Load Shedding and Restoration." IEEE Std C37.117-2007: c1.

[IEEE'73]
IEEE, comittee report (1973). "Dynamic Models for Steam and Hydro Turbines in Power System Studies." power apparatus and systems, ieee transactions on **PAS-92**(6): 1904.

[IEEE/CIGRE'04]
IEEE/CIGRE, Joint Task Force on Stability Terms and Definitions (2004). "Definition and Classification of Power System Stability." IEEE Transactions on Power Systems **19**(2): 1387-1401.

[Ingber'89]
Ingber, L. (1989). "Very Fast Simulated Re-Annealing." Mathl. Comput. Modelling **12**: 967-973.

[Ingber'93]
Ingber, L. (1993). "Simulated annealing: Practice versus theory." Mathl. Comput. Modelling **18**(11): 29-57.

[Jardini'00]
Jardini, J. A., C. M. V. Tahan, et al. (2000). "Daily load profiles for residential, commercial and industrial low voltage consumers." Power Delivery, IEEE Transactions on **15**(1): 375.

[Jenkins'83]
Jenkins, L. (1983). Optimal load shedding algorithm for power system emergency control. 1983 Proceedings of the International Conference on Systems, Man and Cybernetics. Bombay and New Delhi, India, IEEE.

[Johnson'89]
Johnson, D. S., C. R. Aragon, et al. (1989). "Optimization by Simulated Annealing: An Experimental Evaluation; Part I, Graph Partitioning." Oper. Res. **37**(6): 865 - 892.

[Jones'88]
Jones, J. R. and W. D. Kirkland (1988). "Computer algorithm for selection of frequency relays for load shedding." Computer Applications in Power, IEEE **1**(1): 21.

[Jung'02]
Jung, J., L. Chen-Ching, et al. (2002). "Adaptation in load shedding under vulnerable operating conditions." Power Systems, IEEE Transactions on **17**(4): 1199.

[Kakimoto'03]
Kakimoto, N. and K. Baba (2003). "Performance of gas turbine-based plants during frequency drops." Power Systems, IEEE Transactions on **18**(3): 1110.

[Kaufmann'90]
Kaufmann, L. and P. J. Rousseeuw (1990). Finding Groups in Data: An Introduction to Cluster Analysis, Wiley.

[Kendall'09]
Kendall, A., W. Han, et al. (2009). Numerical solution of ordinary differential equations. Chichester, John Wiley & Sons.

[Kirkpatrick'83]
Kirkpatrick, S., C. D. J. Gelatt, et al. (1983). "Optimization by Simulated Annealing." Science **220**(4598): 671-677.

[Koczara'04]

Koczara, W., N. Al-Khayat, et al. (2004). Decoupled generation with additional degree of freedom. Industrial Electronics, 2004 IEEE International Symposium on.

[Kottick'96]
Kottick, D. and O. Or (1996). "Neural-networks for predicting the operation of an under-frequency load shedding system." IEEE Transactions on Power Systems **11**(3): 1350.

[Kundur'94]
Kundur, P. (1994). Power system stability and control. New York, McGraw-Hill.

[Kunitomi'01]
Kunitomi, K., A. Kurita, et al. (2001). Modeling frequency dependency of gas turbine output. Power Engineering Society Winter Meeting, 2001. IEEE.

[Kuri-Morales'02]
Kuri-Morales, A. F. and J. Gutiérrez-García (2002). Penalty Functions Methods for Constrained Optimization with Genetic Algorithms: A Statistical Analysis. Proceedings of the 2nd Mexican International Conference on Artificial Intelligence (MICAI 2002), Mérida, Yucatán, México.

[Larsson'02]
Larsson, M. and C. Rehtanz (2002). Predictive frequency stability control based on wide-area phasor measurements. 2002 IEEE Power Engineering Society Summer Meeting, Piscataway, NJ, USA, IEEE.

[Leite da Silva'90]
Leite da Silva, A. M. and V. L. Arienti (1990). "Probabilistic load flow by a multilinear simulation algorithm." Generation, Transmission and Distribution, IEE Proceedings C **137**(4): 276.

[Levine'99]
Levine, W. S., Ed. (1999). The Control Handbook (Volume 1). Boca Raton, CRC Press.

[Li'06]
Li, Z. and Z. Jin (2006). UFLS design by using f and integrating df/dt. 2006 IEEE/PES Power Systems Conference and Exposition. Atlanta, GA, USA, IEEE.

[Ljung'87]
Ljung, L. (1987). System Identification: Theory for the User. Enlewood Cliffs (NJ, USA), Prentice-Hall.

[Lokay'68]
Lokay, H. E. and V. Burtnyk (1968). "Application of Underfrequency Relays for Automatic Load Shedding." IEEE Transactions on Power Apparatus and Systems **PAS-87**(3): 776.

[Lopes'00]
Lopes, J. A. P., M. A. Mitchell, et al. (2000). Optimum determination of under-frequency load shedding strategies using a genetic algorithm approach. Proceedings of the Thirty-Second Annual North American Power Symposium. Waterloo, Ont., Canada, Univ. Waterloo. **vol.1**.

[Lopes'99]
Lopes, J. A. P., W. Wong Chan, et al. (1999). Genetic algorithms in the definition of optimal load shedding strategies. PowerTech Budapest 99. Budapest, Hungary, IEEE.

[Lopez'08]

Lopez, A., J. C. Montao, et al. (2008). "Power System Frequency Measurement Under Nonstationary Situations." Power Delivery, IEEE Transactions on **23**(2): 562.

[Lukic'98]
Lukic, M., I. Kuzle, et al. (1998). An adaptive approach to setting underfrequency load shedding relays for an isolated power system with private generation. MELECON '98. 9th Mediterranean Electrotechnical Conference. Proceedings, Tel Aviv, Israel, IEEE.

[Lundy'86]
Lundy, M. and A. Mees (1986). "Convergence of an annealing algorithm." Math. Prog. **34**: 111-124.

[Machowski'97]
Machowski, J., J. W. Bialek, et al. (1997). Power System Dynamics and Stability. Chichester.

[Mak'91]
Mak, T. S. and C. K. Law (1991). Spinning reserve and under-frequency load shedding strategies for the interconnected China Light power system. Advances in Power System Control, Operation and Management, 1991. APSCOM-91., 1991 International Conference on.

[Maliszewski'71]
Maliszewski, R. M., R. D. Dunlop, et al. (1971). "Frequency actuated load shedding and restoration I: Philosophy." IEEE Transactions on Power Apparatus and Systems **PAS-90**(4): 1452.

[Mansour'97]
Mansour, Y., A. Y. Chang, et al. (1997). "Large scale dynamic security screening and ranking using neural networks." Power Systems, IEEE Transactions on **12**(2): 954.

[Martínez'93]
Martínez, M., G. Winter, et al. (1993). "La optimización mediante algoritmos genéticos del proceso de deslastre y reposición de carga." Vector Plus.

[Matsuura'09]
Matsuura, M. (2009). "Island breezes." Power and Energy Magazine, IEEE **7**(6): 59.

[McLlwaine'86]
McLlwaine, S. A., C. E. Tindall, et al. (1986). "Frequency tracking for power system control." Generation, Transmission and Distribution, IEE Proceedings C **133**(2): 95.

[Metropolis'53]
Metropolis, N., A. W. Rosenbluth, et al. (1953). "Equation of State Calculation by Fast Computing Machines." Journal of Chemistry Physics **21**: 1087-1091.

[Michie'94]
Michie, D., D. J. Spiegelhalter, et al. (1994). Machine Learning, Neural and Statistical Classification. Upper Saddle River (NJ, USA), Prentice Hall.

[Min'91]
Min, Y., S.-B. Hong, et al. (1991). Analysis of power-frequency dynamics and designation of under frequency load shedding scheme in large scale multi-machine power systems. Advances in Power System Control, Operation and Management, 1991. APSCOM-91., 1991 International Conference on.

[Mitchell'00a]

Mitchell, M. A. (2000a). Optimization of under-frequency load shedding strategies through the use of a neural network and a genetic algorithm. INESC, Universidade do Porto. **Master**.

[Mitchell'00b]
Mitchell, M. A., J. A. P. Lopes, et al. (2000b). Using a neural network to predict the dynamic frequency response of a power system to an under-frequency load shedding scenario. Power Engineering Society Summer Meeting, 2000. IEEE.

[MITyC'06]
MITyC, Ministerio de Industria, Turismo y Comercio (2006). RESOLUCIÓN de 28 de abril de 2006, de la Secretaría General de Energía, por la que se aprueba un conjunto de procedimientos de carácter técnico e instrumental necesarios para realizar la adecuada gestión técnica de los sistemas eléctricos insulares y extrapeninsulares. ANEXO. Boletín oficial del estado.

[MITyC'09]
MITyC, Ministerio de Industria, Turismo y Comercio (2009). Registro de instalaciones de producción en régimen especial. www.mityc.es/energia/electricidad/RegimenEspecial/Paginas/Index.aspx.

[Mohd Zin'04]
Mohd Zin, A. A., H. Mohd Hafiz, et al. (2004). A review of under-frequency load shedding scheme on TNB system. National Power and Energy Conference. PECon 2004. Proceedings. Kuala Lumpur, Malaysia, IEEE.

[Moore'96]
Moore, P. J., J. H. Allmeling, et al. (1996). "Frequency relaying based on instantaneous frequency measurement." Power Delivery, IEEE Transactions on **11**(4): 1737.

[Morren'06]
Morren, J., S. W. H. de Haan, et al. (2006). "Wind turbines emulating inertia and supporting primary frequency control." Power Systems, IEEE Transactions on **21**(1): 433.

[Morrow'91]
Morrow, D. J., D. J. Morrow, et al. (1991). Low-cost under-frequency relay for distributed load shedding. Power System Monitoring and Control, 1991., Third International Conference on.

[Mostafa'97]
Mostafa, M. A., M. E. El-Hawary, et al. (1997). "A computational comparison of steady state load shedding approaches in electric power systems." IEEE Transactions on Power Systems **12**(1): 30.

[Neimane'01]
Neimane, V. (2001). Distribution network planning based on statistical load modeling applying genetic algorithms and Monte-Carlo simulations. Power Tech Proceedings, 2001 IEEE Porto.

[NERC'08]
NERC (2008). UFLS Regional Reliability Standard Characteristics.

[New'77]
New, W. C. (1977). "Load Shedding, Load Restoration and Generator Protection Using Solid-state and Electromechanical Underfrequency Relays." General Electric Company Publication GET-6449.

[NGET'09]
NGET (2009). "The Grid Code."

[Niebur'91]

Niebur, D. and A. J. Germond (1991). Power system static security assessment using the Kohonen neural network classifier. Power Industry Computer Application Conference, 1991. Conference Proceedings.

[Nirenberg'92]
Nirenberg, S. A., D. A. McInnis, et al. (1992). "Fast acting load shedding." IEEE Transactions on Power Systems **7**(2): 873.

[Nordel'07]
Nordel (2007). Nordic Grid Code.

[Novosel'96]
Novosel, D., K. T. Vu, et al. (1996). Practical protection and control strategies during large power-system disturbances. 1996 IEEE Transmission and Distribution Conference Proceedings. Proceedings of the, New York, NY, USA, IEEE.

[Pai'81]
Pai, M. A. (1981). Power System Stability: Analysis by the Direct Method of Lyapunov, North-Holland.

[Parniani'06]
Parniani, M. and A. Nasri (2006). SCADA based under frequency load shedding integrated with rate of frequency decline. 2006 IEEE Power Engineering Society General Meeting. Montreal, Que., Canada, IEEE.

[Pereira'03]
Pereira, L., J. Undrill, et al. (2003). "A New Thermal Governor Modeling Approach in the WECC." Power Systems, IEEE Transactions on **18**(2).

[Phadke'83]
Phadke, A. G., J. S. Thorp, et al. (1983). "A New Measurement Technique for Tracking Voltage Phasors, Local System Frequency, and Rate of Change of Frequency." power apparatus and systems, ieee transactions on **PAS-102**(5): 1025.

[POWER HECO'09]
POWER HECO (2009). PUC Investigation of December 26, 2008 Oahu Island-Wide Power Outage. Outage Report.

[Pradhan'05]
Pradhan, A. K., A. Routray, et al. (2005). "Power system frequency estimation using least mean square technique." Power Delivery, IEEE Transactions on **20**(3): 1812.

[Prasetijo'94]
Prasetijo, D., W. R. Lachs, et al. (1994). "A new load shedding scheme for limiting underfrequency." IEEE Transactions on Power Systems **9**(3): 1371.

[REE'95]
REE (1995). Criterios generales de protección del sistema eléctrico peninsular español, REE.

[REE'98]
REE (1998). Atlas de la demanda eléctrica Española. Proyecto INDEL. Madrid (Spain).

[REE'05]
REE (2005). Criterios generales de protección de los sistemas eléctricos insulares y extrapeninsulares, REE.

[REE'08]
REE (2008). El sistema eléctrico español 08.

[REE'09]

REE (2009). Boletín mensual sistema eléctrico canario. Enero - Junio. available at www.ree.es.

[Rodrigues'99]
Rodrigues, M. S., J. C. S. Souza, et al. (1999). Automatic contingency selection based on a pattern analysis approach. Electric Power Engineering, 1999. PowerTech Budapest 99. International Conference on.

[Rodriguez'09]
Rodriguez, A. and J. Ruperez (2009). Low frequency impact on Diesel engine, REE.

[Rodríguez'05]
Rodríguez, J., M. González, et al. (2005). Un esquema centralizado de deslastre de cargas para pequeños sistemas aislados. 9th Spanish Portuguese Congress on Electrical Engineering (9CHLIE), Marbella (Spain).

[Rojas'96]
Rojas, R. (1996). Neural Networks. Berlin, Springer.

[Rouco'08]
Rouco, L., J. L. Zamora, et al. (2008). Impact of wind power generators on the frequency stability of synchronous generators. Cigré Session 2008, Paris.

[Rouco'99]
Rouco, L., J. L. Zamora, et al. (1999). A Comprehensive Tool for Identification of Excitation and Speed-governing Systems for Power System Stability Studies. 13th Power Systems Compuation Conference (PSCC '99), Trondheim (Norway).

[Routray'02]
Routray, A., A. K. Pradhan, et al. (2002). "A novel Kalman filter for frequency estimation of distorted signals in power systems." Instrumentation and Measurement, IEEE Transactions on **51**(3): 469.

[Rubinstein'08]
Rubinstein, Y. R. (2008). Simulation and the Monte Carlo Method, John Wiley & Sons, Inc.

[Saberi'96]
Saberi, A., L. Zongli, et al. (1996). "Control of linear systems with saturating actuators." Automatic Control, IEEE Transactions on **41**(3): 368.

[Sachdev'85]
Sachdev, M. S. and M. M. Giray (1985). "A Least Error Squares Technique For Determining Power System Frequency." power apparatus and systems, ieee transactions on **PAS-104**(2): 437.

[Sanaye-Pasand'06]
Sanaye-Pasand, M. and M. Davarpanah (2006). A new adaptive multidimensional load shedding scheme using genetic algorithm. 2005 Canadian Conference on Electrical and Computer Engineering. Saskatoon, Sask., Canada, IEEE.

[Seppala'95]
Seppala, A. (1995). Statistical distribution of customer load profiles. Energy Management and Power Delivery, 1995. Proceedings of EMPD '95., 1995 International Conference on.

[Seyedi'09]
Seyedi, H. and M. Sanaye-Pasand (2009). "Design of New Load Shedding Special Protection Schemes for a Double Area Power System." American Journal of Applied Sciences **6**(2): 317-327.

[Seyedi'06]

Seyedi, H., M. Sanaye-Pasand, et al. (2006). Design and simulation of an adaptive load shedding algorithm using a real network. 2006 IEEE Power India Conference. Piscataway, NJ, USA, IEEE**:** 5.

[Shokooh'05]
Shokooh, S., T. Khandelwal, et al. (2005). Intelligent Load Shedding Need for a Fast and Optimal Solution. IEEE PCIC Europe, Basel.

[Shrestha'05]
Shrestha, G. B. and K. C. Lee (2005). Load shedding schedules considering probabilistic outages. Power Engineering Conference, 2005. IPEC 2005. The 7th International.

[Siemens'97]
Siemens (1997). SIPROTEC 7RW600 Numerical Votlage, Frequency and Overexcitation Protection.

[Siemens'05a]
Siemens (2005a). PSS/E 30.2 Program Application Guide (Volume II).

[Siemens'05b]
Siemens (2005b). PSS/E 30.2 Program Operation Manual (Volume II).

[Sigrist'10a]
Sigrist, L., I. Egido, et al. (2010a). Ajuste de las protecciones de frecuencia de los clientes interrumpibles de los sistemas eléctricos canarios. CIGRÉ España - Jornada Técnica de Gestión de la Demanda. ETSII UPM (Madrid).

[Sigrist'08]
Sigrist, L., I. Egido, et al. (2008). Representative contingency identification using data mining. Electrical and Electronics Engineers in Israel, 2008. IEEEI 2008. IEEE 25th Convention of.

[Sigrist'10b]
Sigrist, L., I. Egido, et al. (2010b). "Representative Operating and Contingency Scenarios for the Design of UFLS Schemes." IEEE Transactions on Power Systems **25**(2): 906.

[Singh'10]
Singh, R., B. C. Pal, et al. (2010). "Statistical Representation of Distribution System Loads Using Gaussian Mixture Model." Power Systems, IEEE Transactions on **25**(1): 29.

[Skiena'98]
Skiena, S. S. (1998). The Algorithm Design Manual. New York (NY, USA), Springer.

[SolarPACES'01]
SolarPACES (2001). Concentrating Solar Power in 2001. An IEA/SolarPACES Summary of Present Status and Future Prospects.

[Stanton'72]
Stanton, K. N. (1972). "Dynamic Energy Balance Studies for Simulation of Power-Frequency Transients." power apparatus and systems, ieee transactions on **PAS-91**(1): 110.

[Stern'92]
Stern, J. M. (1992). "Simulated Annealing with a Temperature Dependent Penalty Function." INFORMS JOURNAL ON COMPUTING **4**(3): 311-319.

[Stott'87]
Stott, B., O. Alsac, et al. (1987). "Security analysis and optimization." Proceedings of the IEEE **75**(12): 1623.

[Subramanian'71]

Subramanian, D. K. (1971). "Optimum Load Shedding Through Programming Techniques." IEEE Transactions on Power Apparatus and Systems **PAS-90**(1): 89.

[Szu'87]
Szu, H. H. and R. L. Hartley (1987). "Nonconvex optimization by fast simulated annealing." Proceedings of the IEEE **75**(11): 1538.

[Terzija'06]
Terzija, V. V. (2006). "Adaptive underfrequency load shedding based on the magnitude of the disturbance estimation." IEEE Transactions on Power Systems **21**(3): 1260.

[Thalassinakis'04]
Thalassinakis, E. J. and E. N. Dialynas (2004). "A Monte-Carlo simulation method for setting the underfrequency load shedding relays and selecting the spinning reserve policy in autonomous power systems." IEEE Transactions on Power Systems **19**(4): 2044.

[Thalassinakis'06]
Thalassinakis, E. J., E. N. Dialynas, et al. (2006). "Method Combining ANNs and Monte Carlo Simulation for the Selection of the Load Shedding Protection Strategies in Autonomous Power Systems." Power Systems, IEEE Transactions on **21**(4): 1574.

[Thomas'01]
Thomas, D. W. P. and M. S. Woolfson (2001). "Evaluation of frequency tracking methods." Power Delivery, IEEE Transactions on **16**(3): 367.

[Thompson'94]
Thompson, J. G. and B. Fox (1994). "Adaptive load shedding for isolated power systems." IEE Proceedings-Generation, Transmission and Distribution **141**(5): 491.

[Tor'04]
Tor, O. B., U. Karaagac, et al. (2004). Step-Response Tests of a Unit at Ataturk Hydro Power Plant and Investigation of the Simple Representation of Unit Control System. IEEE PES, 36th North American Power Symposium, University of Idaho.

[Treewittayapoom'90]
Treewittayapoom, C. (1990). Studies on the coordination among steps of an underfrequency load shedding scheme. CIGRE. Proceedings of the 33rd Session. International Conference on Large High Voltage Electric Systems, Paris, France, CIGRE.

[UCTE'04]
UCTE (2004). Operation Handbook Policy 1: Load-Frequency Control and Performance. **C.4**.

[UCTE'06]
UCTE (2006). Final report - System disturbance on 4 November 2006. Brussels (Belgium).

[Vittal'07]
Vittal, E., J. D. McCalley, et al. (2007). Wind Penetration Limited by Thermal Constraints and Frequency Stability. Power Symposium, 2007. NAPS '07. 39th North American.

[von Lanzenhauer'74]

von Lanzenhauer, C. H. and W. N. Lundberg (1974). "The n-fold convolution of a mixed density and mass function." ASTIN Bulletin International Actuarial Association **8**(1).

[Wah'99]
Wah, B. W. and T. Wang (1999). Simulated Annealing with Asymptotic Convergence for Nonlinear Constrained Global Optimization. CP '99: Proceedings of the 5th International Conference on Principles and Practice of Constraint Programming.

[White'84]
White, S. R. (1984). Concepts of scale in simulated annealing. IEEE Conference on Computer Design, Port Chester (NY).

[Yeniay'05]
Yeniay, Ö. (2005). "Penalty Function Methods for Constrained Optimization with Genetic Algorithms." Mathematical and Computational Applications **10**(1): 45-56.

[You'02]
You, H., V. Vittal, et al. (2002). "Self-Healing in Power Systems: An Approach Using Islanding and Rate of Frequency Decline Based Load Shedding." Power Engineering Review, IEEE **22**(12): 62.

[Zabinsky'03]
Zabinsky, Z. B. (2003). Stochastic Adaptive Search for Global Optimization. Norwell, MA, Kluwer Academic Publishers.

APPENDIX A

MATLAB TOOLBOX

A-1 INTRODUCTION

The design of conventional UFLS schemes principally relies on time-domain simulations. Within the scope of a research project undertaken in collaboration with the Spanish system operator (REE), a toolbox prototype has been created which allows both simulating and designing UFLS schemes under numerous operating and contingency scenarios. The Spanish system operator currently uses the Underfrequency Load-Shedding Scheme Applications (UFLSA) toolbox. However, this toolbox is not conceived to replace other transient simulation programs such as PSS/E. The main goal is to be able to quickly simulate numerous operating and contingency scenarios and to design and analyze in an automated manner UFLS schemes. Figure A-1 shows the start-up interface of the toolbox.

Figure A-1: Start-up interface.

A-2 STRUCTURE AND OPERATION OF THE TOOLBOX

Figure A-2 shows the structure of the UFLSA toolbox. First, the toolbox processes data of the detailed dynamic models of the generating units as well as data corresponding to different operating scenarios. Instead of detailed dynamic model data, field-test data can also be read. In a further step, the generic second-order models representing the generating units are tuned using dynamic model data. It is also possible to tune the model using unit responses obtained from field tests. Finally, the toolbox allows not only simulating UFLS schemes considering different operating and contingency scenarios but also designing and analyzing such UFLS schemes. Subsequently, the main features of the UFLSA toolbox are resumed.

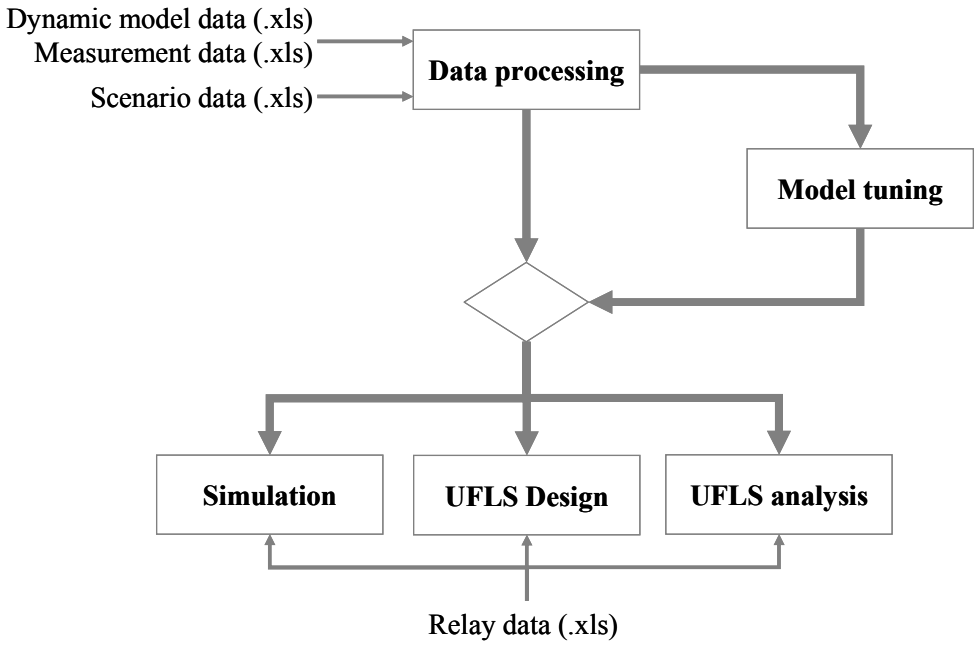

Figure A-2: Toolbox structure.

A-2-1 Data processing

In a first step, data corresponding to detailed dynamic models and to the operating scenarios needs to be read. Alternatively, measured field-test data can be read instead of detailed dynamic model data. This information is read from two distinct Excel Files. Figure A-3 shows the interface for reading the data.

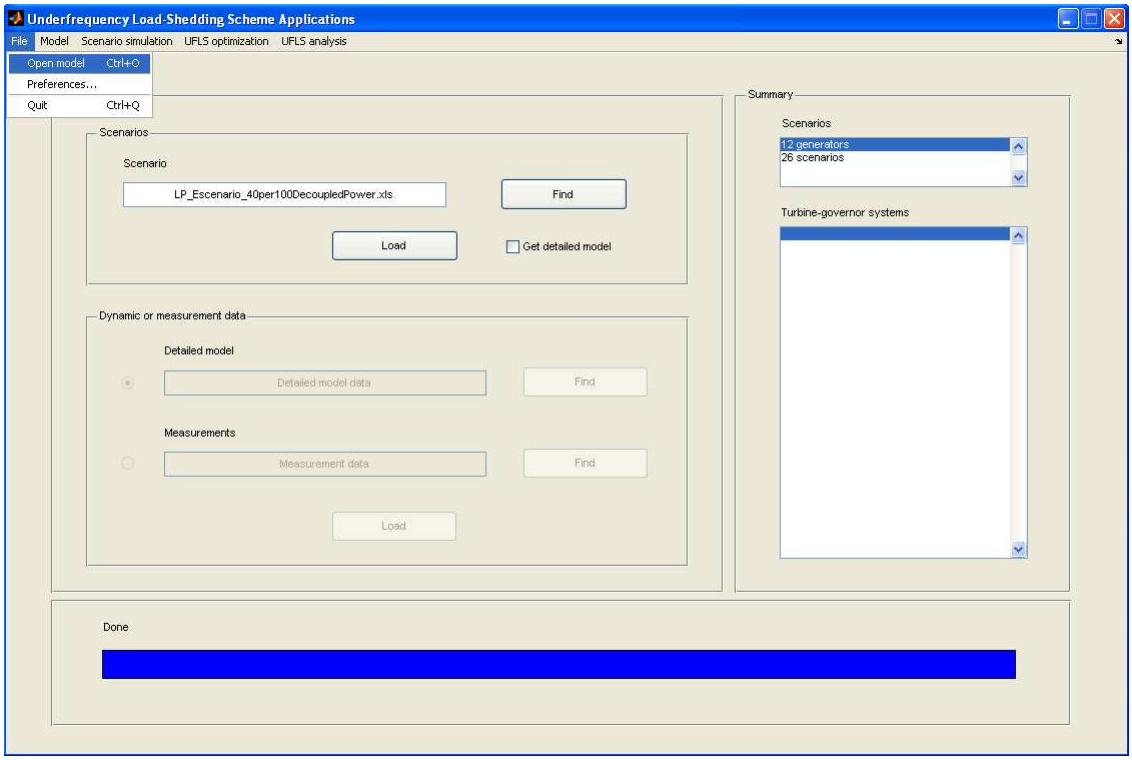

Figure A-3: Interface for processing the data corresponding to both the dynamic models and the operating scenarios.

The data of the dynamic models follow the nomenclature of the PSS/E software package. Of particular interest are the data of the turbine-governor system models. To date, the toolbox can handle the following turbine-governor system models:

- DEGOV1
- IEEEG1
- GAST2A
- GASTWD

Figure A-4 shows an example of the structure of the Excel file containing the detailed dynamic models. The dynamic model shown is a DEGOV1 model.

IDBUS	MODEL	I	Droop control	T1	T2	T3	K	T4	T5	T6	TD	TMAX	TMIN	DROOP	TE
11	'DEGOV1'	1	0	0	0	0.25	1.2	2	0.1	0.1	0.12	0.828	0	0.05	0

Figure A-4: Example of the structure of the dynamic model Excel file.

If measurement data is available, the Excel file should have a structure as shown in Figure A-5. In fact, the structure of this Excel file basically coincides with the structure of the PSS/E simulation output file (headers, etc. have been deleted). However, the user must provide the turbine-governor gain (inverse of the droop).

	Time	SPD BUS 11	PMEC BUS 11	SPD BUS 12	PMEC BUS 12
Gain		20	20	20	20
	0.05	-0.0014294	0.39943	-0.0014294	0.39943
	0.1	-0.0028588	0.39886	-0.0028588	0.39886
	0.15	-0.0042882	0.3983	-0.0042882	0.3983
	⋮	⋮	⋮	⋮	⋮

Figure A-5: Example of the structure of the measurement Excel file.

The data of the scenarios contain the different operating scenarios as well as additional information on the generating units. Figure A-6 shows the structure of the Excel file of the scenarios. The user must provide the data corresponding to the grey cells. The toolbox fills automatically the white cells. Assure that bus numbers coincide with those of the dynamic model or measurement data.

	Bus	11	15	16	17	18
	Nombre	/NAM TYP1/	/NAM TYP2/	/NAM TYP3/	/NAM TYP4/	/NAM TYP5/
	k (en MBASE)	20	20	20	20	21.25
	H (s)	1.75	2.16	1.88	2.10	6.50
	MBASE (MVA)	5.4	9.4	9.6	15.75	26.82
	Pmax	4	7	7	12	22.8
	Pmin	2.5	3.5	3.5	7	0
	B1	1.44	1.32	1.43	1.32	0.89
	B2	0	0	0	0	0
	A1	18.64	18.38	18.66	18.31	5.66
	A2	3.98	2.70	3.85	2.71	3.48
Escenarios	1	2.35	3.41	3.69	10.41	0
	2	0	3.41	4.26	9.26	0
	3	0	3.41	3.29	9.55	0
	4	0	3.41	3.69	8.96	0
	5	0	3.41	3.29	9.35	0

Figure A-6: Example of the structure of the scenario Excel file.

A-2-2 Tuning of the generic second-order model

As shown in chapter 3, generating units can be represented by a generic second-order model of the turbine-governor systems. In other words, some generating units might be accurately represented by a first-order model, whereas others require a second-order model. Thus, in a second step, the parameters of the generic second-order model are tuned such that the response of the generic second-order model is as close as possible to the response of fully detailed dynamic model or to the actual measurement data.

Figure A-7 shows the interface for tuning the generic second-order models. The toolbox allows tuning the generic second-order model in several ways. First, the user can specify if models are tuned using either open-loop or closed-loop structures. The former apply a ramp at turbine-governor system reference of both the generic second-order model and the detailed model and compare their open-loop responses. The latter apply a step at turbine-governor system reference of both the generic second-order model and the detailed model and compare their closed-loop responses. If measurement data is available, the user must verify whether these measurements have been realized using an open-loop or closed-loop configuration. Second, the user can specify which model type has to be tuned (e.g. first-order model or second-order model with one zero, etc.) or if the most adequate model type should be chosen.

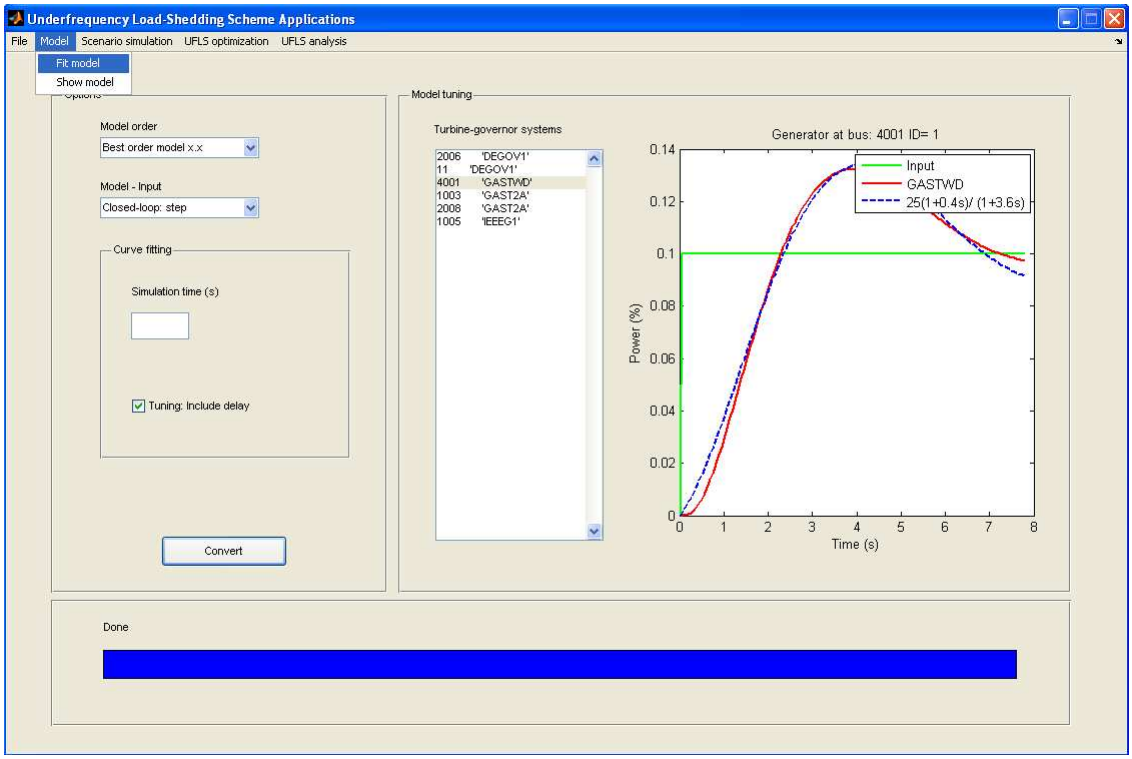

Figure A-7: Interface for tuning the generic second-order model.

It must be noted that this stage is only necessary if the parameters of the simplified model have not already been determined in advance and saved in the scenario data Excel file (i.e. the white cells of the scenario data Excel file are empty).

A-2-3 Simulation of the power system

Once the data has been processed and the model has been tuned, the toolbox is able to simulate different operating and contingency scenarios. Simulations are based on the system frequency dynamics (SFD) model described in chapter 3. Simulations are realized by means of numerical integrations of the system of non-linear differential

equations corresponding to the SFD model. Heun's method is used to numerically integrate this system of non-linear differential equation.

The toolbox allows automatically simulating the loss of the largest and the smallest generator for each operating scenario. Furthermore, it is possible to simulate the loss of specific generators for specific operating scenarios. Finally, it is also possible to simulate all possible operating and contingency scenarios or representative operating and contingency scenarios. Figure A-8 shows the interface for simulating an UFLS scheme taking into account various operating and contingency scenarios.

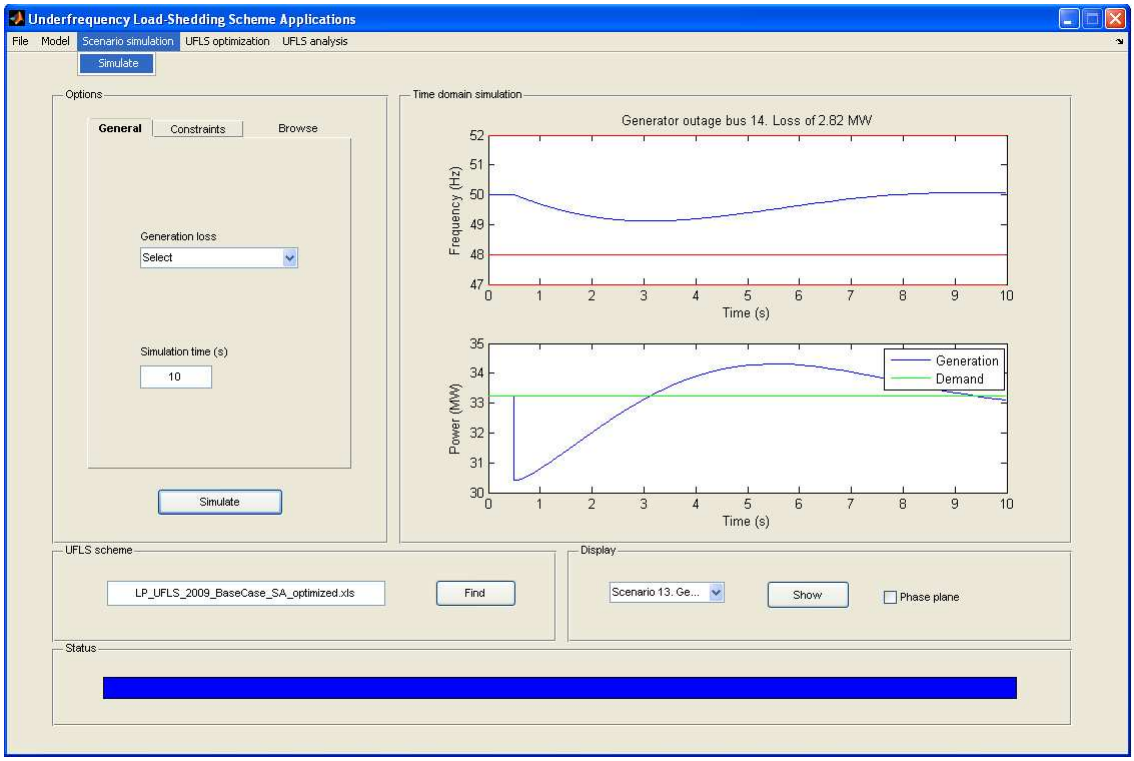

Figure A-8: Simulation of an UFLS scheme.

Simulation time is adjustable. Integration step can be modified by the user via the submenu "Preferences…" in the menu "File". The parameters of the UFLS schemes are read from the relay data Excel file. Since the toolbox allows simulating and designing both static and semi-adaptive UFLS schemes, the parameters of the UFLS scheme may correspond to underfrequency relays and/or ROCOF relays. Figure A-9 shows the structure of the Excel file of the relay data. All parameters must be provided by the user.

Underfrequency relay					
Name	**Bus**	**ω (Hz)**	**tint (s)**	**topn (s)**	**Step size (%)**
Sf1	2101	48.81	0.6	0.2	7.1
Sf2	2102	48.81	0.9	0.2	0.6

ROCOF relays						
Nombre	**Bus**	**ω (Hz)**	**dω/dt (Hz/s)**	**tint (s)**	**topn (s)**	**Step size (%)**
Df1	2101	49.5	-1.8	0.1	0.2	7.1
Df2	2102	49.5	-1.8	0.1	0.2	0.6
Df3	3101	49.5	-1.8	0.1	0.2	14.5
Df4	3102	49.5	-1.8	0.1	0.2	3.6

Figure A-9: Example of the structure of relay data Excel file.

A-2-4 Design of UFLS schemes

As presented in chapter 4, the design of an efficient and robust UFLS schemes comprises two tasks: the selection of adequate operating and contingency scenarios and the application of an optimization algorithm. Once the operating and contingency scenarios have been selected, the optimization algorithm adjusts relay parameters such that the objective function is minimized.

A-2-4-1 Selection of operating and contingency scenarios

The selection of the adequate operating and contingency scenarios can be done manually or by means of cluster analysis. Cluster Analysis refers to the partitioning of a data set into clusters, so that the data in each subset ideally share some common trait and differ from the data in other subsets. There exist different methods based on advanced statistical and modeling techniques. The toolbox offers various statistic measures and clustering algorithms such as K-Means, Fuzzy C-Means and KSOM. Operating and contingency scenarios determined by clustering algorithms are called representative operating and contingency scenarios. In addition, the toolbox allows graphically representing representative operating and contingency scenarios using time-domain plots, principal component analysis, silhouette plots, etc. Figure A-10 shows the interface for determining representative operating and contingency scenarios.

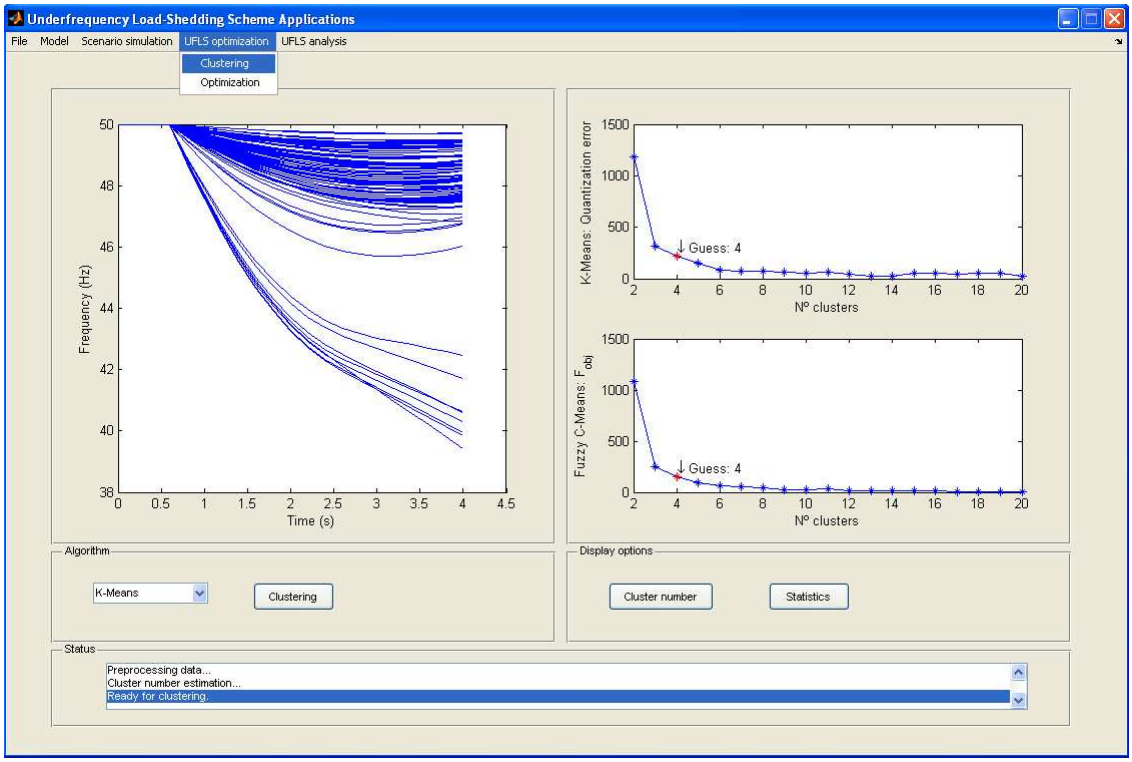

Figure A-10: Interface for determining operating and contingency scenarios.

The user can initially adjust the simulation time and determine whether individual or multiple outages of generating units are contemplated. Integration step can be modified via the submenu “Preferences…” in the menu “File”. The toolbox offers an initial estimation of the appropriate number of clusters (4-2-3). All relevant parameters of the clustering algorithms are modifiable.

A-2-4-2 Tuning of UFLS schemes

As shown in chapter 4, the tuning of UFLS scheme parameters is transformed into an optimization problem. The most general objective function for the optimization algorithm minimizes both the shed load and the minimum frequency deviation for all selected operating and contingency scenarios. The optimization formulation also includes some constraints on system response and UFLS performance. Either manually selected operating and contingency scenarios or scenarios selected by clustering methods can be used.

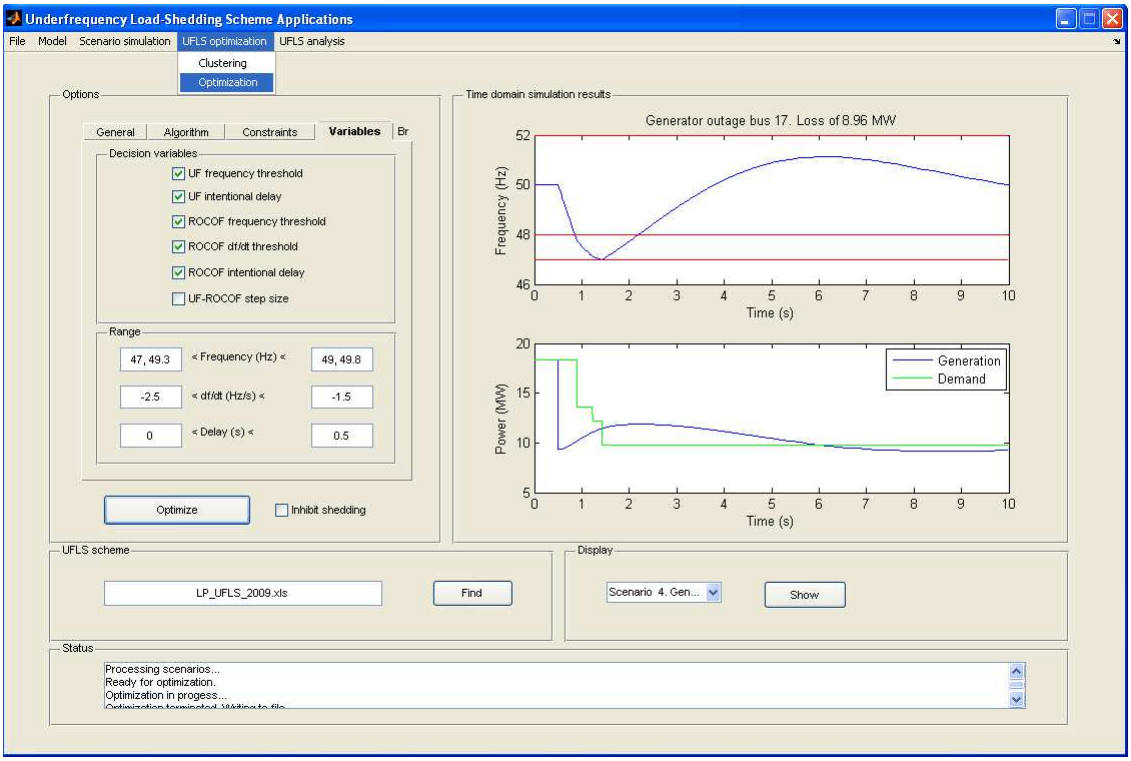

Figure A-11: Tuning of UFLS schemes using optimization techniques.

Figure A-11 shows the interface for the tuning of UFLS schemes using optimization techniques. The toolbox allows choosing the optimization algorithm to be applied such as Simulate Annealing, Genetic Algorithms or Sequential Quadratic Programming, and the objective function to be used. Apart from the objective function aiming at minimizing the amount of shed load, various composite objective functions including a frequency-dependent term can be chosen. Further, the toolbox allows defining and modifying the constraints to be imposed such as constraints on minimum and maximum allowable frequencies, on the amount of shed load, etc. Analogously, the decision variables and their corresponding value ranges can be specified by the user.

A-2-5 Analysis of UFLS schemes

As seen in chapter 5, the design of UFLS schemes is based upon certain assumptions on the response of the power system to a disturbance. Of particular interest are variations of the step sizes of UFLS schemes. These variations are due to feeder-load variations, feeder outages or breaker failure. In addition, the effect of inactive governor could also be analyzed. Monte-Carlo simulations are used to evaluate the impact step-size variations and inactive governors.

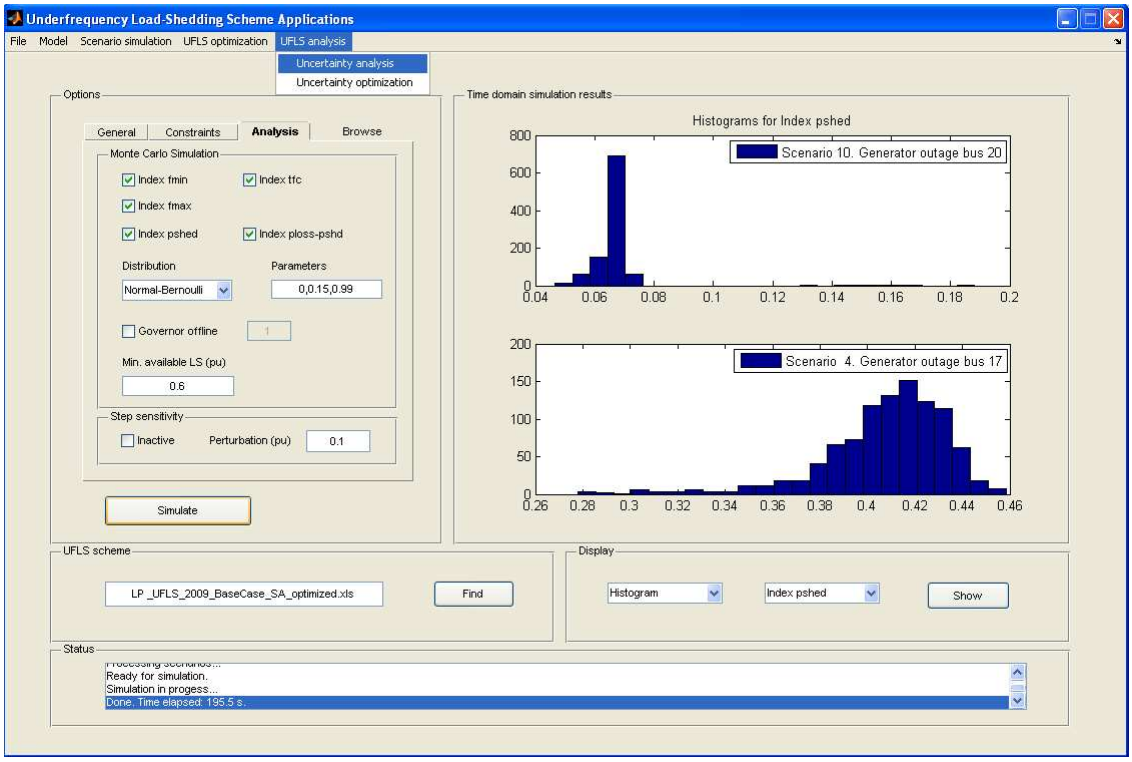

Figure A-12: Analysis of UFLS schemes using Monte-Carlo simulations.

Figure A-12 shows the interface for the analysis of UFLS schemes using Monte-Carlo simulations. The number of runs and the number of simulations as well as the simulation time can be specified by the user. Variations of step sizes are implemented by means of statistical distributions. The user can select a distribution function of a list of various distribution functions and specify its corresponding parameters. Further, the toolbox allows including the effect of randomly selected inactive governors. The minimum amount of available load to be shed can be adjusted, too. Finally, various graphic tools enable to analyze the results obtained from the Monte-Carlo simulations.

A-3 CONCLUSIONS

This appendix presented the UFLSA toolbox developed for simulation as well as design and analysis of UFLS schemes of small isolated power systems. The toolbox employs the SFD model developed in chapter 3 to simulate the response of the power system to a set of possible disturbances. Similarly, design and analysis of UFLS schemes are based on simulations. A simulation refers to the numerical integration of a system of non-linear differential equations. UFLSA toolbox uses Heun's numerical integration method.

The toolbox realizes the following tasks:

- Data processing. Data either contain detailed parameters of the turbine-governor systems or field-test measurements and operating scenarios of the power system of interest.
- Tuning of the generic second-order model. If the parameters of the generic second-order model have not been provided and previously determined, the UFLSA toolbox tunes these parameters such that the output of the generic second-order model resembles as much as possible measurement data or the output of the detailed model.

- Simulation of the power system to one or several contingencies. These contingencies either correspond to the outages of the smallest or largest generating units for each operating scenario or to outages selected by the user or to outages determined by a cluster analysis.
- Design of robust and efficient UFLS schemes. The design of an efficient and robust UFLS schemes comprises two tasks: the selection of adequate operating and contingency scenarios using clustering algorithms and the application of an optimization algorithm to the problem of UFLS scheme parameter tuning. In the optimization stage, the user chooses if representative scenarios or manually selected scenario are used. The user also determines the constraints, objective function, optimization algorithm as well as decision variables, i.e. the UFLS scheme parameters.
- Analysis of UFLS schemes. The analysis of UFLS schemes and the study of the impact of step-size variations in particular are based on Monte-Carlo simulations.

APPENDIX B

PHASE-PLANE ANALYSIS

B-1 INTRODUCTION

Throughout this dissertation, special attention has been paid to conventional UFLS schemes since most of the UFLS schemes employed today are conventional schemes applying underfrequency and rate of change of frequency (ROCOF) relays. These schemes basically shed a predefined amount of load according to settings determined offline. Nevertheless, progress in technology, giving rise to faster and cheaper devices communication infrastructure, could allow implementing advanced UFLS schemes in the future [Terzija'06]. This appendix deals with phase-plane methods which could be used to asses frequency stability and the problem of load shedding.

Phase-plane methods have been widely used for studying the effects of nonlinearities in second-order feedback systems [Levine'99]. They usually consist in sketching state phase-plane trajectories by means of numerical solutions for various initial conditions, slope plots, explicit solutions or isocline plots. An example of graphical phase-plane analysis has been shown in chapter 3. This example illustrated the impact of UFLS schemes on short-term frequency dynamics in the ω–$d\omega/dt$ (frequency versus rate of change of frequency) phase plane.[1] A classical use of phase-plane analysis is made within assessment of angular power-system stability using Lyapunov's first integral method [Pai'81]. In fact, given a Lyapunov function (e.g., energy function), a region of stability can be defined by a separatrix in the δ–ω (angle versus frequency) phase plane. Lyapunov functions represent the primary tool for the stability analysis of non-linear systems [Levine'99]. They verify the stability of a given trajectory, and they also provide an estimate of its region of attraction.

Use of phase-plane analysis for the problem of short-term frequency stability has been made in [Terzija'06], [Chuvychin'96] and [Elkateb'89]. In [Elkateb'89] and [Terzija'06], phase-plane (or locus) plots have been used for the purpose of sketching

[1] Note that $d\omega/dt$ is not a state variable and thus, the ω–$d\omega/dt$ is not a proper state phase plane but rather a derived one.

state trajectories in the ω–p (frequency versus mechanical power) and the ω–dω/dt phase plane, but only the work presented in [Terzija'06] recognizes the possibilities of using the ω–dω/dt phase plane for the synthesis of adaptive UFLS schemes. Such a synthesis has been proposed in [Chuvychin'96]. Assuming that UFLS relays are able to measure both frequency and rate of change of frequency, phase-plane analysis could be incorporated into relay logic, determining power-system status by means of a generation boundary curve. This boundary curve, which has been obtained considering an unregulated machine connected to an infinite bus, allows detecting generation deficiency and determining adequate load-shedding actions.

This appendix presents new frequency protection schemes based on ω–dω/dt phase-plane analysis and on the definition of frequency stability boundary in particular. Due to their nature, these frequency protection schemes belong to advanced UFLS schemes. The definition of a frequency stability boundary is inspired by the definition of the region of angular stability in the δ–ω phase plane. Thus, in a first step, assessment of angular stability using a Lyapunov function revised. Subsequently, derivation of frequency stability boundary is presented and compared with the generation boundary curve defined in [Chuvychin'96]. Finally, some implementations of the frequency stability boundary are shown.

B-2 REGION OF ANGULAR STABILITY

It has been shown in chapter 3 (see e.g. Figure 3-1) that the response of a power system to a power imbalance can be described in four stages. In particular, during the first few seconds and preceding the stages of frequency dynamics, the system's behavior is dominated by rotor swings due to rotor angle oscillations. It is in this first stage where generating units could loose synchronism because of large rotor swings and where the assessment of angular stability is of primary concern.

The determination of the region of angular stability is easily shown for a power system where a single machine is connected to the infinite bus. Neglecting damping, rotor swing equation can be stated as follows:

$$\begin{aligned} 2H\dot{\omega} &= p_m - p_e \\ &= p_m - \frac{e_1 v}{x_e}\sin\delta \end{aligned} \tag{B.1}$$

where p_m is the mechanical power, e_1 is the internal voltage magnitude of the machine, v is the magnitude of the voltage of the infinite bus and x_t is the reactance corresponding to the post-fault system between the generator internal node and the infinite bus. The state equations for equation (B.1) are:

$$\begin{aligned} \Delta\dot{\delta} &= \omega_0 \Delta\omega \\ \Delta\dot{\omega} &= \frac{p_m}{2H} - \frac{1}{2H}\frac{e_1 v}{x_t}\sin\delta \end{aligned} \tag{B.2}$$

with $\Delta\delta = \delta - \delta_s$ and $\Delta\omega = \omega - 1$ and where δ_s is the angle corresponding to the initially stable system. By applying the method of first integrals, a Lyapunov function V can be obtained. From equation (B.2), one obtains

$$\frac{d\Delta\delta}{d\Delta\omega} = \frac{2H\omega_0\Delta\omega}{p_m - \frac{e_1 v}{x_t}\sin\left(\delta_s + \Delta\delta\right)}$$

and integrating from $(0,0)$ to $(\Delta\delta,\Delta\omega)$ yields after some manipulations to:

$$V(\delta,\omega)=\frac{1}{2}2H\omega_0(\omega-1)^2-\frac{e_1 v}{x_t}(\cos\delta-\cos\delta_s)-p_m(\delta-\delta_s) \tag{B.3}$$

The Lyapunov function of equation (B.3) can be interpreted as an energy function. In fact, the first term corresponds to the kinetic energy, whereas the second and the third term correspond to the potential energy. Since the system is conservative, the Lyapunov function V must remain constant. Figure B-1 shows contours for various values of the Lyapunov function V. The contour passing through the saddle point (δ_u,*1*) and defined by the constant V-curve $V(\delta,\omega) = V(\delta_u, \omega=1)$ is called the separatrix. δ_u is the angle for which instability occurs. The closed region inside of the separatrix defines then a region of stability.

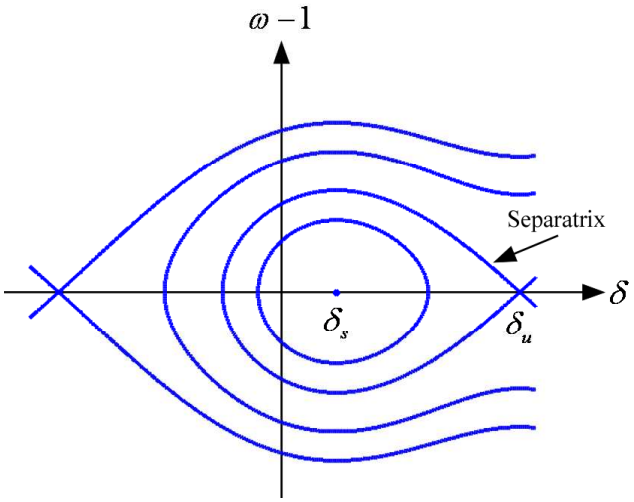

Figure B-1: Constant V-contours and the region of stability δ– ω phase plane.

B-3 REGION OF FREQUENCY STABILITY

The principal idea behind the elaboration of a frequency stability boundary is the ability to predict if a power system remains stable following a disturbance, similar to the assessment of angular power-system stability using Lyapunov's method. If state trajectories are outside the region of stability, adequate emergency control must be undertaken (e.g., load shedding) to stabilize the system.

B-3-1 Review of generation boundary curve

In [Chuvychin'96], the determination of power-system status by means of a generation boundary curve has been presented. This boundary curve has been obtained considering the simple case of an unregulated machine connected to an infinite bus. The dynamics of an unregulated machine (i.e., the machine is not under active governor control) can be stated as follows [Anderson'77]:

$$\Delta t_m=-t_{m0}\Delta\omega \tag{B.4}$$

or by dint of the typical assumption that torque and power are nearly identical in pu:

$$\Delta p_m=-p_{m0}\Delta\omega \tag{B.5}$$

with $\Delta\omega = \omega - 1$.[2] In other words, variations of the mechanical torque t_m are uniquely due to speed variations since governor control is inactive.

Considering the swing equation of equation (B.1) and adding a term related to the load-damping factor D yields to:

$$2H\dot{\omega} = p_m - p_e - D(\omega - 1)$$

Considering now variations in mechanical power due to speed variations results in:

$$2H\dot{\omega} = p_{m0} + \Delta p_m - p_e - D(\omega - 1) \tag{B.6}$$

and by using equation (B.5), one obtains:

$$2H\dot{\omega} = p_{m0} - p_{m0}(\omega - 1) - p_e - D(\omega - 1)$$

Assuming now constant demand and knowing that $p_e = p_{m0} = 1$ leads to equation (B.7):

$$2H\dot{\omega} = -(\omega - 1) - D(\omega - 1) \tag{B.7}$$

The generation boundary curve of equation (B.7) is illustrated in Figure B-2. H and D are set to 2.3 s and 0 pu, respectively. Points above the boundary curve represent a surplus of generation, whereas points below the curve indicate a deficiency of generation. For example, the point (49 Hz,0 Hz/s) would indicate a deficiency of generation since it is below the generation boundary curve. In addition, this boundary curve describes somehow the behavior of the power system. In fact, immediately after a loss of generation of 0.23 pu, the point (ω,dω/dt) would move to the point (50 Hz,-2.5 Hz/s). Subsequently, this point would move along a line parallel to the boundary curve, in the direction of descending frequency and ascending rate of change of frequency.

---

[2] These equations can be derived from the equation relating mechanical power and mechanical torque as follows:

$$T_m = \frac{P_m}{\omega}$$

Considering variations around the operating point yields to:

$$\Delta T_m = \frac{1}{\omega_0}\Delta P_m - \frac{P_{m0}}{\omega_0^2}\Delta\omega$$

Since the machine is not under active governor control, mechanical power variation is zero. Converting into pu results finally in:

$$dt_m = -t_{m0}\,d\omega$$

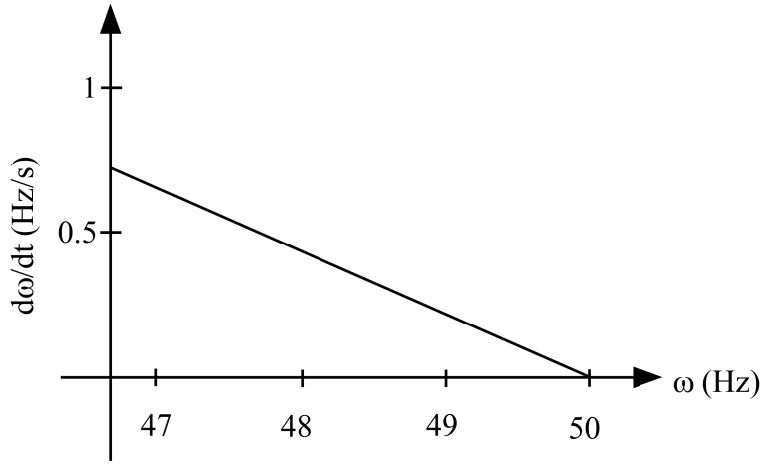

Figure B-2: Generation boundary curve in the ω–dω/dt phase plane [Chuvychin'96].

B-3-2 Definition of frequency stability boundary

The drawback of the generation boundary approach based on an unregulated machine resides in the fact that turbine-governor system dynamics are completely omitted. Further, generation boundary curves uniquely informs on power imbalance. The proposed definition of frequency stability boundary allows assessing frequency stability as the separatrix does in the case of angular stability.

Consider a power system consisting of n generating units and neglect for now non-linearities. If first-order generator models were considered, the power-system response following a disturbance is described by the following system of linear differential equations:

$$\begin{aligned} 2H\Delta\dot{\omega} &= \sum_{i=1}^{n}\Delta p_{m,i} - \Delta p_d \\ \Delta\dot{p}_{m,i} &= -\frac{1}{T_i}\left(\Delta p_{m,i} + K_i\Delta\omega\right) \end{aligned} \tag{B.8}$$

where H is the equivalent inertia and K_i and T_i the gain and time constant of the *ith* generator model, respectively. If generating units are modeled by a second-order model (see also section 3-3), either its first-order version could be derived or the parameter a_1 of the second-order model could be used. During the first instants after the contingency, the response of the power system can be approximated as follows:

$$\begin{aligned} 2H\Delta\dot{\omega} &= \sum_{i=1}^{n}\Delta p_{m,i} - \Delta p_d \\ \Delta\dot{p}_{m,i} &= -\frac{K_i}{T_i}\Delta\omega \end{aligned} \tag{B.9}$$

This formulation is equivalent to the assumption that all generators are modeled by an isochronous-like governor. Note the conflictive control due to two integrators in series, which will result in a cyclic behavior as shown in equation (B.14). Differentiating equation (B.9) yields to:

$$2H\Delta\ddot{\omega} = -\sum_{i=1}^{n}\frac{K_i}{T_i}\Delta\omega - \Delta\dot{p}_d$$

and by applying the Laplace transform, one obtains:

$$2Hs^2\Delta\omega(s)+\sum_{i=1}^{n}\frac{K_i}{T_i}\Delta\omega(s)=-s\Delta p_d(s)$$

This expression is a more elegant version of the idea of "breaking the loop" presented in [Egido'10] and allows summing power outputs of the *n* generators without creating a (*n*+1)th-order system. Modeling the contingency by a step of size Δp of the demand, equation (B.10) is obtained, which describes the response of the power system in terms of frequency.

$$\Delta\omega(s)\left(2Hs^2+\sum_{i=1}^{n}\frac{K_i}{T_i}\right)=-\Delta p \tag{B.10}$$

Rearranging and defining the equivalent gain as $\hat{K}=\sum_{i=1}^{n}\frac{K_i}{T_i}$ results in:

$$\Delta\omega(s)=-\frac{\Delta p}{\hat{K}}\sqrt{\frac{\hat{K}}{2H}}\frac{\sqrt{\frac{\hat{K}}{2H}}}{\left(s^2+\frac{\hat{K}}{2H}\right)} \tag{B.11}$$

The application of the inverse Laplace transforms yields to the time domain response $\Delta\omega(t)$:

$$\Delta\omega(t)=-\frac{\Delta p}{\hat{K}}\sqrt{\frac{\hat{K}}{2H}}\sin\left(\sqrt{\frac{\hat{K}}{2H}}t\right) \tag{B.12}$$

The rate of change of frequency is given by:

$$\Delta\dot{\omega}(t)=-\frac{\Delta p}{2H}\cos\left(\sqrt{\frac{\hat{K}}{2H}}t\right) \tag{B.13}$$

Eliminating time explicitly from equations (B.12) and (B.13) yields to a function describing an ellipsis in the ω–dω/dt phase plane:[3]

$$\frac{\Delta\omega^2}{\Delta\omega_{\min}^2}+\frac{\Delta\dot{\omega}^2}{\Delta\dot{\omega}_{\max}^2}=1 \tag{B.14}$$

where

$$\Delta\omega_{\min}=-\frac{\Delta p}{\hat{K}}\sqrt{\frac{\hat{K}}{2H}} \tag{B.15}$$

and

$$\Delta\dot{\omega}_{\max}=-\frac{\Delta p}{2H} \tag{B.16}$$

Knowing the system parameters *H*, K_i and T_i, it is possible to determine the critical loss Δp for which frequency does not fall bellow the minimum allowable frequency (e.g. 47.5 Hz or $\Delta\omega_{min}$ = -0.05 pu). Once, the critical loss is known, $\Delta\dot{\omega}_{\max}$ can be readily determined. Finally, the frequency stability boundary can be described as:

[3] This makes sense because of the conflictive control caused by two integrators connected in series.

$$\Delta\dot{\omega} \le \sqrt{\Delta\dot{\omega}_{\max}^2 \left(1 - \frac{\Delta\omega^2}{\Delta\omega_{\min}^2}\right)} \tag{B.17}$$

Obviously, the system is stable while state trajectories remain within the boundary of stability, .i.e. inside the region of stability. Equation (B.17) is graphically illustrated in Figure B-3. Note that the frequency stability boundary is in general only valid in the third quadrant since subsequently, the assumption of the equivalent gain is usually not applicable anymore.

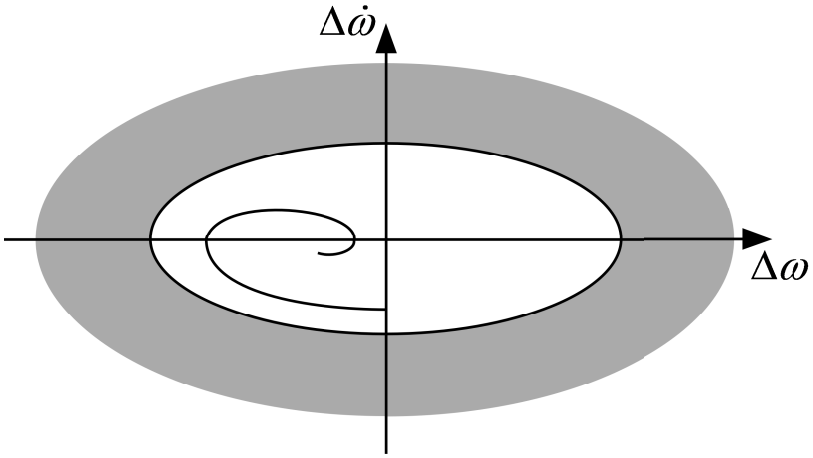

Figure B-3: Illustration of stability boundary in the ω–dω/dt phase plane.

So far, generator output limitations have not been considered. Clearly, if spinning reserve is smaller than the amount of lost generation, the system becomes unstable (unless load is shed). Since the region of stability is defined by ignoring explicitly load-shedding actions, the problem of limited generator output is easily included into the definition of frequency stability boundary. In fact, (B.15) modifies as follows:

$$\Delta p = \min\left(-\Delta\omega_{\min}\sqrt{2H\hat{K}}, \Delta p_{max}\right) \tag{B.18}$$

where Δp_{max} is the upper limit of the generator output. Consequently, $\Delta\omega_{min}$ needs to be recalculated with the final Δp if amount of lost generation is bigger than the amount of available spinning reserve. $\Delta\dot{\omega}_{\max}$ can be readily determined using equation (B.16). For the sake of completeness, it must be highlighted that this approach of dealing with generator output limitations is a simplification since only the total amount of spinning reserve is considered but not the output limitations of each single generating unit.

B-3-3 Determination of frequency stability boundary by Lyapunov theory

The question arises if it is also possible to find a Lyapunov function V able to describe a region of frequency stability and if the proposed frequency stability boundary is a separatrix of this Lyapunov function. A function $V(\mathbf{x}_s)$ is called a Lyapunov function if the following conditions are fulfilled [Pai'81]:

$$\begin{aligned} V(\mathbf{x}_s) &\ge 0, \quad \forall \mathbf{x}_s \\ \dot{V}(\mathbf{x}_s) &\le 0 \end{aligned} \tag{B.19}$$

Consider for this purpose a modified version of equation (B.9) which takes into account the non-linearity introduced by the limited generator output:

$$\begin{aligned} 2H\Delta\dot{\omega} &= sat(\Delta p_m) \\ \Delta\dot{p}_m &= -\hat{K}\Delta\omega \end{aligned} \tag{B.20}$$

where *sat*(•) is a saturation function [Saberi'96]. Clearly, if the saturation function is linear and passes through the origin and minimum allowable frequency is omitted, the system defined by equation (B.20) is stable in $\mathbb{R}^2$. Applying the first integral method yields to the following Lyapunov function *V*:

$$V(\Delta\omega, \Delta p_m) = \frac{\hat{K}}{2}\Delta\omega^2 + \frac{1}{2H}\int_0^{\Delta p_m} sat(\sigma)d\sigma \tag{B.21}$$

If $sat(\sigma)=sign(\sigma)min(\sigma,\sigma_{lim})$, with σ_{lim} being a limit (e.g. the upper generation output limit Δp_{max}), then equation (B.21) results in:

$$V(\Delta\omega, \Delta p_m) = \frac{\hat{K}}{2}\Delta\omega^2 + \frac{1}{2H}\begin{cases} \frac{1}{2}\Delta p_m^2, & \Delta p_m \le \Delta p_{\max} \\ \frac{1}{2}\Delta p_{\max}^2 + \Delta p_m \Delta p_{\max}, & \Delta p_m > \Delta p_{\max} \end{cases} \tag{B.22}$$

where Δp_{max} is the upper limit of the generator output. Without loss of generality, it has been supposed that all generating units have the same saturation function. If saturation functions were different, an equivalent saturation function, defined as the sum of the single saturation functions, could be considered. This is shown in Figure B-4.

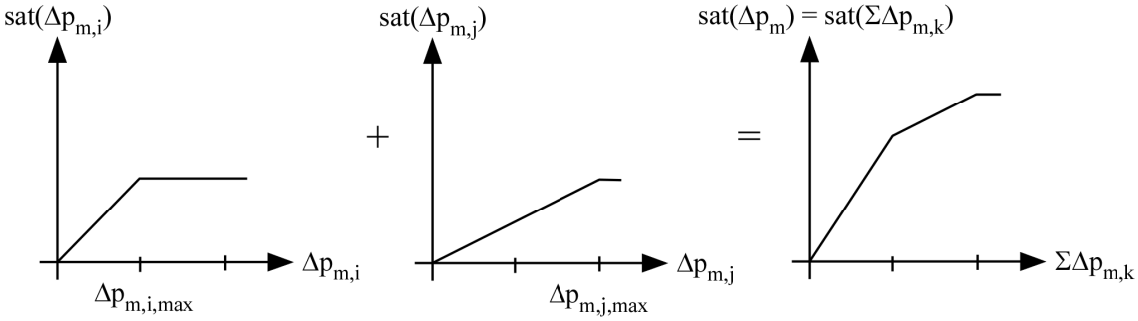

Figure B-4: Equivalent saturation function.

As long as the generator output is smaller than its limit, which has been supposed in the previous section, equation (B.22) reduces to:

$$V(\Delta\omega, \Delta p_m) = \frac{\hat{K}}{2}\Delta\omega^2 + \frac{1}{2H}\frac{1}{2}\Delta p_m^2$$

or

$$V(\Delta\omega, \Delta\dot{\omega}) = \frac{\hat{K}}{2}\Delta\omega^2 + \frac{2H}{2}\Delta\dot{\omega}^2 \tag{B.23}$$

Equation (B.23) is a Lyapunov function since *V(•)* is always equal to or bigger than 0 and since its derivative is always equal to 0. Now, equation (B.14) can be written as follows:

$$\frac{\Delta\omega^2}{\Delta p^2}2H\hat{K}+\frac{\Delta\dot{\omega}^2}{\Delta p^2}(2H)^2=1$$

$$\frac{\hat{K}}{2}\Delta\omega^2+\frac{2H}{2}\Delta\dot{\omega}^2=\frac{1}{2}\frac{\Delta p^2}{2H}$$

$$=\frac{1}{2}2H\left(\frac{\Delta p}{2H}\right)^2$$

$$=\frac{1}{2}2H\Delta\dot{\omega}_{\max}^2$$

Thus, the stability boundary described by equation (B.14) can be interpreted as a separatrix, limiting equation (B.23) to values smaller than or equal to $H\Delta\dot{\omega}_{\max}^2$. In other words, the frequency stability boundary is a Lyapunov function, which allows assessing frequency stability of a power system. Representing system trajectories after disturbances in the ω–dω/dt phase plane, control actions, such as load shedding, could be initiated based on the frequency stability boundary.

B-3-4 Application example

Frequency stability region is described by an ellipsis-like boundary in ω–dω/dt phase plane. The stability boundary function depends on the operating scenario. In fact, operating scenarios directly influence the parameters of the power-system model and especially the equivalent inertia H as well as the equivalent gain $\hat{K}$ which in turn depends on the gain and the time constant of the generator model.

To illustrate the determination of the region of frequency stability, the minimum load-demand scenario without decoupled power generation of the La Palma power system is considered. Table B-1 displays this operating scenario. Table B-2 shows parameters of the first-order generator models of the La Palma power system.

Table B-1: Low demand generation dispatch scenario of the La Palma power system.

S. O. C.	G11	G12	G13	G14	G15	G16	G17	G18	G19	G20	G21	$P_{G_{tot}}=P_{D_{tot}}$
1	0	0	2.35	0	3.29	3.29	9.16	0	0	0	0	18.09

Table B-2: First-order model parameters of the generating units of the La Palma power system.

Generator	H (s)	K	T (s)	Pmin (MW)	Pmax (MW)
G11	1.75	20	8.26	2.5	4
G12	1.75	20	8.26	2.5	4
G13	1.75	20	8.26	2.5	4
G14	1.73	20	8.26	3	4.5
G15	2.16	20	8.26	3.5	7
G16	1.88	20	8.26	3.5	7
G17	2.1	20	8.26	7	12
G18	6.5	21.25	3.18	0	22.8
G19	2.1	20	8.26	7	12
G20	2.1	20	8.26	7	12
G21	2.1	20	8.26	7	12

The equivalent inertia and the equivalent gain are:

$$H = \frac{\sum_{i=1}^{n} M_{base,i} \cdot H_i}{\sum_{i=1}^{n} M_{base,i}} \quad \text{and} \quad \hat{K} = \frac{\sum_{i=1}^{n} M_{base,i} \cdot \frac{K_i}{T_i}}{\sum_{i=1}^{n} M_{base,i}}$$

where H_i and $M_{base,i}$ are the inertia (with respect to $M_{base,i}$) and the base power of generator i, K_i is the gain of generator i (with respect to $M_{base,i}$) and n is the number of generators.

According to equation (B.17), both $\Delta\omega_{min}$ and $\Delta\dot{\omega}_{\max}$ must be first defined. $\Delta\omega_{min}$ coincides with the minimum allowable frequency and is set to -0.05 pu. $\Delta\dot{\omega}_{\max}$ can be computed by means of equations (B.15) and (B.16). In fact, the critical loss is given by:

$$\Delta p = -\Delta\omega_{\min}\sqrt{2H\hat{K}} = 0.1562\,pu \triangleq 6.27MW$$

which is smaller than the available amount of spinning reserve. Knowing the critical loss, $\Delta\dot{\omega}_{\max}$ is determined by equation (B.16) and amounts to -0.0388 pu/s (-1.94 Hz/s).

As an example, the consecutive outages of all four generating units of minimum load-demand scenario of the La Palma power system are simulated. Figure B-5 shows the system responses as well as the region of frequency stability determined by the stability boundary in the ω–dω/dt phase plane. Three cases are clearly stable since their trajectories are within the stability region. The unstable case corresponds the outage of generating unit G17, producing more than 50% of total load demand. For this particular outage, load-shedding actions are necessary to stabilize the power system.

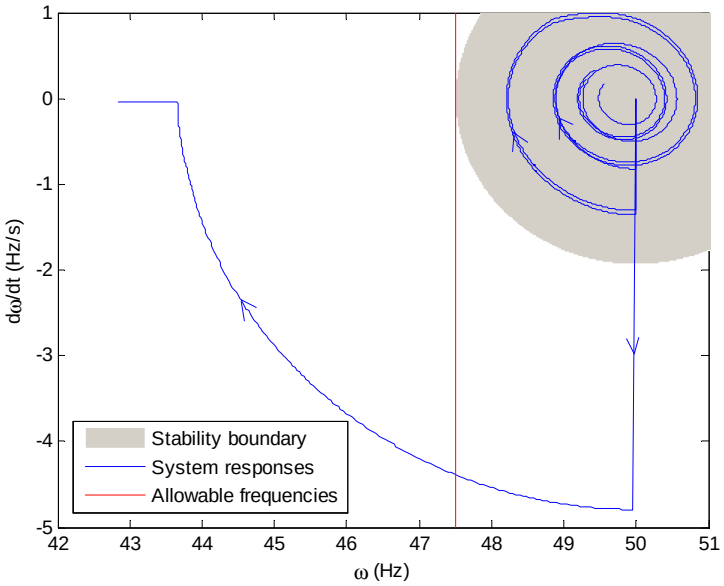

Figure B-5: Power-system response and stability boundary in the ω–dω/dt phase plane.

B-4 APPLICATION OF STABILITY BOUNDARY

An analytical expression has been deduced in the previous section which allows describing the boundary of frequency stability in function of the frequency deviation $\Delta\omega$. Principally, two possible implementations could be envisaged: the first one consists in adding a supplementary signal at the output of present underfrequency relays,

whereas the second option considers a centralized implementation. The latter corresponds to advanced UFLS schemes.

B-4-1 Implementation by means of an additional signal

The implementation of frequency stability boundary is realized by means of a supplementary signal that is added to output signal of the existing underfrequency relays. The supplementary signal depends on the position of the measured point (ω,dω/dt) in the ω–dω/dt phase plane and its distance and directionality with respect to the frequency stability boundary. The supplementary signal is added to the output of the existing underfrequency relays via a logic multiplication.

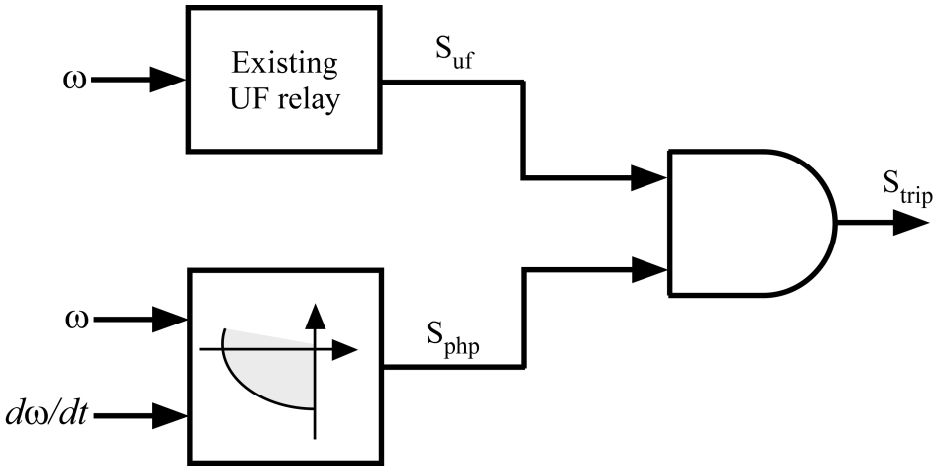

Figure B-6: Implementation by means of an additional signal.

Figure B-6 show the connection scheme of the implementation by means of a supplementary signal. If the underfrequency conditions of the relays are satisfied, the underfrequency relay sends a logic signal S_{uf} of value 1 to the AND port. Similarly, the phase-plane block sends a logic signal S_{php} to the AND port in function of the inputs and according to the imposed conditions. The output signal of the AND port, S_{trip}, corresponds to the logic multiplication of the signals S_{uf} and S_{php}.

B-4-2 Centralized implementation

The implementation is realized in a centralized manner, i.e. the phase plane is implemented in a server which receives frequency and ROCOF as inputs and determines if load must be shed and which amount of load needs to be shed. The requirement of shedding is deduced from the position of the measure point (ω,dω/dt) in the ω–dω/dt phase plane and its distance and directionality with respect to the frequency stability boundary. For example, if the measured point lies within the region of frequency stability and moves away from the stability boundary, it is not necessary to shed load. The amount of shed load could be determined as the difference between the initial loss of generation and the critical lost computed using equation (B.18) [Anderson'90].

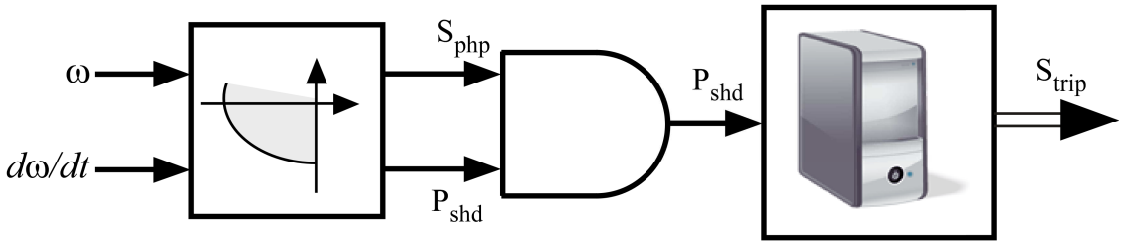

Figure B-7: Centralized implementation.

Figure B-7 shows the scheme of centralized implementation. The phase-plane block sends a logic signal S_{php} to the AND port, depending on its inputs and the imposed conditions. The phase-plane block also determines the amount of load to be shed P_{shd} and sends the corresponding signal to the AND port. The output of the AND port corresponds to the logic multiplication of the signals S_{php} and P_{shd}. In function of the amount of load to be shed, of the availability of loads associated to relays, etc., the server determines to which relays the opening signal S_{trip} must be send.

B-5 CONCLUSIONS

This appendix presented new frequency protection schemes based on ω–dω/dt phase-plane analysis and on the definition of frequency stability boundary in particular. Due to their nature, these frequency protection schemes belong to advanced UFLS schemes.

The definition of a frequency stability boundary is inspired by the definition of the region of angular stability in the δ–ω phase plane and thus, the assessment of angular stability using a Lyapunov function has been revised. The derivation of frequency stability boundary is based upon an elegant version of the idea of "breaking the loop" which allows summing power outputs of *n* generators without creating an (*n*+1)th-order system. It has been shown that the frequency stability boundary is a separatrix, describing a region of frequency stability. This region helps determining if for a particular disturbance load must be shed to guarantee frequency stability. The region of frequency stability is described by an ellipsis in the ω–dω/dt phase plane.

Finally, some implementations making use of the definition of frequency stability boundary have been shown. One implementation simply adds a supplementary signal to the output of the existing underfrequency relay, blocking its trip signal if load shedding is unnecessary. Another option suggests a centralized implementation in a server which determines if load must be shed, what amount of load needs to be shed and which selects in function of this information which relays must be opened.

APPENDIX C

DETAILED TURBINE-GOVERNOR SYSTEMS

C-1 INTRODUCTION

In small isolated power systems, conventional generating units are usually driven by Diesel, gas or steam turbines. This appendix reproduces detailed turbine-governor systems corresponding to these common turbine types. The detailed turbine-governor systems are represented by commonly used standard models from the PSS/E software package model-library [Siemens'05b]; in particular,

- DEGOV1
- GAST2A
- GASTWD
- IEEEG1

C-2 DEGOV1 TURBINE-GOVERNOR SYSTEM

Figure C-1 shows the block diagram of a Diesel-based DEGOV1 turbine-governor system.

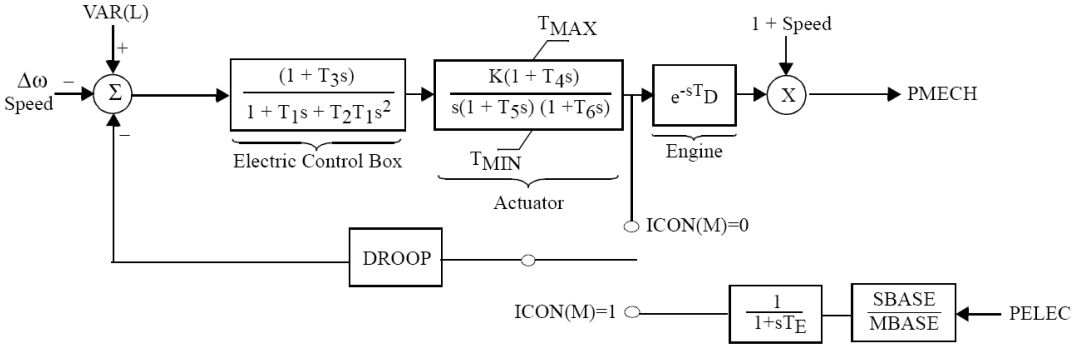

Figure C-1: Block diagram of the DEGOV1 turbine-governor system model [Siemens'05b].

C-3 GAST2A TURBINE-GOVERNOR SYSTEM

Figure C-2 shows the block diagram of a gas-based GAST2A turbine-governor system.

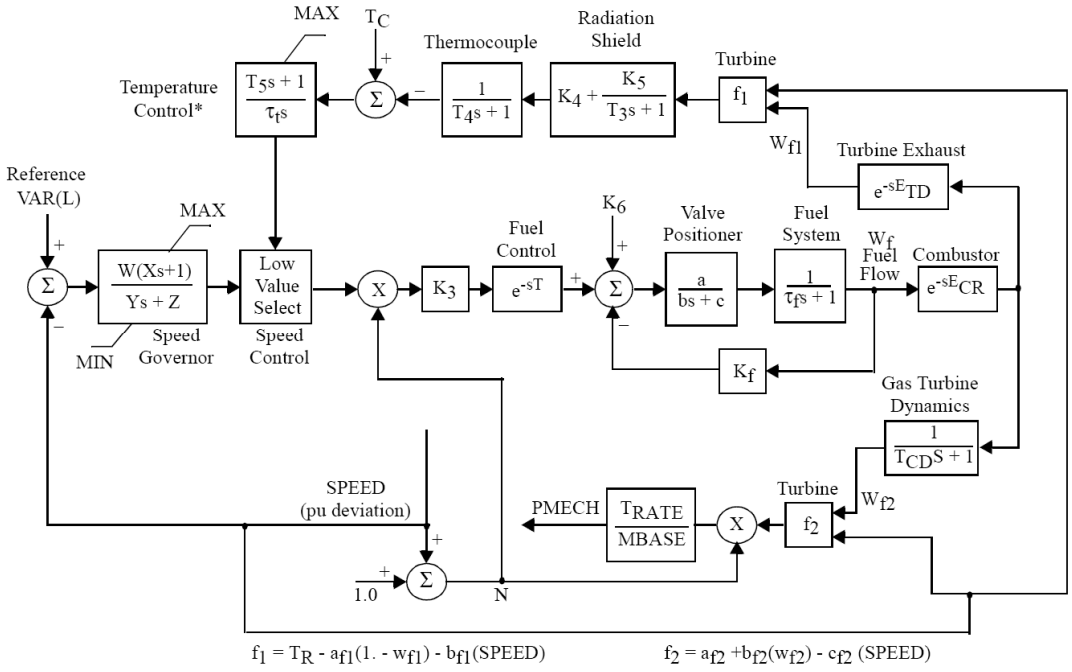

Figure C-2: Block diagram of the GAST2A turbine-governor system model [Siemens'05b].

C-4 GASTWD TURBINE-GOVERNOR SYSTEM

Figure C-3 shows the block diagram of a gas-based GASTWD turbine-governor system.

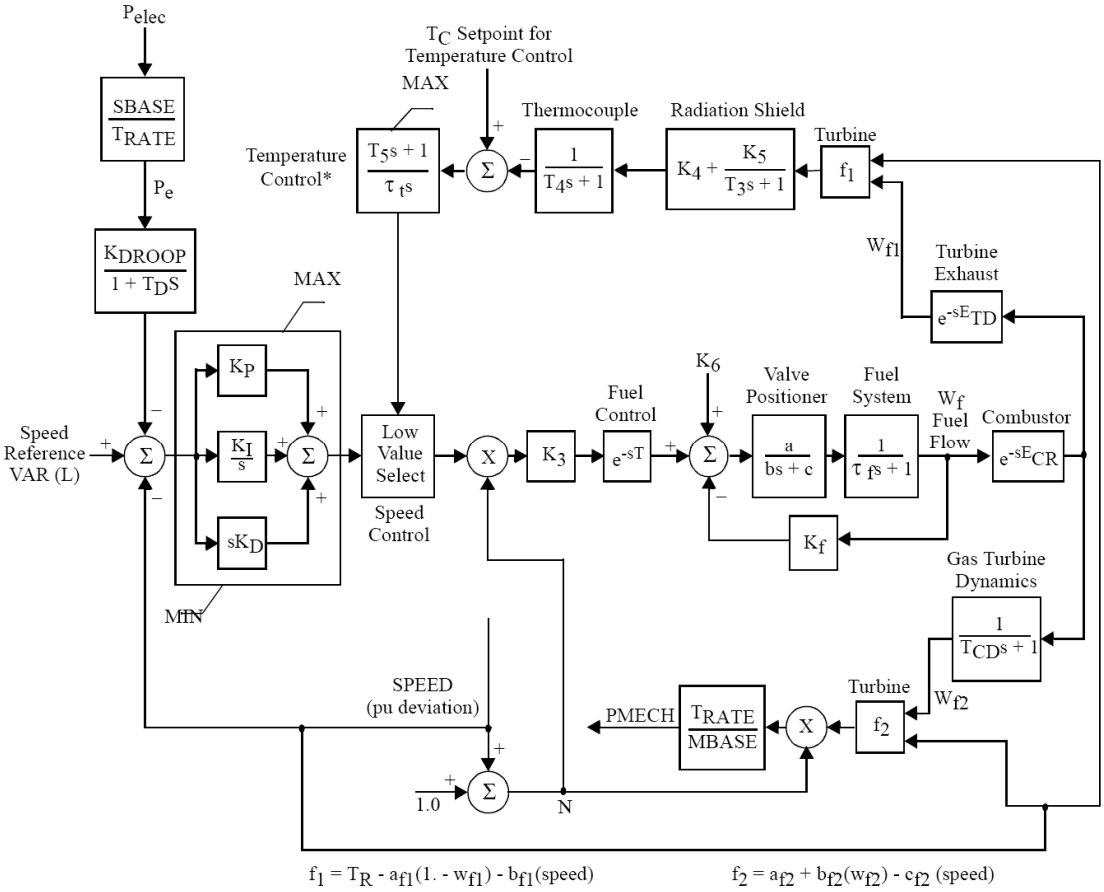

Figure C-3: Block diagram of the GASTWD turbine-governor system model [Siemens'05b].

C-5 IEEEG1 TURBINE-GOVERNOR SYSTEM

Figure C-4 shows the block diagram of a steam-based IEEEG1 turbine-governor system.

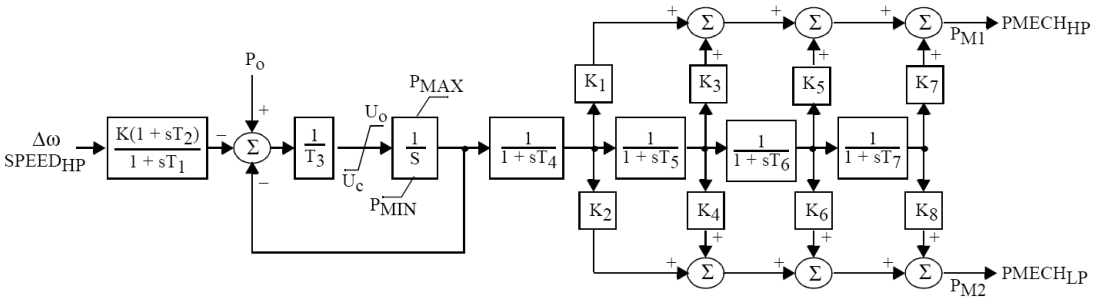

Figure C-4: Block diagram of the IEEEG1 turbine-governor system model [Siemens'05b].